



Attribution–NonCommercial–NoDerivs 2.0 KOREA

You are free to :

- **Share** — copy and redistribute the material in any medium or format

Under the following terms :



Attribution — You must give [appropriate credit](#), provide a link to the license, and [indicate if changes were made](#). You may do so in any reasonable manner, but not in any way that suggests the licensor endorses you or your use.



NonCommercial — You may not use the material for [commercial purposes](#).



NoDerivatives — If you [remix, transform, or build upon](#) the material, you may not distribute the modified material.

You do not have to comply with the license for elements of the material in the public domain or where your use is permitted by an applicable exception or limitation.

This is a human-readable summary of (and not a substitute for) the [license](#).

[Disclaimer](#) 

**A Dissertation for the Degree of Doctor of Philosophy**

**Vitamin B6-Coupled Poly(ester  
amine) Mediated DNA and siRNA  
Delivery via Modulation of  
Intracellular Uptake  
Process for Cancer Therapy**

**August 2015**

**Shambhavi Pandey**

**Department of Biosystems & Biomaterials Science and**

**Engineering**

**Seoul National University**

*Dedicated to*

*My Parents, Beloved Husband*

*&*

*Advisor, Prof. Jong Hoon Chung*

# *ABSTRACT*

---

The innovative methodologies in the broad field of cancer gene therapy promises a number of potential benefits for diagnosis and treatment that are likely to become important in preventing deaths from cancer. DNA synthesis mechanism underlying cancer cell proliferation and mutations can be selected for therapeutic attack to cause cell death or slow the growth of the cancer, which is one of the objectives of the research study. Elevated serine hydroxymethyltransferase (SHMT, one of the components of DNA synthesis machinery) activity has been shown to be coupled with the increased demand for DNA synthesis in rapidly proliferating cancer cells. It is also found that complete knockout of SHMT leads to glycine auxotrophy which leads to impairment in the synthesis of purines and pyrimidines. Therefore the central role of SHMT in nucleotide biosynthesis makes it a suitable anticancer target which can be selectively silenced by delivering siRNA to shut down the whole DNA synthesis machinery in cancer cells. However, the

immense potential of RNAi in anti-cancer therapy is impeded by the non-availability of a suitable delivery agent, off-target effects and induction of innate immune response. Therefore, engineering a non-viral vector which can efficiently deliver the siRNA against SHMT involved in DNA biosynthesis with higher affinity to cancer cells becomes an interesting research area.

Vitamin B6 (VB6) plays an essential role as a coenzyme in various cellular metabolic functions, including DNA biosynthesis for cellular growth and proliferation. VB6 is taken up by cells through facilitated diffusion via VB6 transporting membrane carrier (VTC). In this study, it was demonstrated that the VB6-coupled poly(ester amine) (VBPEA) gene transporter utilizes this uptake mechanism, leading to enhanced vector transport inside the rapidly proliferating cancer cells with relatively high affinity. Physicochemical characterization, cell viability assays, and transfection studies showed VBPEA to meet the standards of a good transfection agent. Competitive inhibition of VBPEA uptake by its structural analogue 4'-deoxypyridoxine hydrochloride revealed the involvement of VB6 specific transporting membrane carrier in

VBPEA internalization in tumor cells. VBPEA elicit higher transfection levels in lung cancer cells (A549) than in normal lung cells (16HBE), indicating that cancer cells which have a high demand for VB6, have a higher affinity for VB6-coupled vector. VB6 coupling to the gene transporter is important to enforce a high level of VTC-mediated endocytosis compared to VB6 alone. This system exemplified how understanding of the VB6 membrane transporter specificity allowed for the design of a VB6-coupled gene transporter with accelerated transfection activity in cancer cells owing to an advanced mode of internalization.

The advancement in study was done by examining its therapeutic application in cancer tissue using RNAi technology. Serine hydroxymethyltransferase isoforms (SHMT1 & SHMT2 $\alpha$ ), which serve as scaffold protein for the formation of a multienzyme complex and generate one-carbon unit for the de novo thymidylate biosynthesis pathway during DNA synthesis, are vitamin B6-dependent enzyme. Cancer cells with high proliferation intensity need increased SHMT activation which enforces the facilitated-diffusion of VB6 for the

continuous functioning of thymidylate synthase cycle. Therefore, SHMT knockdown presents an alternative approach to prevent DNA synthesis in cancer cells; however, its potential to inhibit cancer growth remains unknown so far. Here it was demonstrated that VB6 coupled to poly(ester amine) enforces a high level of VTC-mediated endocytosis of the complexed SHMT1 siRNA (siSHMT1) to interrupt the thymidylate biosynthesis pathway of cancer cells. The detrimental effect of SHMT1 knockdown on the disintegration of multienzyme complex resulted in cell cycle arrest and a decrease in cell's genomic DNA content, leading to enhanced apoptotic events in cancer cells. A reduction in tumor size was observed with constant SHMT1 suppression in xenograft mice. This study illustrates how silencing the SHMT1 expression inhibits cancer growth and the increased VB6 channeling for sustenance of cancer cells promotes VB6-coupled vector to elicit enhanced delivery of siSHMT1.

**Keywords:** Vitamin B6, Poly(ester amine), Membrane carrier, Gene transporter, Serine hydroxymethyl transferase 1, siRNA.

**Student number:** 2011-31353

## *Objectives of the Dissertation*

---

The research study aims at designing a polymer-based non-viral cationic vector with innocuous profile and capable of enhancing cellular uptake in cancer cells to find its application in cancer gene therapy. The first objective of the dissertation is to develop vitamin B6-coupled vector that demonstrate high delivery efficacy in cancer cells together with endosomal escape and degradation properties to ensure efficient transfection activity. In order to overcome the major intracellular trafficking barriers, mechanistic investigation of the vector as to how it modulates the uptake in cancer cells and enhances transgene expression becomes the second objective to study. The final goal is to explore the cancer treatment strategy using RNAi technology to knockdown the function of a VB6 dependent enzyme involved in some vital function of cancer progression.

Chapter 1 of the dissertation is a detailed introduction to the broad field of gene therapy describing its history, limitations, applications, criteria,

strategies, clinical trials, present progress and future prospective. The treatment strategies are addressed mainly in relation to cancer therapeutics.

Chapter 2 focuses on the development of vitamin B6-coupled poly(ester amine) (VBPEA) gene transporter with each component of the vector explaining its specific intended function while delivering the DNA in the cancer cells. VB6 is attached to the branches of the polymer backbone to increase its affinity towards cancer cells; the PEI 1.2 kDa polymer ensures its non-cytotoxic behavior and endosomal escape capability, and finally the ester linkages between the polymer fragments incorporate degradability into the vector.

In chapter 3 the mechanism of enhanced uptake in cancer cells, endocytosis routes of the vector and the role of VB6 in increasing the overall transfection efficiency of the polymer is addressed.

Chapter 4 throws light on the use of RNAi technology in cancer treatment. It illustrates the silencing efficiency of VBPEA using various marker siRNAs in cancer cells.

Chapter 5 elaborates the importance on ceasing the DNA synthesis machinery of the cancer cells in order to stop their growth and proliferation. Emphasis is given on the central role of serine hydroxymethyltransferase 1 (SHMT1) enzyme (VB6 dependent enzyme) in DNA biosynthesis and how it can be used as a strategy to control the cancer cell cycle and progression. The chapter demonstrates nucleotide biosynthesis arrest in cancer cells by silencing the SHMT1 function via SHMT1 siRNA efficiently delivered by VBPEA in vitro and in vivo. The silencing effect on the DNA synthesis and cell cycle of the cancer cells and on the tumor growth is precisely illustrated.

# *CONTENTS*

---

Abstract.....	i
Objectives of the Dissertation.....	v
Contents.....	viii
List of Tables .....	xii
List of Figures.....	xiii
List of Abbreviations .....	xviii
<b>Chapter 1. Introduction to Gene Therapy .....</b>	<b>1</b>
1.1 Historical background of gene therapy .....	1
1.2 Current scenario of gene therapy .....	9
1.3 Cancer gene therapy .....	12
1.4 Gene delivery vectors.....	20
1.5 Need for the non-viral vector mediated gene delivery .....	20
1.6 Non-viral gene delivery systems .....	22
1.7 Biological barriers for cellular uptake.....	24
1.8 Criteria for successful cancer gene therapy.....	31

1.9	Strategies to use nanotechnology in cancer gene therapy .....	32
1.10	Objective of the study .....	37
1.11	Conclusion.....	37

## **Chapter 2. Synthesis & Transfection Efficiency of**

### **Vitamin B6-Coupled Poly(ester amine) Gene Transporter**

.....	<b>39</b>	
2.1	Introduction .....	39
2.2	Materials and Methods .....	43
2.3	Results .....	52
2.4	Discussion .....	71
2.5	Conclusion.....	73

## **Chapter 3. Membrane Transport Mechanism of**

### **Vitamin B6-Coupled Poly(ester amine)..... 74**

3.1	Introduction .....	74
3.2	Materials and Methods .....	75
3.3	Results .....	81
3.4	Discussion .....	92
3.5	Conclusion.....	97

<b>Chapter 4. Gene Silencing Efficiency of Vitamin B6-Coupled Poly(ester amine)</b> .....	<b>99</b>
4.1 Introduction .....	99
4.2 Literature Review .....	101
4.3 Materials and Methods .....	105
4.4 Results .....	113
4.5 Discussion .....	122
4.6 Conclusion.....	122
<b>Chapter 5. Nucleotide Biosynthesis Arrest by Silencing SHMT1 Function</b> .....	<b>124</b>
5.1 Introduction .....	124
5.2 Literature Review .....	129
5.3 Materials and Methods .....	151
5.4 Results .....	166
5.5 Discussion .....	190
5.6 Conclusion.....	193
<b>Chapter 6. Summary</b> .....	<b>195</b>
References .....	198

List of Publications .....	236
Acknowledgement .....	238

# *LIST OF TABLES*

---

- Table 2.1 Characterization of VBPEA polymer
- Table 4.1 siRNA sequences of GFP, luciferase and scrambled
- Table 5.1 Purity of genomic DNA
- Table 5.2 Tumor volume measurements during the one month treatment in xenograft mice

# *LIST OF FIGURES*

---

Figure 1.1 Timeline highlighting important milestones in gene therapy

Figure 1.2 Statistics of the number of gene therapy clinical trials

Figure 1.3 Current scenario of the phases of gene therapy clinical trials

Figure 1.4 Graphical representation of the various diseases addressed by gene therapy

Figure 1.5 Schematic representation of immunotherapy

Figure 1.6 Schematic representation of oncolytic virotherapy

Figure 1.7 Schematic representation of gene transfer therapy

Figure 1.8 Various gene transporting vectors used in clinical trials

Figure 1.9 Intracellular barriers for non-viral gene transfer

Figure 1.10 An artistic representation depicting the proton sponge hypothesis

Figure 1.11 Nanotechnological strategies for diagnosis, treatment and targeting of cancer cells

Figure 2.1 Synthesis scheme of vitamin B6-coupled poly(ester amine) (VBPEA)

Figure 2.2  $^1\text{H-NMR}$  spectra of VBPEA, PEA, and VB6 in  $\text{D}_2\text{O}$

Figure 2.3 Electrophoretic mobility shift assay of VBPEA/DNA polyplexes

Figure 2.4 Dynamic light scattering microscopic measurements

Figure 2.5 Particle size in various percent serum concentrations

Figure 2.6 EF-TEM images

Figure 2.7 Cytotoxicity of VBPEA/DNA complexes

Figure 2.8 *In vitro* transfection studies of VBPEA/DNA complexes

Figure 2.9 Percent transfection efficiency measured by FACS

Figure 2.10 FACS studies showing transfection efficiency of VBPEA polyplexes

Figure 2.11 Transfection of VBPEA/DNA complexes in presence of serum

Figure 2.12 *In vivo* luciferase protein expressions

Figure 3.1 Carrier-mediated uptake of VBPEA

Figure 3.2 Confocal microscopic images

Figure 3.3 VB6 coupling enhances cellular uptake

Figure 3.4 Uptake study of VBPEA/pGL3 by primary cells vs. cancer cells

Figure 3.5 Cytotoxicity of in 16HBE (human) and LA4 (mouse) normal lung cell lines

Figure 3.6 Effect of caveolae- and clathrin- endocytic inhibitors on transfection

Figure 3.7 Bafilomycin A1 studies

Figure 3.8 Diagrammatic representation of VBPEA/DNA uptake mechanism

Figure 4.1 Mechanism of RNA interference

Figure 4.2 Physicochemical characterization of VBPEA/siRNA complexes

Figure 4.3 Cytotoxicity of VBPEA/siRNA complexes

Figure 4.4 Study of VBPEA<sup>T</sup>/siRNA nanoplex uptake and degradation

Figure 4.5 Cytotoxicity measurements of VBPEA<sup>T</sup>/siRNA

Figure 4.6 GFP silencing efficiency of VBPEA/siRNA complexes

Figure 4.7 Luciferase silencing efficiency of VBPEA/siLuc polyplexes

Figure 5.1 Schematic illustration of silencing events after the delivery of VBPEA/siSHMT1

Figure 5.2 Metastasis shown in the bone marrow from carcinoma of prostate gland

Figure 5.3 Checkpoints and inputs of regulatory information to the cell cycle control system

Figure 5.4 Progression of benign tumor to malignant tumor

Figure 5.5 The stages of progression in cancer development

Figure 5.6 A single mutation is not enough to cause cancer

Figure 5.7 Photograph of cells collected from the surface of uterine cervix

Figure 5.8 The basic structure of nitrogenous bases and their synthetic requirements

Figure 5.9 Thymidylate synthase cycle

Figure 5.10 Reaction catalyzed by SHMT

Figure 5.11 SHMT1 gene silencing efficiency of VBPEA/siSHMT1 complexes

Figure 5.12 Western blot analysis of SHMT1

Figure 5.13 SHMT1 gene silencing efficiency is enhanced by VTC-mediated endocytosis

Figure 5.14 Effect of SHMT1 knockdown on the proliferative behavior of A549 cells

Figure 5.15 SHMT1 knockdown onsets the apoptotic events in A549 cells

Figure 5.16 SHMT1 knockdown affected DNA synthesis

Figure 5.17 SHMT1 knockdown resulted in cell cycle arrest

Figure 5.18 FACS analysis

Figure 5.19 SHMT1 knockdown decreased the total genomic DNA content

Figure 5.20 *In vivo* bioimaging

Figure 5.21 Reduction of tumor size in xenograft mice

Figure 5.22 Immunohistochemistry

Figure 5.23 *In vivo* TUNEL assay

# *LIST OF ABBREVIATIONS*

---

ATP	Adenosine triphosphate
bPEI	Branched polyethyleneimine
CPP	Cell-penetrating peptides
DHFR	Dihydrofolate reductase
DLS	Dynamic light scattering microscope
DMSO	Dimethyl sulphoxide
DNA	Deoxyribonucleic acid
EDTA	Ethylenediaminetetra acetic acid
EMA	European Medicines Agency
EMSA	Electrophoretic mobility shift assay
EU	European Union
GFP	Green fluorescent protein
GPC	Gel permeation chromatography
HGPRT	Hypoxanthine-guanine phosphoribosyl transferase
HMW	High molecular weight
LMW	Low molecular weight

MTT	3-(4, 5-Dimethyl thioazol-2-yl)-2, 5-diphenyl tetrazolium bromide
NaCNBH <sub>4</sub>	Sodium cyanoborohydride
NLS	Nuclear localization sequence
NMR	Nuclear magnetic resonance
NPCs	Nuclear pore complexes
PNA	Peptide nucleic acid
RGD	Arginine-Glycine-Aspartic acid peptide
RNA	Ribonucleic acid
RNAi	RNA interference
SDS-PAGE	Sodium dodecyl sulfate polyacrylamide gel electrophoresis
SHMT	Serine hydroxymethyltransferase
siRNA	Small interfering ribonucleic acid
siScr	Scrambled small interfering ribonucleic acid
TEM	Transmission electron microscope
TILs	Tumor-infiltrating lymphocytes
TRITC	Tetramethylrhodamine isothiocyanate
TYMS	Thymidylate synthase
VB6	Vitamin B6

# CHAPTER 1

## *Introduction to Gene Therapy*

---

### **1.1 Historical background of gene therapy**

Gene therapy is the introduction of an exogenous nucleic acid with therapeutic potential into the target cell to induce desirable cellular response for the treatment of inherited or acquired diseases [1]. Figure 1.1 is highlighting some of the milestones during the history of gene therapy. The concept of gene therapy had its beginning since 1928 when Frederick Griffith first described the transformation in pneumococcus bacteria [2]. In his study he reported that the non-virulent R form of Type I pneumococcus when mixed with heat-inactivated virulent S form of Type II pneumococcus was transformed into virulent S form and developed infection. Since the original virulent S form of Type II pneumococcus was heat-inactivated, he also concluded that R form must have also transformed from Type I to Type

II. With the aim to identify the substance that was responsible for transformation, Avery and McCarty in 1944 demonstrated that it was deoxyribonucleic acid (DNA) which was transferred and caused transformation [3]. Later in 1952, Joshua Lederberg together with Norton Zinder uncovered another mechanism of genetic transfer in bacteria in addition to transformation, termed as transduction [4] where the genetic material was transferred between bacterial strains not in the form of pure DNA but instead bacteriophage carried DNA from one bacterium to another. This fundamental discovery explained how bacteria of different species could gain resistance to the same antibiotic very quickly with phage mediated transfer of genetic material. This phenomenon instigated the research of its potential benefit as a tool for transferring hereditary traits and was soon extended to eukaryotic viruses also.

It was then known that cells are able to take up foreign DNA. However, there was no successful documentation of heritable transformation of a biochemical trait, until 1962, when Waclaw Szybalski while doing

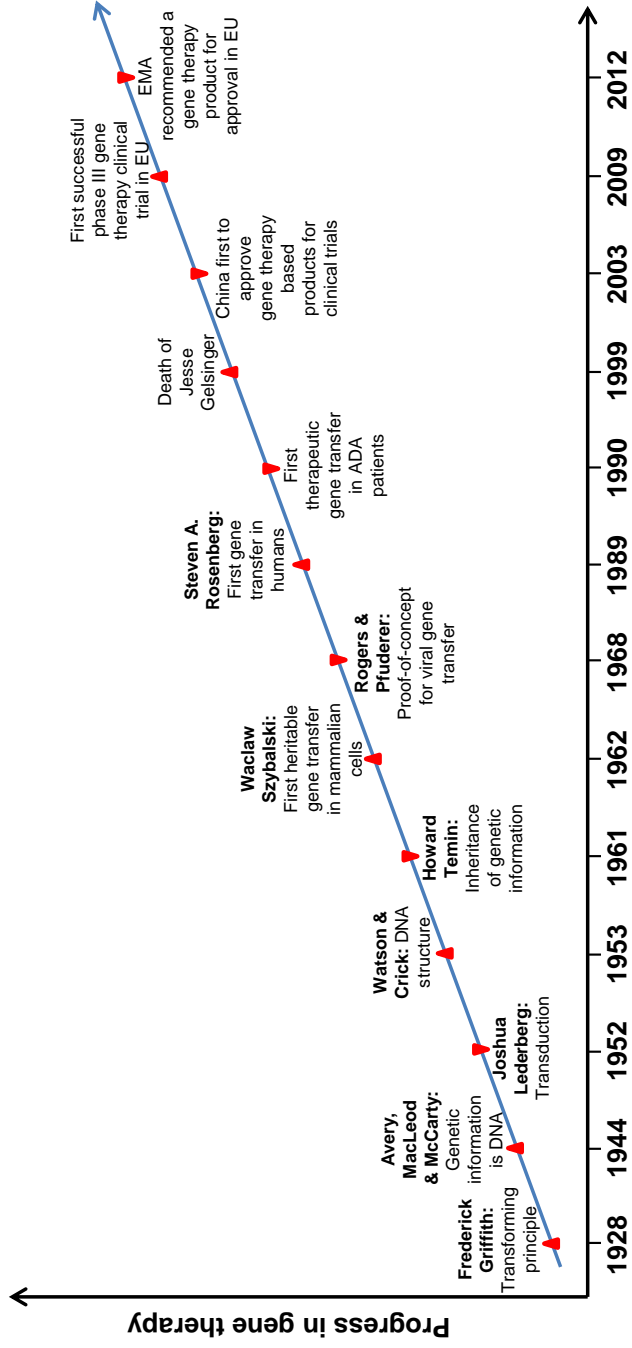


Figure 1.1. Timeline highlighting some of the important milestones towards the progress of gene

pioneering work on lambda phages published his study “DNA-mediated heritable transformation of a biochemical trait” [5], wherein cells that had been genetically modified could be selected based on their phenotype. In brief, cells need dihydrofolate reductase (DHFR) for the de novo synthesis of nucleic acids. When DHFR is inhibited by aminopterin the cell uses an alternate salvage pathway, which utilizes the enzyme hypoxanthine-guanine phosphoribosyl transferase (HGPRT) that catalyzes the conversion of hypoxanthine to inosine monophosphate and guanine to guanosine monophosphate. Based on this knowledge, Szybalski used derivatives of the human bone marrow cell line, whereof some were HGPRT<sup>(+)</sup> and some HGPRT<sup>(-)</sup>. When these cells were grown in a cocktail of aminopterin, hypoxanthine and thymidine (i.e. the HAT medium), only the HGPRT<sup>(+)</sup> cells were able to synthesize DNA and survived. The next Szybalski did that he transformed HGPRT<sup>(-)</sup> cells with the DNA isolated from HGPRT<sup>(+)</sup> cells and observed that HGPRT<sup>(-)</sup> cells then did not die in HAT medium. Hence, Szybalski’s work became the first documented evidence of heritable gene transfer in mammalian cells. It was now demonstrated that a genetic defect could be rescued by transferring functional DNA

from a foreign source and that it could be inherited in the daughter cells. A decade later the same method became key to a Nobel-winning invention of monoclonal antibodies [6].

The first step towards gene therapy was laid by Howard Temin when he discovered that viruses which were able to transfer genetic material were also capable of infecting with specific inheritable genetic mutations through chromosomal insertion [7]. This observation unveiled the conundrum that genetic information could flow only from DNA to RNA; instead the genetic information could also flow from RNA to DNA. It became apparent for the potential of viruses as a tool in delivering desirable genes into cells of interest which gave rise to a new approach in genetic engineering for treating genetic diseases. An initial proof-of-concept of virus mediated gene transfer was demonstrated by Rogers et al. where they used tobacco mosaic virus as a vector vehicle to introduce a polyadenylate stretch to the viral RNA [8]. In 1973, they performed the first direct human gene therapy trial by using the wild-type Shope papilloma virus, believed to encode the gene for arginase activity. The virus was introduced into two girls suffering

from a urea cycle disorder with intention to transfer the arginase gene [9, 10]. Unfortunately, the trial failed which later was revealed after genome sequencing that Shope papilloma virus genome actually does not encode an arginase.

In 1982, Martin Cline successfully inserted foreign genes into mouse bone marrow stem cells using recombinant DNA and that these modified cells were further able to partially repopulate the bone marrow of other mice [11]. Encouraged by these results, in 1990, Cline became the first to attempt this therapeutic approach of using recombinant DNA in humans for treating patients suffering from  $\beta$ -thalassemia. Such patients suffer from severe and life-threatening anaemia due to a genetic defect in their beta-globulin gene that deficit them from producing beta-globulin portion of haemoglobin protein. Cline initiated the therapy in two such patients, though without the approval from the UCLA Institutional Review Board.

The first officially approved clinical trial by the Recombinant DNA Advisory Committee (RAC) in December 1988 was performed by S.A. Rosenberg to track the movements of modified tumor-infiltrating

lymphocytes (TILs) in cancer patients [12]. He already succeeded in demonstrating that TILs modified with interleukin-2 treatment resulted in regression of metastatic melanoma in some patients [13]. Before performing the clinical trials, he initially tested the effectiveness of genetically modified TILs against tumors by introducing a retroviral mediated marker gene (bacterial NeoR gene) and studied their distribution and survival in circulation, lymph nodes or at tumor sites [12, 14, 15]. Based on this initial trial he received approval for treating two patients with advanced melanoma. He used ex vivo modified TILs expressing tumor necrosis factor (Rosenberg, 1992) and re-administered back into the patients which showed no tumor growth at the injection site and no viable tumor cells were evidenced in the surgically resected sections after 3 weeks of injection [15]. At the same time of Rosenberg's studies, Michael R. Blaese was the first to conduct gene therapy using a therapeutic gene [16]. After the approval by FDA in 1990 to perform gene therapy trials in humans, two adenosine deaminase deficient (ADA-SCID) children, were treated with their own ex vivo modified white blood cells to express the normal gene for

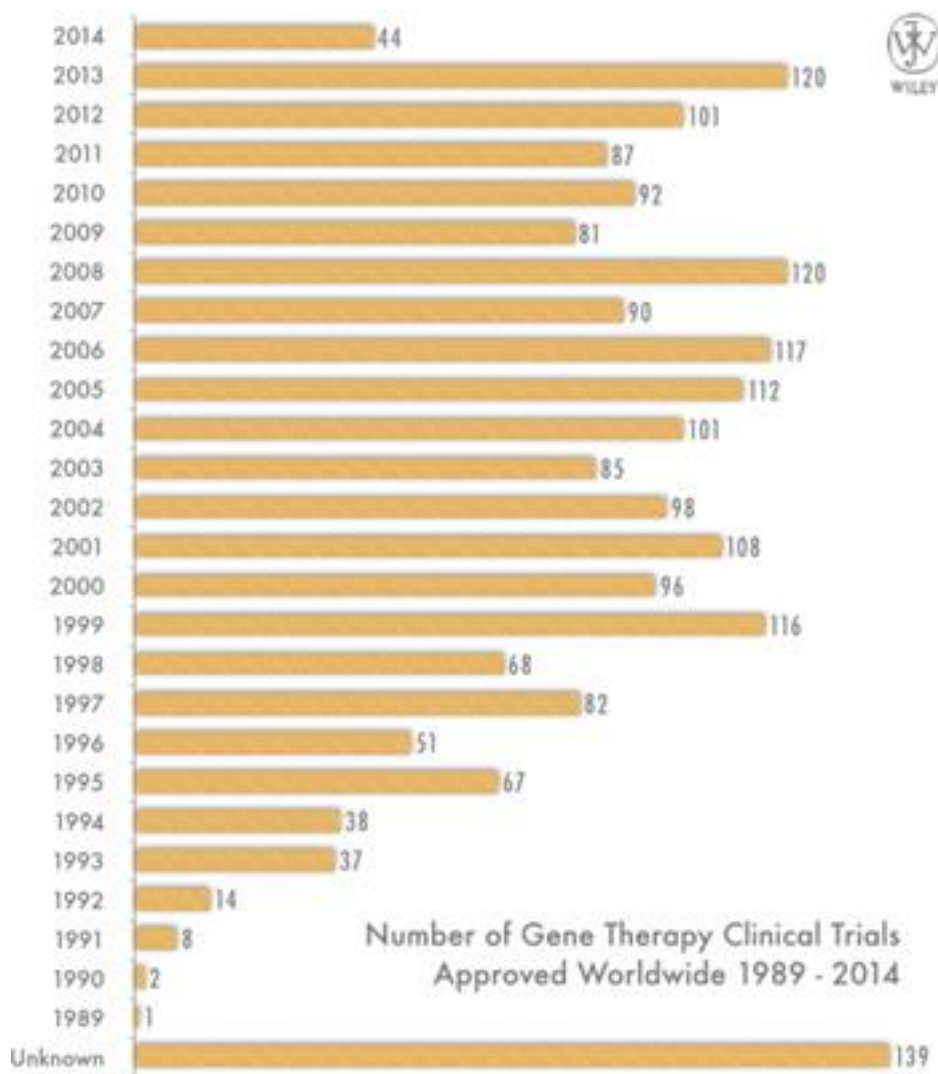


Figure 1.2. Statistics of the number of gene therapy clinical trials approved worldwide until 2014. Adopted from Ref [17].

making adenosine deaminase. After this ADA-SCID trial was also started in the EU [18] and laid the pavement for further trials to treat several other diseases with higher gene transfer efficiency (direct in vivo gene delivery) [19], until the tragic death of Jesse Gelsinger [20]. With Gelsinger's death the worst scenario of viral mediated gene therapy became apparent when virus administration generated immediate immune response to result in multi-organ failure and death [20].

## **1.2 Current scenario of gene therapy**

China was the first country to approve a gene therapy based product for clinical use named Gendicine™ in 2003 [21, 22]. Two years later, China's State Food and Drug Administration (SFDA) granted permission for clinical use of another product, Oncorine™ [23]. In 2004, Cerepro® , developed by Ark Therapeutics Group plc, received permission for its commercial supplies for the first time in the EU as gene-based medicines and by 2008 it became the first adenoviral vector to complete phase III clinical trial [24]. In addition, promising results have been observed in recent gene therapy clinical trials for Leber's

congenital amaurosis [25],  $\beta$ -thalassemia [26, 27], X-linked severe combined immunodeficiency (SCID-X1) [28] and ADA-SCID [29], haemophilia B [27], Wiskott-Aldrich syndrome [30], metachromatic leukodystrophy [31], choroideremia [32], and HIV [33]. Finally, the EMA recommended for the first time a gene therapy product Glybera, originally developed by Amsterdam Molecular Therapeutics and now marketed by UniQure, for clinical approval in the EU on July 19th 2012 [34]. Figure 1.2 shows the number of gene therapy clinical trials approved worldwide from 1989 to 2014 [17]. Since 1999 the number of clinical trials has increased worldwide to make gene therapy as the future treatment procedure and sooner or later be part of the standard care for a variety of genetically linked diseases. However, the majority of gene therapy clinical trials are in phase I, phase II or phase I/II trials [17, 35] to determine the maximum tolerable doses of gene delivery vectors and to identify the transgene products and the activity of the new agents in patients. Phase III, phase IV and single subject gene therapy clinical trials are limited but work is in progress to develop and translate this technique into a clinical reality (Figure 1.3).



Figure 1.3. Current scenario of the phases of gene therapy clinical trials.

Adopted from Ref [17].

### **1.3 Cancer gene therapy**

Contrary to the belief that only inherited single-gene disorders could be possibly treated with gene therapy [36], it was later realized in 1980s that cancer is also a disease of complex gene disorders where the technology could find its widespread application. After the first clinical trial for cancer gene therapy by Steven A. Rosenberg and R. Michael Blaese's groups [12] in 1991 a remarkable progress have been made in the past two decades in an attempt to meet the specific therapeutic needs and replace the conventional treatments with far reaching negative side effects. To date, 2076 gene therapy clinical trials have been approved for treating various diseases (Figure 1.4) [17], out of which cancer diseases outscores with 64.1% of maximum number of clinical trials.

The field of cancer gene therapy treatments can be broadly categorized into immunotherapy, oncolytic virotherapy and gene transfer.

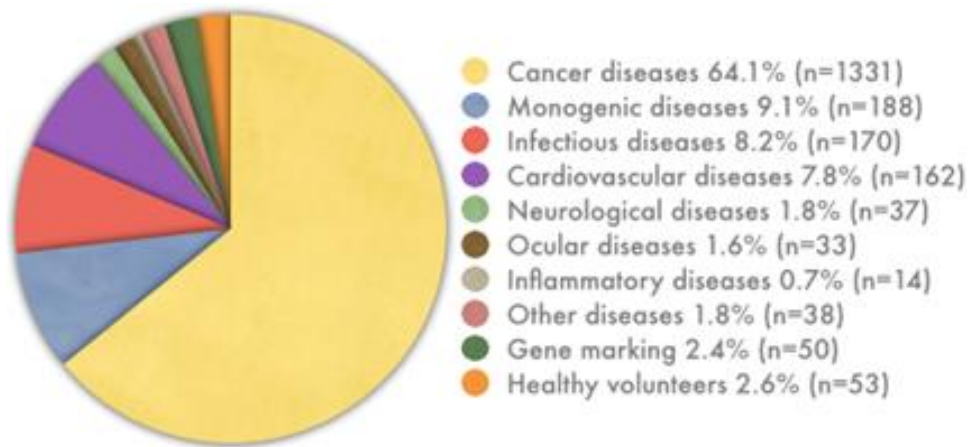


Figure 1.4. Graphical representation of the various diseases addressed by gene therapy in clinical trials, most of which were performed to treat cancer and soon became the major interest [17].

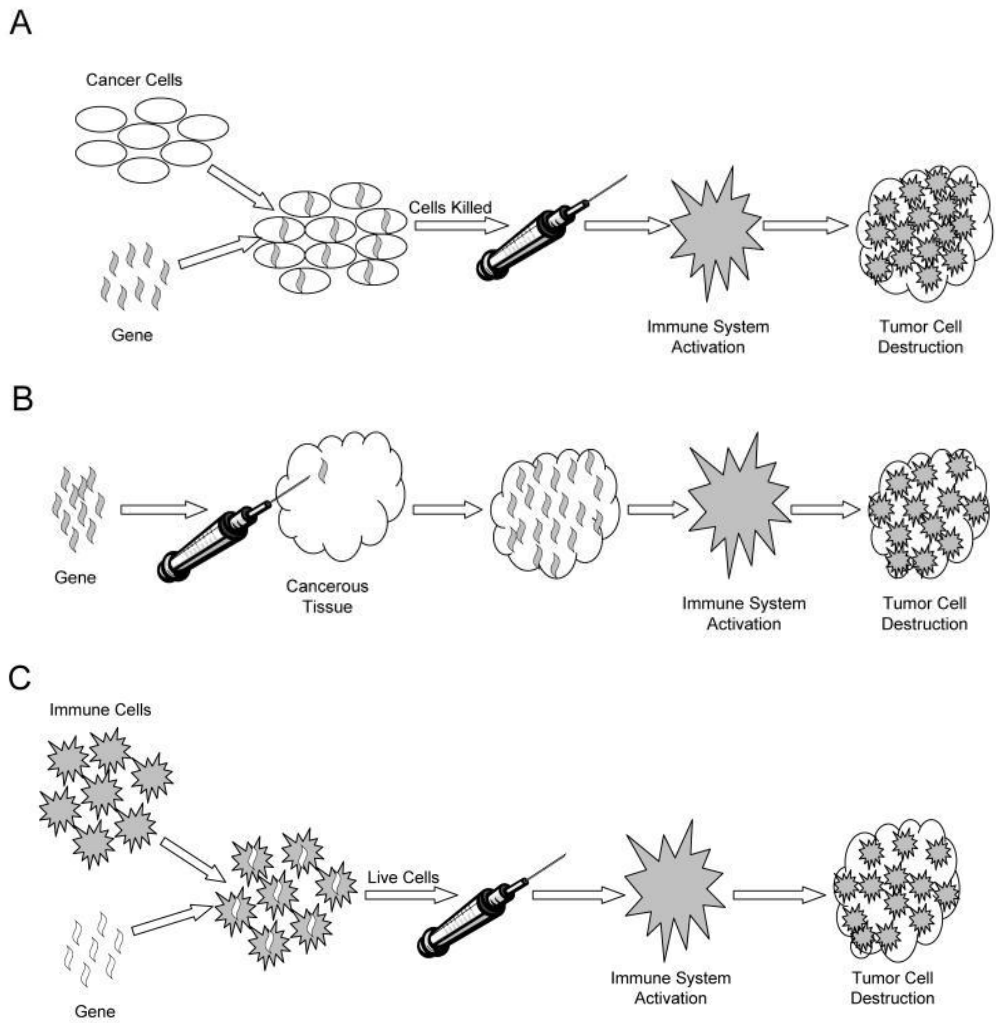


Figure 1.5. Schematic representation of immunotherapy. (A) Immunotherapy with altered cancer cells. (B) Immunotherapy with genes delivered in vivo. (C) Immunotherapy using patient's altered immune cells. Adopted from Ref [37].

**1.3.1. Immunotherapy:** Immunotherapy means to boost one's immune system to target and destroy cancer cells, but limited success has been achieved with traditional immunotherapy, as cancer cells tend to evolve mechanisms that evade immune detection [37]. Currently recombinant cancer vaccines are created to make the cancer cells more recognizable to patient's immune system by the addition of one or more genes (cytokine genes) that produce highly antigenic and immunostimulatory cellular debris. These cellular contents are incorporated into a vaccine (Figure 1.5 A) [38]. Alternatively, immunostimulatory genes (cytokines) can be delivered to the tumor in vivo which upon expression will unmask the cells from immune evasion (Figure 1.5 B) [39]. Another immunotherapy strategy is to directly alter the patient's immune system by adding a tumor antigen or other stimulatory gene into mononuclear circulating blood cells or bone marrow gathered from the patient in order to sensitize it to the cancer cells (Figure 1.5 C) [40].

**1.3.2. Oncolytic virotherapy:** In this strategy genetically engineered viruses are used to target and destroy cancer cells through the propagation of the virus, expression of cytotoxic proteins and cell lysis while remaining innocuous to the rest of the body cells (Figure 1.6)

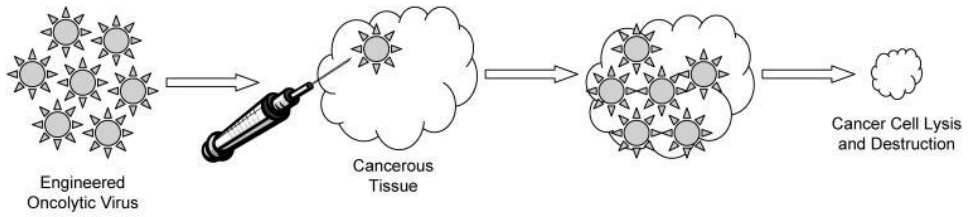


Figure 1.6. Schematic representation of oncolytic virotherapy. Adopted from Ref [37].

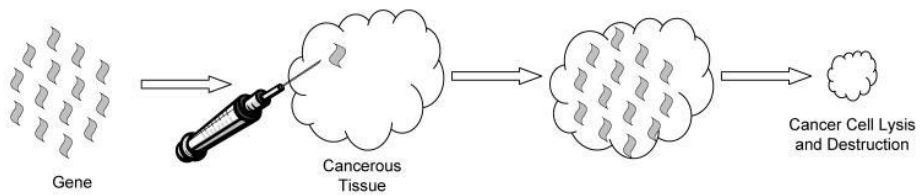


Figure 1.7. Schematic representation of gene transfer therapy. Adopted from Ref [37].

[41]. However, several stumbling blocks for oncolytic virotherapy in humans includes the clearance of viral particles before its infection in cancer cells by patient's immune system and the use of replication competent viral particles often calls for increased safety precautions, making clinical trials more expensive and cumbersome. **1.3.3. Gene transfer:** This is a radically new treatment paradigm which involves introduction of a foreign gene into the cancer cell or surrounding tissue. Genes including suicide genes, antiangiogenesis genes and cellular stasis genes are inserted into the cancer cell chromosome using either viral or non-viral gene delivery vectors, depending upon the desired specificity and length of time required for gene expression (Figure 1.7) [42]. However, this technique requires efficient delivery of therapeutic gene to the target cells without getting integrated into unwanted cell types, such as reproductive tissues.

In a summary, the strategies that have been designed and tested for cancer gene therapy are listed below [17, 35]:

1. The tumor suppressor genes such as p53 hold a check on the controlled division of cells by inducing apoptosis [43]. When

its function becomes awry, cancer establishment and progression could be controlled by replacing the defective tumor suppressor genes with wild type;

2. oncogenes e.g. ras transformed from its proto-oncogenic forms can be inactivated to block its expression;
3. drug sensitivity genes could be delivered that can convert a pro-drug to a cytotoxic drug upon their expression in cancer cells;
4. stimulation of immune responses against cancer cells; or
5. multi-drug resistance genes could be delivered to normal cells so that high chemotherapeutic doses could be given to cancer cells.

Specifically introducing these genetic materials at the target site could become a promising technology for the treatment of cancer, but targeting tumor cells and an appropriate gene transport vector are pre-requisites, the lack of which has rendered this approach clinically less effective.

### Vectors Used in Gene Therapy Clinical Trials

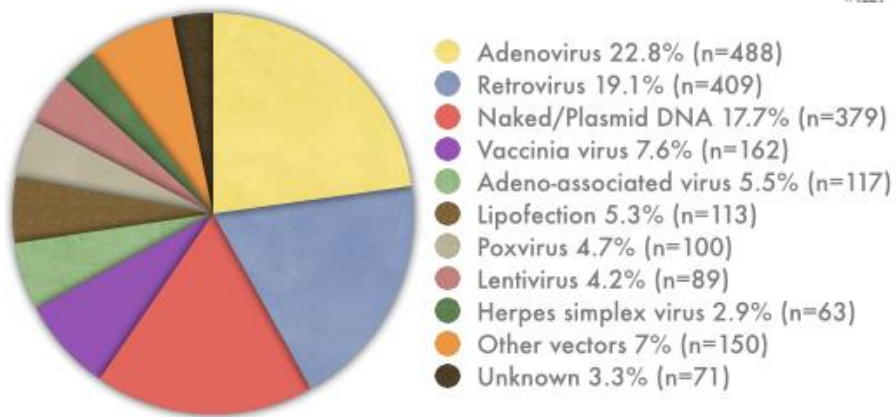


Figure 1.8. Various gene transporting vectors used in clinical trials. Adenovirus and retrovirus are most commonly used viral vectors in clinical trials. Non-viral mediated gene transfer, including naked DNA and liposomes has occupied 24% of all the clinical trials so far. Adopted from Ref [17].

## **1.4 Gene delivery vectors**

The various strategies to deliver exogenous, functional genes to cells could promise for the future treatment of a variety of human diseases, provided that these delivery methods are safe, efficient, and selective. To ensure efficient delivery of genes various vectors are being used in clinical trials including both viral and non-viral vectors, each with its own characteristic advantages and disadvantages. 42% of the clinical trials used adenovirus and retrovirus due to their high gene transfer efficiency and 24% of them used non-viral vectors chiefly considering the safety concerns in therapy (Figure 1.8). Viral vector mediated gene delivery is referred to as transduction while that mediated with non-viral vector is known as transfection.

## **1.5 Need for the non-viral vector mediated gene delivery**

Replication-defective recombinant viruses have considerable appeal in clinical use due to their natural ability to infect cells and delivering genes efficiently. However, these vectors do have significant practical

limitations. For instance, recombinant retroviruses do not transfer genes into non-replicating cells, though do so in culture cells and thus are generally inefficient *in vivo*. Due to the limited packaging capacity of many of these viruses large gene inserts cannot be delivered. In addition, the tropism of specific recombinant viruses can restrict their use. Some viral vectors can be cytotoxic by stimulating severe immune responses which was highlighted during the gene therapy treatment of an 18-year old young patient, Jesse Gelsinger, who died (1999) due to multiple organ failure as a result of the immune response against the infusion of genetically altered adenoviral vectors [20]. Moreover, non-pathogenic viral vectors might become activated following infection with wild-type or helper viruses and produce replication-competent recombinant virus [44], as evidenced in children with X-linked SCID who developed leukemia after receiving a retroviral gene therapy [45]. Because of primarily the safety concerns, the development of non-viral gene delivery vectors has received considerable attention. Moreover, non-viral vectors can be easily constructed and modified, scaled up for large production and show high gene carrying capacity.

## 1.6 Non-viral gene delivery systems

Non-viral systems include a variety of physical, non-infectious methods like calcium phosphate co-precipitation [46], liposomes [47], DEAE-dextran [48], microinjection [49], gene-particle bombardment [50], electroporation [51], ultrasound [52] and cationic polymers [53].

**1.6.1. Electroporation:** In this method electric pulses are applied across the cell membrane which creates transient membrane permeation due to trans-membrane potential difference. This destabilized membrane allows DNA insertion.

**1.6.2. Ultrasound:** This can be used to deliver ultrasound energy directly to an object and genes transport into cells can be achieved by the alteration of vascular permeability in a method called sonoporation.

**1.6.3. Gene-particle bombardment:** This method uses a gene gun for the direct injection of genes into the cell nucleus or other organelles. The payload used is a heavy metal particle coated with DNA.

**1.6.4. Cationic liposomes:** Cationic liposomes are synthetic vectors composed of lipid molecules with a positively charged head group. Liposomes do not encapsulate DNA, but instead the DNA becomes heavily condensed by cationic lipids that completely or partially cover the plasmid. Although it was initially believed that the lipid-DNA complexes fuse with the cell membrane and deliver DNA into the cytoplasm, it is now suggested that the DNA uptake requires endocytosis.

**1.6.5. Cationic polymers:** Cationic polymers are synthetic vectors which form condensed complexes (polyplexes) with nucleic acid due to electrostatic interactions between positive charge of polymers and negative charge on nucleic acid. This condensation results in nanosized particles which facilitate the delivery of genes into the cell. It is shown that the degree of condensation of the complexes is correlated with the level of transgene expression. Complexes measuring 80–100 nm in diameter are most effective for gene transfer [54]. Moreover, the use of polymeric vectors provides flexibility in their design, modification and synthesis for large scale production. Cationic molecules, such as

polymethacrylates [55], polypeptides [56, 57], celluloses [58], chitosan [59, 60], dendrimers including polyamidoamine or PAMAM dendrimers [61, 62], poly(vinyl pyrrolidone) [63], and polyamine polymers [64] are the most widely researched polymeric agents for their use in delivering genes. The excess positive charge present on their nanosized complexes in aqueous solutions lead to the interaction with anionic cell membranes and subsequent uptake into target cells. An effective gene delivery vector then disassembles to release the nucleic acid near nucleus to which it protected against the intracellular degradation [65]. Cyclodextrin based polymer has been used by Davis et al in phase I clinical trials in 2009 for delivering siRNA in patients with solid tumor [66].

## **1.7 Biological barriers for cellular uptake**

Non-viral gene therapy vectors which include naked DNA, cationic lipid/DNA complexes (lipoplex), polymer/DNA complexes (polyplex) or combinations of lipids and polymers are highly desirable tools for delivering genes into cells. However, they need to cross the various cellular barriers for trafficking of payload up till the nucleus (Figure

1.9). (i) The vector must traverse the plasma membrane, (ii) then escape the endosome and pass through the dense cytoskeletal network, (iii) and finally enter the nucleus for the desired transgene expression. Since the non-viral vectors lack the innate mechanisms to deliver and express the genetic material they carry, much work needs to be done at characterizing them to overcome these barriers.

**1.7.1. Plasma membrane:** Plasma membrane represents the first barrier for cellular uptake. Naked DNA is not able to associate efficiently with the cell membrane and get internalized due to the negative charge density present on both the DNA and the membrane [67]. Cationic polymers circumvent this problem by neutralizing the negative charge of DNA and forming nanosized polyplexes, thereby associating with the plasma membrane due to electrostatic interactions which is mediated by heparin sulfate proteoglycans on the cell surface. This trigger endocytosis of the polyplexes and nucleic acid gains entry inside the cell. Endocytosis leads to invagination of the plasma membrane at specific domains characterized by lipid raft/protein depending on the chosen endocytic pathways to form endocytic

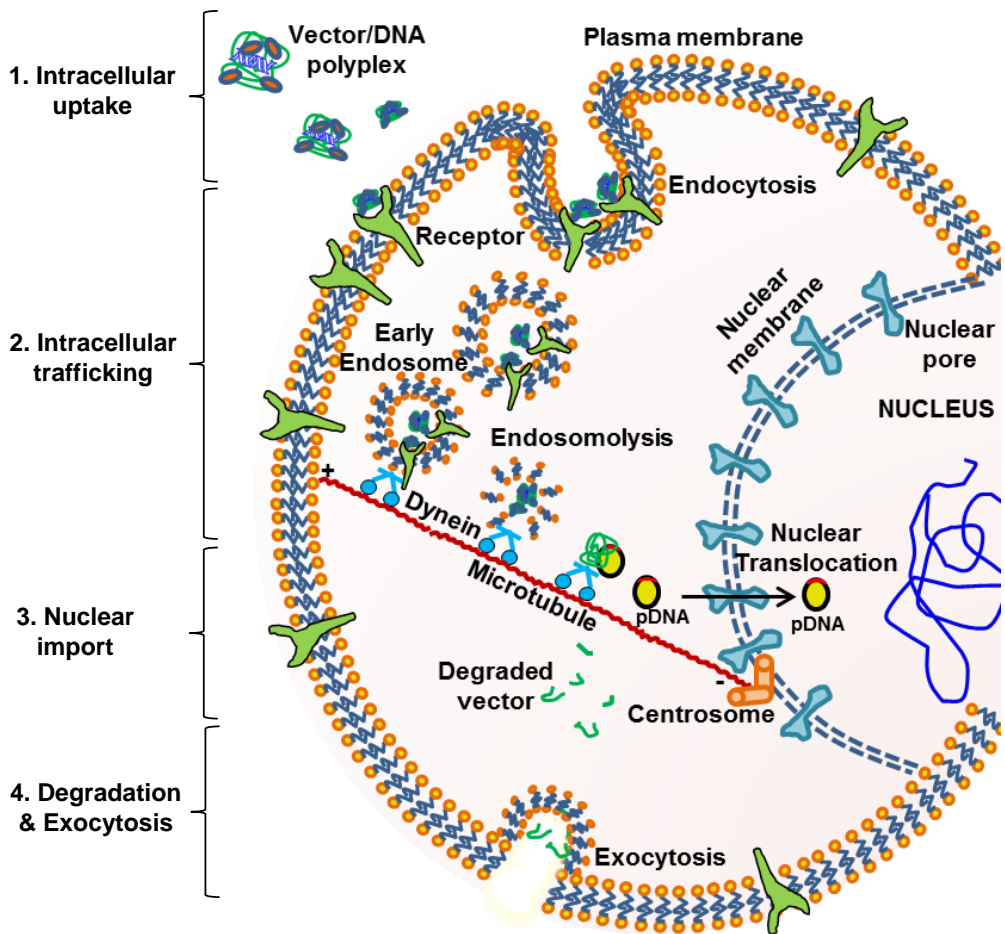


Figure 1.9. Intracellular barriers for non-viral gene transfer. Depiction of the journey of polyplexes after crossing the cellular uptake barriers, unloading the nucleic acid in cytoplasm, nuclear translocation, and transgene expression in the cell nucleus.

vesicles containing the polyplexes. The choice of endocytic pathways such as clathrin-mediated endocytosis, clathrin-independent endocytosis, caveolae-mediated endocytosis, macropinocytosis and phagocytosis [68-70] largely depends on the size of particle and the cell type [71, 72]. It was shown by Rejman et al. that the particles < 200 nm were taken up by the clathrin-dependent pathway, whereas larger particles (200-500nm) entered through another caveolae-mediated endocytosis [71]. Particles > 500 nm undergo micropinocytosis [73]. Alternatively, cell-penetrating peptides (CPPs) can be used to facilitate cell entry in an endocytosis-independent manner [74].

**1.7.2. Endosomal release and cytoplasmic trafficking:** The early endosomes carrying the polyplexes mature to late endosomes in ~ 5 min and is accompanied by a decrease in pH from 7.0 to 5.9. After about 30 min there is an additional pH drop from 6.0 to 5.0 when the late endosomes convert into lysosomes with aim to degrade the vesicular material [69]. Thus, escaping the endosomal trapping before its maturation into lysosomes becomes necessary for the polyplexes and becomes a rate-limiting step in the transgene expression.

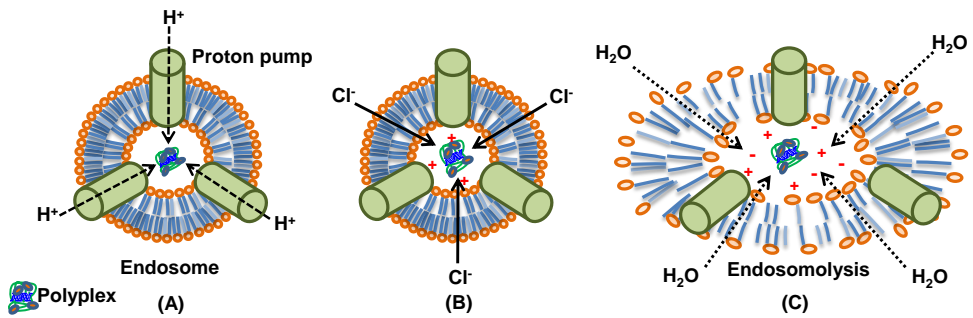


Figure 1.10. An artistic representation depicting the proton sponge hypothesis. (A) Accumulation of proton into endosomes by proton pumps; (B) the protons are accompanied with influx of chloride ions; and (C) builds up an osmotic pressure of water that eventually ruptures the endosomal membrane.

Degradation in the lysosomal acidic environment of the polyplexes can be avoided by employing the proton-sponge effect [75] or by incorporation of fusogenic and pore-forming peptides to the polymers [76]. The polyplexes of polyamidoamine (PAMAM) and pEI [77] can disrupt the endosomes by proton sponge mechanism (Figure 1.10) due to the presence of protonable amines in the polymer branches. PEI has amino nitrogen at every third atom which can be protonated within the acidifying endosomes to impart it a very high buffering capacity. Proton accumulation consequently leads to influx of chloride ions thereby resulting in osmotic swelling and subsequent lysis of endosome to release the entrapped components [75].

The released polyplex with bound nucleic acid is now exposed to cytoplasmic nucleases that can degrade the free nucleic acid. Although the condensed nucleic acids are protected against the nuclease degradation by the polymeric shield, it remains unprotected when once freed by the polymer [78]. Hence, it is of very importance that the polymer also dissociates the nucleic acid in the vicinity of nucleus so that the nucleic acid enters the nucleus before nuclease degradation.

Also the viscosity of cytoplasm poses another diffusional barrier for the mobility of macromolecules [79, 80]. It has been shown that the macromolecules utilize the microtubule network including the motor protein, dynein for its trafficking to the nucleus [81, 82]. A multiprotein complex mainly composed of transcription factors, is involved that bridges the interaction between the macromolecule and dynein and facilitates the movement of macromolecule along microtubules [83].

**1.7.3. Nuclear import:** The final physical barrier to transgene expression is the import of DNA into the nucleus. Nuclear trafficking of DNA from the perinuclear region into the interior of the nucleus largely depends on its size [84]. DNA fragments of size < 250 bp can enter the nucleus by passive diffusion through nuclear pore complexes (NPC), while larger fragments of DNA up to 1 kb need active transport which is a slow and highly inefficient process [82]. Several studies have shown that transfected DNA enters the nucleus during mitosis phase of cell division due to the breakdown of nuclear envelope [85], which could be the case for untroubled DNA entry in the nucleus of fast dividing cancer cells. In case of non-dividing cells the DNA can be

attached with single or multiple nuclear localization sequences (NLS) to stimulate its nuclear entry and augment transgene expression [86].

## **1.8 Criteria for successful cancer gene therapy**

Successful cancer gene therapy depends upon the ability of the vector to specifically target cancer cells, enter the cell and obtain sufficient levels of gene expression.

The following requirements should be fulfilled by an ideal delivering vector for efficient cancer gene therapy.

1. Safe to administer without generating immunogenicity,
2. should be inert to avoid causing any associated diseases,
3. large therapeutic gene carrying capacity,
4. protecting the therapeutic molecule against degradation during its voyage to the nucleus,
5. specifically target the cancer cells without harming the normal body tissues,
6. increase the cellular uptake for transgene expression, and
7. Its self-degradation after delivering the therapeutic molecule to

avoid cytotoxicity and detection by immune system.

Non-viral vectors fulfill most of the above mentioned criteria but usually at the expense of lower gene transfer efficiency than viral vectors. In addition, they result in short-lived expression and generally lack specificity making them difficult for delivering genes in vivo. However, if they can be perfected to a dependable and efficient vehicle for targeted gene delivery in vivo, will lead to further improvements in the overall technology and emerge as the future treatment procedure.

## **1.9 Strategies to use nanotechnology in cancer gene therapy**

The unique challenges for cancer treatment include their small size, high multiplicity and metastasis to diverse organs during advanced stages of cancer. Nanoparticles have many potential benefits for diagnosing and treating cancer, including the ability to transport therapeutic molecules to cancer sites, as well as targeting specific cell populations with erroneous cellular functions. Thus, integrating engineering sciences with cancer biology may expand the capabilities

of nanotechnology-based tools in targeting, detection and particle trafficking for treating cancer. Although nanotherapeutics have reached the clinic, for example, liposome-encapsulated doxorubicin (doxil) [88], protein nanoparticles containing paclitaxel (abraxane) [89], iron oxide nanoparticles (ferumoxytol) [90], we expect that future generation nanotherapeutics will ensure new capabilities in targeting and early detection of diseased cancer sites.

Nanomaterial-based therapeutic approaches are currently under huge development for the strategies to diagnose, treat and target cancer (Figure 1.11).

**1.9.1. Diagnosis:** Stimulus, such as molecular binding event or change in ionic concentration can be detected by the nanomaterial and may respond to the stimulus by releasing therapeutic molecule, or degrading, or chemically modifying drugs in vivo.

**1.9.1. Therapeutic mechanisms:** Nanotherapeutics can be used to carry small molecule drugs or biomacromolecules (proteins or siRNA), or act

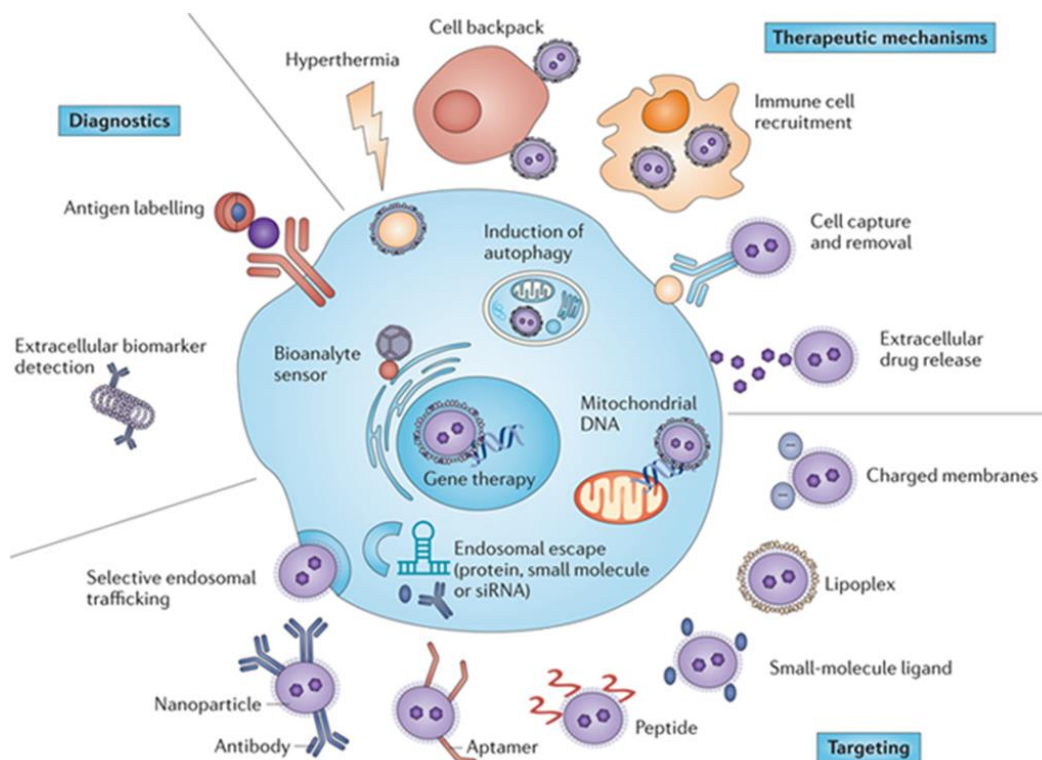


Figure 1.11. The figure summarizes nanotechnological strategies for diagnosis, treatment and specific targeting of cancer cells. Adopted from Ref [87].

as vehicles for immunotherapy and thermal absorption including targeting the diseased site, eliciting drug release, and increasing half-life of drug by changing its pharmacokinetics [91]. This ensures to reduce off-target effects on non-diseased cells and also lower the drug amount needed to be administered [88, 92]. Moreover, thermo-ablative therapy, that is, killing tumor cells by heat energy, can be augmented by activating nanomaterials localized in diseased tissue using magnetic fields, infrared light or radio-frequency[93-96]. Removal of nanomaterials from the in vivo system after its job is done is equally important as the therapeutic process. Hence, the nanomaterials are constructed with linkages to ensure its degradation or removal after a certain time.

**1.9.1. Targeting cancer:** Antibody-based targeting ligands, conjugated with drug or polymer are being used clinically as nanodelivery systems to target cancer cells [97, 98]. Similarly, linking short peptides [99, 100], such as RGD, or aptamers (nucleic acid ligands) [101, 102] to nanoparticles can increase their binding specificity. Peptide nucleic acids (PNAs) are also used in which they bind with high affinity to

complimentary DNA strand and the peptide backbone covalently modifies targeting ligand [103]. Small-molecule-binding domains, such as the folate receptor [104], vitamin B12 receptors [105] which are overexpressed in certain cancer cell types, demonstrate high affinity to the nanotherapeutics coated with their respective ligand molecules. The cellular uptake of such nanotherapeutics is enhanced by the receptor-mediated endocytosis in the specific cells with the receptors on their cell surface. This way indiscriminant transgene expression can be avoided. The ligand is covalently linked to a cationic polymer. The polymer electrostatically interacts with the negatively-charged phosphates of the DNA backbone and forms a stable polymer/DNA complex of nanoscale size suitable for cellular uptake. The polymer must also contain an endosomolytic agent to avoid degradation in the endosomal compartment [106].

Multiple therapeutic functions can be combined into a single platform and such nanoparticles can be used to target specific cells/tissues and reach particular subcellular compartments by carefully considering the biology of cancer process and engineer nanomaterials accordingly.

## **1.10 Objective of the study**

The research study focuses on enhancing the transfection efficiency of transgene transported by cationic polymer specifically to the cancer cells. For this a cationic polymer was constructed such that it is itself innocuous to the cells simultaneously contains a ligand to enhance its cellular uptake in cancer cells. Degradable linkages were incorporated to ensure its degradation after delivering the cargo in the vicinity of cell nucleus. The ligand vitamin B6 was inserted in the polymer branches via covalent bonding to incorporate targeting property in the polymer specifically for cancer. The next chapter 2 deals with this idea and demonstrates the synthesis and mechanistic investigations of the vitamin B6 coupled polymer, VBPEA, for the enhanced cellular uptake of cationic polyplexes by cancer cells.

## **1.11 Conclusion**

An ideal gene delivery system for cancer gene therapy should effectively condense and protect therapeutic nucleic acid, increase its cellular uptake specifically in cancer cells, and release the nucleic acid

at the site of action. Nanomaterial tools can address to the needs of cancer therapy that are only now starting to be realized in the clinic. Many of the past impediments to treatment, like safety, targeting, endosomal escape, polymer toxicity and non-degradability, lower transfection efficiency, etc. are being actively researched and overcome. In the present research study, the solution to the above mentioned problems in cancer gene therapy are tried to address and applied in vivo to discern its therapeutic potential.

# CHAPTER 2

## *Synthesis & Transfection Efficiency of Vitamin B6-Coupled Poly(ester amine) Gene Transporter*

---

### **2.1 Introduction**

Non-viral gene delivery systems are superior to highly-efficient viral methods in a way being safer as they do not induce unwanted immune responses or aberrant gene expressions [107, 108]. However, the low transfection efficiency of non-viral vectors remains a major drawback to their widespread clinical application. Therefore, method optimization for the development of non-viral vector is essential to improve host cell internalization and thus transfection activity so that

the efficacy equivalent to viral vector-mediated gene delivery can be achieved [109]. Recent research focused on these challenges is dedicated to make non-viral method a future treatment for a myriad of genetic disorders. Poly (L-lysine), polyethylenimine (PEI), chitosan, PAMAM dendrimer, and cationic liposomes are a few of the commonly studied non-viral agents that can self-assemble with and condense DNA into nanoplexes suitable for endocytosis [110, 111]. The PEI-based gene delivery system is an excellent candidate as a non-viral vector due to its unique endosome escape capability; however, its high molecular weight (HMW) increases cytotoxicity due to non-discharged aggregate accumulation on the cell surface, which impairs important membrane functions [64]. One approach to reduce cytotoxicity is to cross-link low molecular weight (LMW)-PEI with degradable linkages to make HMW polymer that can condense and protect nucleic acid for efficient transfection and can be discharged into small fragments upon degradation [112]. In addition, incorporation of ligands such as folic acid, mannose, galactose and synthetic peptides into vectors can enhance transfection by encouraging specific pathways of cellular internalization [113, 114]. Active targeting can be beneficial in two

ways: first, coupling a targeting moiety to the vector can facilitate its exclusive uptake into specific cell types, and second, non-specific interactions can be reduced by shielding the positive surface charges of the vector [115]. Hence, the target site, the targeting ligand, and the physicochemical properties of the polyplexes should be carefully considered in the development of gene delivery vectors [116] .

In general, vitamins achieve facilitated entry into most cells with relative specificity. The specific receptors/carriers involved in the uptake of vitamin B<sub>6</sub> (pyridoxine), B<sub>7</sub> (biotin), B<sub>9</sub> (folic acid), B<sub>12</sub> (cobalamin), and other vitamins have been previously studied [117-119]. Therefore, their specific receptor/carrier-mediated entry can be utilized as a biological mechanism for the delivery of pharmacological compounds into cells. Vitamin B<sub>6</sub> (VB<sub>6</sub>) is an essential micronutrient required for the normal growth and function of nearly all cell types. VB<sub>6</sub> plays a vital role as a cofactor for a large number of essential apoenzymes that carry out various metabolic functions [120]. Since tumor cells, owing to high metabolic activity, have high demand for VB<sub>6</sub>, the VB<sub>6</sub>-coupled molecules can also achieve entry into the tumor

cells through the specific VB<sub>6</sub> transporting membrane carriers (VTCs). In a previous work, VB<sub>6</sub> was found to facilitate the cellular uptake of small peptides and peptide-oligonucleotide conjugates through VTCs [121, 122]. Although VB<sub>6</sub> has been modified to transport small molecules, its ability to increase the cellular uptake of gene transporters with a higher affinity in cancer cells has never been documented.

Previously, poly(ester amine) (PEA) synthesized by a Michael addition reaction between LMW-PEI and glycerol dimethacrylate (GDM) as a cross linker was reported to show high transfection efficiency due to the glycerol backbone which facilitates cellular entry by exerting hyperosmotic effects along with PEI amine groups that help in fast endosomal release. Moreover, the polyester backbone ensures the degradability of the polymer into smaller fragments by its biphasic degradation pattern, making it easier to be exocytosed [123]. Based on these aforementioned characteristics, we synthesized a vitamin B<sub>6</sub>-coupled poly(ester amine) (VBPEA) gene transporter in which VB<sub>6</sub> was covalently coupled with a degradable PEA backbone synthesized from 1.2k branched PEI (bPEI) cross linked with GDM. The VBPEA

was expected to show enhanced transfection efficiency due to the specific uptake process of VB<sub>6</sub> combined with the degradable property of PEA. Hence, it was anticipated that VB<sub>6</sub> coupled to a polycationic gene delivery vehicle could encourage specific and enhanced cellular uptake via endocytosis and achieve a pharmacological response by binding to its specific membrane carrier.

## **2.2 Materials and Methods**

### **2.2.1. Materials**

bPEI (Mn: 1.2k and 25k), dimethyl sulfoxide (DMSO), pyridoxal 5'phosphate (PLP), sodium cyanoborohydride (NaCNBH<sub>4</sub>), and 3-(4, 5-dimethyl thiazol-2-yl)-2, 5-diphenyl tetrazolium bromide (MTT) reagent were purchased from Sigma (St. Louis, MO, USA). Luciferase reporter, pGL3- vector with SV-40 promoter and enhancer encoding firefly (*Photinus pyralis*) luciferase was obtained from Promega (Madison, WI, USA). The green fluorescent protein (GFP) gene was obtained from Clontech (Palo Alto, CA, USA). All other chemicals used in this study were of analytical reagent grade.

### **2.2.2. Synthesis of vitamin B<sub>6</sub>-coupled poly(ester amine) (VBPEA)**

VBPEA was synthesized in a two-step reaction in which LMW bPEI was cross linked with GDM to form PEA, which was then coupled with the active form of VB<sub>6</sub> (pyridoxal 5'phosphate, PLP) to produce the VBPEA gene transporter.

#### ***2.2.2.1. Synthesis of PEA***

PEA was synthesized by a Michael addition reaction between LMW-bPEI (1.2k) and GDM [124]. Briefly, GDM and LMW-PEI were separately dissolved in anhydrous methanol. The GDM solution was added slowly to the LMW-PEI solution at a stoichiometric ratio of 1:2 at 60°C with constant stirring for 24 h. The reaction mixture was subsequently dialyzed at 4°C for 24 h using a Spectra/Por membrane (MW cut-off 3.5k; Spectrum Medical Industries, Inc., Los Angeles, CA, USA) against distilled water. Finally, the copolymer was lyophilized and stored at 0°C.

#### ***2.2.2.2. Synthesis of VBPEA***

10 mol% of the total primary amines present in PEA were reacted with pyridoxal 5'phosphate (PLP) to form a transient Schiff base, which was subsequently reduced with NaCNBH<sub>4</sub> to obtain VBPEA [121] . Briefly, a 10 mL aqueous solution of PLP (1 mg/mL) was added dropwise to a 50 mL aqueous solution of PEA (1 g) and NaHCO<sub>3</sub> (100 mg) at RT and stirred vigorously for 24 h. Subsequently, NaCNBH<sub>4</sub> (50 mg) was added to reduce the Schiff base to a secondary amine. The reaction mixture was dialyzed with a Spectra/Por membrane (MW cut-off 3.5 k) against distilled water at 4°C for 24 h. The solution was finally lyophilized and stored at 0°C until use.

### **2.2.3. Characterization of VBPEA**

<sup>1</sup>H NMR spectra of VBPEA and PEA in D<sub>2</sub>O were recorded using an Advanced 600 spectrometer (Bruker, Germany). The absolute molecular weight of the VBPEA polymer was measured by gel permeation chromatography coupled with multiangle laser light scattering (GPC-MALLS) using a Sodex OHpack SB-803 HQ (Phenomenex, Torrells, CA, USA) column (column temperature 25°C; flow rate 0.5 mL/min).

#### **2.2.4. Gel retardation assay**

VBPEA was complexed with DNA (0.3 µg, pGL3 control) at various N/P ratios (0.5, 1, 3, 5 and 10) for 30 min at RT in autoclaved water with the total volume adjusted to 20 µL. 1X loading dye (Biosesang, Korea) was added, and the samples were resolved on a 0.8% agarose gel in 1X TAE buffer containing ethidium bromide (EtBr, 0.1 µg/mL). Gel electrophoresis was conducted at 100 V for 40 min in 1X TAE running buffer, and images were captured under ultraviolet illumination.

#### **2.2.5. DNA protection and release assay**

The ability of VBPEA to protect DNA was assessed by treating VBPEA/DNA (N/P 10) with DNase I. The prepared VBPEA/DNA complexes and free DNA were incubated separately with DNase I (1 µL, 50 units) in DNase/Mg<sup>2+</sup> digestion buffer containing Tris-Cl (50 mM, pH 7.6) and MgCl<sub>2</sub> (10 mM) at 37°C for 30 min. The DNase was inactivated by adding 4 µL EDTA (250 mM in 1 N NaOH) and incubated for another 30 min at RT. Finally, protected DNA was released from the complexes with the addition of 5 µL 1% sodium

dodecyl sulfate (SDS) in distilled water for 2 h. Released DNA was detected by resolving on a 0.8% agarose gel (with 0.1  $\mu\text{g}/\text{mL}$  EtBr) in 1X TAE running buffer at 100 V for 40 min.

#### **2.2.6. Measurement of particle size and zeta potential**

A dynamic light scattering spectrophotometer (DLS 8000, Otsuka Electronics, Osaka, Japan) was used to measure the size and zeta potential of the VBPEA/DNA complexes in comparison to the PEA/DNA and PEI25k/DNA complexes with 90 and 20 scattering angles at 25°C, respectively. The samples were incubated for 30 min in distilled water at N/P ratios of 5, 10, 20 and 30 with a 40  $\mu\text{g}/\text{mL}$  final DNA concentration in a total volume of 1 mL. In order to investigate the effects of serum proteins on the stability of VBPEA/DNA complexes (N/P 20) compared to PEA/DNA (N/P 20) and PEI25k/DNA complexes (N/P 10), serum concentrations of 0%, 10%, 20%, and 30% were added to the prepared complexes and their sizes were then measured.

#### **2.2.7. Observation of VBPEA/DNA complexes**

The morphology and size of the VBPEA/DNA complexes (at N/P 20) and the PEI25k/DNA complexes (at N/P 10) were confirmed by EF-TEM (LIBRA 120, Carl Zeiss, Germany). Prepared VBPEA/DNA and PEI25k/DNA complexes were loaded on a carbon grid, stained with 1% uranyl acetate for 10 s, washed with distilled water, and dried for an additional 10 min. Samples were then analyzed under an electron microscope.

#### **2.2.8. Cell culture and animals**

Adenocarcinoma human alveolar basal epithelial cells (A549) were maintained in Roswell Park Memorial Institute (RPMI)-1640 culture medium. Human cervix carcinoma cells (HeLa) and human liver hepatocellular carcinoma cells (HepG2) were cultured in Dulbecco's modified Eagle's medium (DMEM, low glucose) containing 10% heat-inactivated fetal bovine serum (FBS, HyClone, Logan, UT, USA) with 1% penicillin/streptomycin. All cells were maintained under standard culture conditions of 37°C and 5% CO<sub>2</sub>.

Animals were obtained from Orient Bio Inc. (Republic of Korea) and

kept in a laboratory animal facility maintained at  $23 \pm 2^{\circ}\text{C}$  and  $50 \pm 20\%$  relative humidity and under a 12 h light/dark cycle. All experimental protocols were reviewed and approved by the Animal Care and Use Committee at Seoul National University (SNU-120409-3).

### **2.2.9. Cytotoxicity assay**

VBPEA *in vitro* cytotoxicity was evaluated by MTT assay in three cell lines (A549, HeLa, and HepG2) and compared with that of PEA and PEI25k. At monolayer confluency, cells were trypsinized and seeded in a 24-well plate at  $10 \times 10^4$  initial cell density in 1 mL growth media and allowed to grow to 80% confluency prior to polyplex treatment. Cells were treated at various N/P ratios (5, 10, 20, 30, 40, and 50) in serum-free medium that was changed with serum-containing medium after 3 h. Thirty-six hours later, 500  $\mu\text{L}$  of MTT solution in 1X PBS (0.5 mg/mL) was added to each well and incubated for an additional 3 h. The medium was carefully aspirated, leaving purple formazan crystals, which were dissolved in DMSO (500  $\mu\text{L}$ ). Dissolved formazan (100  $\mu\text{L}$ ) from each well were transferred to 96-well plate and absorbance was

measured at 540 nm using a VERSAmax tunable microplate reader (Sunnyvale, CA, USA). All experiments were conducted in triplicate.

#### **2.2.10. In vitro transfection in the absence and presence of serum**

Transfection studies were performed in A549, HeLa and HepG2 cells at an initial cell density of  $10 \times 10^4$  in 24-well plate. At 80% cell confluency, VBPEA/pGL3 (1  $\mu$ g), PEA/pGL3, and PEI25k/pGL3 polyplexes were treated at various N/P ratios (5, 10, 20, 30 and 40) in serum-free medium, which was exchanged with fresh media containing serum (10% FBS) after 3 h. After the cells were kept under standard incubation conditions for 24 h, luciferase assay was performed according to the manufacturer's protocol. A chemiluminometer (Autolumat, LB953; EG&G Berthold, Germany) was used to measure relative light units (RLUs) normalized with protein concentration in cell extract estimated using a BCA protein assay kit (Pierce Biotechnology, Rockford, IL, USA). The effect of serum on polyplex stability for its possible use in biological systems was investigated in the A549 cell line. At N/P 20, cells were transfected with 0%, 10%, 20%, and 30% serum concentrations in 24-well plate, and luciferase

assay was performed as described above. Transfection activity was measured in triplicate as RLU/mg protein.

#### **2.2.11. Flow cytometry measurement**

Flow cytometry was performed to estimate the percent transfection efficiency of VBPEA/tGFP (1  $\mu$ g) polyplexes in A549 cells in comparison with PEA/tGFP and PEI25k/tGFP polyplexes. Transfected cells were harvested with 0.25% trypsin/EDTA and washed twice with 1X PBS. Cells expressing GFP acquired from a total of 10,000 cells were scored through a FACS calibrator system (Becton-Dickinson, San Jose, CA, USA) to determine the percent transfection.

#### **2.2.12. In vivo biodistribution**

Intravenous injection of VBPEA/pGL3 complexes was performed in Balb/c mice (4 mice/group) to analyze *in vivo* biodistribution. For these experiments, VBPEA and PEA (at N/P 20) were complexed with pGL3 (30  $\mu$ g) in normal saline (final volume 100  $\mu$ L). Similarly, naked DNA in normal saline was used as a control. Complexes were delivered to 6-week old Balb/c mice intravenously (i.v.) through the tail vein using a

40 U insulin syringe (1 mL with a needle size 0.30 x 8 mm). After four days of gene delivery, animals were sacrificed by cervical dislocation and all vital organs were dissected. Organs were washed with chilled normal saline, weighed, chopped, and suspended to 25% w/v homogenate in 2.5X cell lysis buffer (Promega, USA) and centrifuged (10,000 rpm, 10 min, 4°C). Cell lysate (100 µL) from each sample was assayed for luciferase activity using a chemiluminometer.

## **2.3 Results**

### **2.3.1. Synthesis and physicochemical characterization of VBPEA**

The terminal amines of PEA were reacted with the aldehyde group of VB<sub>6</sub> (pyridoxal 5'phosphate) at the 4' position to form an unstable transient Schiff base, which was reduced with NaCNBH<sub>4</sub> (Figure 2.1).

The synthesized VBPEA was characterized for its composition, DNA condensation and protection ability, size, zeta potential and morphology of its complexes with DNA. The composition of VBPEA as analyzed through <sup>1</sup>H NMR spectroscopy shows intense peaks at around 8.0 ppm, representing protons in the pyridoxal ring of VB<sub>6</sub>.

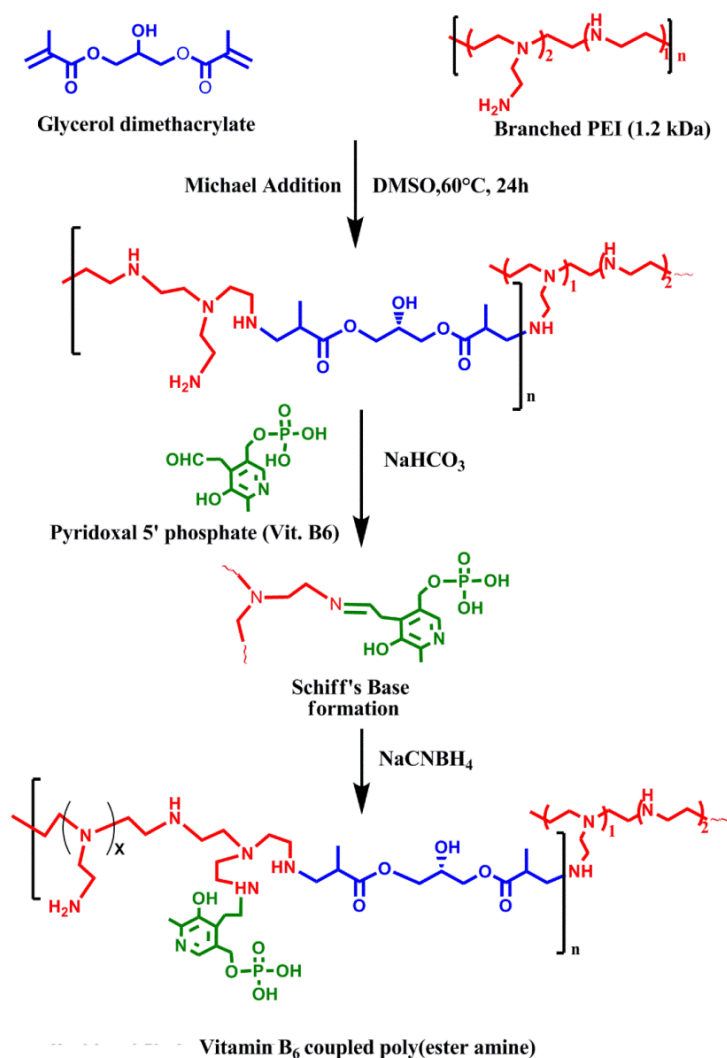


Figure 2.1. Synthesis scheme of vitamin B<sub>6</sub>-coupled poly(ester amine) (VBPEA). The terminal amines of poly(ester amine) (PEA) were reacted with the aldehyde group of VB<sub>6</sub> to form an unstable Schiff base, which was reduced with  $\text{NaCNBH}_4$  to form VBPEA.



Table 2.1. Characterization of VBPEA

MW of reactants (Da)		Composition of PEA (mol-%) *	Composition of VB <sub>6</sub> (mol-%) *	M.W. (Da) †	Polydispersity index (PDI)
PEA	VB <sub>6</sub>				
5,000	247	90.23	9.77	5,000-	1.12
-				6,150	
5,200					

\* Determined by <sup>1</sup>H NMR

† Determined by GPC

Presence of PEA backbone in VBPEA was confirmed by methyl peaks visible at 1.1 ppm and 2.4 ppm. A comparative NMR of VB<sub>6</sub> (pyridoxal), PEA, and VBPEA is shown in figure 2.2. The composition of VB<sub>6</sub> in VBPEA as estimated by NMR was about 9.77 mol-% and the MW of VBPEA measured by GPC was 5000-6000 Da (Table 2.1), which indicated appropriate size of polymer to link with DNA and form stable polyplexes.

Gel retardation assay further demonstrated the ability of VBPEA to condense DNA by completely retarding DNA migration in the agarose gel at an N/P ratio of 5 (Figure 2.3A), suggesting a high VBPEA complexation capacity. Further, through DNA protection and release assay VBPEA showed to protect the complexed DNA as visible in lane 4 of Figure 2.3B to suggest its protection against intracellular DNase degradation.

The condensation of DNA with VBPEA resulted in nanoscale particle sizes appropriate for cellular uptake, confirmed by dynamic light scattering spectrophotometer (DLS) and EF-TEM. DLS revealed a decreasing trend in VBPEA/DNA nanoplex sizes with increasing N/P

ratio (Figure 2.4A), which is in accordance with the increasing zeta potential from +35 to +41 mV (Figure 2.4B). The increase in zeta potential from lower to higher N/P ratio provides increased DNA condensation, leading to a decrease in nanoplex sizes. After a certain limit of compactness of ~ 110 nm (at N/P 20), nanoplex sizes began to increase, probably due to subtle play of electrostatic and repulsive forces of interaction. It is noteworthy that VBPEA showed a reduction in its zeta potential as compared to PEA, most likely due to VB<sub>6</sub> coupling.

The polyplex sizes estimated with increasing serum concentrations showed a continuous increase in the hydrodynamic diameter of PEI25k/DNA due to aggregation with serum proteins, which generates polyplex sizes unsuitable for cellular uptake. In contrast, VBPEA/DNA showed no significant change in polyplex sizes, suggesting minimal interaction with serum proteins and favorable transfection (Figure 2.5). This can be attributed to the coupled VB<sub>6</sub> and hydroxyl groups of PEA backbone, which obstructed interactions between serum proteins and

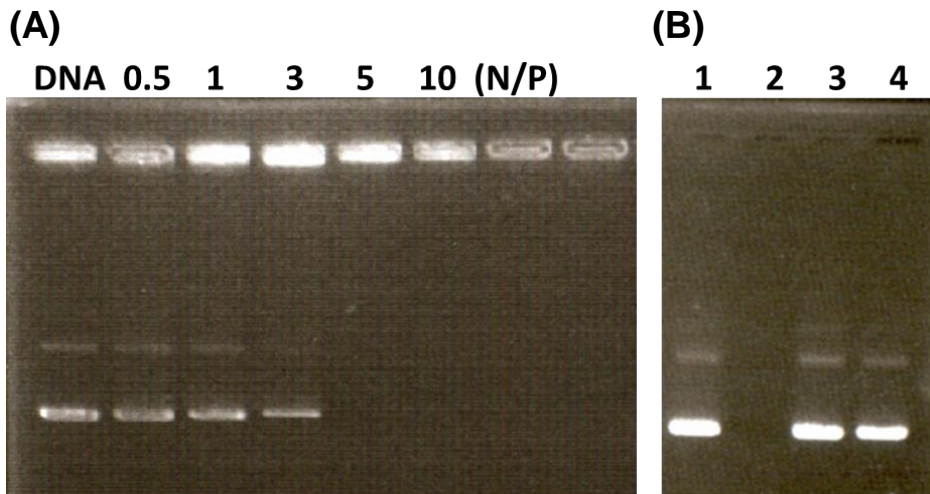


Figure 2.3. Electrophoretic mobility shift assay. (A) Gel electrophoresis of VBPEA/pGL3 (0.1  $\mu\text{g}$ ) complexes at various N/P ratios (0.5 to 10). (B) DNA protection and release assay. DNA was released by adding 1% SDS to VBPEA/pGL3 complexes at an N/P ratio of 10: (Lane 1) pGL3 without DNase I, (Lane 2) pGL3 with DNase I, (Lane 3) VBPEA/pGL3 complexes without DNase I, and (Lane 4) VBPEA/pGL3 complexes with DNase I.

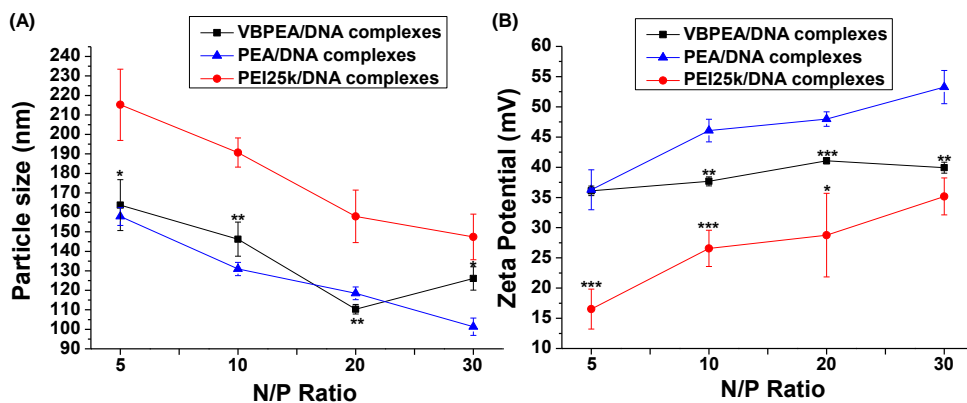


Figure 2.4. Dynamic light scattering microscopic measurements of VBPEA/DNA polyplexes at various N/P ratios. (A) VBPEA/pGL3 particle size without serum. (B) VBPEA/pGL3 zeta potential (n = 3, error bar represents SD) (\*p < 0.05; \*\*p < 0.01; \*\*\*p < 0.001, one-way ANOVA).

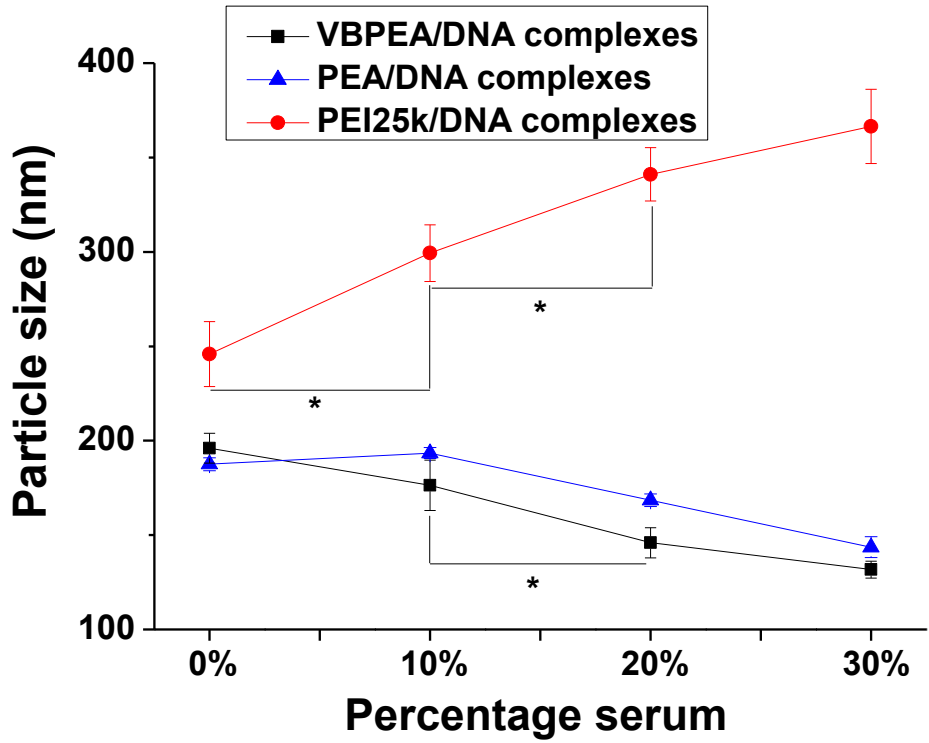


Figure 2.5. VBPEA/pGL3 particle size in various percent serum concentrations (n = 3, error bar represents SD) (\*p < 0.05; \*\*p < 0.01; \*\*\*p < 0.001, one-way ANOVA).

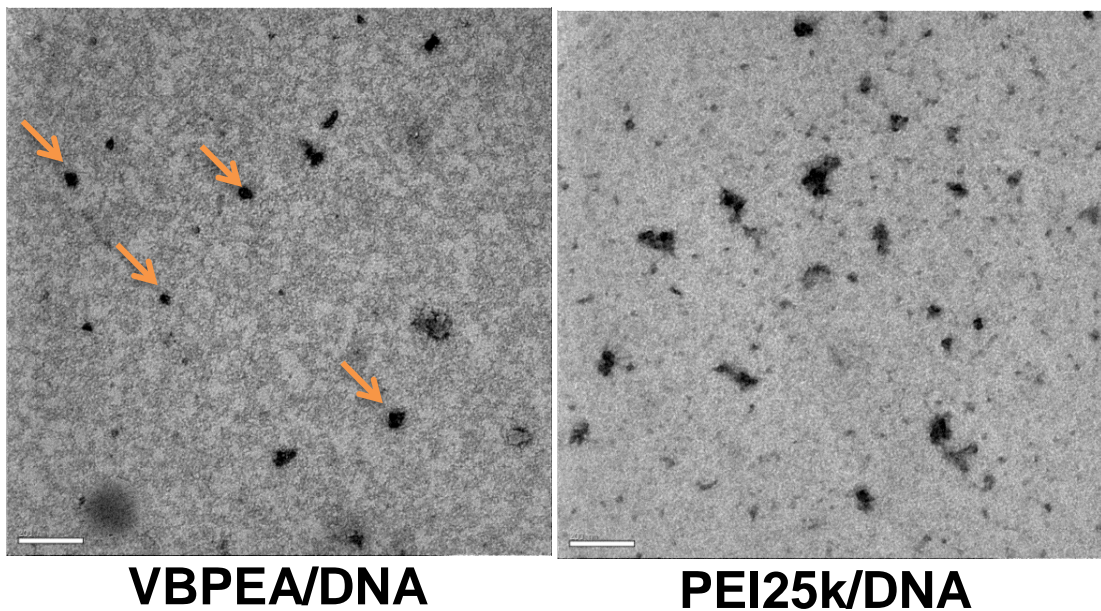


Figure 2.6. EF-TEM images of VBPEA/pGL3 and PEI25k/pGL3 complexes at an N/P ratio of 20.

the positive charges of the PEA backbone, ensuring its stability in an anionic environment. EF-TEM images also showed the VBPEA/DNA complexes to have a uniform size distribution (<120 nm) with well-defined spherical morphologies and no aggregation allowing their easy uptake, in comparison to PEI25k/DNA (Figure 2.6).

### **2.3.2. Enhanced *in vitro* cell viability and transfection efficiency of VBPEA/DNA complexes**

Enhancement in cell viability by VBPEA due to VB<sub>6</sub> coupling was demonstrated by MTT assay that shows >98% cell viability in A549, HeLa, and HepG2 mammalian carcinoma cell lines in comparison to PEA/DNA (~85-90%) and PEI25k/DNA (~70%) complexes (Figure 2.7).

*In vitro* VBPEA/pGL3 transfection in A549, HeLa, and HepG2 cell lines showed increase in transfection efficiency from N/P 5 to 40 due to the increasing positive charge density, leading to more efficient DNA complexation. However, the level of luciferase gene expression with PEA was comparatively lower than VBPEA. VBPEA (N/P 20)

resulted in a 5-20 fold increase in luciferase expression over PEA (N/P 20) and a 12-30 fold increase over PEI 25k (N/P 10) (Figure 2.8). VBPEA showed 40-45 % transfection efficiency compared to 30-35% efficiency of PEA and 10-13% efficiency of PEI 25k (Figure 2.9) as measured by flow cytometry (Figure 2.10). The crucial result is the increased transfection of VBPEA over PEA, which indicated the probable involvement of a VB<sub>6</sub>-mediated internalization.

Furthermore, VBPEA transfection in presence of serum (Figure 2.11) initially showed stable expression of transgenic product until 20% serum concentration, after which only a slight decrease in transfection was observed due to aggregated serum proteins on VBPEA. The results are in accordance with the aforementioned particle size measurements at various percent serum concentrations.

### **2.3.3. In vivo biodistribution of VBPEA/DNA complexes**

The biodistribution of VBPEA/pGL3 complexes in a Balb/c mouse model showed a moderate level of luciferase gene expression in most of the vital organs, with the highest expression in the spleen, followed

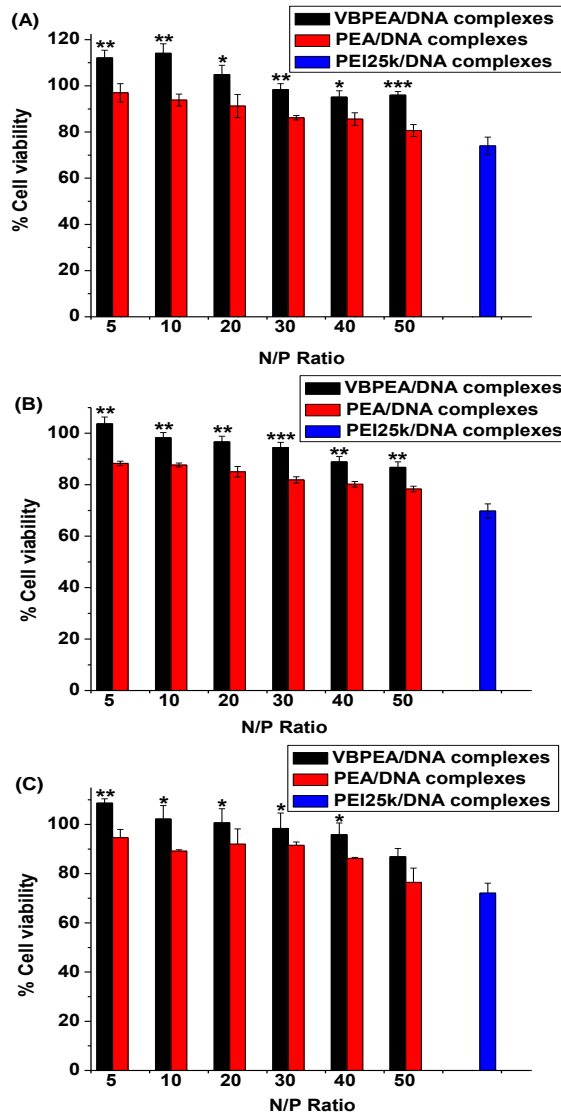


Figure 2.7. Cytotoxicity of VBPEA/DNA (pGL3) complexes at various N/P ratios in different cell lines. (A) A549, (B) HeLa, and (C) HepG2 (n= 3, error bar represents SD) (\*p < 0.05; \*\*p < 0.01; \*\*\*p < 0.001, one-way ANOVA).

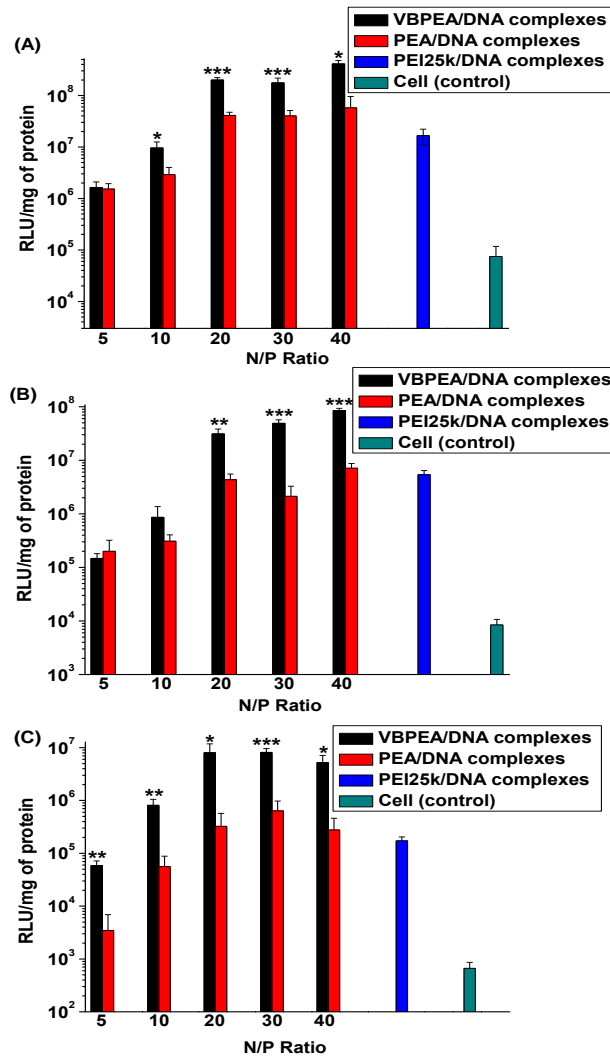


Figure 2.8. In vitro transfection studies of VBPEA/DNA complexes. In vitro transfection in serum free medium at various N/P ratios in different cell lines: (A) A549, (B) HeLa, and (C) HepG2 (n = 3, error bar represents SD) (\*p < 0.05; \*\*p < 0.01, \*\*\*p < 0.001, one-way ANOVA).

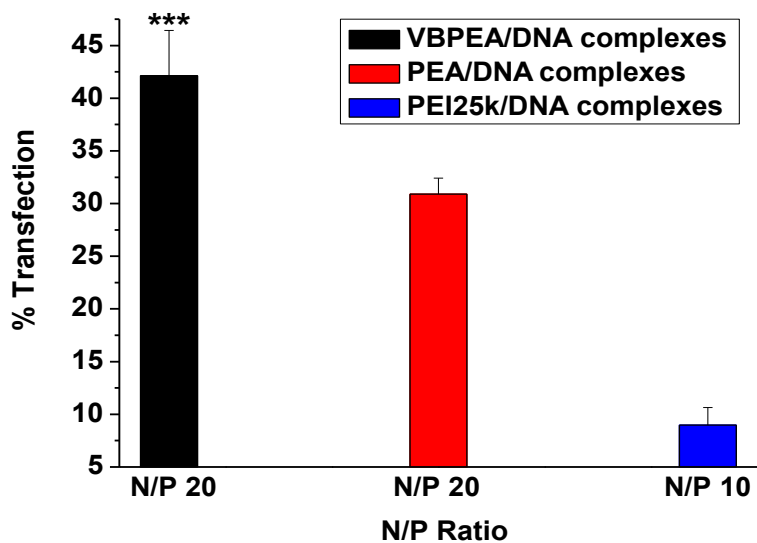


Figure 2.9. Percent transfection efficiency as measured by flow cytometry (n= 3, error bar represents SD) (\*p < 0.05; \*\*p < 0.01, \*\*\*p < 0.001, one-way ANOVA).

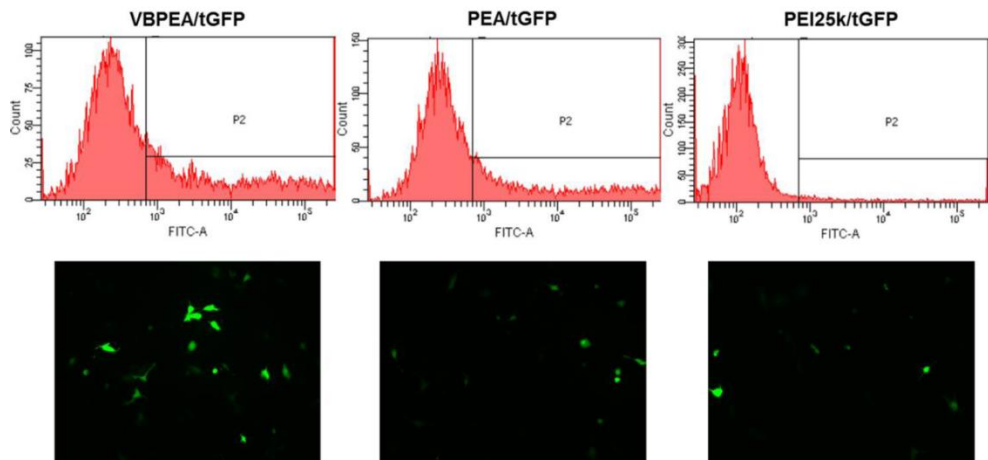


Figure 2.10. FACS studies showing transfection efficiency of VBPEA/tGFP, PEA/tGFP and PEI25k/tGFP complexes in A549 cells with corresponding transfection images.

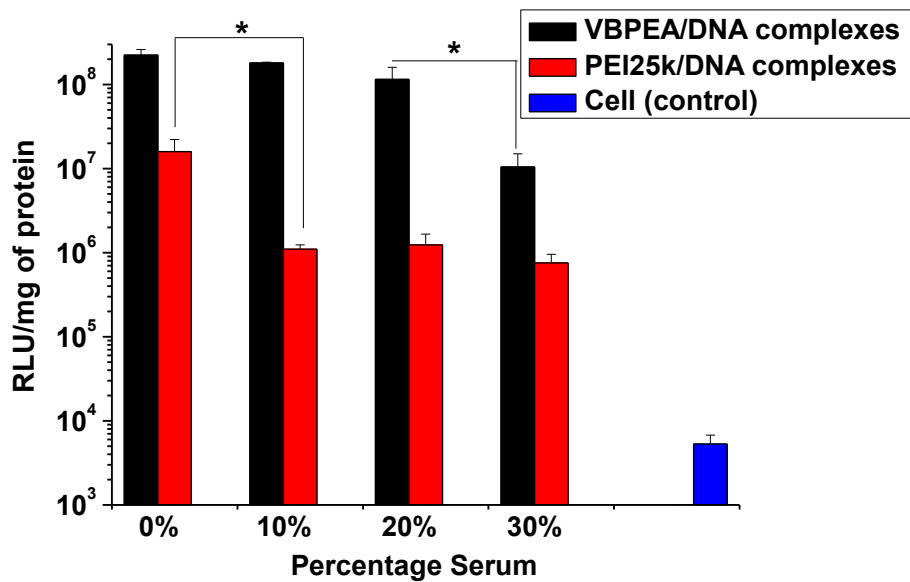


Figure 2.11. Transfection of VBPEA/DNA complexes in various percent serum concentrations in A549 cells (n= 3, error bar represents SD) (\*p < 0.05; \*\*p < 0.01, \*\*\*p < 0.001, one-way ANOVA).

by the lung, brain, liver, and kidney, with minimum expression in the heart (Figure 2.12). VB<sub>6</sub> enhanced the cellular uptake, especially in the liver, lung, and brain, which typically shows lower levels of transgene expression due to restricted entry of therapeutics [124, 125]. Immediately after i.v. injection, polyplexes tend to aggregate with blood cells and plasma components, resulting in a large accumulation of polyplexes in the fine capillaries of the lung, where they extravasate into lung tissues due to vascular leakage of ~60 nm polyplexes. Larger polyplexes are released into circulation, with high concentrations found in liver cells [115]. VB<sub>6</sub> is metabolized by the liver resulting in high accumulation in the liver [126]. Therefore, luciferase delivered by VBPEA, but not by PEA, was expressed in mouse liver.

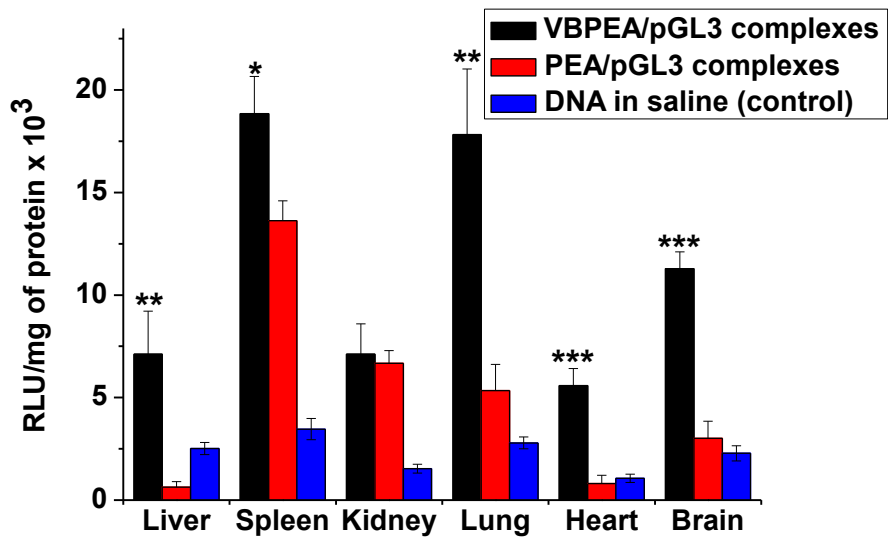


Figure 2.12. In vivo luciferase protein expression after i.v. injection in Balb/c mice showing biodistribution of VBPEA/pGL3 complexes in comparison to PEA/pGL3 complexes and naked pGL3 (n = 4, error bar represents SD) (\*p < 0.05; \*\*p < 0.01, \*\*\*p < 0.001, one-way ANOVA).

## 2.4 Discussion

Our findings show that, with the modification of internalization pathway and mode of cellular uptake, a gene transporter can enhance transfection efficiency in cancer cells. Using VB<sub>6</sub>, coupled to poly(ester amine) backbone, we sought that VB<sub>6</sub> could trail the gene transporter to its specific intracellular route. Interest aroused towards VB<sub>6</sub> due to its unequalled catalytic versatility as a cofactor and widespread involvement in various cellular processes [110, 127]. VB<sub>6</sub> utilizes the common reaction feature of forming a Schiff base (aldimine) between its electrophilic carbonyl group and nucleophilic amines on enzymes [128]. The amino groups of PEA play a similar elegant role in forming the VB<sub>6</sub>-coupled gene transporter via Schiff base formation. The robustness of VBPEA was demonstrated by its ability to protect nucleic acids against DNase degradation and its biocompatibility was verified by over 98% cell viability. The nanosized structure (<170 nm) with optimum surface charge of VBPEA/DNA polyplexes makes it suitable for cellular uptake. In addition, 20-30 folds higher transfection efficiency of VBPEA relative to PEA and PEI25k nanoplexes

demonstrated the involvement of VB<sub>6</sub> specific membrane carriers in uptake process, owing to which the VBPEA gene transporter showed potential for use in gene therapy.

The molecular weight and surface charge of polyplexes plays a crucial role in determining their cytotoxicity. High surface charge of PEI25k tends it to aggregate on the membrane surface and impairs important membrane functions, thereby reducing cell viability [123]. Therefore, LMW PEI was used in VBPEA. VB<sub>6</sub> coupled to the PEA backbone further reduced the surface charge and converted cytotoxic primary amines [129] to less toxic secondary amines, and resulted in the polyplexes no longer being deleterious to cells. In addition, formation of LMW degradation products after polyester backbone hydrolysis into respective acid and alcohol reduces the detrimental cytological effects [123]. The hydroxyl groups in PEA that offer greater cell viability by reducing the surface charge through the formation of hydrogen bonds with DNA gives further biocompatibility to VBPEA in addition to that conferred by the degradable ester linkages. These characteristics function together to give VBPEA an innocuous profile. Polyplex sizes

less than 200 nm helps in an easy cellular internalization, and a positive zeta potential enables it to condense DNA into nanoplexes that brings it in close proximity with the anionic cell membrane [130]. Despite the reduced zeta potential of VBPEA compared to PEA due to VB<sub>6</sub> coupling, the enhancement in the transfection efficiency of VBPEA both *in vitro* and *in vivo* is its most striking feature (Figure 2.8, 2.12), that suggests for the presence of a specialized cellular uptake mechanism due to incorporation of VB<sub>6</sub>.

## **2.5 Conclusion**

This study provides a proof-of-principle strategy for using vitamin B<sub>6</sub>-coupled poly(ester amine) (VBPEA) as a gene transporter for gene delivery to cancer cells with reduced cytotoxicity and increased transfection efficiency. The current research suggests VBPEA is a promising anticancer therapeutic entity that modulates vector delivery and will be able to perform myriad of productive gene modulations by the expression of transgenic products.

# CHAPTER 3

## *Membrane Transport Mechanism of Vitamin B<sub>6</sub>-Coupled Poly(ester amine)*

---

### **3.1 Introduction**

Vitamin B<sub>6</sub> (VB<sub>6</sub>) is an essential micronutrient required for the normal cellular growth and function. It is taken up by the body from exogenous food sources and absorbed by the intestine. Most of the absorbed VB<sub>6</sub> is transported to the liver and taken up by facilitated diffusion through specific VB<sub>6</sub> transporting membrane carriers (VTCs) into the cells [119]. VB<sub>6</sub> plays a vital role as a cofactor for a large number of essential apoenzymes that carry out various metabolic functions [120]. Serine hydroxymethyltransferase (SHMT) is one of the VB<sub>6</sub>-dependent enzymes involved in DNA biosynthesis. This enzyme activity is

enhanced for DNA duplication in the proliferating tumor cells that results in increased consumption of VB<sub>6</sub> [131]. Consequently, to meet the VB<sub>6</sub> needs of tumor cells, VB<sub>6</sub> uptake from neighboring tissues is increased [132, 133]. Since tumor cells have high demand for VB<sub>6</sub>, it was anticipated that the VB<sub>6</sub>-coupled molecules can also achieve VTC-mediated entry into the tumor cells with higher affinity than the normal cells.

## **3.2 Materials and Methods**

### **3.2.1. Materials**

bPEI 25kDa, pyridoxal 5'phosphate (PLP), genistein, chlorpromazine, methyl-β-cyclodextrin, bafilomycin A1 and 4'-deoxypyridoxine hydrochloride were purchased from Sigma (St. Louis, MO, USA). Luciferase reporter, pGL3- vector with SV-40 promoter and enhancer encoding firefly (*Photinus pyralis*) luciferase was obtained from Promega (Madison, WI, USA). Tetramethylrhodamine isothiocyanate (TRITC) and YOYO-1 iodide (Molecular Probes, Invitrogen, Oregon,

USA) fluorescent dyes were used for confocal microscopy. All other chemicals used in this study were of analytical reagent grade.

### **3.2.2. Cell culture and isolation of mouse primary lung cells**

Adenocarcinoma human alveolar basal epithelial cells (A549) and mouse lung adenoma cells (LA-4) were maintained in Roswell Park Memorial Institute (RPMI)-1640 culture medium. Human bronchial epithelial cells (16-HBE) were cultured in DMEM/Ham's F-12 medium containing 10% heat-inactivated fetal bovine serum (FBS, HyClone, Logan, UT, USA) with 1% penicillin/streptomycin. All cells were maintained under standard culture conditions of 37°C and 5% CO<sub>2</sub>.

To obtain lung single cell suspensions, lungs were removed from mice (6 weeks old) and kept separately in DMEM/F-12 medium containing 0.5 mg/mL collagenase D (Roche Applied Science, Indianapolis, IN, USA) and 100 µg/mL DNase I (Sigma-Aldrich). Tissues were minced with scissors, incubated for 1 h at 37°C and then passed through a 70 µm Falcon cell strainer (BD Labware). RBC lysis was performed using ACK lysis buffer (Gibco) followed by centrifugation (800 rpm, 10 min).

The cell pellet was resuspended in DMEM/Ham's F-12 medium (10% FBS and 1% antibiotic). Cells were counted and seeded in a 24-well plate.

### **3.2.3. In vitro transfection**

Transfection studies were performed in A549, LA-4 and 16-HBE cells at an initial cell density of  $10 \times 10^4$  in 24-well plate. At 80% cell confluency, VBPEA/pGL3 (1  $\mu$ g), PEA/pGL3, and PEI25k/pGL3 polyplexes were treated at various 20 N/P ratio in serum-free medium, which was exchanged with fresh media containing serum (10% FBS) after 3 h. After the cells were kept under standard incubation conditions for 24 h, luciferase assay was performed according to the manufacturer's protocol. A chemiluminometer (Autolumat, LB953; EG&G Berthold, Germany) was used to measure relative light units (RLUs) normalized with protein concentration in cell extract estimated using a BCA protein assay kit (Pierce Biotechnology, Rockford, IL, USA). Transfection activity was measured in triplicate as RLUs/mg protein.

### **3.2.4. Mechanistic studies for VBPEA high transfection efficiency:**

#### ***3.2.4.1. 4'-Deoxypyridoxine competition assay***

To investigate the role of VB<sub>6</sub> in enhancing cellular internalization, a competitive inhibition study was performed using 4'-deoxypyridoxine, a structural analogue of VB<sub>6</sub>. 4'-Deoxypyridoxine was added to 80% confluent A549 cells at concentrations of 0, 1, 2, 5, 10, and 20 mM, and the cells were incubated for 10 min before the addition of VBPEA/DNA and PEA/DNA polyplexes. *In vitro* luciferase assay was performed 24 h later.

#### ***3.2.4.2. VBPEA inhibition study by confocal microscopy***

A Carl Zeiss LSM 710 inverted laser scanning confocal microscope was used to monitor intracellular trafficking of TRITC-labeled VBPEA and YOYO-1-labeled pDNA in A549 cells in the presence and absence of 4'-deoxypyridoxine. TRITC (25 μL, 1 mg/100 μL in DMF) was added to VBPEA (1 mL, 10 mg/mL in H<sub>2</sub>O) to block ~1% of its total amines and stirred overnight. Unreacted TRITC was removed by washing with ethyl acetate (3 × 2 mL), which was then lyophilized and

resuspended in water. pDNA (1  $\mu$ g) was labeled with YOYO-1 iodide (2  $\mu$ L, 1 mM solution in DMSO) by stirring for 2 h at  $25 \pm 1^\circ\text{C}$  in the dark and then stored at  $-20^\circ\text{C}$ . A549 cells seeded in 6-well plate at  $20 \times 10^4$  cells/well were transfected with dual-labeled VBPEA/DNA complexes with and without 4'-deoxypyridoxine. After 120 min of incubation, cells were washed with  $1\times$  PBS 3 times with 500  $\mu$ L and fixed with 4% paraformaldehyde for 10 min at  $4^\circ\text{C}$ . DAPI was used to counter-stain the nuclear DNA of fixed cells, and images were procured from confocal microscopy.

#### ***3.2.4.3. Effect of free and coupled VB<sub>6</sub> on gene transfection***

The effect of VBPEA in comparison to VB<sub>6</sub> alone in enhancing transfection was demonstrated by transfecting A549 cells with PEA/pGL3 complexes (N/P 20) with 0, 5, 20, 50, and 100  $\mu$ M VB<sub>6</sub>. These transfection results were compared with VBPEA/pGL3 (N/P 20)-mediated transfection.

#### ***3.2.4.4. Comparison of VBPEA affinity towards cancer cells and normal cells***

Mouse primary lung cells seeded in 24-well plate at a density of  $10 \times 10^4$  cells/well were washed with PBS and transfected with VBPEA/DNA complexes (N/P 20) in serum-free medium. After 3 h, the medium was replaced with fresh DMEM/F-12 complete medium. Similarly, mouse lung adenoma LA4 cells, human adenocarcinoma A549, and human bronchial epithelial 16HBE cells were also transfected. After 24 h, luciferase expression was analyzed and compared between normal and cancer cells.

#### ***3.2.4.5. Comparison of PEA and VBPEA endocytosis pathways***

The route of VBPEA uptake was analyzed by inhibiting various endocytosis pathways and their subsequent effect on transfection was observed. For the investigation of clathrin-mediated endocytosis, A549 cells were treated with chlorpromazine at concentrations of 1, 2 and 3  $\mu\text{g}/\text{mL}$  and incubated for 1 h before adding VBPEA/DNA complexes. Similarly, caveolae-mediated uptake was examined using the inhibitors  $\beta$ -methyl cyclodextrin (2.5, 6.5 and 10  $\text{mg}/\text{mL}$ ) and genistein (100, 200, and 300  $\mu\text{M}$ ). After 1 h of incubation with inhibitors, A549 cells were transfected and luciferase expression was measured 24 h later.

#### ***3.2.4.6. Proton sponge effect by PEI in VBPEA***

To ensure the endosomal escape of VBPEA, the vacuolar-type H<sup>+</sup>-ATPase endosome proton pump was inhibited by bafilomycin A1 and the effect on transfection was observed. For this, A549 cells were seeded in 24-well plate at an initial cell density of  $10 \times 10^4$ . Confluent cells (80%) were pretreated with bafilomycin A1 (200 nM in DMSO) for 10 min, after which the inhibitor was aspirated and VBPEA/DNA and PEI25k/DNA polyplexes were added. Luciferase expression was measured after 24 h as described above.

### **3.3 Results**

#### **3.3.1. Competitive inhibition of VBPEA/DNA complexes by 4'-deoxyribose reveals VTC mediated uptake**

A549 cells transfected with VBPEA/DNA and PEA/DNA complexes in the presence of 4'-deoxyribose (structural analogue of VB<sub>6</sub>) showed a sudden decrease in VBPEA transfection to the level of PEA-mediated transfection efficiency at an inhibitor concentration of 1 mM (Figure 3.1). On the other hand, no significant inhibitor effect in

PEA/DNA transfection activity was observed, suggesting that 4'-deoxypyridoxine competitively inhibits the binding of VB<sub>6</sub> present in VBPEA/DNA polyplexes to VTC and decelerates polyplex uptake. Owing to the PEA backbone, VBPEA still retains transfection potential and does not completely lose transfection efficacy; instead, only VB<sub>6</sub>-specific uptake is hindered by 4'-deoxypyridoxine. This suggests the active participation of a VB<sub>6</sub>-specific uptake mechanism via a membrane carrier favoring accelerated internalization of VBPEA. Moreover, confocal images showed that VBPEA/DNA polyplexes internalization was decreased in the presence of 4'-deoxypyridoxine due to the decreased accessibility of VTC to VBPEA (Figure 3.2).

### **3.3.2. VB<sub>6</sub> coupling enhances cellular uptake of PEA polyplexes in cancer cells**

In order to prove the role of coupled VB<sub>6</sub>, we analyzed the transfection activity of PEA/DNA in the presence of free VB<sub>6</sub> compared to the amount of coupled VB<sub>6</sub> in VBPEA. VB<sub>6</sub> in a non-coupled state had no contribution in increasing the transfection activity of PEA even at 100 μM concentration of VB<sub>6</sub> (Figure 3.3). In contrast, the VB<sub>6</sub> coupled to

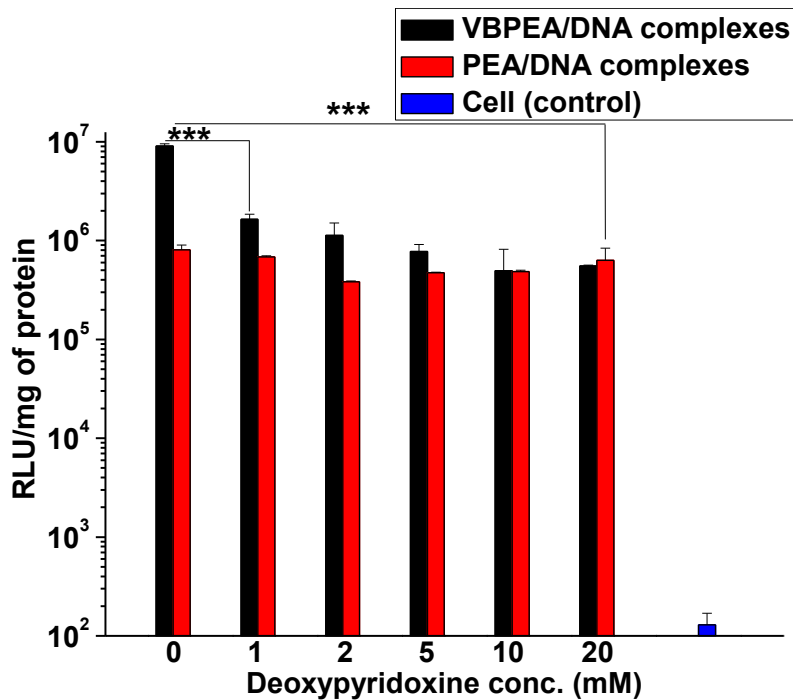


Figure 3.1. Carrier-mediated uptake of VBPEA evidenced by 4'-deoxyripyridoxine (a structural analog of VB6) competitive inhibition (n = 3, error bar represents SD) (\*\*\*)p < 0.001, one-way ANOVA).

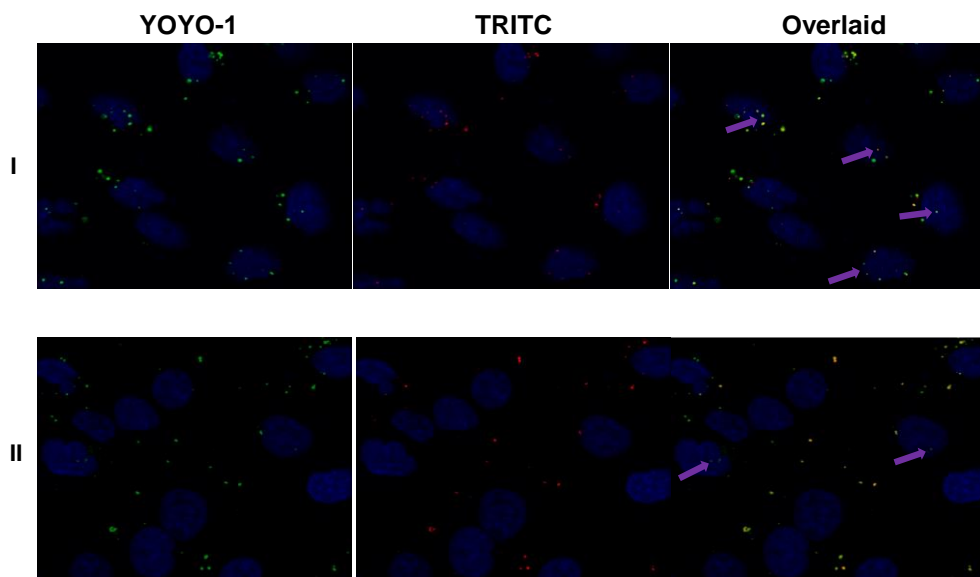


Figure 3.2. Confocal microscopic images of A549 cells taken after VBPEA/DNA polyplex treatment for 120 min (I) in the absence of 4'-deoxypyridoxine and (II) in the presence of 4'-deoxypyridoxine. VBPEA labeled with TRITC (red), pDNA labeled with YOYO-1 (green) and nuclear DNA labeled with DAPI (blue).

PEA drastically elevated the gene delivering capacity. Based on these results, it can be concluded that free VB<sub>6</sub> is easily transported across the cell membrane through VTC without affecting the transfection efficiency of PEA, whereas VB<sub>6</sub> coupled to PEA is unable to pass through the VTC owing to its large polyplex sizes, which may result in endocytosis of the inactivated VTC along with the VBPEA polyplex.

To investigate the increased affinity of cancer cells for VBPEA relative to normal cells, a comparative transfection study using human and mouse primary lung and cancer cells with VBPEA/DNA complexes was conducted. Primary cells showed lower transfection relative to their respective cancer cells (Figure 3.4), illustrating that VBPEA/DNA polyplex uptake is favored in tumors, most likely due to their need for excess VB<sub>6</sub> to support their uncontrolled growth and proliferation. However, normal cells, the growth and proliferation of which is under strong control, have a comparatively lower affinity for VB<sub>6</sub>, and thus showed lower transfection activity. To verify that normal cells were not affected by cellular cytotoxicity, a cell viability assay was performed to show no toxic effects of VBPEA/DNA complexes (Figure 3.5).

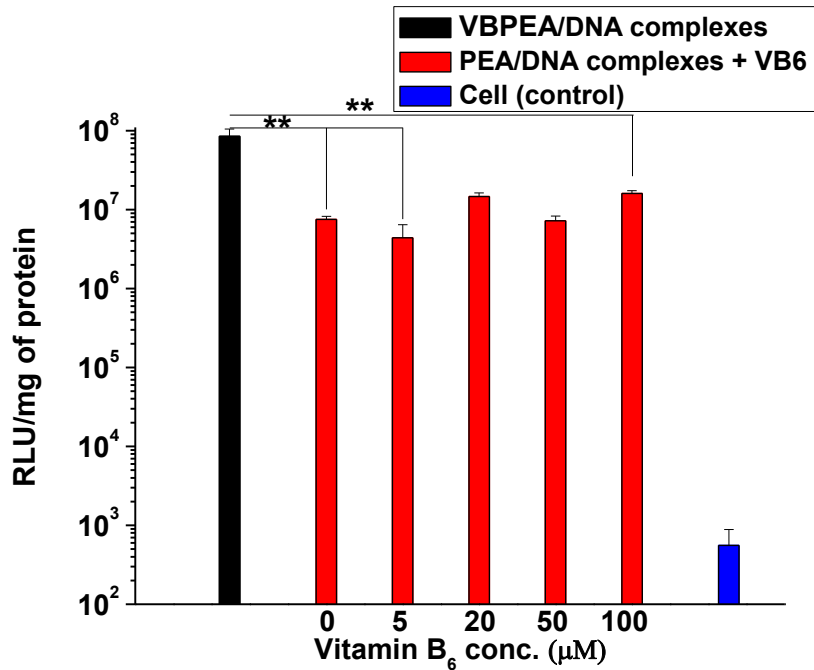


Figure 3.3. VB6 coupling enhances cellular uptake of PEA polyplexes in cancer cells. Effect of coupled VB6 in VBPEA compared to free VB6 in gene delivery (n = 3, error bar represents SD), (\*p < 0.05; \*\*p < 0.01, \*\*\*p < 0.001, one-way ANOVA).

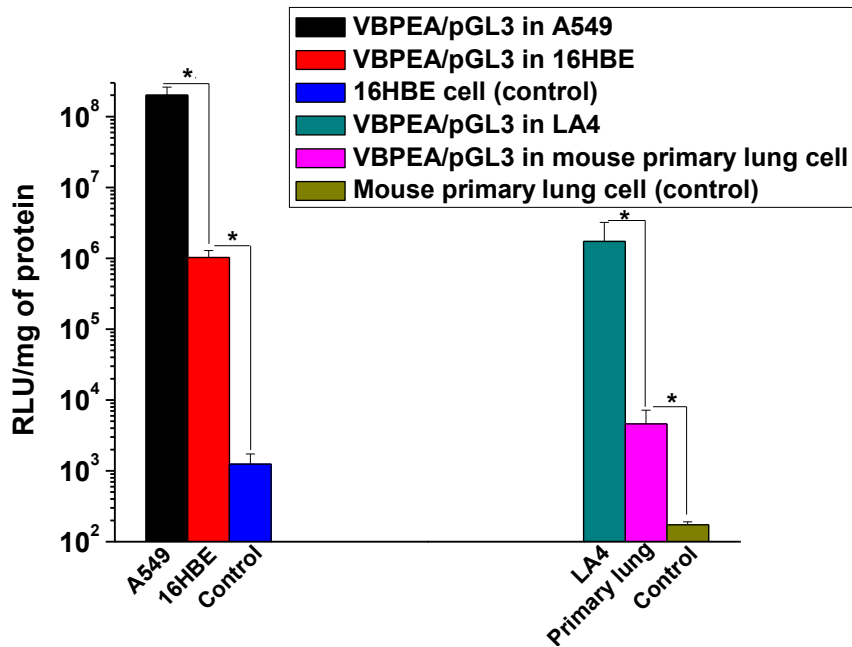


Figure 3.4. Uptake study of VBPEA/pGL3 by primary cells vs. cancer cells in human and mouse lung cell lines showing enhanced uptake by cancer cells (n = 3, error bar represents SD), (\*p < 0.05; \*\*p < 0.01, \*\*\*p < 0.001, one-way ANOVA).

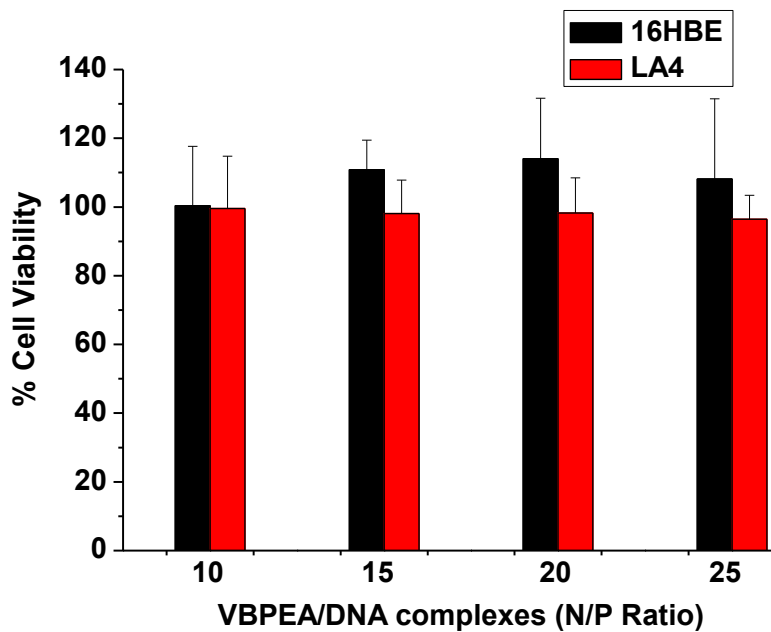


Figure 3.5. Cytotoxicity of VBPEA/DNA complexes in 16HBE (human) and LA4 (mouse) normal lung cell lines at various N/P ratios. (n = 3, error bar represents SD).

### **3.3.3. VBPEA elicit clathrin- and caveolae-mediated endocytosis and endosomal escape**

Caveolae endocytic inhibitors  $\beta$ -methyl cyclodextrin and genistein, which deplete the cholesterol rafts of caveolae, result in a gradual decrease in VBPEA and PEA-mediated transfection, suggesting a caveolae route of internalization utilized by both transporters. In contrast, clathrin-mediated endocytosis studied using chlorpromazine inhibitor showed decreased transfection of VBPEA/DNA complexes, whereas PEA/DNA complexes showed no loss in transfection (Figure 3.6). The clathrin pathway is likely to be initiated by VBPEA because of the involvement of VTCs in its uptake process, whereas PEA does not follow clathrin-mediated endocytosis due to the lack of carrier participation. Furthermore, inhibition of vacuolar type  $H^+$ -ATPases by bafilomycin A1 showed a 1000-fold decrease in the transfection of VBPEA, suggesting the ability of VBPEA to induce endosome acidification (Figure 3.7). The inhibitor prevented endosomal acidification and hence ceased its bursting to release the transporter.

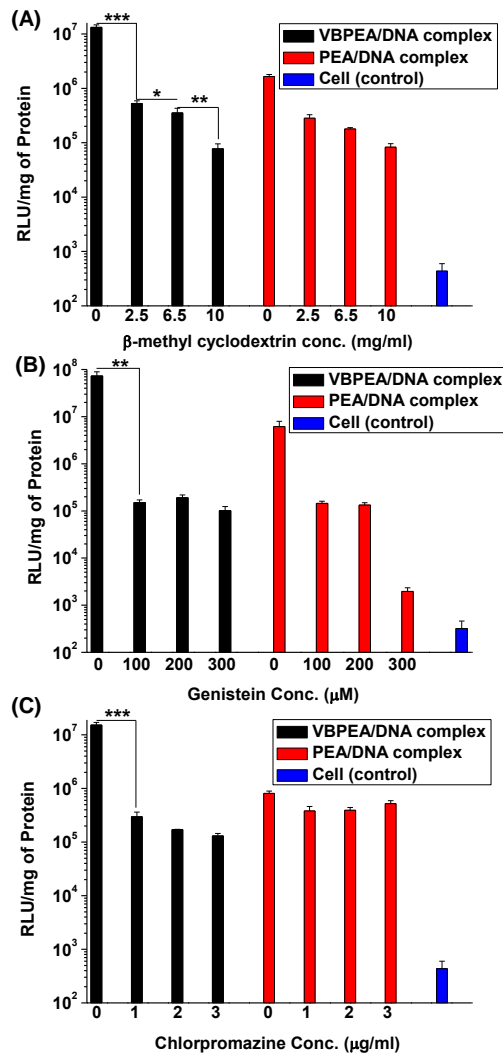


Figure 3.6. Effect of caveolae- and clathrin- endocytic inhibitors on transfection. Caveolae-endocytic inhibitors (A)  $\beta$ -methyl cyclodextrin, (B) genistein and clathrin-endocytic inhibitor (C) chlorpromazine. (n = 3, error bar represents SD), (\*p < 0.05; \*\*p < 0.01, \*\*\*p < 0.001, one-way ANOVA).

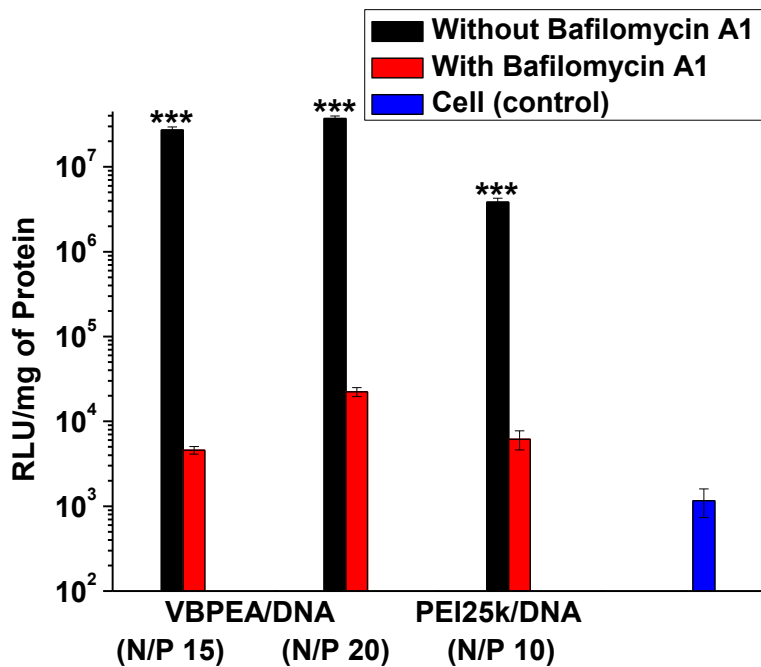


Figure 3.7. Bafilomycin A1 studies to show endosomal escape ability of VBPEA. (n = 3, error bar represents SD), (\*\*\*)p < 0.001, one-way ANOVA).

### 3.4 Discussion

The enhancement in transfection efficiency of VBPEA both *in vitro* and *in vivo* relative to PEA (Figure 2.8, 2.12), suggests the involvement of VB<sub>6</sub> specific membrane carriers in its uptake process due to incorporated VB<sub>6</sub>. The coupled VB<sub>6</sub>-mediated uptake of polyplexes was investigated by the effect of 4'-deoxyripyridoxine, which is a structural analog of VB<sub>6</sub>, on the transfection efficiency of VBPEA and PEA. It was observed that 4'-deoxyripyridoxine reduced the transfection activity of VBPEA but had no effect on PEA transfection, suggesting that 4'-deoxyripyridoxine competitively inhibited VBPEA cellular uptake by obstructing VB<sub>6</sub>-mediated cellular entry. This indicated the involvement of VTCs in polyplex transport into cells. When VTCs on the cell membrane were competitively inhibited, the VB<sub>6</sub> in VBPEA is unable to enhance transfection. Confocal studies in the presence of inhibitor also showed a reduction in the internalization of polyplexes compared to that in the absence of inhibitor. This hypothesis was further supported when PEA along with unbound VB<sub>6</sub> experienced no enhancement in expression of transgenic product. We concluded that

the addition of free VB<sub>6</sub> to PEA/DNA complexes exerted no effect on complex internalization; instead, VB<sub>6</sub> itself easily passed through the membrane carrier. This clearly demonstrated the role of VB<sub>6</sub>-coupled to PEA in enhancing polyplex uptake by co-transporting the vector with VB<sub>6</sub> attached to the VTC. A speculative representation of the involvement of VTC in VBPEA/DNA transport into cell is shown in Figure 3.8A. VBPEA-mediated transfection was found to be sensitive to bafilomycin A1, a specific inhibitor of vacuolar-type H<sup>+</sup>-ATPases [134], suggesting that PEI has a role in the endosomal release of VBPEA/DNA complexes via a ‘proton sponge’ effect, helping it to escape the aggressive endosomal nucleases in the cytoplasm. However, it is noteworthy that, even in the presence of bafilomycin A1, VBPEA showed an approximately 10-fold higher level of transfection than PEI25k (Figure 3.7), suggesting that increased cellular uptake is more important than endosomal escape in order to achieve high transfection.

In general, VB<sub>6</sub> is absorbed into the bloodstream from the intestine via simple diffusion, where it travels in its activated form (PLP). Before cellular uptake, it is dephosphorylated by a membrane-bound alkaline

phosphatase and enters the cell via a VTC through facilitated diffusion. Pyridoxal kinase rephosphorylates it to PLP so that it can participate in various cellular catalytic reactions [119, 126]. A schematic representation of a hypothetical mechanism of enhanced transfection of VBPEA based on available mechanistic studies is shown in figure 3.8B. Cells displaying VTC on their membrane specifically transport VB<sub>6</sub> inside cells; however, these membrane carriers are not able to transport the VB<sub>6</sub> in VBPEA/DNA polyplexes due to their large sizes. Consequently, polyplexes bound to the inactivated VTC are endocytosed as a cellular clearing mechanism. Its sojourn towards lysosomal fusion is halted due to the proton sponge effect, which leads to endosomal escape and subsequent gene delivery into the nucleus. In addition endocytosis inhibition studies of VBPEA showed both clathrin- and caveolae-mediated endocytosis, indicating the involvement of VTC in the VBPEA internalization process.

Since VB<sub>6</sub> is essential for the growth and proliferation of cells, it becomes an important requisite for cancerous tissues. In addition, there is evidence that serine hydroxymethyltransferase (SHMT), a VB<sub>6</sub>-

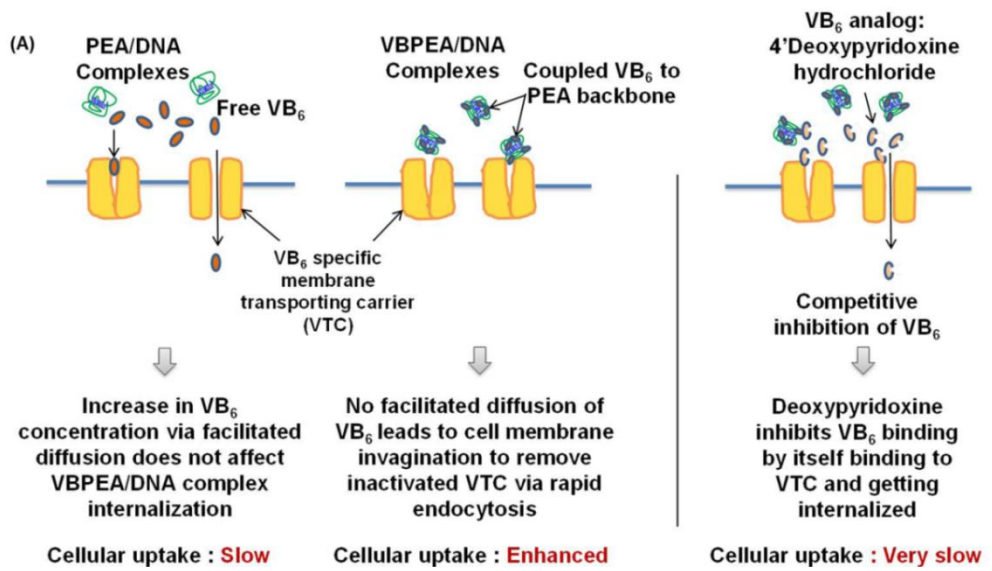


Figure 3.8. (A) A speculative representation of the involvement of a VTC in VBPEA/DNA transport. Figures do not represent the scale of the molecule.

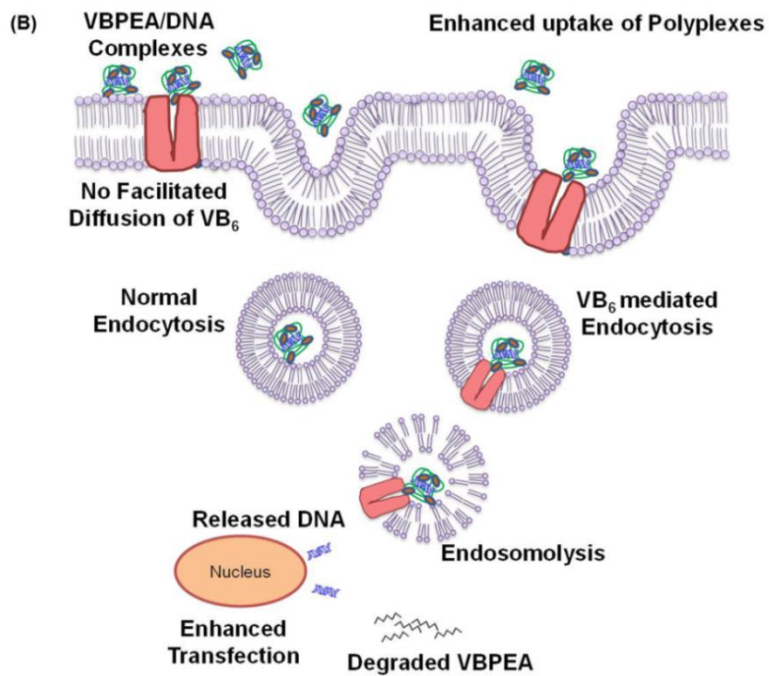


Figure 3.8. (B) A schematic representation of a hypothetical mechanism of cellular internalization of VBPEA/DNA complexes. Figures do not represent the scale of the molecule.

dependent enzyme, is associated with the increased demand for DNA biosynthesis during tumor proliferation. In order to support their uncontrolled proliferation, tumors have a constant need for this vitamin to synthesize DNA [133]. Due to this cancer cells show higher affinity towards VBPEA coupled with VB<sub>6</sub> and hence elevated transfection level was observed in comparison to normal cells. Therefore, we anticipate that our newly synthesized gene transporter can be used in cancer gene therapy with specificity and efficiency to deliver therapeutic siRNA targeting VB<sub>6</sub>-dependent enzymes. The attributes of VB<sub>6</sub> demonstrated in the present study show its potential applications in developing more profound gene and drug delivery systems.

### **3.5 Conclusion**

Competitive inhibition studies with 4'-deoxyribose indicated that VTCs play a crucial role in enhancing the cellular uptake of VBPEA, which was inactivated by the attachment of large polyplexes and resulted in endosome formation. Although the exact mechanism of the enhanced affinity of VBPEA towards cancer cells is not clear at this point, we speculate that, in order to support their uncontrolled growth

and proliferation, cancer cells constantly require VB<sub>6</sub> for various metabolic reactions, resulting in increased VBPEA uptake. Ongoing studies are focusing on the cellular signaling mechanism involved in increasing the affinity of VBPEA in cancer cells and exploring its therapeutic applications using siRNA.

# CHAPTER 4

## *Gene Silencing Efficiency of Vitamin B6-Coupled Poly(ester amine)*

---

### 4.1 Introduction

The phenomena RNA interference (RNAi) first discovered in the nematode worm *Caenorhabditis elegans*, is a conserved biological response of double-stranded RNA (~ 21 nucleotides long) which impose resistance to both endogenous parasitic and exogenous pathogenic nucleic acids and regulates the expression of genes post transcriptionally [135]. Fire, Mello and colleagues discovered that dsRNA mixture was at least tenfold more potent in triggering silencing effect than the sense or antisense RNAs alone [136]. Since then RNAi has become a valuable research tool, both *in vitro* and *in vivo*, because

synthetic dsRNA can selectively and robustly suppress the products of specific genes of interest when introduced into cells.

RNAi can be induced either by miRNA or siRNA. Both function via the same mechanism and using the similar silencing machinery, the difference lies in their origin. miRNA originates from a single strand RNA looped on itself which on cutting by Dicer appears double stranded. On the other hand, siRNA is actually formed from a double stranded RNA. Moreover, miRNA is synthesized endogenously in the cell to regulate the expression of genes whereas siRNA has exogenous origin which is foreign to cell.

RNAi technology is welcomed as one of the greatest medical advancements since antibiotics, with the potential to knockdown the genes that are responsible for cancer advancement, yet most laboratories are working dedicatedly to translate this RNAi technology from just a research tool into a usable therapeutic strategy. A major obstacle for RNAi remains the efficient delivery of these small molecules to the targeted cell type in vivo. Hence, the development of a suitable vector candidate with a conjugated targeting ligand becomes

the major area of research. Therefore, owing to higher affinity towards cancer cells, VBPEA gene transporter portrays an appropriate vector for delivering siRNA into the cancer cells.

## **4.2 Literature Review**

### **4.2.1. Components of RNAi machinery**

**Dicer** is an endoribonuclease that cleaves dsRNA and generates short dsRNA fragments called small interfering RNA (siRNA ~ 20-23 nucleotides long) with two base long 3' overhang and 5' phosphorylated terminus, both required for activity [137].

**RISC** is RNA-induced silencing complex. This multiprotein complex has helicase, exonuclease, endonuclease and homology searching proteins. Initially RISC is inactive until it is transformed into active form by unwinding of the siRNA duplex; loss of sense strand called as passenger strand and remains attached with the another antisense strand of siRNA called as the guide strand.

**Antisense** (guide) strand of siRNA defines specificity of RNAi by

guiding the RISC complex to its complementary mRNA. This strand serves as a template for recognizing the specific mRNA after which RISC activates the RNase activity and cleaves the mRNA, resulting in decreased level of protein translation and efficiently turning off the gene [138].

**Argonaute** protein acts as a slicer which functions as the catalytic component of the RISC complex. These proteins are key players in RNA silencing which can bind small non-coding RNAs and control protein synthesis, affect mRNA stability and even participate in the production of a different class of RNAs called Piwi interacting RNAs. These proteins are also responsible to some extent for the selection of guide strand and destruction of passage strand [139].

#### **4.2.2. Mechanism of RNAi**

A sequential RNAi pathway is illustrated in figure 4.1.

**A.** Introduction of dsRNA precursor triggers the RNAi pathway in cell's cytoplasm which accounts for the initiation of gene silencing.

**B.** Dicer which is a large multidomain cytoplasmic RNase III endonuclease enzyme cleaves the dsRNA precursor to produce double stranded fragments of small interfering RNA (siRNA) of approximately 21-23bp length with two base long 3'overhangs. Dicer producing siRNA is ATP dependent process with substrate specificity to dsRNA. It also need a dsRNA binding protein called R2D2 which has two dsRNA binding domains and function in association with RNase enzyme of dicer forming a heterodimeric complex [141]. It is unclear which of these domains physically bind to siRNA but is believed that siRNA binds at the interface between dicer and R2D2. This induces a conformational change in either or both the proteins allowing them to bind to siRNA simultaneously [142].

**C.** The next step is characterized by the formation of silencing complex called RISC (RNA Induced Silencing Complex). The double stranded siRNA unwinds and one out of the two single strands referred to as guide strand assembles into RISC. The other strand called passenger strand is degraded. The core of the RISC complex was found to be composed of highly conserved Argonaute (Ago) protein which has

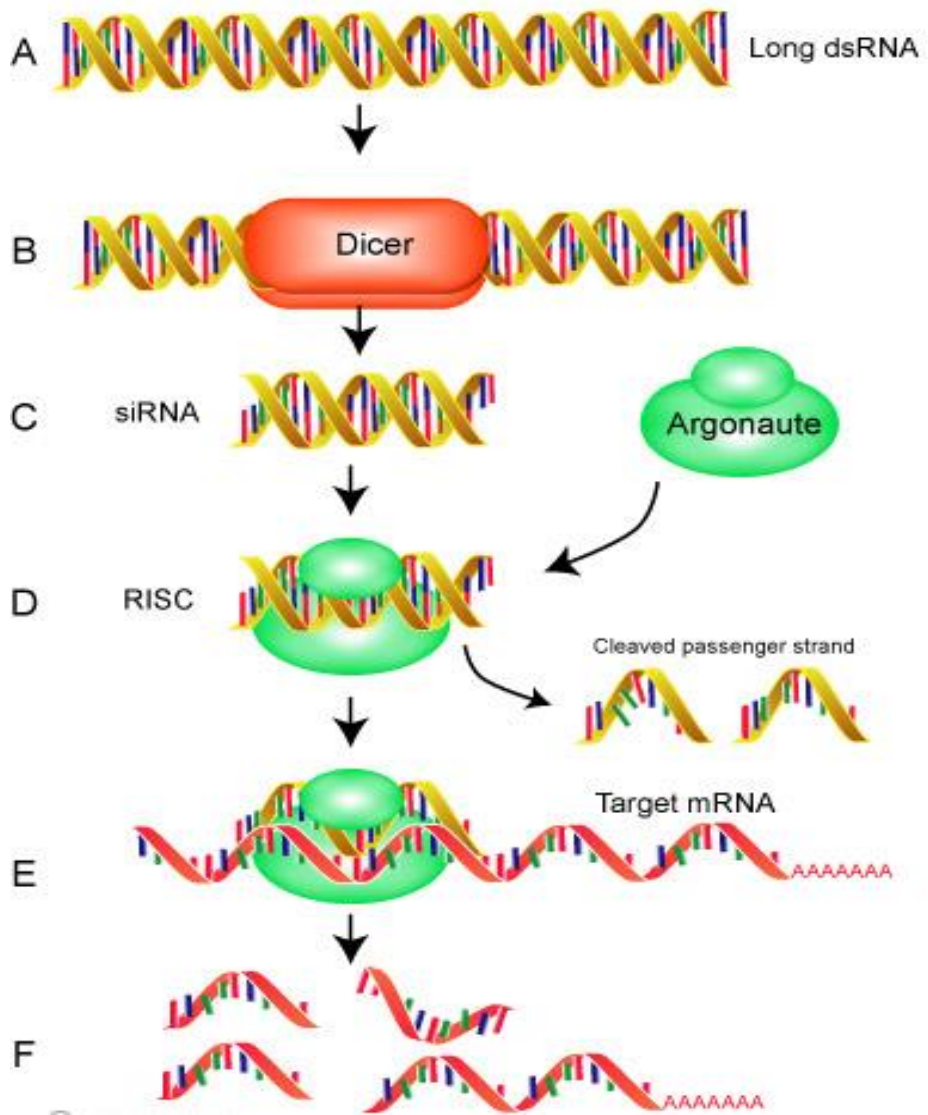


Figure 4.1. Mechanism of RNA interference. Adopted from Ref [140].

structural similarity with RNase H ribonuclease [143]. The Ago proteins serve to be the catalytic subunit of RISC. The orientation of the RISC with siRNA creates a thermodynamic asymmetry that helps in the separation of guide strand from the passenger strand [144].

This Ago protein dependent complex converts the pre-RISC containing the duplex siRNA into holo-RISC containing the guide strand of siRNA, by removing the passenger strand [144].

**D.** Antisense siRNA guide strand then guides the RISC to complementary mRNA molecules. The 5' end of siRNA acts as a target recognition site.

**E.** RISC cleaves the mRNA. The Ago subunit of holo-RISC acts as RNase H and cleaves the target mRNA backbone.

**F.** This leads to specific post transcriptional gene silencing.

## **4.3 Materials and Methods**

### **4.3.1. Materials**

bPEI 25kDa, and 3-(4, 5-dimethyl thiazol-2-yl)-2, 5-diphenyl tetrazolium bromide (MTT) reagent were purchased from Sigma (St. Louis, MO, USA). Luciferase reporter, pGL3- vector with SV-40 promoter and enhancer encoding firefly (*Photinus pyralis*) luciferase was obtained from Promega (Madison, WI, USA). The green fluorescent protein (GFP) gene was obtained from Clontech (Palo Alto, CA, USA). Nonspecific scrambled siRNA (siScr), luciferase siRNA and GFP siRNA (siGFP) (Table 4.1) were purchased from Genolution Pharmaceuticals, Inc. (Seoul, South Korea). All other chemicals used in this study were of analytical reagent grade.

#### **4.3.2. Synthesis and characterization of VBPEA/siRNA polyplexes**

The cationic VBPEA polymer at N/P 20 was electrostatically bound with siGFP (100 pM) in ultra-pure molecular grade water (WelGENE, S. Korea) (30 min incubation at RT) to form VBPEA/siGFP polyplexes. VBPEA/siRNA polyplexes were characterized using a transmission electron microscope (EF-TEM) (LIBRA 120, Carl Zeiss, Germany) and a dynamic light scattering spectrophotometer (DLS 8000, Otsuka Electronics, Osaka, Japan). The specimens for TEM were prepared by

Table 4.1. siRNA sequences

<b>siRNA</b>	<b>Sense (5'→3')</b>	<b>Anti-sense (5'→3')</b>
siRNA scrambled	CGUACGCGGAAUACUUCGAUU	UCGAAGUAUUCCGCGUACGUU
siRNA GFP	GUUCAGCGUGUCCGGCGAGUU	CUCGCCGGACACGCUGAACUU
siRNA Luciferase	CUUACGCUGAGUACUUCGAUU	UCGAAGUACUCAGCGUAAGUU

drop-coating the VBPEA/siRNA (N/P 20) polyplex dispersion onto a carbon grid and then dried for 2 h, after which it was stained with 1% uranyl acetate (10 s) and observed for its morphology. DLS samples were prepared at various N/P ratios (5, 10, 20, and 30) of VBPEA/siGFP polyplexes with 40  $\mu\text{g}/\text{mL}$  siGFP and then measured for their hydrodynamic size and zeta potential with  $90^\circ$  and  $20^\circ$  scattering angles at  $25^\circ\text{C}$ .

#### **4.3.3. Electrophoretic mobility shift assay (EMSA)**

VBPEA/siRNA polyplexes were characterized for siRNA retardation and protection assay. For siRNA retardation assay, VBPEA was complexed with siRNA (1  $\mu\text{g}$ ) for 30 min at RT at various N/P ratios (0.5, 1, 2, 3, and 5). The complexed samples and equivalent amounts of free siRNA with 1X loading dye (Biosesang, Korea) were added in individual wells in a 2% agarose gel (with 0.1  $\mu\text{g}/\text{mL}$  EtBr) casted in 1X TAE buffer. The samples were resolved for 40 min in 0.5X TAE running buffer at 100 V, and images were captured under ultraviolet illumination. For RNase protection assay, VBPEA/siRNA (N/P 20) polyplexes and free siRNA were incubated with RNase (1  $\mu\text{g}/\mu\text{L}$ ) at

37°C. After 30 min, RNase was inactivated by adding 5  $\mu$ L EDTA (100 mM) at 70°C for 10 min and incubated for another 30 min at RT. Finally, the protected siRNA was released from the complexes with the addition of 5  $\mu$ L 1% sodium dodecyl sulfate (SDS) for 2 h and resolved on a 2% agarose gel (with 0.1  $\mu$ g/mL EtBr) in 0.5X TAE running buffer at 100 V for 40 min.

#### **4.3.4. Cell culture**

Low passage adenocarcinoma human alveolar basal epithelial (A549) cells were cultured in T-75 culture flasks (Nunc, Thermo Scientific) in 15 mL complete medium containing Roswell Park Memorial Institute (RPMI)-1640 (HyClone Laboratories, USA) supplemented with 10% heat-inactivated fetal bovine serum (FBS, HyClone Laboratories, USA) and 1% antibiotic cocktail of streptomycin and penicillin. Cells were maintained under standard culture conditions of 37°C and 5% CO<sub>2</sub> for 4 or 5 days, with the culture duration selected to maintain cells under exponential growth and reach ~80% confluency. Cells were then trypsinized, centrifuged at 1200 RPM for 5 min to pellet cells and counted using hemocytometer to seed the cells for experimental assays.

#### **4.3.5. Confocal microscopy**

TRITC (Molecular Probes, Invitrogen, Oregon, USA) (25  $\mu$ L, 1 mg/100  $\mu$ L in DMF) was added to VBPEA (1 mL, 10 mg/mL in H<sub>2</sub>O) to block ~1% of its total amines, and the mixture was then stirred overnight (VBPEA<sup>T</sup>). Unreacted TRITC was removed by washing with ethyl acetate (3 x 2 mL), which was then lyophilized and resuspended in water. A549 cells were seeded at a density of 3 x 10<sup>5</sup> cells/well in a cover glass bottom dish (SPL Lifesciences, Korea) and incubated for 24 h in humidified chamber. Cells were transfected with VBPEA<sup>T</sup>/siRNA complexes and further incubated for 3 h, 2 d, 3 d, 5 d, 6 d, and 7 d to study the degradation profile of VBPEA polyplexes. The transfected A549 cells with fluorescently labeled complexes were washed 3 times with 1X PBS and then fixed with 4% paraformaldehyde for 10 min at 4°C. DAPI was used to counter-stain the nuclear DNA of fixed cells, and images were procured using a Leica SP8 X STED super-resolution laser scanning confocal microscope to monitor fluorescently labeled VBPEA<sup>T</sup>/siRNA complexes inside the treated A549 cells.

#### **4.3.6. Cell viability assay**

Cytotoxicity of VBPEA/siRNA (N/P 20), PEA/siRNA (N/P 20) and PEI25k/siRNA (N/P 10) polyplexes at various siRNA concentrations (0, 50, 100, 150 pM) and after different incubation times (3 h, 2 d, 5 d, 7d) were measured by the reduction of a tetrazolium component (3-(4,5-dimethylthiazol-2-yl)-2,5-diphenyltetrazolium bromide, or MTT) (Sigma, St. Louis, Mo, USA) into insoluble purple colored formazan crystals by the mitochondria of the viable cells. Polyplex transfected A549 cells that had been incubated in a 24-well plate ( $10 \times 10^4$  initial cell density/well) for 48 h were then incubated with MTT reagent (0.5 mg/mL in 1X PBS) for 3 h, followed by the addition of DMSO (500  $\mu$ L) to solubilize the colored crystals, and absorbance was measured at 540 nm using a Sunrise<sup>TM</sup> TECAN ELISA reader (Grödig, Austria).

#### **4.3.7. Silencing of luciferase activity**

A549 cell were transfected with Lipofectamine<sup>TM</sup>/pGL3 complexes in serum-free medium. After 3 h, the medium was aspirated and VBPEA/siLuc or siScr and PEA/siLuc or siScr complexes (N/P 20) were added containing 50, 75, 100 and 150 pM siRNA concentrations. Cells were incubated for additional 3 h, after which medium was

replaced with complete medium containing 10% serum. Finally, 24 h later luciferase expression was measured by luciferase assay and normalized with the protein concentration in the cell extract. The luciferase silencing efficiency was calculated as the relative percentage of luciferase activity to the control cells without siRNA treatment.

#### **4.3.8. GFP silencing efficiency by VBPEA**

A549 cells at 70% confluency ( $3 \times 10^5$  initial cell density/well) in a 6-well plate were transfected with Lipofectamine/tGFP (1  $\mu$ g) complex in serum-free medium according to the manufacturer's protocol (Invitrogen, Oregon, USA). After 3 hours, the medium was replaced with fresh serum-free RPMI-1640 medium with the VBPEA/siGFP complex (N/P 20) containing 100 pM of siRNA. The silencing efficiency was then compared with that of PEA/siGFP (N/P 20) and PEI25k/siGFP (N/P 10) mediated silencing. After 3 hours of incubation, the medium was again replaced with 10% serum-containing medium. After an additional 48 h, the silencing efficiency was measured using flow cytometry (BD Biosciences, San Jose, CA, USA). The percentage of GFP silencing in the cells treated with VBPEA/siGFP complexes

was calculated after normalizing the results with respective mock-treated cells and then compared to the silencing of the VBPEA/siScr-treated group. Nonspecific scrambled siRNA (siScr) and GFP siRNA (siGFP) (Table 4.1) were purchased from Genolution Pharmaceuticals, Inc. (Seoul, South Korea).

## **4.4 Results**

### **4.4.1. VBPEA represents an efficient siRNA transporter**

Electrophoretic mobility shift assay demonstrated VBPEA's high complexation ability with siRNA and its ability to protect siRNA against intracellular RNase degradation (Figure 4.2a, b). Dynamic light scattering spectrophotometry (DLS) and EF-TEM images showed nanosized VBPEA/siRNA polyplexes suitable for cellular uptake. A decreasing trend in VBPEA/siRNA polyplex size (from 180 to 110 nm) and zeta potential (from +44 to +38 mV) suggest stronger condensation of VBPEA with siRNA with increasing N/P ratios (Figure 4.2c). EF-TEM images showed a uniform particle size distribution (< 100 nm)

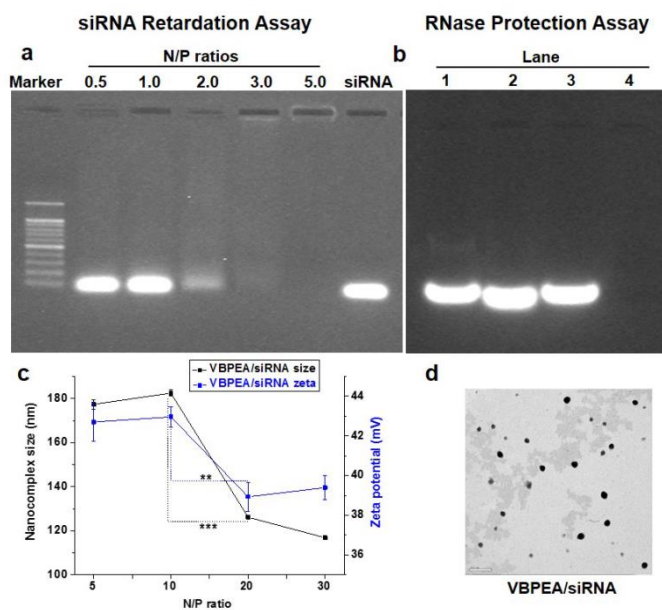


Figure 4.2. Physicochemical characterization of VBPEA/siRNA complexes. (a) Gel electrophoresis of VBPEA/siRNA (0.1  $\mu\text{g}$ ) complexes at various N/P ratios (0.5, 1, 2, 3, and 5) shows complete siRNA retardation at an N/P ratio of 3. (b) RNase protection and release assay. Complexed siRNA with VBPEA (N/P 20) was released using 1% SDS: (Lane 1) VBPEA/siRNA complexes without RNase; (Lane 2) VBPEA/siRNA complexes with RNase (1  $\mu\text{g}/\mu\text{L}$ ) demonstrates the protection of the siRNA; (Lane 3) free siRNA without RNase; (Lane 4) free siRNA with RNase (1  $\mu\text{g}/\mu\text{L}$ ) shows its complete degradation. (c) Particle size and zeta potential of VBPEA/siRNA complexes at various N/P ratios (5, 10, 20, and 30) shows its size  $\sim 110$  nm and zeta potential +38 mV ( $n = 3$ , error bar represents SD) (\*\* $P < 0.01$ ; \*\*\* $P < 0.001$ , one-way ANOVA). (d) EF-TEM image of VBPEA/siRNA (N/P 20) complexes shows its size  $\sim 100$  nm (scale bar: 200 nm).

without aggregation (Figure 4.2d), suggesting their efficient cellular uptake.

#### **4.4.2. Enhanced in vitro cell viability and degradation profile of VBPEA/siRNA complexes**

The lower surface charge and non-aggregation of the VBPEA polyplexes (Figure 4.2c, d) does not disrupt the integrity of the cell membrane surface [123, 145] which results in higher cell viability of VBPEA/siRNA complexes (> 98%) in comparison to PEA/siRNA (~85-95%) and PEI25k/siRNA (~60%) complexes (Figure 4.3) in A549 cells. In addition, the presence of degradable ester linkages in VBPEA backbone (Figure 2.1) ensured a gradual disappearance of VBPEA after 3 h, 2, 3, 5, 6, and 7 days of transfection (Figure 4.4) by hydrolyzing into smaller degradation products that can be exocytosed [146]. Therefore, the occurrence of vesicles was observed to increase with time (maximum on day 5). This further increases the cell viability of VBPEA complexes (Figure 4.5) and makes VBPEA innocuous for cellular uptake.

#### **4.4.3. GFP silencing efficiency of VBPEA/siGFP complexes**

The gene silencing efficiency of vectors was analyzed by suppressing transgenic GFP expression in A549 cells. VBPEA/siGFP exhibited 67% GFP silencing in comparison to 41% by PEA/siGFP, 32% by PEI25k/siGFP and negligible by naked siGFP and complexes with non-specific scrambled siRNA (siScr) (Figure 4.6).

#### **4.4.4. Luciferase silencing efficiency of VBPEA/siLuc complexes**

Luciferase expression was silenced with luciferase siRNA (siLuc). VBPEA/siLuc showed an increased silencing efficiency reaching upto 94% in comparison to PEA/siLuc. The silencing activity becomes stable after 100 pM of siRNA concentration. As expected, nonspecific scrambled siRNA (siScr) and naked siLuc exhibited negligible silencing (Figure 4.7). Cell viability assay verifies that the improved VBPEA-mediated gene silencing was not affected by cellular cytotoxicity (Figure 4.3). The results reflect the potential of VBPEA to silence VB<sub>6</sub> dependent enzymes which are involved in cancer cell proliferation as an anticancer therapeutic strategy.

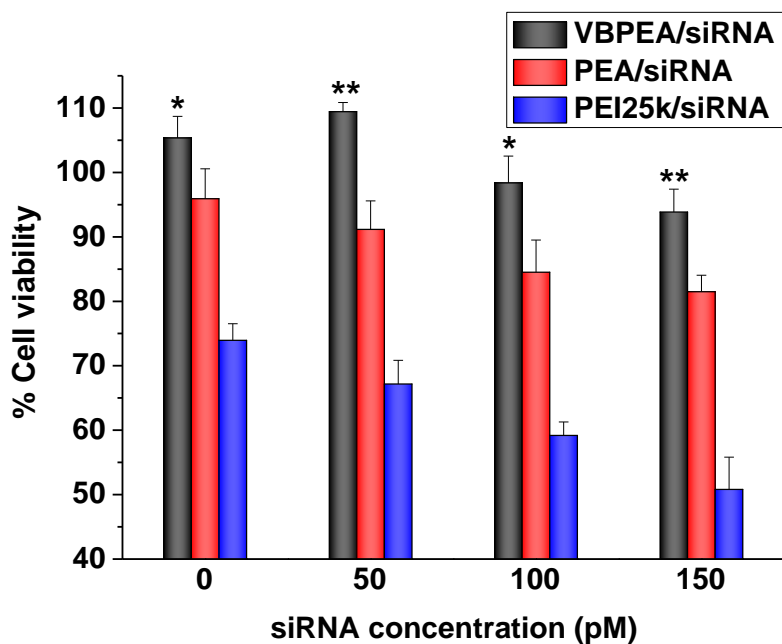


Figure 4.3. Cytotoxicity of VBPEA/siRNA complexes at various siRNA concentrations (0, 50, 100, 150 pM) show no cytotoxicity. (n = 3, error bar represents SD) (\*P < 0.05; \*\*P < 0.01, one-way ANOVA).

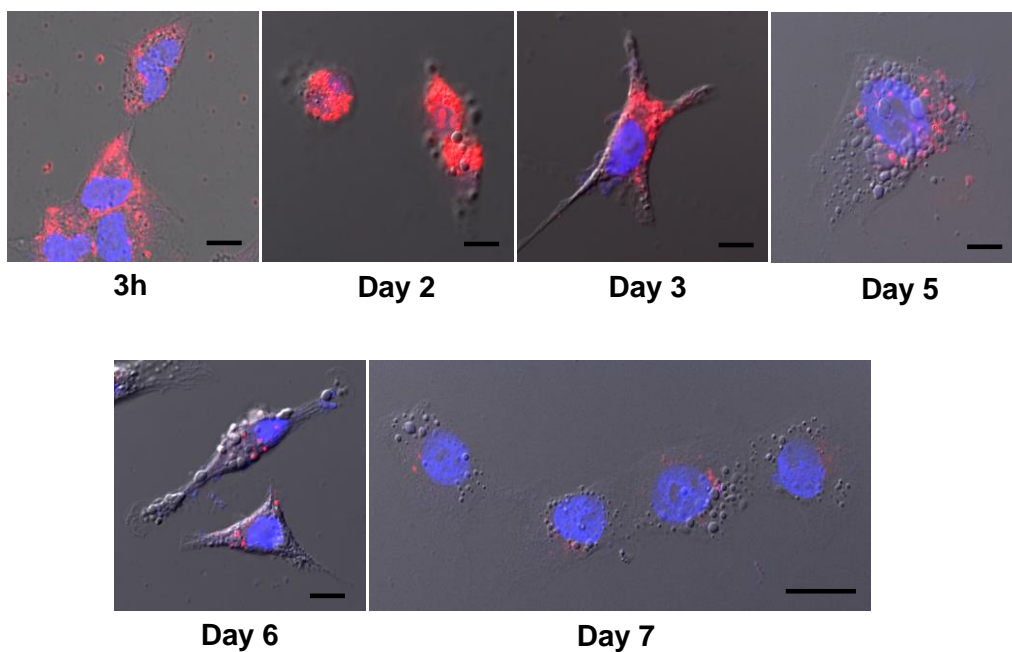


Figure 4.4. Study of VBPEA<sup>T</sup>/siRNA nanoplex uptake and degradation in A549 cells. Confocal microscopic images of A549 cells with DAPI nuclear staining (blue), observed up to 7 days following transfection with TRITC-labeled VBPEA<sup>T</sup> (red). VBPEA<sup>T</sup> after cellular uptake (3 h) (scale bar: 10  $\mu\text{m}$ ) is gradually degraded up to day 7 (scale bar: 20  $\mu\text{m}$ ), and the occurrence of vesicular structures represents the increased exocytosis of fragmented VBPEA<sup>T</sup>.

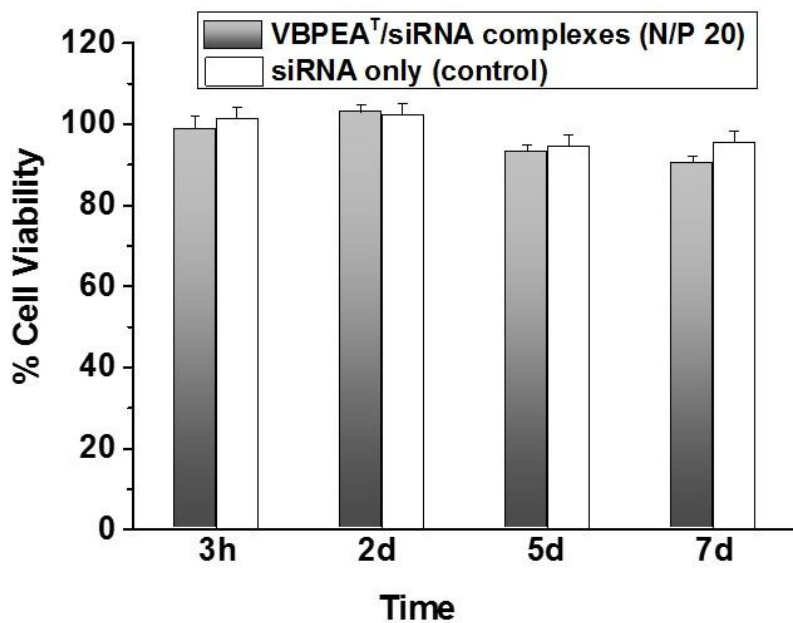


Figure 4.5. Cytotoxicity measurements of VBPEAT/siRNA (N/P 20) complexes by MTT assay after 3 h, 2d, 5d, and 7d of transfection in A549 cells show no cytotoxic effects. Statistical significance was determined using one-way ANOVA (n = 3, error bar represents SD).

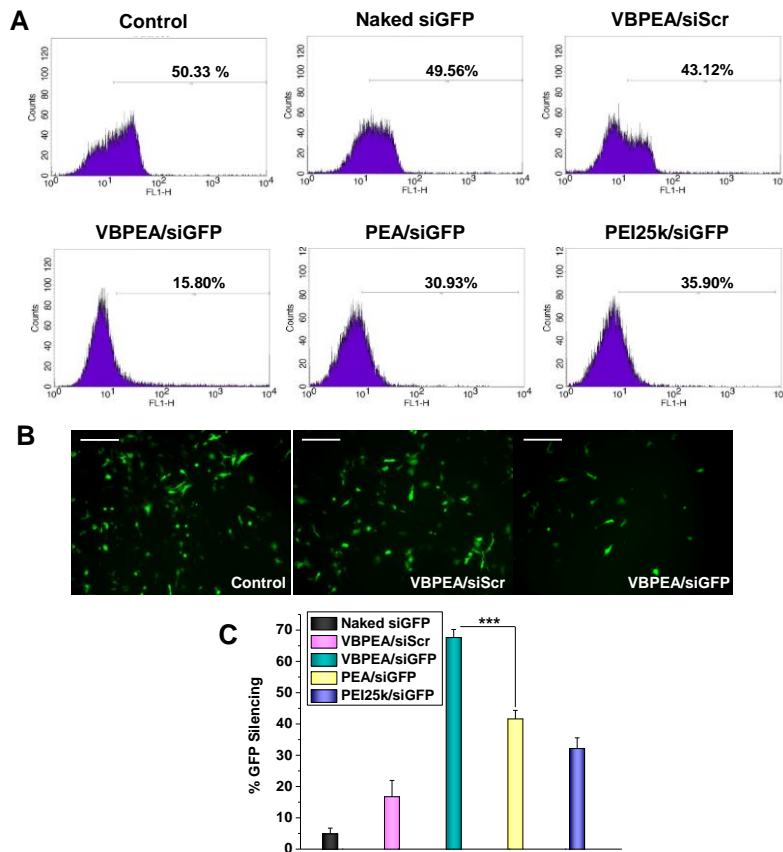


Figure 4.6. GFP silencing efficiency of VBPEA/siRNA complexes in A549 cells. (A) Pre-transfected GFP gene was silenced using siGFP (100 pM) complexed with VBPEA (N/P 20), and transgene expression was measured using FACS. (B) Corresponding transfection images were taken with a Nikon fluorescence microscope (scale bar: 500  $\mu$ m) to show maximum GFP suppression by VBPEA mediated siGFP delivery. (C) %GFP silencing was calculated in reference to the control cells without siGFP treatment, and maximum silencing was found to be mediated by VBPEA (67%) (n = 3, error bar represents SD) (\*P < 0.05; \*\*P < 0.01, one-way ANOVA).

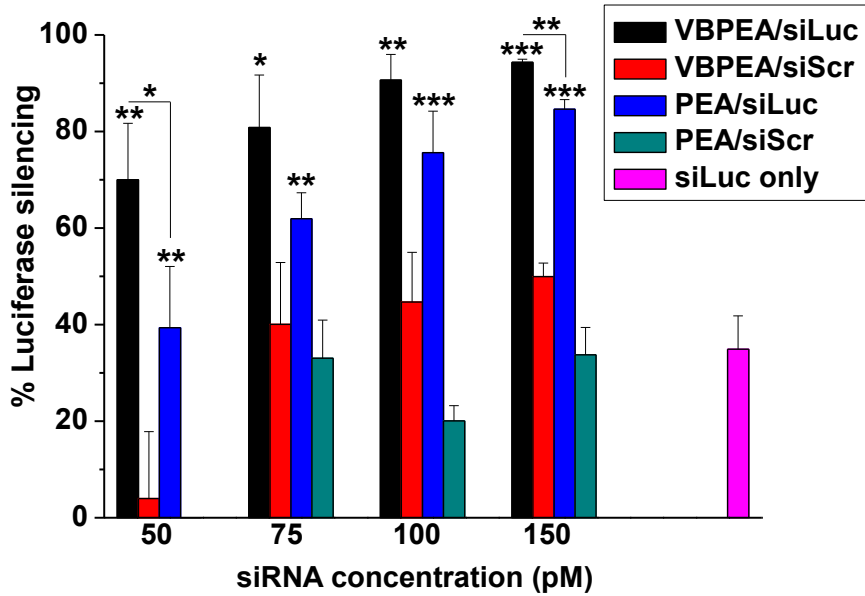


Figure 4.7. Silencing efficacy of VBPEA/siLuc and PEA/siLuc complexes in A549 cells compared to the respective scrambled siRNA (siScr) group (n = 3, error bar represents SD), (\*p < 0.05; \*\*p < 0.01, \*\*\*p < 0.001, one-way ANOVA).

## **4.5 Discussion**

VBPEA resulted not only in ~100 nm size of compact nanoplexes after complexation with siRNA, but also demonstrated to protect the complexed siRNA against nuclease degradation in the biological milieu. VBPEA/siRNA complexes showed high cell viability due to the presence of ester linkages in the polymer backbone. This was responsible for its gradual degradation and subsequent exocytosis by hydrolyzing into respective acid and alcohol degradation products of smaller molecular weights. Therefore, a higher silencing efficiency of VBPEA over PEA and PEI25k nanoplexes was achieved in cancer cells that showed the potential of VBPEA gene transporter for its use in cancer gene therapy.

## **4.6 Conclusion**

RNA interference through siRNA, shRNA, miRNA has contributed to the better understanding of neoplasia and proposes a great promise for anti-cancer therapeutics. A long term accumulation of genetic and epigenetic aberrations take the form of cancer. There is not one reason

for the cause of cancer and creates heterogeneity among patients. Therefore, there are different responses to the standard therapeutic approaches. It necessitates for analyzing molecular profiles of individual cancer patients and to develop a personalized therapy programs. This therapeutic approach requires specificity and adaptability to the particular patient which could be rendered by the RNAi technique. To imply the RNAi technology against cancer, the limitations of target selection, delivery agent, and off-target effects need to be considered. However, novel RNAi and delivery vectors with the conjugated vitamin B6 as a targeting ligand may solve the problem and hopefully help in the development of effective anti-cancer therapy.

# CHAPTER 5

## *Nucleotide Biosynthesis Arrest by Silencing SHMT1 Function*

---

### 5.1 Introduction

Serine hydroxymethyltransferase (SHMT) is one of the components of a multi-enzyme complex involved in the *de novo* thymidylate biosynthesis pathway that catalyzes a reaction to generate one-carbon supply for the downstream synthesis of thymidylate, purine and methionine [147]. During cell proliferation, SHMT isoforms cytoplasmic SHMT1 & mitochondrial SHMT2 $\alpha$  are found in high concentrations due to their active participation in DNA biosynthesis [148] performing two major functions. First, it catalyzes the reversible conversion of serine to glycine by transferring serine-carbon to tetrahydrofolate (THF) yielding methylene-THF, the one-carbon donor

which methylates dUMP to dTMP for the synthesis of thymine nucleotides [147, 149]. Second, it serves as a scaffold protein essential for multi-enzyme complex formation [148]. This metabolic complex associates with the nuclear lamina and is enriched at sites of DNA replication initiation during the S and G2/M phases of cell cycle [148] (Figure 5.1A, B). Due to its pivotal role in the *de novo* thymidylate biosynthesis, the only cellular pathway for thymine synthesis [149], SHMT expression becomes a rate limiting factor [148]. Therefore, SHMT activity is correlated with an increased demand for DNA biosynthesis and is evidenced in fast proliferating tumor cells to preferentially channel serine for rapid DNA duplication [133, 150, 151]. Alternatively, the abnormal SHMT overexpression may influence the process of carcinogenesis in terms of both the development and genesis of tumor. Consequently, the central role of SHMT in nucleotide biosynthesis makes SHMT an attractive target [151], whereby reducing its activity could cease the DNA synthesis machinery of cancer cells. Moreover, cancer cells have greater requirements for nucleotides and, therefore, are more sensitive than normal cells towards the inhibition of nucleotide biosynthesis [149]. Although SHMT2 found to be

overexpressed in certain cancer cell lines and silencing of this isoform slows down proliferation to some extent [152], the effect of SHMT1 silencing on cancer progression has yet not been sufficiently explored.

Among the three enzymes of the thymidylate synthase cycle, SHMT1 is the only enzyme that remains uninvestigated as a target for chemotherapy [153]. The other two enzymes, thymidylate synthase (TYMS) and dihydrofolate reductase (DHFR) are targeted by clinically practiced chemotherapeutic drugs [149, 154-156]. However, the emergence of drug resistance is a major problem for the prolonged use of these drugs [157, 158], making it necessary for an alternative approach to target SHMT1. In this study, we propose a siRNA technology based SHMT1 silencing-mediated cancer therapy with presumably no chance for the development of drug resistance. However, in spite of specificity, potency and versatility to silence the expression of a desired gene [159], the high therapeutic potential of siRNA approach to the treatment of severe and chronic diseases has not yet been successfully translated clinically, owing to major limitations such as difficult cellular uptake, low transfection capability, short half-life

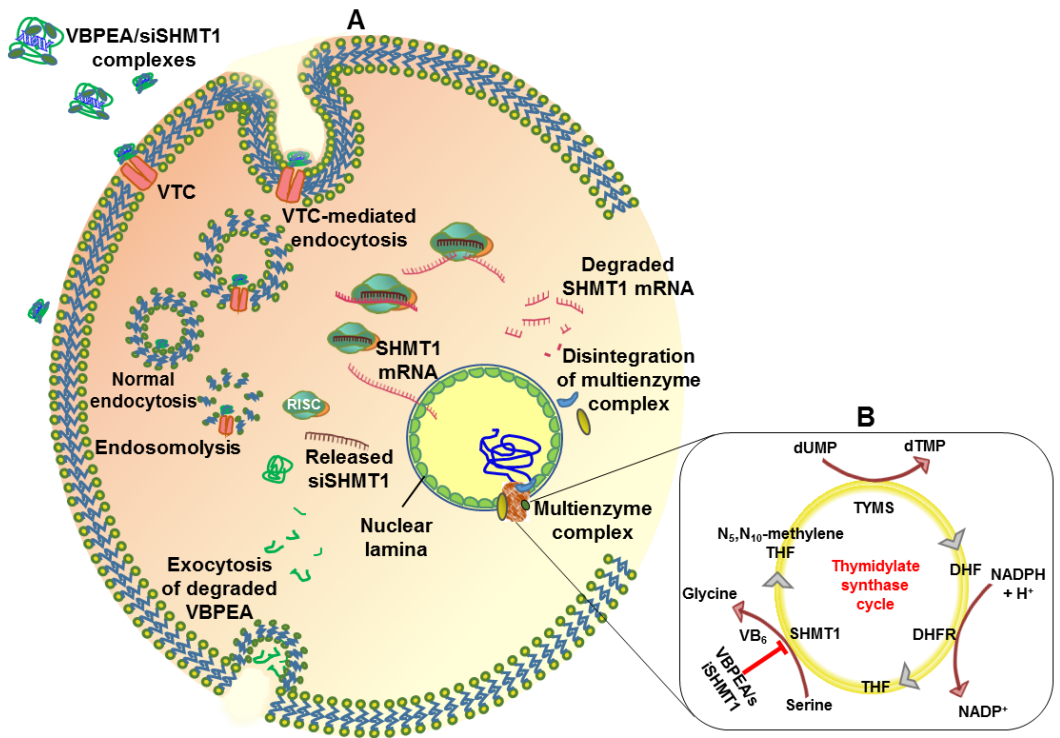


Figure 5.1. Schematic illustration of silencing events after the delivery of VBPEA-mediated siSHMT1 (A) VBPEA-mediated SHMT1 silencing, (B) interruption of thymidylate synthase cycle. Figures do not represent the scale of the molecules.

and insufficient bioavailability [160]. Thus, an efficient transporter for SHMT1 siRNA (siSHMT1) delivery is a vital requisite between siRNA technology and its therapeutic applications.

Vitamin B<sub>6</sub>-coupled poly(ester amine) (VBPEA) recently synthesized in our laboratory (Figure 2.1) shows high transfection activity in cancer cells, due to VB<sub>6</sub> coupling that utilizes the VB<sub>6</sub> transporting membrane carrier (VTC)-mediated uptake mechanism, leading to enhanced vector transport [146, 161, 162].

Interestingly, SHMT1 is one of the VB<sub>6</sub>-dependent enzymes that become functional when the VB<sub>6</sub> cofactor is bound to its active site [151, 163]. Due to its involvement in various cellular metabolic processes, VB<sub>6</sub> availability is expected to augment the process of carcinogenesis by keeping the DNA synthesis machinery functional through SHMT1 catalyzed reactions [164]. Consequently, VB<sub>6</sub> uptake from the neighboring tissues increases to support tumor growth [132, 133]. In short, the increased DNA requirement enhances SHMT1 activity [151, 165] which enforces increased VB<sub>6</sub> uptake in cancer cells than normal cells [146, 151, 164] and therefore a vector coupled to VB<sub>6</sub>

may experience enhanced cellular uptake [146, 166, 167]. Hence, we hypothesize that due to the increased membrane transport efficiency of VBPEA [146], the complexed siSHMT1 could be trailed along with the vector inside the cell. Accordingly, we investigated the efficacy of VBPEA/siSHMT1 system to down regulate the overexpressed SHMT1 gene responsible for rapid DNA synthesis in cancer cells both *in vitro* and in xenograft mice. Because SHMT1 controls a fundamental rate limiting step in DNA synthesis, silencing its activity is anticipated to result in decreased cell proliferation and tumor growth inhibition. Therefore, the impact of SHMT1 knockdown on the integrity of multi-enzyme complex, cell cycle and DNA synthesis of cancer cells was assessed.

## **5.2 Literature Review**

Cancer being one of the most prevalent diseases of the world reflects disturbances of the basic rules of cell behavior in a multicellular organism. The body of an animal represents a society or ecosystem composed of individual cells which are reproducing by programmed cell division and well organized into collaborative tissues. The only

difference from ecological system is the lack of natural selection and competition where the basic rule is self-sacrifice as all the somatic cells are destined to die after propagating their clonal progeny. But in cancer selfish behavior of individual mutant cells within the population of somatic cells prosper at the expense of their neighbors leading to the destruction of the whole cellular society [168].

Cancer cells are neoplastic (uncontrolled proliferation) and malignant (invade and colonize surrounding tissues). A general concept is that a single cell mutation causes additional mutations on proliferation of the cell to result in a full blown tumor. The tumor cells may further metastasize giving rise to secondary tumors, difficult to eradicate surgically. Therefore, in order to devise rational ways to cure it, the understanding of the cancer cell's inner malfunctioning and intercommunication with other cells is necessary [169]. Neoplastic cell proliferation is often associated with a block in differentiation whereby the stem cells continue to divide which can be curbed by promoting cell differentiation. The tumor cells must cross the basal lamina to become malignant which can be obstructed by designing specific antibodies to

interfere its invasion. The characteristic of the cancer cells to easily mutate helps them to develop resistance to anticancer drugs. However, the DNA metabolism underlying such mutations can be selected for therapeutic attack which is the focus of discussion in this chapter.

The prevailing anticancer therapy includes surgical removal of the benign tumor if detected at an early stage, or destruction with toxic chemicals or radiation which are toxic to the normal cells as well. Moreover, eradication of every single cancer cell is very difficult. Hence, an alternative approach is in demand for cancer therapy. Fire and Mello who received Noble Prize for discovering RNA interference (RNAi) in 1998, have opened an era for increased understanding of the molecular mechanisms involved in the development of cancer and devising probable therapeutics against cancer by performing targeted gene silencing [136]. RNAi is a post-transcriptional process whereby the transcribed mRNA is degraded by a double stranded RNA molecule to regulate the gene expression [170]. Since the remarkable breakthrough, RNAi therapeutics has gained considerable advancements against various diseases including viral infections and

cancer [171].

## **5.2.1. Cancer cell growth and proliferation**

### ***5.2.1.1. Key behavior of cancer cells in general***

1. Self-sufficient – the cancer cells reproduce in defiance to normal restraints because they become self-supportive for the supply of nutrients and oxygen.
2. Insensitive to anti-proliferative extracellular signals –The normal cells that stop dividing due to contact inhibition, the abnormal cells continue dividing to give rise to neoplasm – a relentlessly growing mass of abnormal cells, which become impervious to anti-proliferative signals.
3. Less prone to apoptosis – Due to development of certain mutations cancer cells escape the programmed cell death mechanism and keep dividing to form a tumor.
4. Defective in intracellular control mechanisms (abnormal proliferation) - The cancer cells in contrast to normal cells

which are under strong vigilance of cell cycle check points, defy and surpass the cell cycle control system.

5. Induce help from normal stromal cells – To compensate the increased demand of nutrition, cancer cells drive it from their neighboring stromal cells.
6. Induce angiogenesis – Angiogenesis is a key feature of tumor growth and proliferation to support their need for blood supply and exchange of gases in deep seated compact cell mass.
7. Escape from their home tissue – Tumor becomes seriously dangerous when it becomes malignant, that is, capable of invading the surrounding tissues usually far away from the original tissue. Tumor cells break loose, enter the blood stream and form secondary tumors at other sites in the body (Figure 5.2).
8. Genetically unstable – Cancer is caused by mutations that cause cells not only to grow indefinitely but also uncontrollably and invasively. They are genetically unstable due to establishment



Figure 5.2. Metastasis shown in the bone marrow from carcinoma of prostate gland. Adopted from Ref [140].

of multiple mutations which may be developed as an effect of mutagens.

9. Produce telomerase - Telomeres are specialized sequence of hundreds to thousands of tandem repeats at the ends of eukaryotic chromosomes which in normal somatic cells are lost (50-200 nucleotides) per cell division. DNA polymerase is unable to replicate these lost nucleotides. This loss of genetic material is what leads to aging and apoptosis (programed cell death). Telomerase is a ribonucleoprotein (enzyme) that synthesizes telomeric DNA which prevents the loss in telomere length. Although telomerase is suppressed in normal somatic cells, it is activated in cancer cells allowing the cells to replicate indefinitely as an immortal cell line [172].

#### ***5.2.1.2. Normal cell division with various check points***

The cell cycle control system is a set of coordinating proteins functioning cyclically which regulates the cell division at specific check points (Figure 5.3). These proteins have been conserved over a billion years through evolution. The two basic components of this system are: activating proteins called cyclins and cyclin dependent

kinases (Cdk), the complexes of which together regulate the normal cell cycle [173].

#### ***5.2.1.3. Tumor proliferation and uncontrolled division***

When the cell crosses all the cell cycle barriers it leads to duplication of cell. Cancer cells due to mutation keeps the cell cycle proteins in their active state to continuously replicate the DNA and divide the cell in uncontrolled fashion. The localized tumor mass is called benign which can be surgically removed but when it takes the form of metastases it migrates and invades other tissues to colonize in various body parts impossible to surgical removal and usually fatal (Figure 5.4 & 5.5).

#### ***5.2.1.4. Most cancers derive from a single abnormal cell***

A single cell that has undergone some heritable changes enables it to outgrow its neighbors. A single mutation is not sufficient to convert a healthy cell into a cancer cell. The genesis of a cancer is evidenced by the fact that it requires several independent mutational accidents to occur together in one cell. These events may then cause the establishment of cancer which further proliferate and invade the neighboring tissues (Figure 5.6).

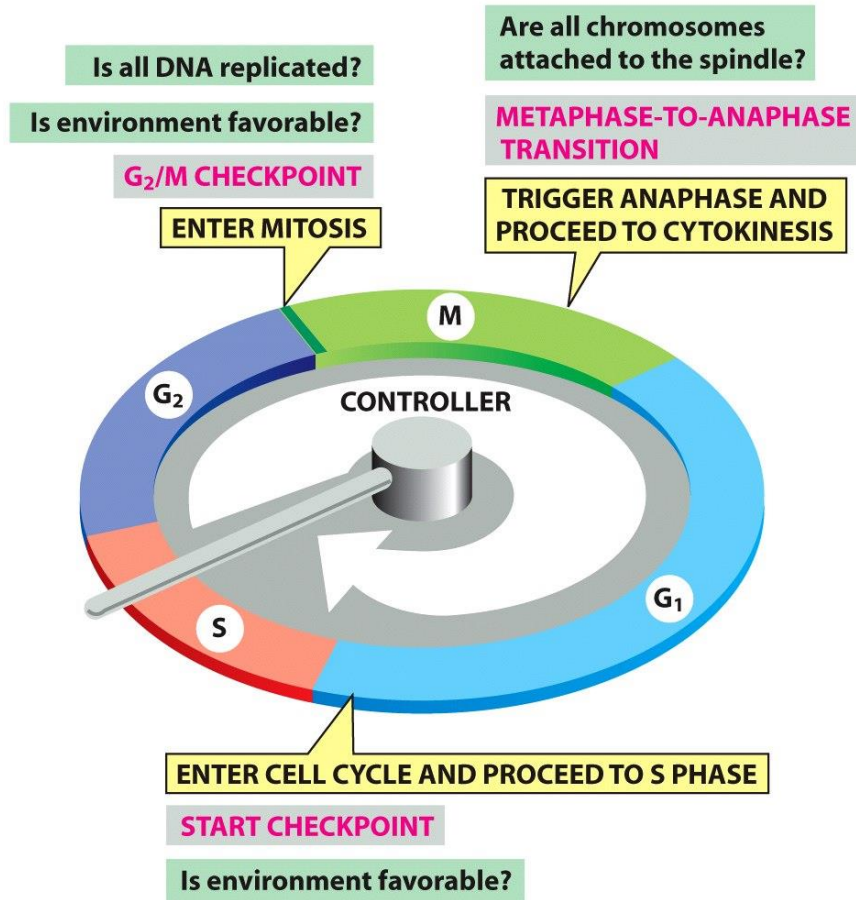


Figure 5.3. Checkpoints and inputs of regulatory information to the cell cycle control system. Adopted from Ref [140].

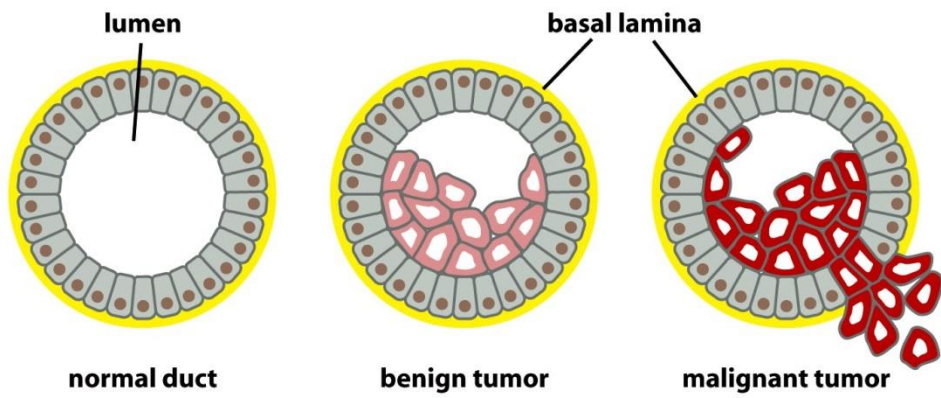


Figure 5.4. Progression of benign tumor (adenoma) to malignant tumor (adenocarcinoma). Adopted from Ref [140].

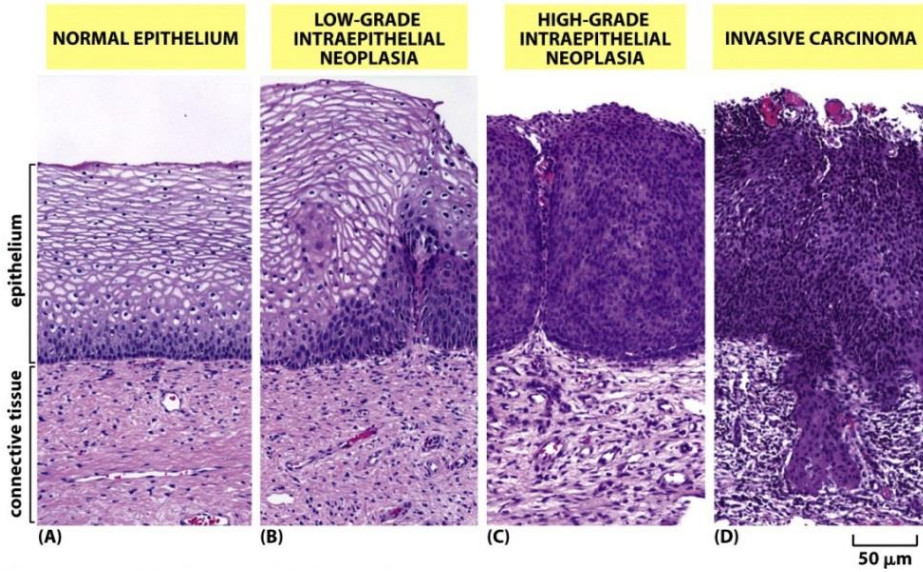


Figure 5.5. The stages of progression in cancer development of epithelium of uterine cervix. Adopted from Ref [140].

#### ***5.2.1.5. Cancer develop in slow stages from mildly aberrant***

Cancer begins as a disorder characterized by nonlethal overproduction of cells which continues for several years before changing into a much more rapid cell proliferation and illness progression that usually leads to death of the patient in few months. The descendants of a single mutant ancestor evolve through successive cycles of mutation and natural selection. The later rapidly dividing cells are characterized with the presence of large nucleus and comparatively less cytoplasm due to the rapid division of cells without paying attention to cell growth as visible in figure 5.7c.

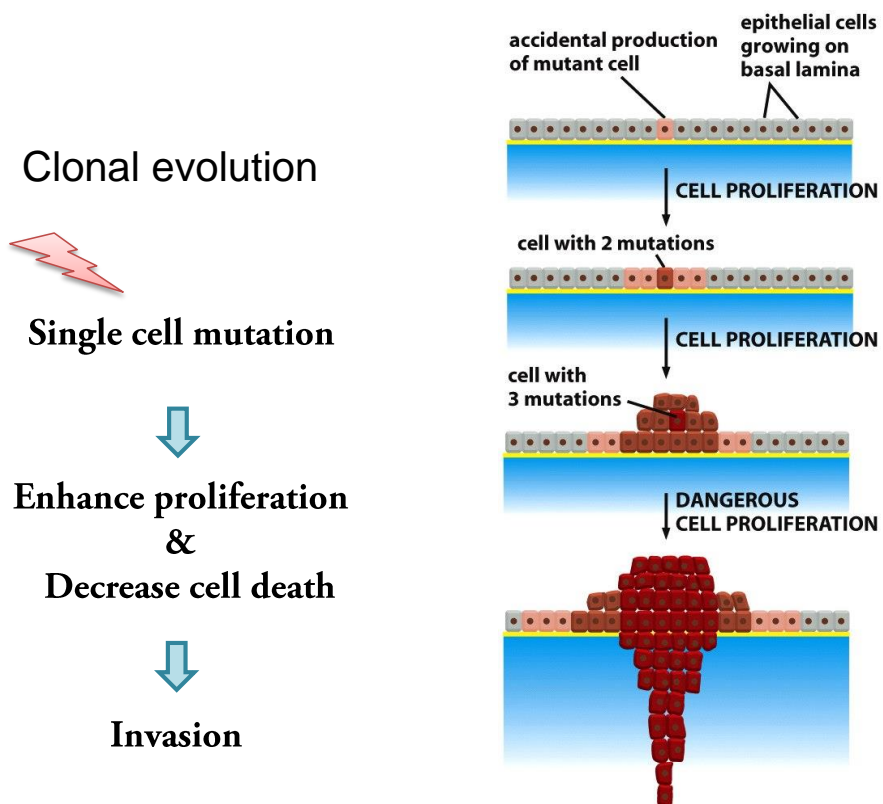


Figure 5.6. A single mutation is not enough to cause cancer. Adopted from Ref [140].

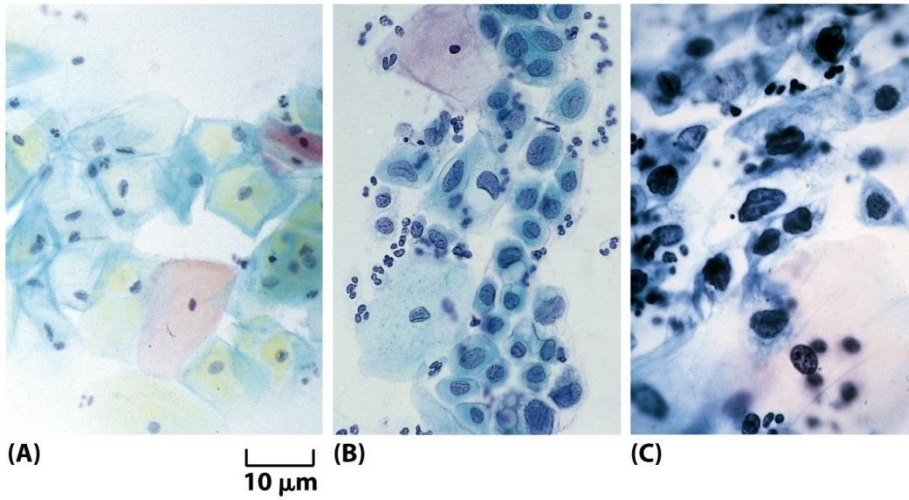


Figure 5.7. Photograph of cells collected from the surface of uterine cervix. Adopted from Ref [140].

## **5.2.2. DNA synthesis**

### ***5.2.2.1. DNA synthesis activity increases during cancer development***

DNA replication, together with repair mechanisms and cell cycle control, are the most important cellular processes necessary to maintain correct transfer of genetic information to the progeny [174]. The cell divides when DNA is completely replicated. Any error during DNA synthesis is proofread by DNA polymerase to replace with the correct nucleotide otherwise in the next cell division it may become a permanent mutation which is read as a normal nucleotide by cellular machinery. These mutated cells lead to aberrant cell proliferation with increased DNA synthesis activity during the cancer advancement [175, 176].

DNA replication means polymerization of pre-synthesized nucleotides which is composed of purines and pyrimidines. Both the purines and pyrimidines have some common points in their biosynthetic pathways. The basic difference is in their size due to ring system and therefore their N and C donors differ slightly. The smaller pyrimidine ring has

two fewer nitrogens, and one less carbon than purine ring. A purine is synthesized from 3 amino acids, two formyl-THFs, and one CO<sub>2</sub> whereas a pyrimidine requires two amino acids and CO<sub>2</sub>. For these extra N's and C's the purine ring needs twice as many glutamines and depends on 2 formyl-THFs. Thus, purine assembly relies on multiple amino acids (Figure 5.8).

#### ***5.2.2.2. Regeneration of N<sup>5</sup>,N<sup>10</sup> Methylene tetrahydrofolate - key to DNA synthesis***

The thymidylate synthase cycle shown in figure 5.9 is central to DNA replication as it recycles the folate involved in DNA synthesis. Thymidylate is a key precursor of DNA which is synthesized by the tetrahydrofolate-dependent methylation of deoxyuridylate catalyzed by thymidylate synthase (TYMS) [177]. The methyl group (recall that thymine is 5-methyl uracil) is donated to dUMP by N<sup>5</sup>,N<sup>10</sup>-methylene THF. The produced dTMP is quickly consumed by cancer cells for direct incorporation during DNA replication. Thymidylate synthase shows its unique property by converting THF to dihydrofolate (DHF), the only reaction that yields DHF from THF. In order to continue the

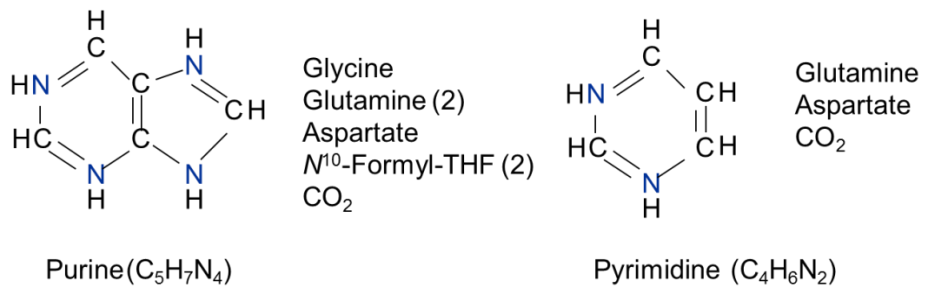


Figure 5.8. The basic structure of nitrogenous bases: purines and pyrimidines and their synthetic requirements.

thymidylate synthase reaction, THF must be regenerated from DHF which is accomplished through dihydrofolate reductase (DHFR). THF is then converted to  $N^5,N^{10}$ -THF via serine hydroxymethyl transferase (SHMT) enzyme by methyl transfer from serine. Serine is reduced to glycine which a precursor for purine synthesis as mentioned in previous section. All the three enzymes TYMS, DHFR and SHMT function in cyclic coordination to generate the precursors of nucleotides displaying the central hub for DNA synthesis.

#### ***5.2.2.3. Role of Serine hydroxymethyltransferase (SHMT)***

Folate dependent one carbon metabolism is essential for the biosynthesis of numerous cellular constituents required for cell growth, and serine hydroxymethyltransferase (SHMT) is central to this process. Folate coenzymes function as donor and acceptor of one carbon unit and the  $\beta$ -carbon of serine is its major source. SHMT is a highly conserved enzyme that catalyzes the reversible conversion of serine and THF into glycine and 5,10-methylene THF, respectively (Figure 5.10). During the S-phase of cell cycle when the cells prepare to proliferate, incorporation of  $\beta$ -carbon of serine into DNA and SHMT activity are

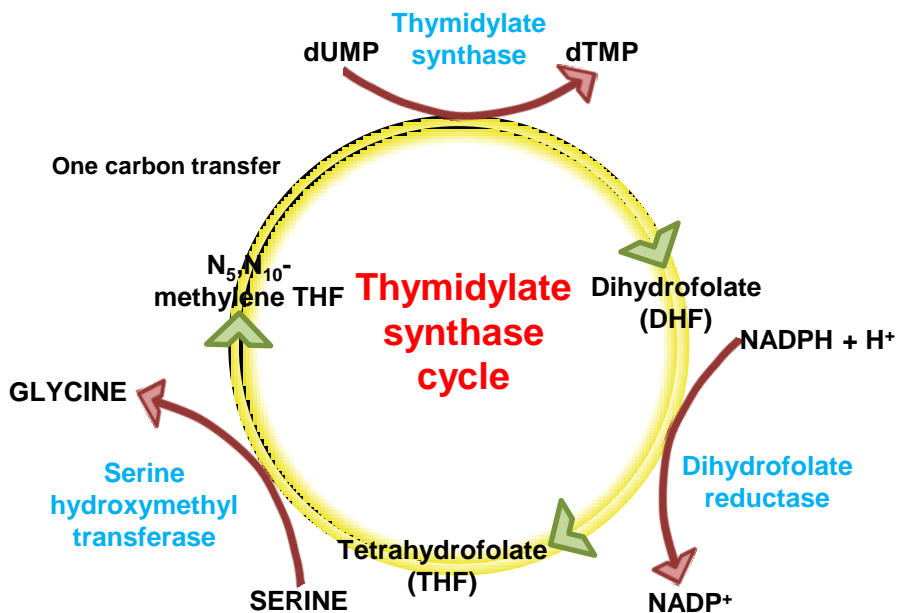


Figure 5.9. Thymidylate synthase cycle displaying the central hub for DNA synthesis by the action of three enzymes TYMS, DHFR and SHMT.

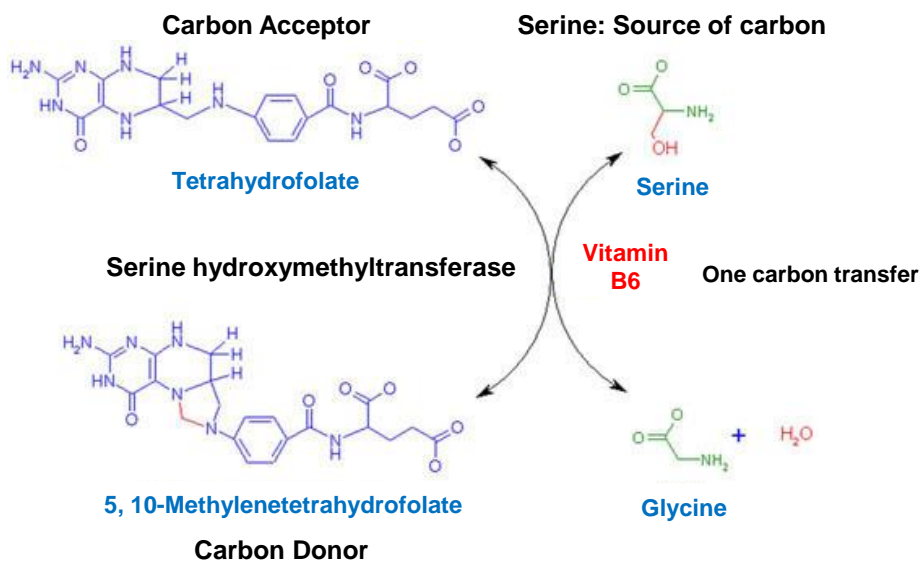


Figure 5.10. The transfer of hydroxyl methyl group of serine to THF to form glycine and 5,10-THF catalyzed by SHMT.

both increased [178].

### **5.2.3. Target proteins for retarding DNA biosynthesis**

DNA is replicated during S-phase of the cell cycle one for each daughter cell. If the DNA replication machinery which involves DNA polymerase and four deoxynucleotides faces incapability in duplicating the DNA, the cell does not divide. Since SHMT, a component enzyme of thymidylate synthase cycle, along with the TYMS and DHFR are involved in DNA synthesis, they may function as the potential anticancer targets.

There could be various technologies and strategies applied to cease the growth and proliferation of cancer cells by interfering their DNA synthesis mechanism. Chemotherapy drugs are used to interfere with thymidylate synthase reaction to decrease dTMP production or dihydrofolate reductase step can be stopped competitively by DHF analogs. Fluorodeoxyuridylate an irreversible inhibitor of TYMS also affects rapidly growing normal cells (hair follicles, bone marrow, immune system, intestinal mucosa). Anti-folates such as aminopterin,

methotrexate, trimethoprim are clinically used as inhibitors for DNA synthesis. But a common problem encountered by using these inhibitors is the emergence of drug resistance because the enhanced mutability of cancer cells help them evade destruction by anticancer drugs [179]. Several researches have been conducted to inhibit TYMS and DHFR but little has been focused on SHMT. Elevated SHMT activity has been shown to be coupled with the increased demand for DNA synthesis in rapidly proliferating cells. It is also found that complete knockout of SHMT leads to glycine auxotrophy. Therefore the central role of SHMT in nucleotide biosynthesis makes it a suitable anticancer target [179, 180].

Another strategy to control the proliferation of cancer cells is the use of RNAi technology (discussed in later section) which will selectively silence the SHMT to shut down the whole DNA synthesis machinery in cancer cells. However, the immense potential of RNAi in anti-cancer therapy is impeded by the non-availability of a suitable delivery agent, off-target effects and induction of innate immune response. These obstacles can be overcome by using nanoparticles of the size below 100

nm which can effectively deliver the siRNA via endosome mediated cellular uptake. The RNAi specificity not only depends upon the sequence homology between siRNA and target mRNA, but also on the homology of 5' end of guide strand which is the major determinant of off-target silencing. Hence, to avoid cross homology of 5' end, siRNA design should be thoroughly considered.

### **5.3 Materials and Methods**

#### **5.3.1. Cell culture and animals**

Low passage adenocarcinoma human alveolar basal epithelial (A549) cells were cultured in T-75 culture flasks (Nunc, Thermo Scientific) in 15 mL complete medium containing Roswell Park Memorial Institute (RPMI)-1640 (HyClone Laboratories, USA) supplemented with 10% heat-inactivated fetal bovine serum (FBS, HyClone Laboratories, USA) and 1% antibiotic cocktail of streptomycin and penicillin. Cells were maintained under standard culture conditions of 37°C and 5% CO<sub>2</sub> for 4 or 5 days, with the culture duration selected to maintain cells under exponential growth and reach ~80% confluency. Cells were then

trypsinized, centrifuged at 1200 RPM for 5 min to pellet cells and counted using hemocytometer to seed the cells for experimental assays.

For animal study four weeks old nude Balb/c mice were obtained from Orient Bio Inc. (Republic of Korea) and kept in a laboratory animal facility maintained at  $23 \pm 2^\circ\text{C}$  and  $50 \pm 20\%$  relative humidity under a 12 h light/dark cycle. All experimental protocols were reviewed and approved by the Animal Care and Use Committee at Seoul National University (SNU-120409-3).

### **5.3.2. Transfection for RNAi silencing of SHMT1**

A549 cells were cultured according to standard techniques as described above. Cells were seeded at a density of  $3 \times 10^5$  cells/well in a 6-well plate; and after 24 h (70% confluent) were transfected with VBPEA/siSHMT1 complexes. The SHMT1 siRNA (siSHMT1) (Sigma, St. Louis, MO, USA) was reconstituted in ultra-pure water (DNase/RNase free) and mixed with VBPEA at an N/P ratio of 20 to a final concentration of 100 pM of SHMT1 siRNA. After 30 min of incubation, A549 cells at ~70% confluency were transfected for 3 h in

serum-free medium. PEA (N/P 20) and PEI25k (N/P 10) were used as positive controls, whereas naked siSHMT1 and scrambled sequence (siScr) negative controls were used in all experiments. For assessment of SHMT1 knockdown, 24 h, 48 h, and 72 h post-transfection total RNA was isolated from cells using QuickGene RNA kit (Fujifilm, Tokyo, Japan), and real-time quantitative PCR (Q-PCR) was performed for SHMT1. Extracted RNA was reverse transcribed to cDNA using the Finnzymes cDNA synthesis kit with MMLV reverse transcriptase (Thermo Fisher Scientific Inc., Vantaa, Finland) and a random primer. The relative abundance of each mRNA species was quantified by qPCR using the hSHMT1 5'-GCTGGGCTACAAAATAGTCA-3' (forward) and 5'-AGGCAATAGAACAGGCTTC-3' (reverse) and hGAPDH 5'-GCCCAATACGACCAAATCC-3' (forward) and 5'-AGTCAGCCGCATCTTCTT-3' (reverse) specific primers from Cosmogenetech, Seoul, Korea. PCR mixtures were prepared with 2X Prime Q-Mastermix containing 2X SYBR<sup>®</sup> Green I (Genet Bio, Nonsan, Korea) according to the manufacturer's protocol. Q-PCR was performed in quadruplicate for each group, with GAPDH as reference gene, using a C1000 Thermal Cycler (BioRad, CA, USA) starting with

10 min of pre-incubation at 95°C followed by 50 amplification cycles with an annealing temperature at 61.3°C. The fluorescent signal intensities were measured and analyzed using C1000Manager Software (BioRad, Hercules, CA, USA).

### **5.3.3. Western blot analysis**

At 48 h post-transfection, cells were harvested and lysed with 1X RIPA lysis buffer (Millipore, MA, USA). A BCA protein assay kit (Thermo scientific, MA, USA) was used to measure the protein concentrations. Equal amounts of the protein (25 µg) from each sample were separated by a Novex NuPAGE 4-12% SDS-PAGE gel (Life technologies, CA, USA), transferred to nitrocellulose membrane using iBlot (Invitrogen, USA) and then non-specific binding sites were pre-blocked with 5% skim milk for 1 h at RT. The membrane was washed and probed with anti-SHMT1 (Santa Cruz Biotechnology Inc., CA, USA) and anti-β-actin (Abfrontier, Seoul, Korea) antibodies (1:500 dilution) overnight at 4°C. Then, the membrane was incubated with secondary antibody (1:1000 dilution) conjugated with HRP (Invitrogen, Carlsbad, CA, USA). Bands were captured using a ChemiDoc<sup>TM</sup> XRS<sup>+</sup> (Biorad, CA,

USA) imaging system. The band intensities were analyzed quantitatively using ImageJ software (NIH, USA) and plotted as the mean pixel value.

#### **5.3.4. Confocal microscopy**

TRITC (Molecular Probes, Invitrogen, Oregon, USA) (25  $\mu$ L, 1 mg/100  $\mu$ L in DMF) was added to VBPEA (1 mL, 10 mg/mL in H<sub>2</sub>O) to block ~1% of its total amines, and the mixture was then stirred overnight (VBPEA<sup>T</sup>). Unreacted TRITC was removed by washing with ethyl acetate (3 x 2 mL), which was then lyophilized and resuspended in water. A549 cells were seeded at a density of 3 x 10<sup>5</sup> cells/well in a cover glass bottom dish (SPL Lifesciences, Korea) and incubated for 24 h in humidified chamber. Cells were transfected with VBPEA<sup>T</sup>/siRNA complexes and further incubated for 120 min. The transfected A549 cells with fluorescently labeled complexes were washed 3 times with 1X PBS and then fixed with 4% paraformaldehyde for 10 min at 4°C. DAPI was used to counter-stain the nuclear DNA of fixed cells, and images were procured using a Carl Zeiss LSM 710 inverted laser scanning confocal microscope with ZEN software to monitor

fluorescently labeled VBPEA<sup>T</sup>/siRNA complexes inside the treated A549 cells.

### **5.3.5. Immunocytochemistry (ICC)**

A549 cells were seeded in an 8-well chamber slide (Lab Tek, Sigma, USA) at  $5 \times 10^4$  initial cell density/well and transfected with the VBPEA/siSHMT1 complexes together with the positive controls. After 48 h, cells were rinsed in 1X PBS and fixed with 4% paraformaldehyde at 37°C for 10 min and then with 1:1 (v/v) methanol:acetone solution at -20°C for an additional 10 min. After fixation, cells were washed twice with ice cold PBS and then permeabilized with ice-cold 0.2% Tween 20 in PBS for 10 min. Non-specific binding was blocked using 10% BSA in 1X PBS for 5 min at RT and then at 4°C for 1 h because cooling prevents endocytosis of antibodies. Cells were incubated with SHMT1 (100 µg/mL) (Santa Cruz Biotechnology Inc., CA, USA) and nuclear lamina specific LAP2 (20 µg/mL) (Millipore, CA, USA) antibodies diluted in 3% BSA at 4°C overnight. After washing several times with PBS, cells were incubated with fluorophore-conjugated secondary antibodies diluted in 3% BSA for 2 h at RT away from light.

Nuclei were stained with DAPI (0.1  $\mu\text{g}/\text{mL}$ ) for 10 min and mounted with Aqua poly/mount (Polysciences, PA, USA). The images were procured from confocal microscopy and the percentage of colocalization was evaluated using a custom designed MATLAB program.

### **5.3.6. EdU and WST proliferation assay**

A549 cells in an 8-well chamber slide were transfected and further grown in complete media containing EdU (5-ethynyl-2'-deoxyuridine, 10 $\mu\text{M}$ ) for 48 h. EdU is a nucleoside analog of thymidine that is incorporated into DNA during active DNA synthesis. The cells were then fixed in 4% paraformaldehyde and permeabilized with 0.5% Triton X-100. EdU detection is based on a copper catalyzed click reaction between an alkyne in EdU and an azide in the Alexa Fluor dye, and was conducted according to the manufacturer's protocol (Click-iT EdU imaging kit, Invitrogen). This is a direct qualitative method for the detection of cell's proliferative ability to evaluate anti-cancer activity. The images were captured using image restoration microscopy (DeltaVision RT, USA). WST colorimetric assay (EZ-Cytox Cell

Viability Assay Kit; Daeillab, Korea) quantified the proliferation ability of the transfected A549 cells in a 96-well plate (10000 initial cell density/well), which was proportional to the intensity of the water soluble formazan formed by the cleavage of tetrazolium salt by the mitochondria of the viable cells. After 0, 1, 2, 3, 4 days of treatment, WST assay was performed according to manufacturer's protocol, and the absorbance was measured at 450 nm using a Sunrise™ TECAN ELISA reader (Grödig, Austria).

#### **5.3.7. In vitro and in vivo TUNEL assay**

The transfected A549 cells in the 8-well chamber slide and the *in vivo* treated tumor sections were analyzed for apoptotic death using a DeadEnd colorimetric TUNEL (TdT mediated dUTP nick end labeling) system from Promega, USA, which end-labels the fragmented DNA of apoptotic cells. The paraffin embedded tissue sections were deparaffinized using xylene and rehydrated by sequentially immersing the slides into 100%, 95%, 85%, 70%, and 50% ethanol. The tissue sections and the cultured cells were fixed with 4% paraformaldehyde for 25 min at RT and washed twice with PBS. The tissue cells and

cultured cells were then permeabilized using proteinase K (20  $\mu\text{g}/\text{mL}$ ) and 0.2% Triton X-100 respectively, for 10 min at RT and rinsed twice with PBS. Biotinylated nucleotides were incorporated at the 3'-OH DNA ends using a recombinant terminal deoxynucleotidyl transferase, (rTdT) enzyme. Horseradish peroxidase-conjugated streptavidin was then bound to biotinylated nucleotides, which were detected with hydrogen peroxide and diaminobenzimide (DAB). The images were captured using a light microscope. Cells treated with DNase I to induce DNA strand breaks were used as a positive control.

#### **5.3.8. Annexin V-FITC Apoptosis Detection Assay**

The supernatant medium from the transfected cells and trypsinized adherent cells were collected and washed twice with cold 1X PBS at 2000 rpm for 5 min at RT. Cells were then washed with cold 1X binding buffer diluted in 1X PBS, and 1.8  $\mu\text{L}$  of FITC-conjugated Annexin V (200  $\mu\text{g}/\text{mL}$ ) (Komabiotech, Korea) which has high affinity for translocated membrane phospholipid phosphatidylserine (PS), was added and incubated for 15 min at RT in dark. The supernatant was removed by centrifugation and the cells were washed with cold 1X

binding buffer (0.5 mL). 10  $\mu$ L of propidium iodide (PI) (30  $\mu$ g/mL) which can bind with nucleic acids, was added and the cells were then analyzed using a BD FACSCalibur I equipped with dual laser (488 nm argon ion laser and 635 nm red diode laser) for the detection of multicolored fluorescent particles in the single sample. As the fluorescent particles intercept the laser light, the scattering of the fluorescent light is detected and the particle's fluorescent intensity is acquired by using BD FACStation software version 6.0.

#### **5.3.9. 4'-Deoxypyridoxine inhibition study**

A549 cells were transfected with VBPEA/siSHMT1 and PEA/siSHMT1 complexes in the presence and absence of 4'-deoxypyridoxine hydrochloride (structural analog of VB<sub>6</sub>) (10 mM) (Sigma, MO, USA) and were harvested 48 h later for western blot analysis as described above to evaluate their effect on the silencing efficiency of SHMT1. Confocal microscopy was also used to visualize the intracellular trafficking of the TRITC-labeled VBPEA<sup>T</sup>/siRNA complexes with and without 4'-deoxypyridoxine. After 120 min of

transfection, the cells were processed for confocal microscopy as previously explained.

#### **5.3.10. Cell synchronization**

After 48 h of treatment, A549 cells in an 8-well chamber slide were provided with Ham's F-12 medium supplemented with 10% FBS, 1% antibiotics, and 2 mM thymidine and incubated for 8 h at 37°C in a CO<sub>2</sub> incubation chamber. The cells were washed twice with 1XPBS and Ham's F-12 medium supplemented with 10% FBS and 1% antibiotics was then added. Cells were incubated for an additional 12 h to progress through S phase.

#### **5.3.11. Cell cycle analysis**

Transfected A549 cells were harvested after 12 h, 24 h, and 72 h, and then washed, pelleted and resuspended in 0.5 mL PBS into a monodisperse cell suspension before fixing it with ice-cold 70% ethanol for 2 h at -20°C. Before the cell cycle analysis, cells were hydrolyzed and stained with PI (50 µg/mL) and RNase (1 µg/mL) in 1X PBS. Analysis was performed using single-color flow cytometry with a

BD FACSCanto II at an excitation wavelength of 488 nm (blue laser) and an emission wavelength range of 564 to 606 nm. Cell fluorescence was measured using a pulse-width area signal which discriminated G2/M cell singlets from G0/G1 cell doublets and gated out the latter. The data was analyzed using BD FACSDiva 5.0 software and the ModFit (Verity software) deconvolution algorithm was used to deconvolute the histograms.

#### **5.3.12. Fluorescence studies for genomic DNA quantification**

At 72 h post-transfection, A549 cells were harvested and genomic DNA was extracted using a PureLink genomic DNA kit (Invitrogen, CA, USA). The purity of the extracted DNA was analyzed by using NanoVue (GE Healthcare Life Sciences, USA) (Table 5.1). The total DNA contents of the samples were measured using a fluorescence based DNA quantitation kit from Sigma. Fluorescence based DNA measurement is highly sensitive and accurate method. The fluorescent dye, Hoechst 33258, bound primarily to AT sequences in the minor groove of double-stranded DNA excites at 360 nm and gives emission spectra at 460 nm. The emission spectra of samples with unknown

Table 5.1. Purity of genomic DNA from the transfected A549 cells after 72 h.

<b>Sample</b>	<b>Control</b>	<b>Naked siSHMT1</b>	<b>VBPEA/ siScr</b>	<b>VBPEA/ siSHMT1</b>	<b>PEA/siSHMT1</b>
<b>Purity</b>	1.948 ± 0.02	1.774± 0.11	1.918± 0.03	1.810± 0.31	1.911± 0.02

DNA concentrations and standard DNA solutions were obtained using a FluoroMate FS-2 fluorescence spectrophotometer (Scinco, WI, USA). A standard DNA curve was calibrated by plotting the known DNA concentrations versus relative fluorescence units. The DNA concentrations of samples were calculated from the standard DNA curve.

### **5.3.13. Tumor implantation, treatment and in vivo bioimaging**

Five weeks old nude Balb/c mice (male, 4 mice/group) were subcutaneously injected with 100  $\mu$ L of a single cell suspension containing  $3 \times 10^6$  luciferase expressing A549 cells (PerkinElmer, MA, USA). The treatment of tumors with siSHMT1 was started after 1 month when the tumor size reached 800-1000  $\text{mm}^3$ . 100  $\mu$ L of VBPEA/siSHMT1 (30  $\mu$ g) complexes (N/P 20) in normal saline was injected directly into the tumor at an interval of 48 h, which continued for one month. PEA/siSHMT1 (N/P 20) and PEI25k/siSHMT1 (N/P 10) complexes prepared under identical conditions were used as vector controls, and normal saline was used as a negative control. The IVIS Imaging system 100 (Xenogen) with Living Image software was used

for tumor bioimaging to analyze the effect of treatment on tumor size. The mice were anaesthetized by intraperitoneal (IP) injection of a Zoletil (40 mg/kg): Rompun (10 mg/kg) (4:1) mixture diluted 8 times in sterile 1X PBS. 200  $\mu$ L of D-luciferin (15 mg/mL stock solution in DPBS) for a 20 g mouse (3 mg/mouse) was injected intraperitoneally and was quickly distributed throughout the body. Tumor-expressed luciferase reacts with luciferin to emit luminescence, which was captured by the IVIS system to show images with intensity proportional to tumor size. Images were captured in the plateau phase which usually occurs after 15 min and lasts for 15-20 min. Tumor volume was also measured using Vernier caliper every week during the treatment. Tumor volume was calculated by using its mean diameter and applying the formula  $m = 0.5 \times a \times b^2$ , where  $a$  and  $b$  are the smallest and largest diameters, respectively. After treatment over one month, the tumors were dissected, chopped, and homogenized, and the protein concentrations of the lysates were measured. Equal amounts of protein (25  $\mu$ g) were separated by SDS-PAGE and transferred onto a nitrocellulose membrane for immunoblot analysis.

#### **5.3.14. Immunohistochemistry (IHC)**

The dissected tumors were fixed in 10% neutral buffered formalin and embedded in paraffin wax. Tissue sections (4-12  $\mu\text{m}$  thick) were prepared using a microtome and placed on positively charged slides and dried in an oven at 60°C. The slides were then deparaffinized, rehydrated and processed for antigen retrieval using 10 mM sodium citrate buffer, pH 6.0 at 95-100°C. Immunostaining with SHMT1 antibody (1:50 dilution) was performed using a mouse specific HRP/DAB detection IHC kit (Abcam, Cambridge, UK). Harris hematoxylin solution (Sigma) was used to stain the nuclei, and images were taken using a light microscope.

#### **5.3.15. Statistical analysis**

Statistical analysis was carried out by one-way ANOVA in conjunction with Bonferroni's test for the comparison of means. A value of  $P < 0.05$  was taken as statistically significant.

### **5.4 Results**

#### **5.4.1. VBPEA efficiently delivers siSHMT1 to silence SHMT1**

SHMT1 suppression by VBPEA/siSHMT1 was observed in A549 cells up to 72 h post-transfection using quantitative real time (Q)-PCR. A remarkable suppression of SHMT1 (~90%) was observed after 48 h of VBPEA/siSHMT1 treatment in comparison to PEA/siSHMT1 (42%) (Figure 5.11A), indicating an enhanced gene silencing efficiency. Further, western blot showed that VBPEA mediated delivery of siSHMT1 resulted in ~60% knockdown of SHMT1 protein expression, which was higher than that obtained by PEA/siSHMT1 (33%) or PEI25k/siSHMT1 (~32%) polyplexes in reference to the control after 48 h (Figure 5.12). Immunocytochemical analysis also showed the suppressed gene expression of SHMT1 by VBPEA/siSHMT1 treatment (Figure 5.11B). The crucial result is the increased gene silencing efficiency of VBPEA over PEA, which is indicative of the involvement of VB<sub>6</sub> in internalization of the polyplex.

#### **5.4.2. Competitive inhibition by 4'-deoxypyridoxine suggests VTC-mediated uptake of VBPEA polyplexes**

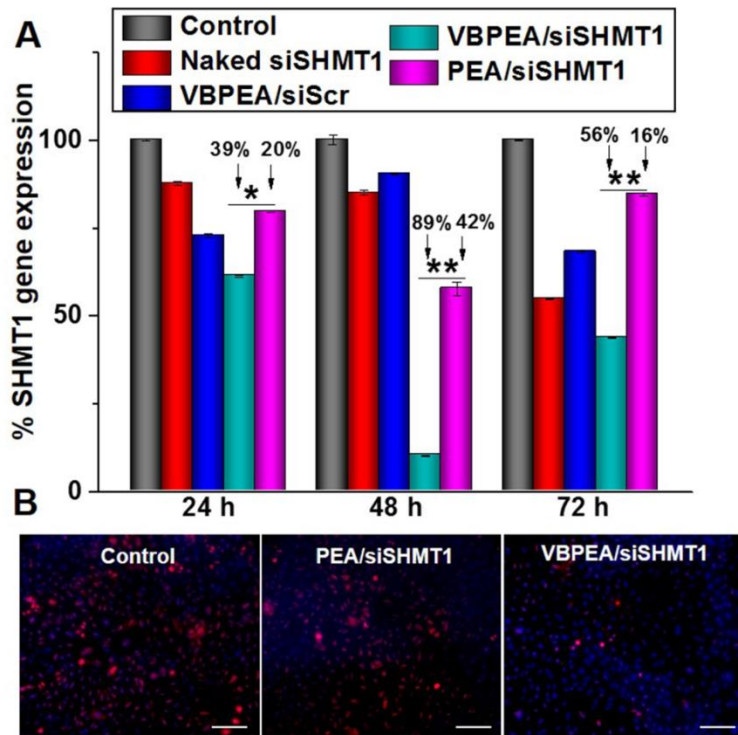


Figure 5.11. SHMT1 gene silencing efficiency of VBPEA/siSHMT1 complexes. (A) SHMT1 gene expression monitored at 24, 48, and 72 h post-transfection in A549 cells using quantitative real-time PCR (Q-PCR). Maximum SHMT1 suppression (~90%) was observed after 48 h by VBPEA/siSHMT1 complexes. Data are expressed as the mean  $\pm$  SEM of 3 experiments. Statistical significance was determined using one-way ANOVA (\* $P < 0.05$ ; \*\* $P < 0.01$ ). (B) Immunocytochemical analysis shows least SHMT1 expression (red) in VBPEA-treated A549 cells in comparison to PEA-treated and control cells after 48 h of transfection (scale bar: 200  $\mu$ m).

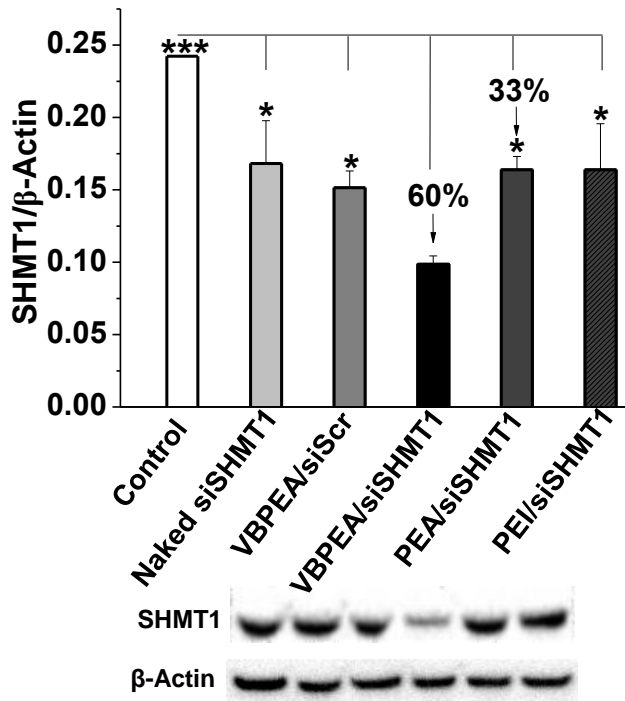


Figure 5.12. Western blot analysis of SHMT1 protein from the lysate of transfected A549 cells after 48 h showing no change in  $\beta$ -actin (42-kDa band) protein expression and a significant decrease in SHMT1 (50-kDa band) protein expression in cells treated with VBPEA/siSHMT1 complexes in contrast to other treated controls. Densitometric analysis of the SHMT1 protein band in reference to the untreated control cells (100% SHMT1 expression) shows a 60% decrease in SHMT1 expression in VBPEA/siSHMT1 treated cells. Data are shown as the mean  $\pm$  SD of 3 independent experiments (\* $P < 0.05$ ; \*\*\* $P < 0.001$ , one-way ANOVA).

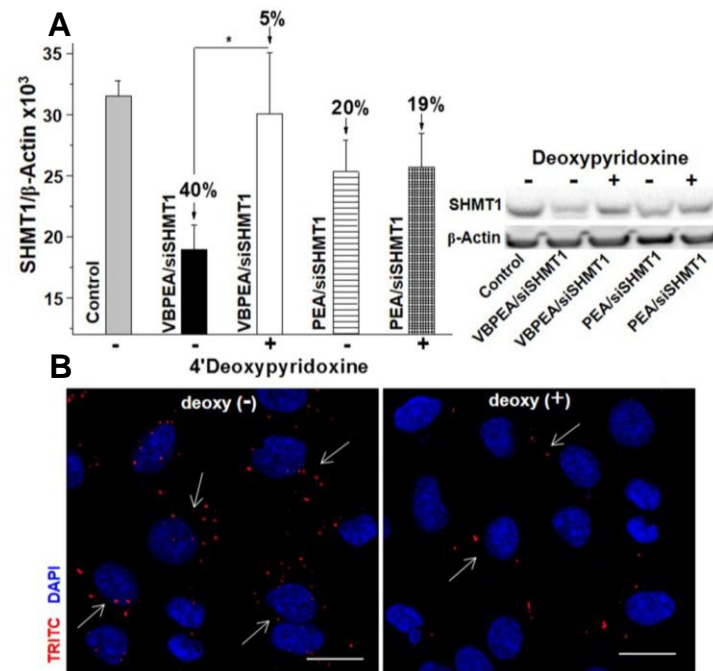


Figure 5.13. SHMT1 gene silencing efficiency of VBPEA/siSHMT1 complexes is enhanced by VTC-mediated endocytosis. (A) Western blot analysis of the A549 cells treated with VBPEA/siSHMT1 and PEA/siSHMT1 complexes (N/P 20) in the absence and presence of 4'-deoxyypyridoxine shows the effect of inhibition only on VBPEA-mediated delivery, whereas the PEA-mediated delivery remained unaffected by the inhibitor. Data are shown as the mean  $\pm$  SD of 3 independent experiments (\* $P < 0.05$ , one-way ANOVA). (B) Confocal microscopic images of A549 cells (scale bar: 20  $\mu$ m) after transfection with the VBPEAT/siRNA polyplex after 120 min show reduced polyplex internalization in the presence of 4'-deoxyypyridoxine (deoxy) competitive inhibitor than in its absence. VBPEA was labeled with TRITC (red) and nuclear DNA was counter-stained with DAPI (blue).

The western blot analysis of A549 cell lysates from VBPEA/siSHMT1 transfected cells showed no suppression of the SHMT1 gene in the presence of 4'-deoxypyridoxine (structural analog of VB<sub>6</sub>) (~5%) than the otherwise silenced SHMT1 in absence of the inhibitor (~40%) (Figure 5.13A). Contrary to this, no significant inhibitory effect was observed in PEA/siSHMT1 transfected cells in the presence (~19%) or absence (~20%) of 4'-deoxypyridoxine, suggesting that 4'-deoxypyridoxine competitively inhibits the binding of VB<sub>6</sub> present in VBPEA/siSHMT1 polyplexes to VTC [146] and decelerates polyplex uptake. Confocal studies in the presence of inhibitor also resulted in reduced polyplex internalization compared to that in the absence of inhibitor due to the decreased accessibility of VTC to VBPEA (Figure 5.13B). This suggests the active participation of a VB<sub>6</sub>-specific uptake mechanism via a membrane carrier (VTC) favoring the accelerated internalization of VBPEA.

#### **5.4.3. SHMT1 knockdown resulted in reduced cell proliferation and increased apoptotic events**

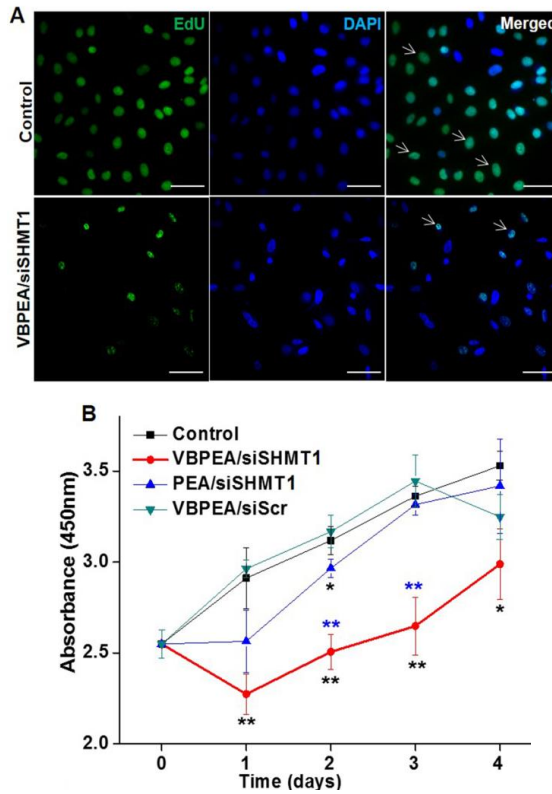


Figure 5.14. Effect of SHMT1 knockdown on the proliferative behavior of A549 cells. (A) EdU proliferation assay showing diminished cell proliferation in the VBPEA/siSHMT1 treated group compared to the untreated control group due to lower EdU nucleotide incorporation in fewer dividing A549 cells (scale bar: 50  $\mu$ m). The arrows indicate the proliferated nuclei (green). (B) WST proliferation assay at day 0, 1, 2, 3, 4 after treatment with polyplexes shows the lowest metabolic activity in VBPEA/siSHMT1 treated A549 cells up to day 3, indicating less cell proliferation. Statistical significance was determined using one-way ANOVA (\* $P < 0.05$ ; \*\* $P < 0.01$ ,  $n = 3$ , error bar represents SD).

VBPEA/siSHMT1 transfected A549 cells exhibited comparatively lesser proliferative behavior than the untreated control cells. EdU incorporation in proliferating cells (green fluorescence) can be assessed for the direct analysis of DNA synthesis and cell proliferation. The results showed hampered cell proliferation (lower number of green nuclei) due to the knockdown of SHMT1 protein expression, in comparison to the untreated control (Figure 5.14A). In addition, WST assay also showed a reduced proliferation of VBPEA/siSHMT1 treated cells until day 3, after which proliferative behavior was restored, due to consumption of the single dose of siSHMT1 (Figure 5.14B). The proliferation was also halted to some extent, but less efficiently by PEA/siSHMT1. PEI25k was excluded due to its high cytotoxicity, which may produce false results.

The non-proliferative cancer cells with silenced SHMT1 are supposed to gradually proceed towards apoptosis, which was evident from features such as cell rounding, membrane blebbing, and detachment from the tissue culture dish. Loss of membrane asymmetry and nuclear disintegration are the characteristic features of apoptotic cells

distinguishable from the necrotic cells [181, 182]. Therefore, enumeration of apoptosis in the treated cancer cells was done for assuring the induction of apoptosis, which serves as a prognostic marker for cancer treatment [183, 184]. The results of colorimetric TUNEL assay, where ends of the apoptosis-induced DNA strand breaks were labeled and detected as dark brown stained nuclei, showed higher DNA fragmentation (dark brown) in VBPEA/siSHMT1 treated cells than the cells treated with PEA and the controls (Figure 5.15A). AnnexinV-PI staining also detects apoptosis, based on the binding of Annexin V with the exposed phospholipid phosphatidylserine and propidium iodide (PI) with DNA on loss of plasma membrane integrity of apoptotic cells [185]. From the FACS results of VBPEA/siSHMT1 treated group, cells that are negative for both Annexin V and PI are considered viable (~35%), whereas cells in early apoptosis are Annexin V positive and PI negative (~3%), and late apoptotic or dead cells are positive for both Annexin V and PI (~62%) (Figure 5.15B). The presence of these three phenotypes within a mixed cell population suggests apoptosis. The proliferation and apoptosis assays suggest that

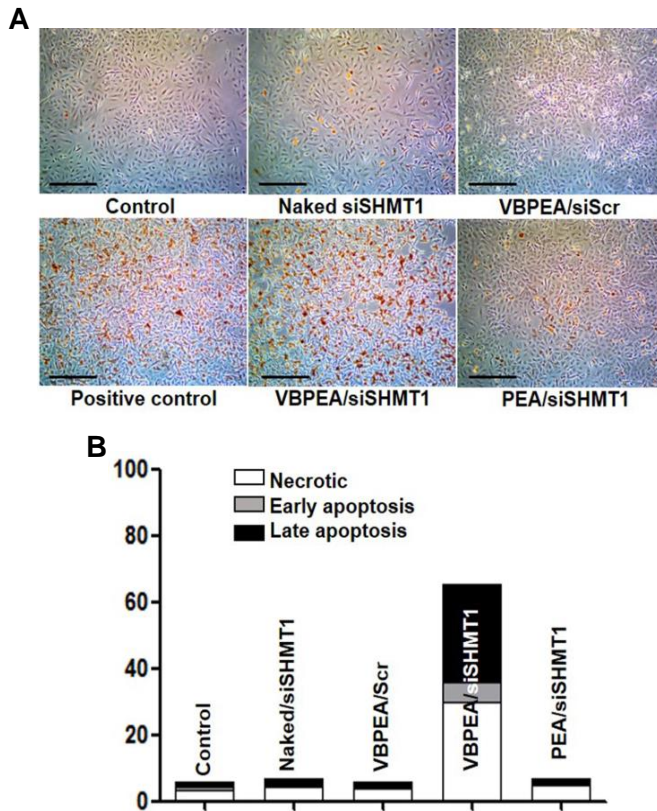


Figure 5.15. SHMT1 knockdown onsets the apoptotic events in A549 cells. (A) TUNEL assay in A549 cells for the comparison of apoptotic events in the various treatment groups shows the maximum apoptosis induction in the VBPEA-mediated siSHMT1 delivery; apoptosis is represented by brown stained nuclei (scale bar: 500  $\mu$ m). (B) AnnexinV-PI staining of transfected A549 cells show >50% apoptotic cell death in VBPEA/siSHMT1 treated cells after 48 h.

antagonizing SHMT1 expression resulted in reduced cell division and apoptotic death of cancer cells.

#### **5.4.4. Knockdown of SHMT1 drastically affects cellular DNA synthesis and arrests cell cycle at sub-G<sub>1</sub> phase**

The three constituent enzymes of the thymidylate biosynthetic pathway, which translocate to the nucleus for DNA replication, form a multienzyme complex where SHMT isoforms (SHMT1 & SHMT2 $\alpha$ ) anchor this metabolic complex at the nuclear lamina [148]. Therefore, the co-localization of SHMT1 with nuclear lamins was investigated during DNA replication at the S phase (cells synchronized at S phase) of the cell cycle. We demonstrated that VBPEA-mediated delivery of siSHMT1 resulted in the decreased incidence of SHMT1 co-localization with the nuclear lamina (Figure 5.16). The results showed approximately 91% co-localization of SHMT1 (red) with the nuclear lamina (green) in the control group, with no significant difference in the siScr treated group (89%), suggesting continued DNA synthesis and cell division (indicated by an arrow in Figure 5.16). In contrast, VBPEA/siSHMT1 treated cells displayed reduced amount of SHMT1

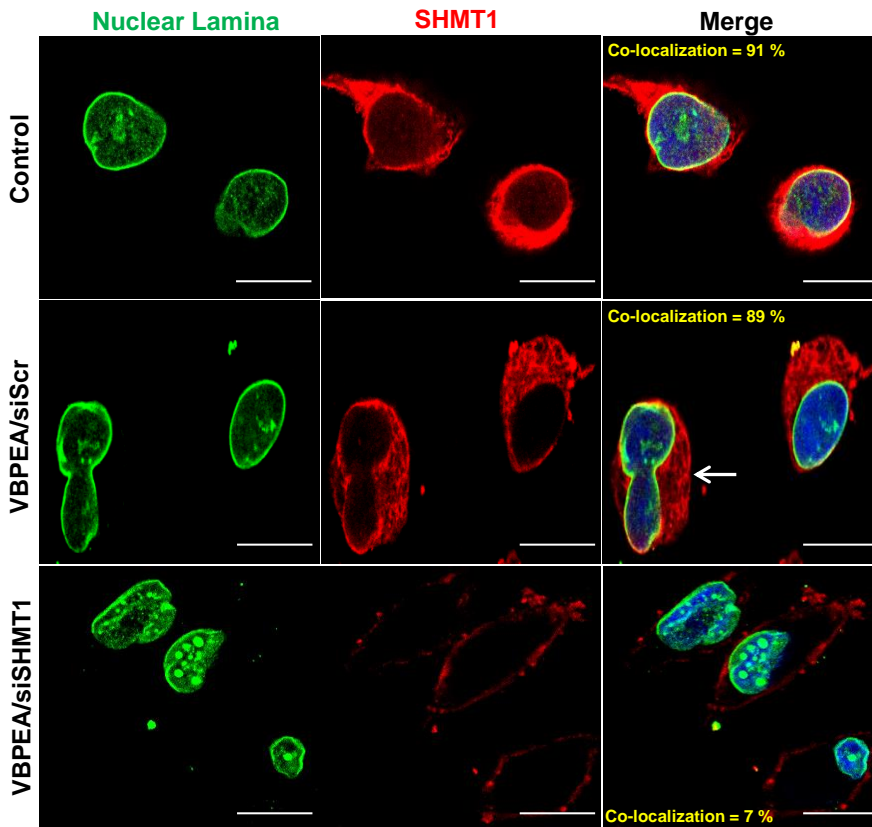


Figure 5.16. SHMT1 knockdown affected DNA synthesis. Co-localization study of SHMT1 (red) with the nuclear lamina (green) of post-transfected A549 cells, synchronized at S phase, showed the least co-localization (7%) with VBPEA/siSHMT1 treated cells in contrast to the control in which ~90% co-localization suggests active DNA synthesis and cell division. The dividing cell in the negative control (VBPEA/siScr treated cells) is indicated by an arrow (scale bar: 20  $\mu$ m).

(less intense red fluorescence), showing only 7% co-localization with the nuclear lamina. These SHMT1 silencing results indicate the disintegration of the *de novo* thymidylate biosynthetic multienzyme complex, which leads to the cessation of DNA synthesis and cell cycle arrest in adenocarcinoma cells.

The cell growth arrest after the delivery of siSHMT1 using VBPEA was confirmed by cell cycle analysis. Since the incidence of DNA replication is much higher in cancer cells than in normal cells, their growth pattern is different where most cells skip cell cycle check points and remain in the G1 phase without exiting the cell cycle [186]. VBPEA-mediated delivery of siSHMT1 is demonstrated to arrest cell cycle progression (Figure 5.17B) that occurred due to the deprivation of nucleotides. A549 cells treated with VBPEA/siSHMT1 together with positive and negative controls were monitored for their growth pattern after 12 h, 24 h, and 72 h of transfection using FACS. On the basis of differences in intensity of PI fluorescence (proportional to DNA content), the population of cells in G0/G1, S, and G2/M phases were identified. A population of cells in G0/G1 phase had uniform, low

DNA content values compared to G2/M cells with twice the DNA content, and S cells with intermediate DNA content. 12 h post-transfection, not much differences were observed in all of the treated and control groups, with most cancer cells (~70%) being present in G1 phase, indicating their re-entry into the cell cycle. 24 h later, while the control cells again entered G1 phase in preparation for the next division cycle, the VBPEA/siSHMT1 treated cells were not observed in G1 phase (2%), suggesting initiation for their retreat from cell division. The crucial results after 72 h showed that the VBPEA/siSHMT1 treated cells exhibited cell cycle arrest in the sub-G1 phase (38%) and were prevented from entering the G1 phase of cell division (Figure 5.17A & 5.18). It is noteworthy that the decrease in the number of S phase cells (after 24 h) has appeared at the sub-G1 phase, where they can be induced for apoptosis. The results are in accordance with the WST proliferation assay where the cell proliferation is seen reduced until day 3 (72 h) (Figure 5.14B).

Because cells were found in the sub-G1 phase after 72 h, the total genomic DNA from all of the treated and control groups were

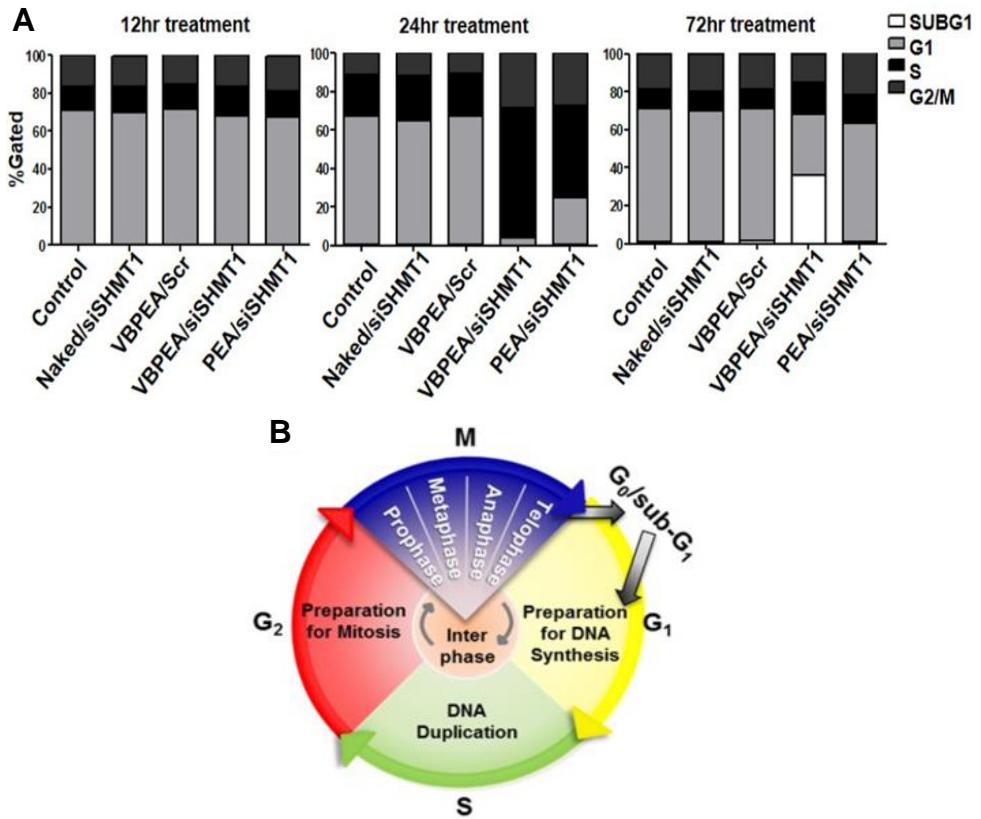


Figure 5.17. SHMT1 knockdown resulted in cell cycle arrest. (A) FACS analysis of the population of A549 cells in different cell growth phases after 12 h, 24 h, and 72 h of treatment with VBPEA/siSHMT1 and PEA/siSHMT1 complexes (N/P 20), showing cell growth arrest due to suppression of SHMT1 gene expression after 72 h. (B) Pictorial presentation of cell cycle progression.

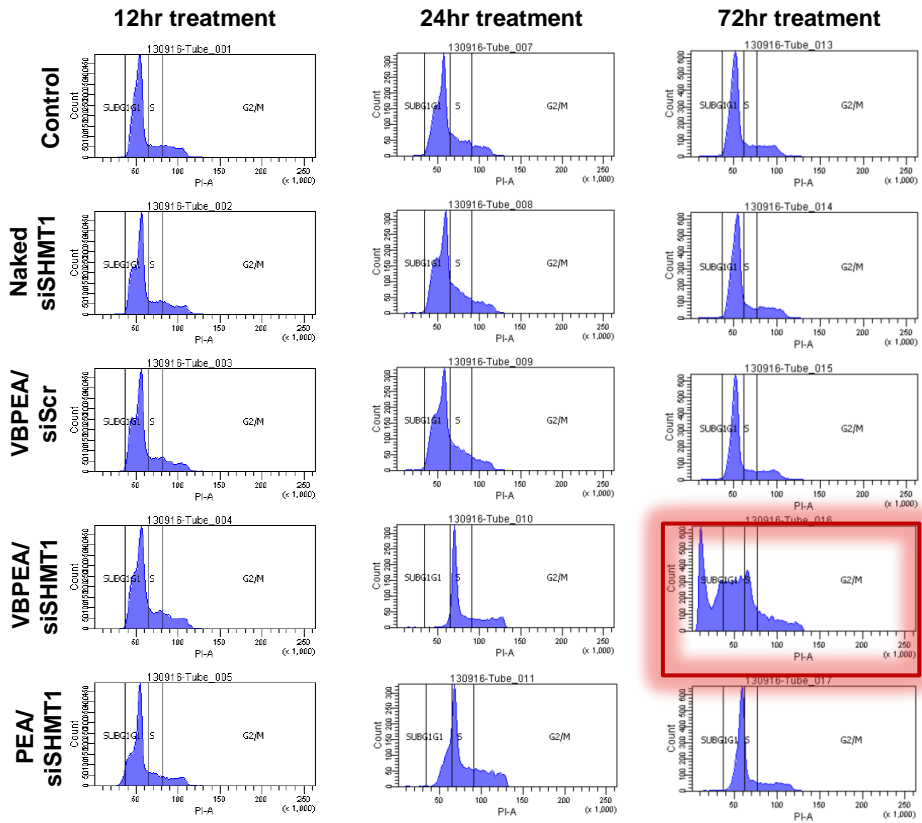


Figure 5.18. FACS analysis of the population of A549 cells present in different cell growth phases after 12 h, 24 h, and 72 h of treatment with VBPEA/siSHMT1 and PEA/siSHMT1 complexes.

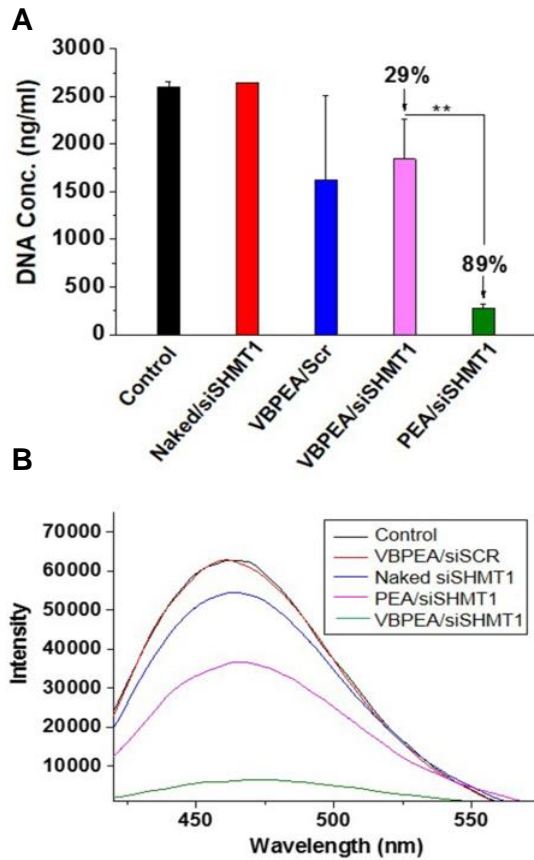


Figure 5.19. SHMT1 knockdown decreased the total genomic DNA content of the cells. (A) The total genomic DNA content and (B) fluorescence intensity of treated A549 cells shows a drastic decrease in genomic DNA content of VBPEA treated cells after 72 h. The fluorescent dye, Hoechst 33258, bound to DNA excites at 360 nm and gives emission spectra at 460 nm. Statistical significance was determined using one-way ANOVA (\*\*P < 0.01, n = 3, error bar represents SD).

quantified after 72 h. The VBPEA group showed an 89% decrease in the genomic DNA concentration, whereas the PEA group showed a 29% decrease in reference to control (Figure 5.19A, B). The results suggest that VBPEA-mediated silencing of SHMT1 arrested the thymidylate synthase cycle and consequently stopped nucleotide biosynthesis. As a result, cell proliferation was also inhibited, leading to apoptotic cell death and lower genomic DNA concentration.

#### **5.4.5. VBPEA-mediated knockdown of SHMT1 retarded tumor growth in xenograft mice**

Instead of systemic, local administration of siRNA avoids the obstacles of low bioavailability, systemic toxicity, rapid excretion and inefficient targeting [187]. Therefore, the luciferase-expressing subcutaneous tumor ( $\sim 1000 \text{ mm}^3$ ) bearing xenograft mice were treated with the local administration of VBPEA/siSHMT1. Bioluminescence images were captured every two weeks during polyplex injection. A gradual decrease in bioluminescence intensity (Figure 5.20) and tumor volume (56%)(Table 5.2) of the VBPEA/siSHMT1 treated group demonstrated

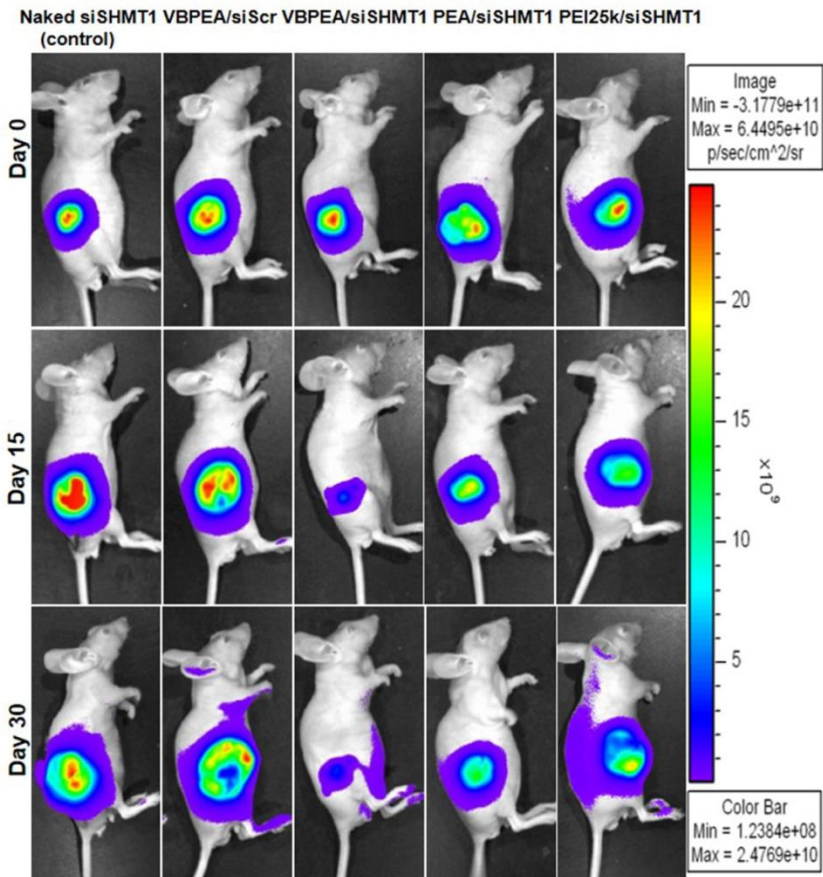


Figure 5.20. The subcutaneous injection of luciferase expressing A549 cells in 5 weeks old nude Balb/c mice ( $n = 4$ ) resulted in tumors  $\sim 1000$  mm<sup>3</sup> in size after a month. VBPEA/siSHMT1 (N/P 20), PEA/siSHMT1 (N/P 20) and PEI25k/siSHMT1 (N/P 10) complexes (with 30  $\mu$ g siSHMT1) were directly administered in the tumor with alternate doses after every 48 h for 4 weeks. Bioluminescence images taken every 15 days show a maximum in vivo tumor retardation resulting from VBPEA-mediated delivery of siSHMT1.

tumor growth inhibition, in contrast to the control groups where tumor has grown several folds than the initial volume (Figure 5.21A). Although the PEA/siSHMT1 and PEI/siSHMT1 treated mice did not show a multifold increase in tumor size, they failed to retard the tumor growth comparative to VBPEA, certainly due to their lower gene transport efficiency. In the subsequent experiments, VBPEA treated group showed a 59% decrease in SHMT1 expression in reference to the control (similar to *in vitro* SHMT1 suppression of 60%), which was higher than that of the PEA (26% decrease) or PEI (19% decrease) treated groups (Figure 5.21B). Immunohistochemical analysis also showed decreased brown staining of the SHMT1 protein throughout the tumor section of VBPEA/siSHMT1-treated group (Figure 5.22). The effect of SHMT1 suppression in VBPEA/siSHMT1-treated tumor is not only seen as diminution in tumor volume but also by the presence of apoptotic cells in tumor section (Figure 5.23) which suggests the significance of SHMT1 inactivation in treating cancer and applicability of VB<sub>6</sub>-coupled vector in enhancing siSHMT1 delivery.

Table 5.2. Tumor volume measurements using Vernier caliper every week during the one month treatment in xenograft mice (n = 4).

<b>Sample</b>	<b>Untreated (mm<sup>3</sup>)</b>	<b>Naked siSHMT1 (mm<sup>3</sup>)</b>	<b>VBPEA/ siScr (mm<sup>3</sup>)</b>	<b>VBPEA/ siSHMT1 (mm<sup>3</sup>)</b>	<b>PEA/ siSHMT1 (mm<sup>3</sup>)</b>	<b>PEI/ siSHMT1 (mm<sup>3</sup>)</b>
<b>Initial</b>	961.4 ± 24.7	889.4± 38.4	1000.5± 31.8	1066.6± 31.1	1138.4± 40.5	1166.4± 40.5
<b>Week 1</b>	2016.5 ± 66.4	1608.2± 69.5	1846.0± 85.6	956.3 ± 52.9	1241.9 ± 93.9	1203.6 ± 76.9
<b>Week 2</b>	2740.8 ± 49.2	2282.8± 68.6	2794.8± 20.7	802.1 ± 79.0	1283.5 ± 56.5	1405.9 ± 56.1
<b>Week 3</b>	3662.0 ± 49.2	3187.1± 60.9	3593.7± 51.6	590.5± 45.6	1488.4± 64.9	1583.5± 45.0
<b>Week 4</b>	4428.9 ± 66.6	4397.7± 53.2	4763.0± 173.2	471.5± 25.0	1504.6± 14.1	1884.9± 77.1

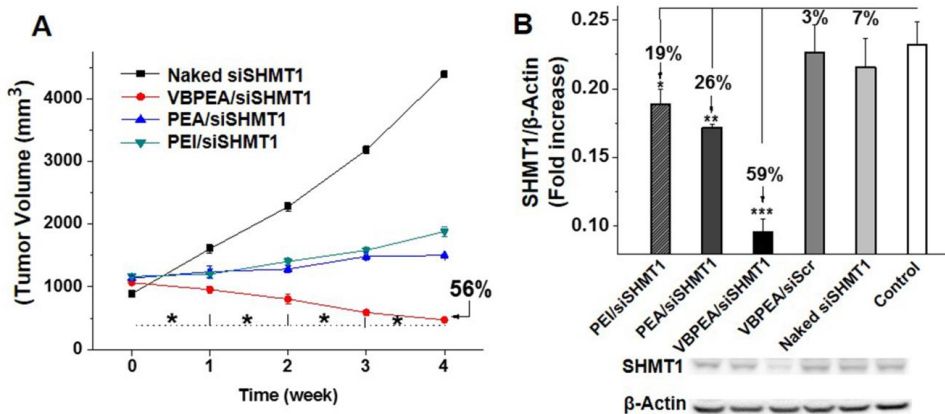


Figure 5.21. Reduction of tumor size in xenograft mice (n = 4). (A) Tumor volumes were measured using Vernier caliper every week during the treatment and ultimately resulted in ~56% reduction in tumor size. Statistical significance was determined using one-way ANOVA (\*P < 0.05, error bar represents SD). (B) Western blot analysis of the tumor mass after 1 month of treatment shows suppressed SHMT1 expression in VBPEA-mediated treated tumor. Data are shown as the mean ± SD of 3 independent experiments (\*P < 0.05; \*\*P < 0.01; \*\*\*P < 0.001, one-way ANOVA).

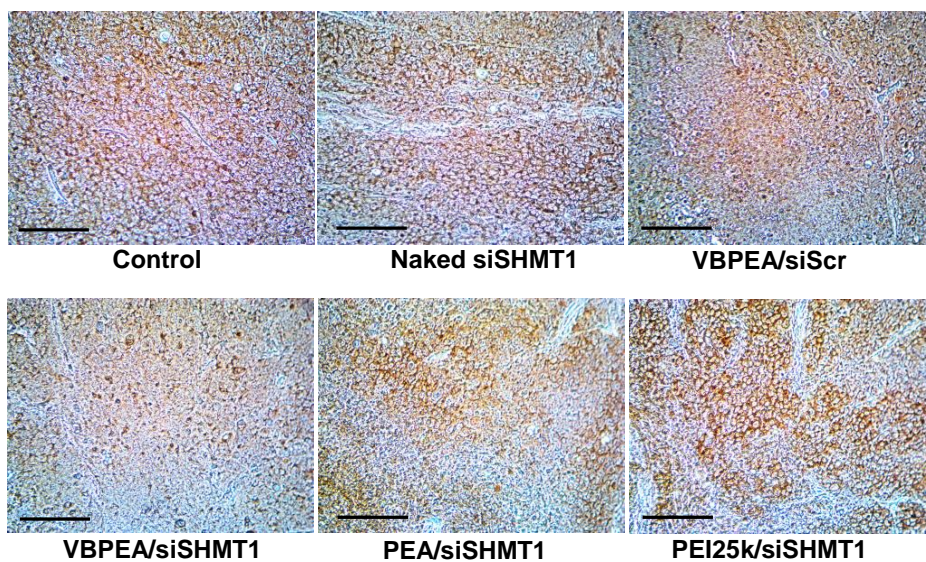


Figure 5.22. Immunohistochemistry of the formalin fixed tumor sections show decreased staining in VBPEA treated tumor section of xenograft mice (n = 4) (scale bar: 500  $\mu$ m), suggesting suppression of SHMT1 gene expression.

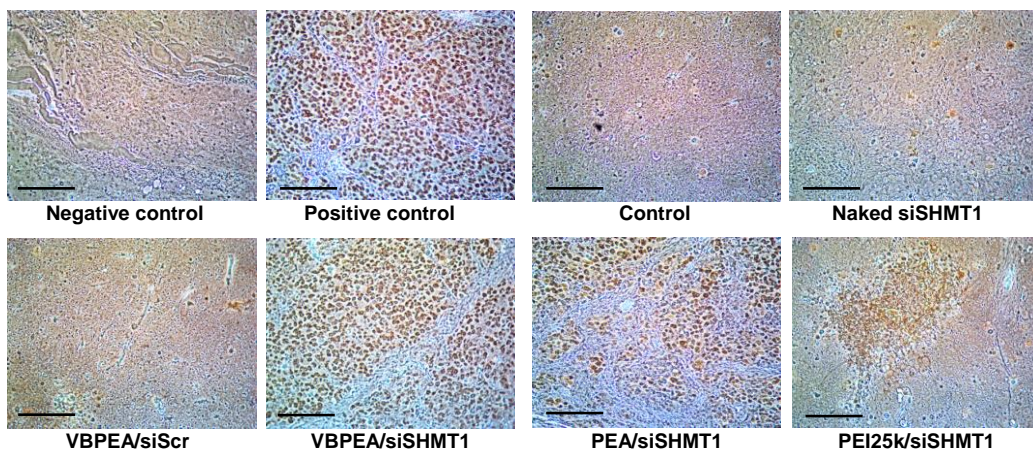


Figure 5.23. In vivo TUNEL assay of formalin fixed tumor sections show a high level of apoptotic events occurring in VBPEA/siSHMT1 treated tumors in xenograft mice (n = 4) (scale bar: 500  $\mu$ m).

## 5.5 Discussion

Our findings show that, by combining the gene silencing technology with the modification of the mode of cellular uptake of polyplex, a control on the growth of the tumor cells could be achieved. Using VB<sub>6</sub>, coupled to poly(ester amine), we sought that VB<sub>6</sub> could trail the vector along with the complexed therapeutic siRNA through its specific VTC-mediated endocytosis [146]. VB<sub>6</sub> has gained attention due to its unequalled catalytic versatility as a cofactor where VB<sub>6</sub> forms a Schiff base (aldimine) between its electrophilic carbonyl group and nucleophilic amines of an enzyme [110, 127, 128]. Similarly, the amines of PEA form a Schiff base with VB<sub>6</sub> and get reduced during the formation of VBPEA. Despite the reduction in the total number of primary amines of the backbone polymer, the enhancement in the transfection capability of VBPEA is its most striking feature [146], which underscores its potential as an efficient carrier of siRNA molecules.

SHMT catalyzed reaction in the thymidylate synthase cycle in addition to dTMP synthesis also produces glycine and methylene-THF, both of

which are the precursors for nucleotide biosynthesis [151]. During cancer progression, the SHMT enzyme is extremely required for continuous synthesis of DNA [151] and therefore, is in constant need for its cofactor, VB<sub>6</sub>. For unobstructed DNA synthesis the cellular uptake of VB<sub>6</sub> is increased in tumor cells [132, 164], due to which VB<sub>6</sub>-coupled VBPEA gains quick entry into the tumor cells in comparison to non-coupled vectors (Figure 5.13A). SHMT plays a central role in carcinogenesis and therefore its therapeutic manipulation raises exciting opportunities as well as challenges in the path towards clinical development. Inhibition of the thymidylate biosynthesis pathway due to SHMT1 knockdown by enhanced delivery of SHMT1 siRNA is expected to introduce a nanotechnology-based approach for the treatment of cancer. The mechanism of VBPEA-mediated SHMT1 silencing was demonstrated to occur via VTC-mediated endocytosis (Figure 5.13A, B). Antagonizing SHMT1 expression severely hampers the DNA synthesis mechanism by disrupting the multienzyme complex, shown by only 7% co-localization (Figure 5.16), which impairs the thymidylate synthase cycle components to assemble at nuclear lamina. The growth pattern of VBPEA/siSHMT1-treated cancer cells showed

~40% of the cell fraction in the sub-G1 phase which secondarily underwent apoptosis. Suppressed SHMT1 could not anchor the multienzyme complex to the nuclear lamina for DNA synthesis that preferentially impaired rapidly proliferating cancer cells and slowed down the tumor growth. That is why, VBPEA/siSHMT1 treated cells displayed inhibition of cell proliferation as well as induction of apoptosis. So, it can be deduced that the loss of SHMT1 function results in the cessation of thymidylate nucleotide (dTMP) synthesis from the thymidylate biosynthesis pathway. Subsequently, dUMP (deoxyuracil monophosphate) instead of dTMP is incorporated into DNA strand during DNA synthesis which leads to high genomic instability and DNA strand breaks in cancer cells [188]. Consequently, this results in apoptotic cell death and a reduction in the genomic DNA content. A speculative representation of the silencing events has been documented in Figure 5.1A.

The obtained *in vivo* results further illustrate that even at an advanced tumor state; the inactivation of SHMT1 *in situ* can bring about substantial decrease in tumor volume. We may conclude that silencing

the SHMT1 expression radically inhibits cancer growth and that this effect is enhanced by delivery via VB<sub>6</sub>-coupled vector comparable to non-coupled vector. Therefore, it is strongly recommended to study and use VB<sub>6</sub>-coupled vectors for carrying the cargo in cancer cells, which has also been suggested by Zhang et al. [122]. The attributes of VBPEA-mediated siSHMT1 delivery demonstrated in the present study suggest its potential applications in developing more profound therapeutic molecules against the uninvestigated therapeutic target SHMT1 and other VB<sub>6</sub>-dependent enzymes involved in cancer sustenance.

## **5.6 Conclusion**

Antagonizing SHMT1 expression in cancer cells using siRNA whose enhanced delivery was ensured by the VB<sub>6</sub>-coupled vector, VBPEA, showed its detrimental effect on the cell cycle and proliferation of cancer cells with subsequent onset of apoptosis. 4'-Deoxypyridoxine inhibition studies indicated the crucial involvement of VTCs in enhancing the cellular uptake of VBPEA complexes by resulting in endosome formation on the attachment of large polyplexes. Based on

the silencing results we infer that in order to support their uncontrolled growth and proliferation, cancer cells constantly need VB<sub>6</sub> for continuous functioning of thymidylate synthase cycle, resulting in enhanced VBPEA uptake. With further success in the xenograft mice model, we offer an efficient alternative to inhibit cancer growth by using VBPEA to curb SHMT1 activation that will envision a new target for cancer treatment.

# CHAPTER 6

## *SUMMARY*

---

To address the safety and specific delivery of the therapeutics to the cancer cells, vitamin B6 coupled cationic polymer was developed as a non-viral vector. PEI 1.2 kDa was used to ensure negligible polymer cytotoxicity and was linked with GDM to make poly(ester amine) (PEA) as the backbone polymer. To ~10% of the nucleophilic amines present throughout the branches of the PEA backbone, VB6 was attached via a Schiff base formation due to its electrophilic carbonyl groups. The vector, vitamin B6 coupled poly(ester amine) (VBPEA), was constructed such that (i) the VB6 provides specificity to the polymer for cancer cells, (ii) the PEI component incorporates endosomal escape property into the vector, and (iii) the PEA backbone contains degradable ester linkages which facilitate the polymer removal from the system after delivering the payload. VB6 serves as a cofactor

to various apoenzymes for cell growth and proliferation. A specific VB6 transporting carrier (VTC) facilitates the entry of VB6 in cells. VB6 present in VBPEA also utilizes this pathway for its cellular uptake. VBPEA due to its size limitation cannot pass through the VTC and consequently end up in VTC-mediated endocytosis of the polyplex. VBPEA owing to endosomal osmolysis property ruptures the endosome and enters the cell cytoplasm to deliver the therapeutic gene in the vicinity of cell nucleus. The cancer cells need VB6 more frequently and in larger amounts to support its rapid proliferation. And, subsequently it takes up the VB6 from the neighboring normal cells. Therefore, cancer cells have higher affinity for VBPEA than the normal cells and VBPEA is spontaneously channeled towards the diseased cancer tissue. Further, therapeutic study using VBPEA was done in vitro and in vivo.

Serine hydroxymethyltransferase (SHMT), a vitaminB6 (VB6)-dependent enzyme, plays a key role during DNA synthesis by generating precursors for nucleotide biosynthesis. Therefore, SHMT expression is drastically increased during cancer proliferation, making it an attractive target for cancer therapy; however, the impact of

SHMT1 knockdown on DNA synthesis machinery of cancer cells was entirely uninvestigated. To address this, SHMT1 siRNA was used and its efficient delivery was ensured by a VB6 coupled vector. The mechanism and detrimental effect of SHMT1 silencing on the cell cycle and proliferation of cancer cells with subsequent onset of apoptosis was demonstrated. SHMT1 silencing resulted in disintegration of the multienzyme complex and thus prevented the functioning of thymidylate synthase cycle in cancer cells. Xenograft tumor mice models were used to show the inhibition of tumor growth by silencing SHMT using VBPEA vector. With the success in xenograft mice model, an efficient alternative to inhibit cancer growth by curbing SHMT1 activation is offered that will envision a new target for cancer treatment.

## *REFERENCES*

---

- [1] Culver K. Gene Therapy—A Handbook for Physician. Mary Ann Liebert, Inc, New York. 1994.
- [2] Griffith F. The Significance of Pneumococcal Types. *Epidemiology & Infection*. 1928;27:113-59.
- [3] Avery OT, MacLeod CM, McCarty M. Studies on the chemical nature of the substance inducing transformation of pneumococcal types: induction of transformation by a desoxyribonucleic acid fraction isolated from pneumococcus type III. *The Journal of Experimental Medicine*. 1944;79:137-58.
- [4] Zinder ND, Lederberg J. Genetic exchange in Salmonella. *Journal of Bacteriology*. 1952;64:679-99.
- [5] Szybalska EH, Szybalski W. Genetics of human cell lines, IV. DNA-mediated heritable transformation of a biochemical trait. *Proceedings of the National Academy of Sciences*. 1962;48:2026-34.

- [6] Wirth T, Parker N, Ylä-Herttuala S. History of gene therapy. *Gene*. 2013;525:162-9.
- [7] Temin HM. Mixed infection with two types of Rous sarcoma virus. *Virology*. 1961;13:158-63.
- [8] Rogers S, Pfuderer P. Use of viruses as carriers of added genetic information. *Nature*. 1968;219:749-51.
- [9] Rogers S, Lowenthal A, Terheggen HG, Columbo JP. Induction of arginase activity with the Shope papilloma virus in tissue culture cells from an argininemic patient. *The Journal of Experimental Medicine*. 1973;137:1091-6.
- [10] Terheggen HG, Lowenthal A, Lavinha F, Colombo JP, Rogers S. Unsuccessful trial of gene replacement in arginase deficiency. *Z Kinder-Heilk*. 1975;119:1-3.
- [11] Mercola KE, Bar-Eli M, Stang HD, Slamon DJ, Cline MJ. Insertion of new genetic information into bone marrow cells of mice:

comparison of two selectable genes. *Annals of the New York Academy of Sciences*. 1982;397:272-80.

[12] Rosenberg SA, Aebersold P, Cornetta K, Kasid A, Morgan RA, Moen R, et al. Gene transfer into humans — Immunotherapy of patients with advanced melanoma, using tumor-infiltrating lymphocytes modified by retroviral gene transduction. *New England Journal of Medicine*. 1990;323:570-8.

[13] Rosenberg SA, Packard BS, Aebersold PM, Solomon D, Topalian SL, Toy ST, et al. Use of tumor-infiltrating lymphocytes and interleukin-2 in the immunotherapy of patients with metastatic melanoma. *New England Journal of Medicine*. 1988;319:1676-80.

[14] Rosenberg SA. Gene therapy for cancer. *JAMA*. 1992;268:2416-9.

[15] Rosenberg SA, Anderson WF, Blaese M, Hwu P, Yannelli JR, Yang JC, et al. The development of gene therapy for the treatment of cancer. *Annals of Surgery*. 1993;218:455-63.

[16] Blaese RM, Culver KW, Miller AD, Carter CS, Fleisher T, Clerici M, et al. T lymphocyte-directed gene therapy for ADA- SCID: Initial trial results after 4 years. *Science*. 1995;270:475-80.

[17] Edelstein ML. Gene therapy clinical trials worldwide. website at: <http://www.wiley.co.uk/genmed/clinical>. *The Journal of Gene Medicine* 2014.

[18] Bordignon C, Notarangelo LD, Nobili N, Ferrari G, Casorati G, Panina P, et al. Gene therapy in peripheral blood lymphocytes and bone marrow for ADA- immunodeficient patients. *Science*. 1995;270:470-5.

[19] Puumalainen AM, Vapalahti M, Agrawal RS, Kossila M, Laukkanen J, Lehtolainen P, et al.  $\beta$ -galactosidase gene transfer to human malignant glioma in vivo using replication-deficient retroviruses and adenoviruses. *Human Gene Therapy*. 1998;9:1769-74.

[20] Stolberg SG. The biotech death of Jesse Gelsinger. *NYTimes Mag*. 1999:136-40, 49-50.

[21] Peng Z. Current status of gendicine in China: Recombinant human Ad-p53 agent for treatment of cancers. *Human Gene Therapy*. 2005;16:1016-27.

[22] Wilson JM. Gendicine: The first commercial gene therapy product. *Human Gene Therapy*. 2005;16:1014-5.

[23] Bischoff JR, Kirn DH, Williams A, Heise C, Horn S, Muna M, et al. An adenovirus mutant that replicates selectively in p53-deficient human tumor cells. *Science*. 1996;274:373-6.

[24] Wirth T, Samaranayake H, Pikkarainen J, Määttä AM, Ylä-Herttuala S. Clinical trials for glioblastoma multiforme using adenoviral vectors. *Current Opinion in Molecular Therapeutics*. 2009;11:485-92.

[25] Maguire AM, High KA, Auricchio A, Wright JF, Pierce EA, Testa F, et al. Age-dependent effects of RPE65 gene therapy for Leber's congenital amaurosis: a phase 1 dose-escalation trial. *The Lancet*. 2009;374:1597-605.

[26] Cavazzana-Calvo M, Payen E, Negre O, Wang G, Hehir K, Fusil F, et al. Transfusion independence and HMGA2 activation after gene therapy of human  $\beta$ -thalassaemia. *Nature*. 2010;467:318-22.

[27] Jessup M, Greenberg B, Mancini D, Cappola T, Pauly DF, Jaski B, et al. Calcium upregulation by percutaneous administration of gene therapy in cardiac disease (CUPID): A phase 2 trial of intracoronary gene therapy of sarcoplasmic reticulum  $\text{Ca}^{2+}$ -ATPase in patients with advanced heart failure. *Circulation*. 2011;124:304-13.

[28] Hacein-Bey-Abina S, Hauer J, Lim A, Picard C, Wang GP, Berry CC, et al. Efficacy of gene therapy for X-linked severe combined immunodeficiency. *New England Journal of Medicine*. 2010;363:355-64.

[29] Aiuti A, Cattaneo F, Galimberti S, Benninghoff U, Cassani B, Callegaro L, et al. Gene therapy for immunodeficiency due to adenosine deaminase deficiency. *New England Journal of Medicine*. 2009;360:447-58.

[30] Boztug K, Schmidt M, Schwarzer A, Banerjee PP, Díez IA, Dewey RA, et al. Stem-cell gene therapy for the Wiskott-Aldrich syndrome. *New England Journal of Medicine*. 2010;363:1918-27.

[31] Biffi A, Montini E, Lorioli L, Cesani M, Fumagalli F, Plati T, et al. Lentiviral hematopoietic stem cell gene therapy benefits metachromatic leukodystrophy. *Science*. 2013;341.

[32] MacLaren RE, Groppe M, Barnard AR, Cottrill CL, Tolmachova T, Seymour L, et al. Retinal gene therapy in patients with choroideremia: initial findings from a phase 1/2 clinical trial. *The Lancet*. 2014;383:1129-37.

[33] Tebas P, Stein D, Tang WW, Frank I, Wang SQ, Lee G, et al. Gene editing of CCR5 in autologous CD4 T cells of persons infected with HIV. *New England Journal of Medicine*. 2014;370:901-10.

[34] Ylä-Herttuala S. Endgame: Glybera finally recommended for approval as the first gene therapy drug in the European union. *Molecular Therapy*. 2012;20:1831-2.

- [35] Edelstein ML, Abedi MR, Wixon J. Gene therapy clinical trials worldwide to 2007—an update. *The Journal of Gene Medicine*. 2007;9:833-42.
- [36] Friedmann T, Roblin R. Gene therapy for human genetic disease? *Science*. 1972;175:949-55.
- [37] Cross D, Burmester JK. Gene Therapy for cancer treatment: past, present and future. *Clinical Medicine & Research*. 2006;4:218-27.
- [38] Kowalczyk DW, Wysocki PJ, A M. Cancer immunotherapy using cells modified with cytokine genes. *Acta Biochimica Polonica*. 2003;50:613-24.
- [39] Nawrocki S, Wysocki PJ, Mackiewicz A. Genetically modified tumour vaccines: an obstacle race to break host tolerance to cancer. *Expert Opinion on Biological Therapy*. 2001;1:193-204.
- [40] Kikuchi T. Genetically modified dendritic cells for therapeutic immunity. *The Tohoku Journal of Experimental Medicine*. 2006;208:1-8.

- [41] Mullen J, Tanabe K. Viral oncolysis for malignant liver tumors. *Ann Surg Oncol*. 2003;10:596-605.
- [42] Patil S, Rhodes D, Burgess D. DNA-based therapeutics and DNA delivery systems: A comprehensive review. *AAPS J*. 2005;7:E61-E77.
- [43] Fridman JS, Lowe SW. Control of apoptosis by p53. *Oncogene*. 2003;22:9030-40.
- [44] Ziady A, Ferkol T. DNA condensation and receptor-mediated gene transfer. *Gene therapy technologies, applications and regulations: from laboratory to clinic* editor: Anthony Meager 2001:13-34.
- [45] Kohn DB, Sadelain M, Glorioso JC. Occurrence of leukaemia following gene therapy of X-linked SCID. *Nat Rev Cancer*. 2003;3:477-88.
- [46] Graham FL, van der Eb AJ. A new technique for the assay of infectivity of human adenovirus 5 DNA. *Virology*. 1973;52:456-67.

- [47] Fraley R, Subramani S, Berg P, Papahadjopoulos D. Introduction of liposome-encapsulated SV40 DNA into cells. *Journal of Biological Chemistry*. 1980;255:10431-5.
- [48] Pagano JS, McCutchan JH, Vaheiri A. Factors influencing the enhancement of the infectivity of poliovirus ribonucleic acid by diethylaminoethyl-dextran. *Journal of Virology*. 1967;1:891-7.
- [49] Gordon JW, Scangos GA, Plotkin DJ, Barbosa JA, Ruddle FH. Genetic transformation of mouse embryos by microinjection of purified DNA. *Proceedings of the National Academy of Sciences*. 1980;77:7380-4.
- [50] Klein TM, Wolf ED, Wu R, Sanford JC. High-velocity microprojectiles for delivering nucleic acids into living cells. *Nature*. 1987;327:70-3.
- [51] Andreason G. Electroporation as a technique for the transfer of macromolecules into mammalian cell lines. *Journal of Tissue Culture Methods*. 1993;15:56-62.

[52] Noble ML, Kuhr CS, Graves SS, Loeb KR, Sun SS, Keilman GW, et al. Ultrasound-targeted microbubble destruction-mediated gene delivery Into canine livers. *Mol Ther*. 2013;21:1687-94.

[53] Samal SK, Dash M, Van Vlierberghe S, Kaplan DL, Chiellini E, van Blitterswijk C, et al. Cationic polymers and their therapeutic potential. *Chemical Society Reviews*. 2012;41:7147-94.

[54] Wagner E, Cotten M, Foisner R, Birnstiel ML. Transferrin-polycation-DNA complexes: the effect of polycations on the structure of the complex and DNA delivery to cells. *Proceedings of the National Academy of Sciences*. 1991;88:4255-9.

[55] Funhoff AM, van Nostrum CF, Lok MC, Kruijtzter JAW, Crommelin DJA, Hennink WE. Cationic polymethacrylates with covalently linked membrane destabilizing peptides as gene delivery vectors. *Journal of Controlled Release*. 2005;101:233-46.

[56] Pouton CW, Lucas P, Thomas BJ, Uduehi AN, Milroy DA, Moss SH. Polycation-DNA complexes for gene delivery: a comparison of the

biopharmaceutical properties of cationic polypeptides and cationic lipids. *Journal of Controlled Release*. 1998;53:289-99.

[57] Zeng J, Wang S. Enhanced gene delivery to PC12 cells by a cationic polypeptide. *Biomaterials*. 2005;26:679-86.

[58] Fayazpour F, Lucas B, Alvarez-Lorenzo C, Sanders NN, Demeester J, De Smedt SC. Physicochemical and transfection properties of cationic hydroxyethylcellulose/DNA nanoparticles. *Biomacromolecules*. 2006;7:2856-62.

[59] Borchard G. Chitosans for gene delivery. *Advanced Drug Delivery Reviews*. 2001;52:145-50.

[60] Huang M, Fong C-W, Khor E, Lim L-Y. Transfection efficiency of chitosan vectors: Effect of polymer molecular weight and degree of deacetylation. *Journal of Controlled Release*. 2005;106:391-406.

[61] Lee CC, MacKay JA, Frechet JMJ, Szoka FC. Designing dendrimers for biological applications. *Nat Biotech*. 2005;23:1517-26.

[62] Bielinska A, Kukowska-Latallo JF, Johnson J, Tomalia DA, Baker JR. Regulation of in vitro gene expression using antisense oligonucleotides or antisense expression plasmids transfected using starburst PAMAM dendrimers. *Nucleic Acids Research*. 1996;24:2176-82.

[63] Mendiratta SK, Quezada A, Matar M, Wang J, Hebel HL, Long S, et al. Intratumoral delivery of IL-12 gene by polyvinyl polymeric vector system to murine renal and colon carcinoma results in potent antitumor immunity. *Gene Therapy*. 1999;6:833-9.

[64] Lungwitz U, Breunig M, Blunk T, Göpferich A. Polyethylenimine-based non-viral gene delivery systems. *European Journal of Pharmaceutics and Biopharmaceutics*. 2005;60:247-66.

[65] Heidel JD, Yu Z, Liu JY-C, Rele SM, Liang Y, Zeidan RK, et al. Administration in non-human primates of escalating intravenous doses of targeted nanoparticles containing ribonucleotide reductase subunit M2 siRNA. *Proceedings of the National Academy of Sciences*. 2007;104:5715-21.

[66] Davis ME. The first targeted delivery of siRNA in humans via a self-assembling, cyclodextrin polymer-based nanoparticle: from concept to clinic. *Molecular Pharmaceutics*. 2009;6:659-68.

[67] Gottfried LF, Dean DA. Extracellular and intracellular barriers to non-viral gene transfer. *Novel Gene Therapy Approaches*. 2013.

[68] Mellman I. Endocytosis and mmolecular sorting. *Annual Review of Cell and Developmental Biology*. 1996;12:575-625.

[69] Mukherjee S, Ghosh RN, Maxfield FR. Endocytosis. *Physiological Reviews*. 1997.

[70] Goldstein JL, Anderson RGW, Brown MS. Coated pits, coated vesicles, and receptor-mediated endocytosis. *Nature*. 1979;279:679-85.

[71] Rejman J, Oberle V, Zuhorn IS, Hoekstra D. Size-dependent internalization of particles via the pathways of clathrin- and caveolae-mediated endocytosis. *Biochem J* 2004;377:159-69.

[72] Douglas KL, Piccirillo CA, Tabrizian M. Cell line-dependent internalization pathways and intracellular trafficking determine

transfection efficiency of nanoparticle vectors. *European Journal of Pharmaceutics and Biopharmaceutics*. 2008;68:676-87.

[73] Nakase I, Tadokoro A, Kawabata N, Takeuchi T, Katoh H, Hiramoto K, et al. Interaction of arginine-rich peptides with membrane-associated proteoglycans is crucial for induction of actin organization and macropinocytosis. *Biochemistry*. 2006;46:492-501.

[74] Luedtke NW, Carmichael P, Tor Y. Cellular Uptake of aminoglycosides, guanidinoglycosides, and poly-arginine. *Journal of the American Chemical Society*. 2003;125:12374-5.

[75] Varkouhi AK, Scholte M, Storm G, Haisma HJ. Endosomal escape pathways for delivery of biologicals. *Journal of Controlled Release*. 2011;151:220-8.

[76] Lee H, Jeong JH, Park TG. A new gene delivery formulation of polyethylenimine/DNA complexes coated with PEG conjugated fusogenic peptide. *Journal of Controlled Release*. 2001;76:183-92.

[77] Sonawane ND, Szoka FC, Verkman AS. Chloride accumulation and swelling in endosomes enhances DNA transfer by polyamine-DNA polyplexes. *Journal of Biological Chemistry*. 2003;278:44826-31.

[78] Lechardeur D, Sohn KJ, Haardt M, Joshi PB, Monck M, Graham RW, et al. Metabolic instability of plasmid DNA in the cytosol: a potential barrier to gene transfer. *Gene Therapy*. 1999;6:482-97.

[79] Kao HP, Abney JR, Verkman AS. Determinants of the translational mobility of a small solute in cell cytoplasm. *The Journal of Cell Biology*. 1993;120:175-84.

[80] Dauty E, Verkman AS. Actin cytoskeleton as the principal determinant of size-dependent DNA mobility in cytoplasm: A new barrier for non-viral gene delivery. *Journal of Biological Chemistry*. 2005;280:7823-8.

[81] Vaughan EE, Dean DA. Intracellular trafficking of plasmids during transfection is mediated by microtubules. *Mol Ther*. 2006;13:422-8.

[82] Mesika A, Kiss V, Brumfeld V, Ghosh G, Reich Z. Enhanced intracellular mobility and nuclear accumulation of DNA plasmids associated with a karyophilic protein. *Human Gene Therapy*. 2005;16:200-8.

[83] Badding MA, Vaughan EE, Dean DA. Transcription factor plasmid binding modulates microtubule interactions and intracellular trafficking during gene transfer. *Gene Ther*. 2012;19:338-46.

[84] Lukacs GL, Haggie P, Seksek O, Lechardeur D, Freedman N, Verkman AS. Size-dependent DNA mobility in cytoplasm and nucleus. *Journal of Biological Chemistry*. 2000;275:1625-9.

[85] Brunner S, Sauer T, Carotta S, Cotten M, Saltik M, Wagner E. Cell cycle dependence of gene transfer by lipoplex, polyplex and recombinant adenovirus. *Gene Therapy*. 2000;7:401-7.

[86] Young JL, Benoit JN, Dean DA. Effect of a DNA nuclear targeting sequence on gene transfer and expression of plasmids in the intact vasculature. *Gene Ther*. 0000;10:1465-70.

[87] Schroeder A, Heller DA, Winslow MM, Dahlman JE, Pratt GW, Langer R, et al. Treating metastatic cancer with nanotechnology. *Nat Rev Cancer*. 2012;12:39-50.

[88] Safra T, Muggia F, Jeffers S, Tsao-Wei DD, Groshen S, Lyass O, et al. Pegylated liposomal doxorubicin (doxil): Reduced clinical cardiotoxicity in patients reaching or exceeding cumulative doses of 500 mg/m<sup>2</sup>. *Annals of Oncology*. 2000;11:1029-33.

[89] Tomao S, Miele E, Spinelli GP, Miele E, Tomao F. Albumin-bound formulation of paclitaxel (Abraxane<sup>®</sup> ABI-007) in the treatment of breast cancer. *Int J Nanomedicine*. 2009;4:99-105.

[90] Harisinghani MG, Saksena M, RW R. A pilot study of lymphotropic nanoparticle-enhanced magnetic resonance imaging technique in early stage testicular cancer: a new method for noninvasive lymph node evaluation. *Urology*. 2005;66:1066-71.

[91] Gabizon A, Shmeeda H, Barenholz Y. Pharmacokinetics of pegylated liposomal doxorubicin. *Clin Pharmacokinet*. 2003;42:419-36.

- [92] Lee J, Sohn JW, Zhang Y, Leong KW, Pisetsky D, Sullenger BA. Nucleic acid-binding polymers as anti-inflammatory agents. *Proceedings of the National Academy of Sciences*. 2011;108:14055-60.
- [93] Lal S, Clare SE, Halas NJ. Nanoshell-enabled photothermal cancer therapy: Impending clinical impact. *Accounts of Chemical Research*. 2008;41:1842-51.
- [94] W. Y, M. A, M. E, A. HES, S. LT, R. SR, et al. Do liposomal apoptotic enhancers increase tumor coagulation and end-point survival in percutaneous radiofrequency ablation of tumors in a rat tumor model? *Radiology*. 2010;257:685-96.
- [95] Baker I, Zeng Q, Li W, Sullivan CR. Heat deposition in iron oxide and iron nanoparticles for localized hyperthermia. *Journal of Applied Physics*. 2006;99:08H106-08H-3.
- [96] Ivkov R, DeNardo SJ, Daum W, Foreman AR, Goldstein RC, Nemkov VS, et al. Application of high amplitude alternating magnetic fields for heat induction of nanoparticles localized in cancer. *Clinical Cancer Research*. 2005;11:7093s-103s.

[97] Jain RK, Lee JJ, Hong D, Markman M, Gong J, Naing A, et al. Phase I oncology studies: Evidence that in the era of targeted therapies patients on lower doses do not fare worse. *Clinical Cancer Research*. 2010;16:1289-97.

[98] Brannon-Peppas L, Blanchette JO. Nanoparticle and targeted systems for cancer therapy. *Advanced Drug Delivery Reviews*. 2004;56:1649-59.

[99] Sarfati G, Dvir T, Elkabets M, Apte RN, Cohen S. Targeting of polymeric nanoparticles to lung metastases by surface-attachment of YIGSR peptide from laminin. *Biomaterials*. 2011;32:152-61.

[100] Yang W, Luo D, Wang S, Wang R, Chen R, Liu Y, et al. TMTP1, a novel tumor-homing peptide specifically targeting metastasis. *Clinical Cancer Research*. 2008;14:5494-502.

[101] Farokhzad OC, Jon S, Khademhosseini A, Tran T-NT, LaVan DA, Langer R. Nanoparticle-aptamer bioconjugates: A new approach for targeting prostate cancer cells. *Cancer Research*. 2004;64:7668-72.

- [102] Shigdar S, Lin J, Yu Y, Pastuovic M, Wei M, Duan W. RNA aptamer against a cancer stem cell marker epithelial cell adhesion molecule. *Cancer Science*. 2011;102:991-8.
- [103] Hanvey J, Peffer N, Bisi J, Thomson S, Cadilla R, Josey J, et al. Antisense and antigene properties of peptide nucleic acids. *Science*. 1992;258:1481-5.
- [104] Wang X, Li J, Wang Y, Koenig L, Gjyzezi A, Giannakakou P, et al. A folate receptor-targeting nanoparticle minimizes drug resistance in a human cancer model. *ACS Nano*. 2011;5:6184-94.
- [105] Arendt JFB, Pedersen L, Nexø E, Sørensen HT. Elevated plasma vitamin B12 levels as a marker for cancer: A population-based cohort study. *Journal of the National Cancer Institute*. 2013.
- [106] Michael SI, Curiel DT. Strategies to achieve targeted gene delivery via the receptor-mediated endocytosis pathway. *Gene Therapy*. 1994;1:223-32.

[107] Lehrman S. Virus treatment questioned after gene therapy death. *Nature*. 1999;401:517-8.

[108] Marshall E. Gene therapy a suspect in leukemia-like disease. *Science*. 2002;298:34-5.

[109] Zhu K, Guo C, Lai H, Yang W, Wang C. Novel hyperbranched polyamidoamine nanoparticle based gene delivery: Transfection, cytotoxicity and in vitro evaluation. *International Journal of Pharmaceutics*. 2012;423:378-83.

[110] Luo D, Saltzman, W. Mark. Synthetic DNA delivery systems. *Nat Biotech*. 2000;18:33-7.

[111] Morille M, Passirani C, Vonarbourg A, Clavreul A, Benoit J-P. Progress in developing cationic vectors for non-viral systemic gene therapy against cancer. *Biomaterials*. 2008;29:3477-96.

[112] Arote RB, Hwang S-K, Lim H-T, Kim T-H, Jere D, Jiang H-L, et al. The therapeutic efficiency of FP-PEA/TAM67 gene complexes via

folate receptor-mediated endocytosis in a xenograft mice model. *Biomaterials*. 2010;31:2435-45.

[113] Delgado D, Gascón AR, del Pozo-Rodríguez A, Echevarría E, Ruiz de Garibay AP, Rodríguez JM, et al. Dextran–protamine–solid lipid nanoparticles as a non-viral vector for gene therapy: In vitro characterization and in vivo transfection after intravenous administration to mice. *International Journal of Pharmaceutics*. 2012;425:35-43.

[114] Liang B, He M-L, Chan C-y, Chen Y-c, Li X-P, Li Y, et al. The use of folate-PEG-grafted-hybranched-PEI nonviral vector for the inhibition of glioma growth in the rat. *Biomaterials*. 2009;30:4014-20.

[115] Merdan T, Kopeček J, Kissel T. Prospects for cationic polymers in gene and oligonucleotide therapy against cancer. *Advanced Drug Delivery Reviews*. 2002;54:715-58.

[116] Hughes JA, Rao GA. Targeted polymers for gene delivery. *Expert Opinion on Drug Delivery*. 2005;2:145-57.

[117] Said HM, Kumar C. Intestinal absorption of vitamins. *Current Opinion in Gastroenterology*. 1999;15:172.

[118] Carver LA, Schnitzer JE. Caveolae: mining little caves for new cancer targets. *Nat Rev Cancer*. 2003;3:571-81.

[119] Said HM, Ortiz A, Ma TY. A carrier-mediated mechanism for pyridoxine uptake by human intestinal epithelial Caco-2 cells: regulation by a PKA-mediated pathway. *American Journal of Physiology - Cell Physiology*. 2003;285:C1219-C25.

[120] Merrill AH, Henderson JM. Diseases associated with defects in vitamin B6 metabolism or utilization. *Annual Review of Nutrition*. 1987;7:137-56.

[121] Zhu T, Stein S. Preparation of vitamin B6-conjugated peptides at the amino terminus and of vitamin B6-peptide-oligonucleotide conjugates. *Bioconjugate Chemistry*. 1994;5:312-5.

[122] Zhang ZM, McCormick DB. Uptake of N-(4'-pyridoxyl)amines and release of amines by renal cells: a model for transporter-enhanced

delivery of bioactive compounds. Proceedings of the National Academy of Sciences. 1991;88:10407-10.

[123] Arote RB, Hwang S-K, Yoo M-K, Jere D, Jiang H-L, Kim Y-K, et al. Biodegradable poly(ester amine) based on glycerol dimethacrylate and polyethylenimine as a gene carrier. The Journal of Gene Medicine. 2008;10:1223-35.

[124] L. B. Thomsen ABL, J. Lichota, T. Moos. Nanoparticle-derived non-viral genetic transfection at the blood-brain barrier to enable neuronal growth factor delivery by secretion from brain endothelium. Current Medicinal Chemistry. 2011;18:3330-4.

[125] Begley DJ. Delivery of therapeutic agents to the central nervous system: the problems and the possibilities. Pharmacology & Therapeutics. 2004;104:29-45.

[126] Merrill AH, Henderson JM. Vitamin B6 metabolism by human liver. Annals of the New York Academy of Sciences. 1990;585:110-7.

[127] Mooney S, Leuendorf J-E, Hendrickson C, Hellmann H. Vitamin B6: A long known compound of surprising complexity. *Molecules*. 2009;14:329-51.

[128] Ortega-Castro J, Adrover M, Frau J, Salvà A, Donoso J, Muñoz F. DFT studies on schiff base formation of vitamin B6 analogues. Reaction between a pyridoxamine-analogue and carbonyl compounds. *The Journal of Physical Chemistry A*. 2010;114:4634-40.

[129] Breunig M, Lungwitz U, Liebl R, Goepferich A. Breaking up the correlation between efficacy and toxicity for nonviral gene delivery. *Proceedings of the National Academy of Sciences*. 2007;104:14454-9.

[130] Merkel OM, Mintzer MA, Sitterberg J, Bakowsky U, Simanek EE, Kissel T. Triazine dendrimers as nonviral gene delivery systems: Effects of molecular structure on biological activity. *Bioconjugate Chemistry*. 2009;20:1799-806.

[131] Skelly JV, Renwick SB, Chave KJ, Sanders PG, Snell K, Baumann U. Purification, crystallization and preliminary X-ray analysis of human recombinant cytosolic serine

hydroxymethyltransferase. *Acta Crystallographica Section D*. 1998;54:1030-1.

[132] Gregory JF. A novel vitamin B6 metabolite may be a circulating marker of cancer. *Nutrition Reviews*. 1992;50:295-7.

[133] Hellmann H, Mooney S. Vitamin B6: A molecule for human health? *Molecules*. 2010;15:442-59.

[134] Yoshimori T, Yamamoto A, Moriyama Y, Futai M, Tashiro Y. Bafilomycin A1, a specific inhibitor of vacuolar-type H(+)-ATPase, inhibits acidification and protein degradation in lysosomes of cultured cells. *Journal of Biological Chemistry*. 1991;266:17707-12.

[135] Hannon GJ. RNA interference. *Nature*. 2002;418:244-51.

[136] Fire A, Xu S, Montgomery MK, Kostas SA, Driver SE, Mello CC. Potent and specific genetic interference by double-stranded RNA in *Caenorhabditis elegans*. *Nature*. 1998;391:806-11.

- [137] Zamore PD, Tuschl T, Sharp PA, Bartel DP. RNAi: Double-stranded RNA directs the ATP-dependent cleavage of mRNA at 21 to 23 nucleotide intervals. *Cell*. 2000;101:25-33.
- [138] Gregory RI, Chendrimada TP, Cooch N, Shiekhattar R. Human RISC couples microRNA biogenesis and posttranscriptional gene silencing. *Cell*. 2005;123:631-40.
- [139] Hutvagner G, Simard MJ. Argonaute proteins: key players in RNA silencing. *Nat Rev Mol Cell Biol*. 2008;9:22-32.
- [140] Bruce Alberts, Alexander Johnson, Julian Lewis, Martin Raff, Keith Roberts, Walter P. Cancer, *Molecular biology of the cell* 5th Edition: Garland Science; 2007.
- [141] Jiang F, Ye X, Liu X, Fincher L, McKearin D, Liu Q. Dicer-1 and R3D1-L catalyze microRNA maturation in *Drosophila*. *Genes & development*. 2005;19:1674-9.

- [142] Liu X JF, Kalidas S, Smith D, Liu Q. Dicer-2 and R2D2 coordinately bind siRNA to promote assembly of the siRISC complexes. *RNA*. 2006;12:1514-20.
- [143] Song J-J, Smith SK, Hannon GJ, Joshua-Tor L. Crystal structure of argonaute and its implications for RISC slicer activity. *Science*. 2004;305:1434-7.
- [144] Schwarz DS, Hutvágner G, Du T, Xu Z, Aronin N, Zamore PD. Asymmetry in the assembly of the RNAi enzyme complex. *Cell*. 2003;115:199-208.
- [145] Lim Y-b, Kim S-m, Suh H, Park J-s. Biodegradable, endosome disruptive, and cationic network-type polymer as a highly efficient and nontoxic gene delivery carrier. *Bioconjugate Chemistry*. 2002;13:952-7.
- [146] Pandey S, Garg P, Lim KT, Kim J, Choung Y-H, Choi Y-J, et al. The efficiency of membrane transport of vitamin B6 coupled to poly(ester amine) gene transporter and transfection in cancer cells. *Biomaterials*. 2013;34:3716-28.

[147] Anderson DD, Stover PJ. SHMT1 and SHMT2 are functionally redundant in nuclear *de novo* thymidylate biosynthesis. PLoS ONE. 2009;4:e5839.

[148] Anderson DD, Woeller CF, Chiang E-P, Shane B, Stover PJ. Serine hydroxymethyltransferase anchors *de novo* thymidylate synthesis pathway to nuclear lamina for DNA synthesis. Journal of Biological Chemistry. 2012;287:7051-62.

[149] Nelson DL, Cox MM. Biosynthesis of amino acids, nucleotides, and related molecules. Lehninger Principles of Biochemistry: W. H. Freeman Publishers; 2013. p. 833-80.

[150] Thorndike J, Pelliniemi T-T, Beck WS. Serine hydroxymethyltransferase activity and serine incorporation in leukocytes. Cancer Research. 1979;39:3435-40.

[151] Renwick SBS, Skelly JVJ, Chave KJK, Sanders PGP, Snell KK, Baumann UU. Purification, crystallization and preliminary X-ray analysis of human recombinant cytosolic serine

hydroxymethyltransferase. *Acta Crystallogr D Biol Crystallogr*. 1998;54:1030-1.

[152] Jain M, Nilsson R, Sharma S, Madhusudhan N, Kitami T, Souza AL, et al. Metabolite profiling identifies a key role for glycine in rapid cancer cell proliferation. *Science*. 2012;336:1040-4.

[153] Amadasi A. Pyridoxal 5'-phosphate enzymes as targets for therapeutic agents. *Current medicinal chemistry*. 2007;14:1291.

[154] Papamichael D. The use of thymidylate synthase inhibitors in the treatment of advanced colorectal cancer: Current status. *The Oncologist*. 1999;4:478-87.

[155] Marsh S. Thymidylate synthase pharmacogenetics. *Invest New Drugs*. 2005;23:533-7.

[156] Schweitzer BI, Dicker AP, Bertino JR. Dihydrofolate reductase as a therapeutic target. *The FASEB Journal*. 1990;4:2441-52.

[157] Wang T-L, Diaz LA, Romans K, Bardelli A, Saha S, Galizia G, et al. Digital karyotyping identifies thymidylate synthase amplification as

a mechanism of resistance to 5-fluorouracil in metastatic colorectal cancer patients. Proceedings of the National Academy of Sciences of the United States of America. 2004;101:3089-94.

[158] Banerjee D, Mayer-Kuckuk P, Capioux G, Budak-Alpdogan T, Gorlick R, Bertino JR. Novel aspects of resistance to drugs targeted to dihydrofolate reductase and thymidylate synthase. *Biochimica et Biophysica Acta (BBA) - Molecular Basis of Disease*. 2002;1587:164-73.

[159] Vicentini F, Borgheti-Cardoso L, Depieri L, Macedo Mano D, Abelha T, Petrilli R, et al. Delivery systems and local administration routes for therapeutic siRNA. *Pharm Res*. 2013;30:915-31.

[160] Ozpolat B, Sood AK, Lopez-Berestein G. Nanomedicine based approaches for the delivery of siRNA in cancer. *Journal of Internal Medicine*. 2010;267:44-53.

[161] Grant BD, Donaldson JG. Pathways and mechanisms of endocytic recycling. *Nat Rev Mol Cell Biol*. 2009;10:597-608.

[162] Wu F, Christen P, Gehring H. A novel approach to inhibit intracellular vitamin B6-dependent enzymes: proof of principle with human and plasmodium ornithine decarboxylase and human histidine decarboxylase. *The FASEB Journal*. 2011;25:2109-22.

[163] Schirch V, Szebenyi DME. Serine hydroxymethyltransferase revisited. *Current Opinion in Chemical Biology*. 2005;9:482-7.

[164] GP T, HP M, GP S. Vitamin B6 and cancer (review). *Anticancer Research*. 1981;1:263-7.

[165] Hans-Georg Eichler RH, Keith Snell. The role of serine hydroxymethyltransferase in cell proliferation: DNA synthesis from serine following mitogenic stimulation of lymphocytes. *Bioscience Reports*. 1981;1:101-6.

[166] Tripathi SK, Gupta N, Mahato M, Gupta KC, Kumar P. Selective blocking of primary amines in branched polyethylenimine with biocompatible ligand alleviates cytotoxicity and augments gene delivery efficacy in mammalian cells. *Colloids and Surfaces B: Biointerfaces*. 2014;115:79-85.

- [167] Arif M, Tripathi SK, Gupta KC, Kumar P. Self-assembled amphiphilic phosphopyridoxyl-polyethylenimine polymers exhibit high cell viability and gene transfection efficiency in vitro and in vivo. *Journal of Materials Chemistry B*. 2013;1:4020-31.
- [168] Cairns J. Mutation selection and the natural history of cancer. *Nature*. 1975;255:197-200.
- [169] Nowell P. The clonal evolution of tumor cell populations. *Science*. 1976;194:23-8.
- [170] Elbashir SM, Harborth J, Lendeckel W, Yalcin A, Weber K, Tuschl T. Duplexes of 21-nucleotide RNAs mediate RNA interference in cultured mammalian cells. *Nature*. 2001;411:494-8.
- [171] Whitehead KA, Langer R, Anderson DG. Knocking down barriers: advances in siRNA delivery. *Nat Rev Drug Discov*. 2009;8:129-38.

[172] Kim NW, Piatyszek MA, Prowse KR, Harley CB, West MD, Ho PL, et al. Specific association of human telomerase activity with immortal cells and cancer. *Science (New York, NY)*. 1994;266:2011-5.

[173] Weinert LHaT. Checkpoints: controls that ensure the order of cell cycle events. *Science*. 1989;246:629-34.

[174] Viviane Castelo Branco Reis FAGT, Marcio José Poças-Fonseca, Marlene Teixeira De-Souza, Diorge Paulo de Souza, João Ricardo Moreira Almeida, Camila Marinho-Silva, Nádia Skorupa Parachin, Alessandra da Silva Dantas, Thiago Machado Mello-de-Sousa, Lídia Maria Pepe de Moraes. Cell cycle, DNA replication, repair, and recombination in the dimorphic human pathogenic fungus *Paracoccidioides brasiliensis*. *Genet Mol Res*. 2005;4:232-50.

[175] Nio Y, Tamura K, Kan N, Inamoto T, Ohgaki K, Kodama H. In vitro DNA synthesis in freshly separated human breast cancer cells assessed by tritiated thymidine incorporation assay: relationship to the long-term outcome of patients. *British Journal of Surgery*. 1999;86:1463-9.

[176] Shirasaka T, Fujii S. DNA synthesis in tumor-bearing rats. *Cancer Research*. 1975;35:517-20.

[177] Narasimha Rao K, Bhattacharya RK, Venkatachalam SR. Thymidylate synthase activity in leukocytes from patients with chronic myelocytic leukemia and acute lymphocytic leukemia and its inhibition by phenanthroindolizidine alkaloids pergularinine and tylophorinidine. *Cancer Letters*. 1998;128:183-8.

[178] Elsea SH, Juyal RC, Jiralerspong S, Finucane BM, Pandolfo M, Greenberg F, et al. Haploinsufficiency of cytosolic serine hydroxymethyltransferase in the Smith-Magenis syndrome, 1995.

[179] Appaji Rao N, Talwar R, Savithri HS. Molecular organization, catalytic mechanism and function of serine hydroxymethyltransferase — a potential target for cancer chemotherapy. *The International Journal of Biochemistry & Cell Biology*. 2000;32:405-16.

[180] Renwick SB, Snell K, Baumann U. The crystal structure of human cytosolic serine hydroxymethyltransferase: a target for cancer chemotherapy. *Structure*. 1998;6:1105-16.

[181] Duvall E, Wyllie AH. Death and the cell. *Immunology Today*. 1986;7:115-9.

[182] Wyllie AH, Kerr JFR, Currie AR. Cell Death: The significance of apoptosis. *International Review of Cytology*: Academic Press; 1980. p. 251-306.

[183] Carson DA, Ribeiro JM. Apoptosis and disease. *The Lancet*. 1993;341:1251-4.

[184] Hickman J. Apoptosis induced by anticancer drugs. *Cancer Metast Rev*. 1992;11:121-39.

[185] van Engeland M, Nieland LJW, Ramaekers FCS, Schutte B, Reutelingsperger CPM. Annexin V-affinity assay: A review on an apoptosis detection system based on phosphatidylserine exposure. *Cytometry*. 1998;31:1-9.

[186] Sherr CJ. Cancer cell cycles. *Science*. 1996;274:1672-7.

[187] Durcan N, Murphy C, Cryan S-A. Inhalable siRNA: Potential as a therapeutic agent in the lungs. *Molecular Pharmaceutics*. 2008;5:559-66.

[188] Herbig K, Chiang E-P, Lee L-R, Hills J, Shane B, Stover PJ. Cytoplasmic serine hydroxymethyltransferase mediates competition between folate-dependent deoxyribonucleotide and S-adenosylmethionine biosyntheses. *Journal of Biological Chemistry*. 2002;277:38381-9.

## *LIST OF PUBLICATIONS*

---

1. **S Pandey\***, P Garg\*, Somin Lee, Yun-Hoon Choung, Pill-Hoon Choung\*\*, and Jong Hoon Chung, Nucleotide biosynthesis arrest by silencing SHMT1 function via vitamin B6-coupled vector and effects on tumor growth inhibition, **Biomaterials**, 35 (2014), 9332-9342.
2. **S Pandey\***, P Garg\*, KT Lim, J Kim, YH Choung, YJ Choi, PH Choung, CS Cho and JH Chung, The efficiency of membrane transport of vitamin B6 coupled to Poly(ester amine) gene transporter and transfection in cancer cells, **Biomaterials**, 34 (2013), 3746-3728.
3. P Garg, **S Pandey**, B Kang, J Kim, K T Lim, M H Cho, T-E Park, Y J Choi, P H Choung, C S Cho and J H Chung, Highly efficient gene transfection by hyperosmotic polymannitol based gene

- transporter through regulation of caveolae and COX-2 induced endocytosis, **J. Mater. Chem. B**, 2 (2014), 2666-2679.
4. J Kim, HN Kim, KT Lim, Y Kim, **S Pandey**, P Garg, YH Choung, PH Choung, KY Suh and JH Chung, Synergistic Effects of Nanotopography and Co-Culture with Endothelial Cells on Osteogenesis of Mesenchymal Stem Cells, **Biomaterials**, 34 (2013), 7257-7268.
  5. P Garg\*, S Kumar\*, **S Pandey**, H Seonwoo, PH Choung, J Koh and JH Chung, Triphenylamine coupled chitosan with high buffering capacity and low viscosity for enhanced transfection in mammalian cells in vitro and in vivo, **J. Mater. Chem. B**, 1 (2013), 6053-6065.
  6. P. Garg\*, S. Pandey\*, Seonwoo Hoon, Seungmin Yeom, Choung Yun-Hoon, Cho Chong-Su, Choung Pill-Hoon and Chung Jong Hoon, Hyperosmotic polydixylitol for crossing blood brain barrier and efficient nucleic acid delivery, **ChemComm**.

NOTE: \*equal contributions



Attribution–NonCommercial–NoDerivs 2.0 KOREA

You are free to :

- **Share** — copy and redistribute the material in any medium or format

Under the following terms :



Attribution — You must give [appropriate credit](#), provide a link to the license, and [indicate if changes were made](#). You may do so in any reasonable manner, but not in any way that suggests the licensor endorses you or your use.



NonCommercial — You may not use the material for [commercial purposes](#).



NoDerivatives — If you [remix, transform, or build upon](#) the material, you may not distribute the modified material.

You do not have to comply with the license for elements of the material in the public domain or where your use is permitted by an applicable exception or limitation.

This is a human-readable summary of (and not a substitute for) the [license](#).

[Disclaimer](#) 

**A Dissertation for the Degree of Doctor of Philosophy**

**Vitamin B6-Coupled Poly(ester  
amine) Mediated DNA and siRNA  
Delivery via Modulation of  
Intracellular Uptake  
Process for Cancer Therapy**

**August 2015**

**Shambhavi Pandey**

**Department of Biosystems & Biomaterials Science and**

**Engineering**

**Seoul National University**

*Dedicated to*

*My Parents, Beloved Husband*

*&*

*Advisor, Prof. Jong Hoon Chung*

# *ABSTRACT*

---

The innovative methodologies in the broad field of cancer gene therapy promises a number of potential benefits for diagnosis and treatment that are likely to become important in preventing deaths from cancer. DNA synthesis mechanism underlying cancer cell proliferation and mutations can be selected for therapeutic attack to cause cell death or slow the growth of the cancer, which is one of the objectives of the research study. Elevated serine hydroxymethyltransferase (SHMT, one of the components of DNA synthesis machinery) activity has been shown to be coupled with the increased demand for DNA synthesis in rapidly proliferating cancer cells. It is also found that complete knockout of SHMT leads to glycine auxotrophy which leads to impairment in the synthesis of purines and pyrimidines. Therefore the central role of SHMT in nucleotide biosynthesis makes it a suitable anticancer target which can be selectively silenced by delivering siRNA to shut down the whole DNA synthesis machinery in cancer cells. However, the

immense potential of RNAi in anti-cancer therapy is impeded by the non-availability of a suitable delivery agent, off-target effects and induction of innate immune response. Therefore, engineering a non-viral vector which can efficiently deliver the siRNA against SHMT involved in DNA biosynthesis with higher affinity to cancer cells becomes an interesting research area.

Vitamin B6 (VB6) plays an essential role as a coenzyme in various cellular metabolic functions, including DNA biosynthesis for cellular growth and proliferation. VB6 is taken up by cells through facilitated diffusion via VB6 transporting membrane carrier (VTC). In this study, it was demonstrated that the VB6-coupled poly(ester amine) (VBPEA) gene transporter utilizes this uptake mechanism, leading to enhanced vector transport inside the rapidly proliferating cancer cells with relatively high affinity. Physicochemical characterization, cell viability assays, and transfection studies showed VBPEA to meet the standards of a good transfection agent. Competitive inhibition of VBPEA uptake by its structural analogue 4'-deoxypyridoxine hydrochloride revealed the involvement of VB6 specific transporting membrane carrier in

VBPEA internalization in tumor cells. VBPEA elicit higher transfection levels in lung cancer cells (A549) than in normal lung cells (16HBE), indicating that cancer cells which have a high demand for VB6, have a higher affinity for VB6-coupled vector. VB6 coupling to the gene transporter is important to enforce a high level of VTC-mediated endocytosis compared to VB6 alone. This system exemplified how understanding of the VB6 membrane transporter specificity allowed for the design of a VB6-coupled gene transporter with accelerated transfection activity in cancer cells owing to an advanced mode of internalization.

The advancement in study was done by examining its therapeutic application in cancer tissue using RNAi technology. Serine hydroxymethyltransferase isoforms (SHMT1 & SHMT2 $\alpha$ ), which serve as scaffold protein for the formation of a multienzyme complex and generate one-carbon unit for the de novo thymidylate biosynthesis pathway during DNA synthesis, are vitamin B6-dependent enzyme. Cancer cells with high proliferation intensity need increased SHMT activation which enforces the facilitated-diffusion of VB6 for the

continuous functioning of thymidylate synthase cycle. Therefore, SHMT knockdown presents an alternative approach to prevent DNA synthesis in cancer cells; however, its potential to inhibit cancer growth remains unknown so far. Here it was demonstrated that VB6 coupled to poly(ester amine) enforces a high level of VTC-mediated endocytosis of the complexed SHMT1 siRNA (siSHMT1) to interrupt the thymidylate biosynthesis pathway of cancer cells. The detrimental effect of SHMT1 knockdown on the disintegration of multienzyme complex resulted in cell cycle arrest and a decrease in cell's genomic DNA content, leading to enhanced apoptotic events in cancer cells. A reduction in tumor size was observed with constant SHMT1 suppression in xenograft mice. This study illustrates how silencing the SHMT1 expression inhibits cancer growth and the increased VB6 channeling for sustenance of cancer cells promotes VB6-coupled vector to elicit enhanced delivery of siSHMT1.

**Keywords:** Vitamin B6, Poly(ester amine), Membrane carrier, Gene transporter, Serine hydroxymethyl transferase 1, siRNA.

**Student number:** 2011-31353

## *Objectives of the Dissertation*

---

The research study aims at designing a polymer-based non-viral cationic vector with innocuous profile and capable of enhancing cellular uptake in cancer cells to find its application in cancer gene therapy. The first objective of the dissertation is to develop vitamin B6-coupled vector that demonstrate high delivery efficacy in cancer cells together with endosomal escape and degradation properties to ensure efficient transfection activity. In order to overcome the major intracellular trafficking barriers, mechanistic investigation of the vector as to how it modulates the uptake in cancer cells and enhances transgene expression becomes the second objective to study. The final goal is to explore the cancer treatment strategy using RNAi technology to knockdown the function of a VB6 dependent enzyme involved in some vital function of cancer progression.

Chapter 1 of the dissertation is a detailed introduction to the broad field of gene therapy describing its history, limitations, applications, criteria,

strategies, clinical trials, present progress and future prospective. The treatment strategies are addressed mainly in relation to cancer therapeutics.

Chapter 2 focuses on the development of vitamin B6-coupled poly(ester amine) (VBPEA) gene transporter with each component of the vector explaining its specific intended function while delivering the DNA in the cancer cells. VB6 is attached to the branches of the polymer backbone to increase its affinity towards cancer cells; the PEI 1.2 kDa polymer ensures its non-cytotoxic behavior and endosomal escape capability, and finally the ester linkages between the polymer fragments incorporate degradability into the vector.

In chapter 3 the mechanism of enhanced uptake in cancer cells, endocytosis routes of the vector and the role of VB6 in increasing the overall transfection efficiency of the polymer is addressed.

Chapter 4 throws light on the use of RNAi technology in cancer treatment. It illustrates the silencing efficiency of VBPEA using various marker siRNAs in cancer cells.

Chapter 5 elaborates the importance on ceasing the DNA synthesis machinery of the cancer cells in order to stop their growth and proliferation. Emphasis is given on the central role of serine hydroxymethyltransferase 1 (SHMT1) enzyme (VB6 dependent enzyme) in DNA biosynthesis and how it can be used as a strategy to control the cancer cell cycle and progression. The chapter demonstrates nucleotide biosynthesis arrest in cancer cells by silencing the SHMT1 function via SHMT1 siRNA efficiently delivered by VBPEA in vitro and in vivo. The silencing effect on the DNA synthesis and cell cycle of the cancer cells and on the tumor growth is precisely illustrated.

# *CONTENTS*

---

Abstract.....	i
Objectives of the Dissertation.....	v
Contents.....	viii
List of Tables .....	xii
List of Figures.....	xiii
List of Abbreviations .....	xviii
<b>Chapter 1. Introduction to Gene Therapy .....</b>	<b>1</b>
1.1 Historical background of gene therapy .....	1
1.2 Current scenario of gene therapy .....	9
1.3 Cancer gene therapy .....	12
1.4 Gene delivery vectors.....	20
1.5 Need for the non-viral vector mediated gene delivery .....	20
1.6 Non-viral gene delivery systems .....	22
1.7 Biological barriers for cellular uptake.....	24
1.8 Criteria for successful cancer gene therapy.....	31

1.9	Strategies to use nanotechnology in cancer gene therapy .....	32
1.10	Objective of the study .....	37
1.11	Conclusion.....	37

## **Chapter 2. Synthesis & Transfection Efficiency of**

### **Vitamin B6-Coupled Poly(ester amine) Gene Transporter**

.....	<b>39</b>	
2.1	Introduction .....	39
2.2	Materials and Methods .....	43
2.3	Results .....	52
2.4	Discussion .....	71
2.5	Conclusion.....	73

## **Chapter 3. Membrane Transport Mechanism of**

### **Vitamin B6-Coupled Poly(ester amine)..... 74**

3.1	Introduction .....	74
3.2	Materials and Methods .....	75
3.3	Results .....	81
3.4	Discussion .....	92
3.5	Conclusion.....	97

<b>Chapter 4. Gene Silencing Efficiency of Vitamin B6-Coupled Poly(ester amine)</b> .....	<b>99</b>
4.1 Introduction .....	99
4.2 Literature Review .....	101
4.3 Materials and Methods .....	105
4.4 Results .....	113
4.5 Discussion .....	122
4.6 Conclusion.....	122
<b>Chapter 5. Nucleotide Biosynthesis Arrest by Silencing SHMT1 Function</b> .....	<b>124</b>
5.1 Introduction .....	124
5.2 Literature Review .....	129
5.3 Materials and Methods .....	151
5.4 Results .....	166
5.5 Discussion .....	190
5.6 Conclusion.....	193
<b>Chapter 6. Summary</b> .....	<b>195</b>
References .....	198

List of Publications .....	236
Acknowledgement .....	238

# *LIST OF TABLES*

---

Table 2.1 Characterization of VBPEA polymer

Table 4.1 siRNA sequences of GFP, luciferase and scrambled

Table 5.1 Purity of genomic DNA

Table 5.2 Tumor volume measurements during the one month  
treatment in xenograft mice

# *LIST OF FIGURES*

---

Figure 1.1 Timeline highlighting important milestones in gene therapy

Figure 1.2 Statistics of the number of gene therapy clinical trials

Figure 1.3 Current scenario of the phases of gene therapy clinical trials

Figure 1.4 Graphical representation of the various diseases addressed by gene therapy

Figure 1.5 Schematic representation of immunotherapy

Figure 1.6 Schematic representation of oncolytic virotherapy

Figure 1.7 Schematic representation of gene transfer therapy

Figure 1.8 Various gene transporting vectors used in clinical trials

Figure 1.9 Intracellular barriers for non-viral gene transfer

Figure 1.10 An artistic representation depicting the proton sponge hypothesis

Figure 1.11 Nanotechnological strategies for diagnosis, treatment and targeting of cancer cells

Figure 2.1 Synthesis scheme of vitamin B6-coupled poly(ester amine) (VBPEA)

Figure 2.2  $^1\text{H-NMR}$  spectra of VBPEA, PEA, and VB6 in  $\text{D}_2\text{O}$

Figure 2.3 Electrophoretic mobility shift assay of VBPEA/DNA polyplexes

Figure 2.4 Dynamic light scattering microscopic measurements

Figure 2.5 Particle size in various percent serum concentrations

Figure 2.6 EF-TEM images

Figure 2.7 Cytotoxicity of VBPEA/DNA complexes

Figure 2.8 *In vitro* transfection studies of VBPEA/DNA complexes

Figure 2.9 Percent transfection efficiency measured by FACS

Figure 2.10 FACS studies showing transfection efficiency of VBPEA polyplexes

Figure 2.11 Transfection of VBPEA/DNA complexes in presence of serum

Figure 2.12 *In vivo* luciferase protein expressions

Figure 3.1 Carrier-mediated uptake of VBPEA

Figure 3.2 Confocal microscopic images

Figure 3.3 VB6 coupling enhances cellular uptake

Figure 3.4 Uptake study of VBPEA/pGL3 by primary cells vs. cancer cells

Figure 3.5 Cytotoxicity of in 16HBE (human) and LA4 (mouse) normal lung cell lines

Figure 3.6 Effect of caveolae- and clathrin- endocytic inhibitors on transfection

Figure 3.7 Bafilomycin A1 studies

Figure 3.8 Diagrammatic representation of VBPEA/DNA uptake mechanism

Figure 4.1 Mechanism of RNA interference

Figure 4.2 Physicochemical characterization of VBPEA/siRNA complexes

Figure 4.3 Cytotoxicity of VBPEA/siRNA complexes

Figure 4.4 Study of VBPEA<sup>T</sup>/siRNA nanoplex uptake and degradation

Figure 4.5 Cytotoxicity measurements of VBPEA<sup>T</sup>/siRNA

Figure 4.6 GFP silencing efficiency of VBPEA/siRNA complexes

Figure 4.7 Luciferase silencing efficiency of VBPEA/siLuc polyplexes

Figure 5.1 Schematic illustration of silencing events after the delivery of VBPEA/siSHMT1

Figure 5.2 Metastasis shown in the bone marrow from carcinoma of prostate gland

Figure 5.3 Checkpoints and inputs of regulatory information to the cell cycle control system

Figure 5.4 Progression of benign tumor to malignant tumor

Figure 5.5 The stages of progression in cancer development

Figure 5.6 A single mutation is not enough to cause cancer

Figure 5.7 Photograph of cells collected from the surface of uterine cervix

Figure 5.8 The basic structure of nitrogenous bases and their synthetic requirements

Figure 5.9 Thymidylate synthase cycle

Figure 5.10 Reaction catalyzed by SHMT

Figure 5.11 SHMT1 gene silencing efficiency of VBPEA/siSHMT1 complexes

Figure 5.12 Western blot analysis of SHMT1

Figure 5.13 SHMT1 gene silencing efficiency is enhanced by VTC-mediated endocytosis

Figure 5.14 Effect of SHMT1 knockdown on the proliferative behavior of A549 cells

Figure 5.15 SHMT1 knockdown onsets the apoptotic events in A549 cells

Figure 5.16 SHMT1 knockdown affected DNA synthesis

Figure 5.17 SHMT1 knockdown resulted in cell cycle arrest

Figure 5.18 FACS analysis

Figure 5.19 SHMT1 knockdown decreased the total genomic DNA content

Figure 5.20 *In vivo* bioimaging

Figure 5.21 Reduction of tumor size in xenograft mice

Figure 5.22 Immunohistochemistry

Figure 5.23 *In vivo* TUNEL assay

# *LIST OF ABBREVIATIONS*

---

ATP	Adenosine triphosphate
bPEI	Branched polyethyleneimine
CPP	Cell-penetrating peptides
DHFR	Dihydrofolate reductase
DLS	Dynamic light scattering microscope
DMSO	Dimethyl sulphoxide
DNA	Deoxyribonucleic acid
EDTA	Ethylenediaminetetra acetic acid
EMA	European Medicines Agency
EMSA	Electrophoretic mobility shift assay
EU	European Union
GFP	Green fluorescent protein
GPC	Gel permeation chromatography
HGPRT	Hypoxanthine-guanine phosphoribosyl transferase
HMW	High molecular weight
LMW	Low molecular weight

MTT	3-(4, 5-Dimethyl thiazol-2-yl)-2, 5-diphenyl tetrazolium bromide
NaCNBH <sub>4</sub>	Sodium cyanoborohydride
NLS	Nuclear localization sequence
NMR	Nuclear magnetic resonance
NPCs	Nuclear pore complexes
PNA	Peptide nucleic acid
RGD	Arginine-Glycine-Aspartic acid peptide
RNA	Ribonucleic acid
RNAi	RNA interference
SDS-PAGE	Sodium dodecyl sulfate polyacrylamide gel electrophoresis
SHMT	Serine hydroxymethyltransferase
siRNA	Small interfering ribonucleic acid
siScr	Scrambled small interfering ribonucleic acid
TEM	Transmission electron microscope
TILs	Tumor-infiltrating lymphocytes
TRITC	Tetramethylrhodamine isothiocyanate
TYMS	Thymidylate synthase
VB6	Vitamin B6

# CHAPTER 1

## *Introduction to Gene Therapy*

---

### **1.1 Historical background of gene therapy**

Gene therapy is the introduction of an exogenous nucleic acid with therapeutic potential into the target cell to induce desirable cellular response for the treatment of inherited or acquired diseases [1]. Figure 1.1 is highlighting some of the milestones during the history of gene therapy. The concept of gene therapy had its beginning since 1928 when Frederick Griffith first described the transformation in pneumococcus bacteria [2]. In his study he reported that the non-virulent R form of Type I pneumococcus when mixed with heat-inactivated virulent S form of Type II pneumococcus was transformed into virulent S form and developed infection. Since the original virulent S form of Type II pneumococcus was heat-inactivated, he also concluded that R form must have also transformed from Type I to Type

II. With the aim to identify the substance that was responsible for transformation, Avery and McCarty in 1944 demonstrated that it was deoxyribonucleic acid (DNA) which was transferred and caused transformation [3]. Later in 1952, Joshua Lederberg together with Norton Zinder uncovered another mechanism of genetic transfer in bacteria in addition to transformation, termed as transduction [4] where the genetic material was transferred between bacterial strains not in the form of pure DNA but instead bacteriophage carried DNA from one bacterium to another. This fundamental discovery explained how bacteria of different species could gain resistance to the same antibiotic very quickly with phage mediated transfer of genetic material. This phenomenon instigated the research of its potential benefit as a tool for transferring hereditary traits and was soon extended to eukaryotic viruses also.

It was then known that cells are able to take up foreign DNA. However, there was no successful documentation of heritable transformation of a biochemical trait, until 1962, when Waclaw Szybalski while doing

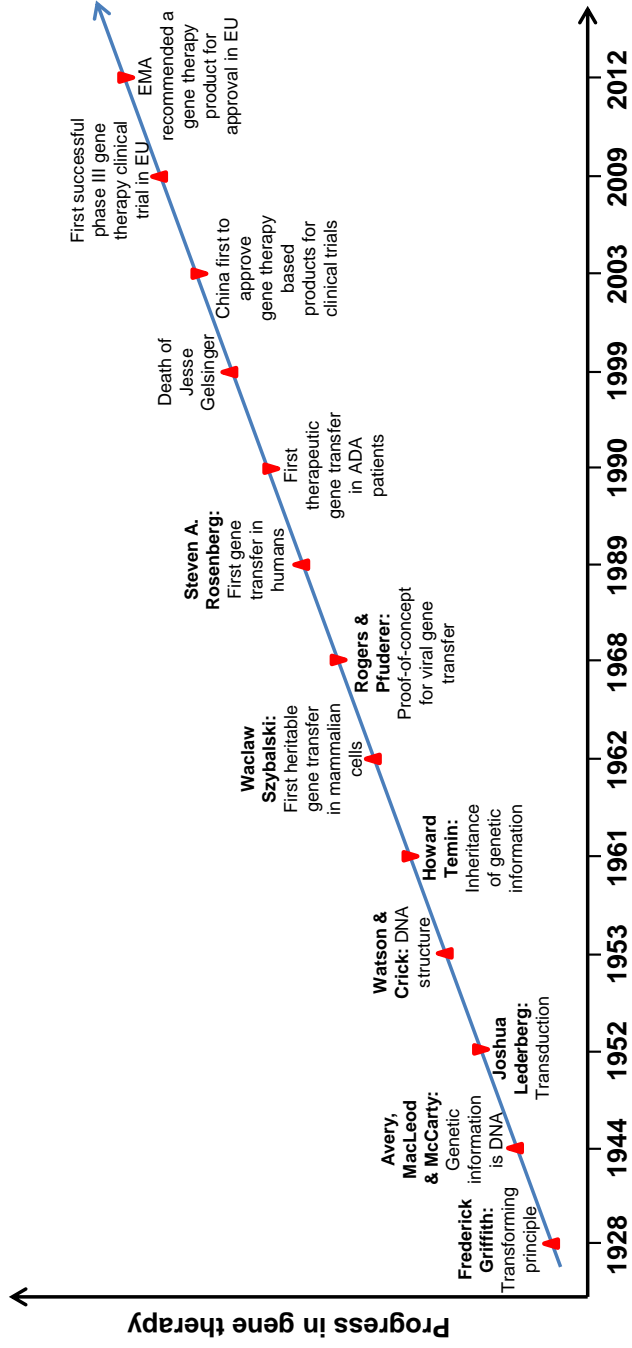


Figure 1.1. Timeline highlighting some of the important milestones towards the progress of gene

pioneering work on lambda phages published his study “DNA-mediated heritable transformation of a biochemical trait” [5], wherein cells that had been genetically modified could be selected based on their phenotype. In brief, cells need dihydrofolate reductase (DHFR) for the de novo synthesis of nucleic acids. When DHFR is inhibited by aminopterin the cell uses an alternate salvage pathway, which utilizes the enzyme hypoxanthine-guanine phosphoribosyl transferase (HGPRT) that catalyzes the conversion of hypoxanthine to inosine monophosphate and guanine to guanosine monophosphate. Based on this knowledge, Szybalski used derivatives of the human bone marrow cell line, whereof some were HGPRT<sup>(+)</sup> and some HGPRT<sup>(-)</sup>. When these cells were grown in a cocktail of aminopterin, hypoxanthine and thymidine (i.e. the HAT medium), only the HGPRT<sup>(+)</sup> cells were able to synthesize DNA and survived. The next Szybalski did that he transformed HGPRT<sup>(-)</sup> cells with the DNA isolated from HGPRT<sup>(+)</sup> cells and observed that HGPRT<sup>(-)</sup> cells then did not die in HAT medium. Hence, Szybalski’s work became the first documented evidence of heritable gene transfer in mammalian cells. It was now demonstrated that a genetic defect could be rescued by transferring functional DNA

from a foreign source and that it could be inherited in the daughter cells. A decade later the same method became key to a Nobel-winning invention of monoclonal antibodies [6].

The first step towards gene therapy was laid by Howard Temin when he discovered that viruses which were able to transfer genetic material were also capable of infecting with specific inheritable genetic mutations through chromosomal insertion [7]. This observation unveiled the conundrum that genetic information could flow only from DNA to RNA; instead the genetic information could also flow from RNA to DNA. It became apparent for the potential of viruses as a tool in delivering desirable genes into cells of interest which gave rise to a new approach in genetic engineering for treating genetic diseases. An initial proof-of-concept of virus mediated gene transfer was demonstrated by Rogers et al. where they used tobacco mosaic virus as a vector vehicle to introduce a polyadenylate stretch to the viral RNA [8]. In 1973, they performed the first direct human gene therapy trial by using the wild-type Shope papilloma virus, believed to encode the gene for arginase activity. The virus was introduced into two girls suffering

from a urea cycle disorder with intention to transfer the arginase gene [9, 10]. Unfortunately, the trial failed which later was revealed after genome sequencing that Shope papilloma virus genome actually does not encode an arginase.

In 1982, Martin Cline successfully inserted foreign genes into mouse bone marrow stem cells using recombinant DNA and that these modified cells were further able to partially repopulate the bone marrow of other mice [11]. Encouraged by these results, in 1990, Cline became the first to attempt this therapeutic approach of using recombinant DNA in humans for treating patients suffering from  $\beta$ -thalassemia. Such patients suffer from severe and life-threatening anaemia due to a genetic defect in their beta-globulin gene that deficit them from producing beta-globulin portion of haemoglobin protein. Cline initiated the therapy in two such patients, though without the approval from the UCLA Institutional Review Board.

The first officially approved clinical trial by the Recombinant DNA Advisory Committee (RAC) in December 1988 was performed by S.A. Rosenberg to track the movements of modified tumor-infiltrating

lymphocytes (TILs) in cancer patients [12]. He already succeeded in demonstrating that TILs modified with interleukin-2 treatment resulted in regression of metastatic melanoma in some patients [13]. Before performing the clinical trials, he initially tested the effectiveness of genetically modified TILs against tumors by introducing a retroviral mediated marker gene (bacterial NeoR gene) and studied their distribution and survival in circulation, lymph nodes or at tumor sites [12, 14, 15]. Based on this initial trial he received approval for treating two patients with advanced melanoma. He used ex vivo modified TILs expressing tumor necrosis factor (Rosenberg, 1992) and re-administered back into the patients which showed no tumor growth at the injection site and no viable tumor cells were evidenced in the surgically resected sections after 3 weeks of injection [15]. At the same time of Rosenberg's studies, Michael R. Blaese was the first to conduct gene therapy using a therapeutic gene [16]. After the approval by FDA in 1990 to perform gene therapy trials in humans, two adenosine deaminase deficient (ADA-SCID) children, were treated with their own ex vivo modified white blood cells to express the normal gene for

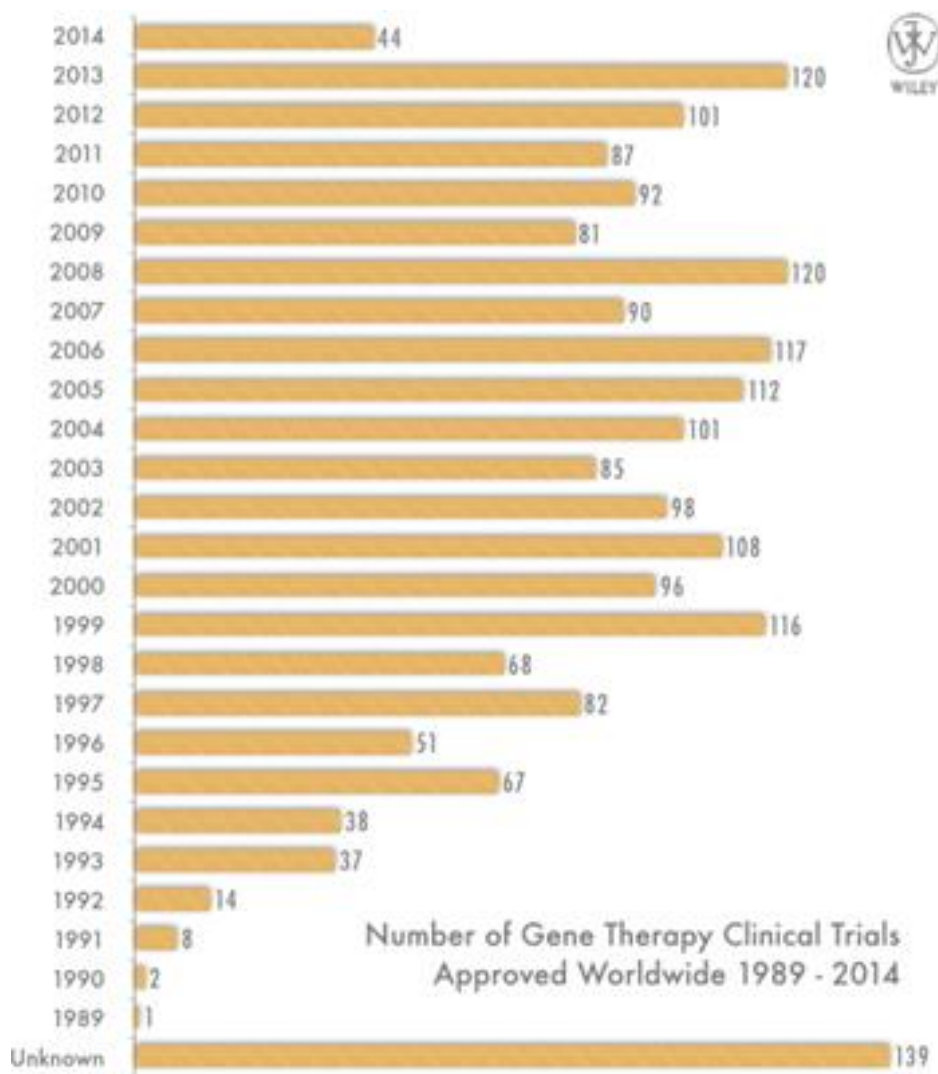


Figure 1.2. Statistics of the number of gene therapy clinical trials approved worldwide until 2014. Adopted from Ref [17].

making adenosine deaminase. After this ADA-SCID trial was also started in the EU [18] and laid the pavement for further trials to treat several other diseases with higher gene transfer efficiency (direct in vivo gene delivery) [19], until the tragic death of Jesse Gelsinger [20]. With Gelsinger's death the worst scenario of viral mediated gene therapy became apparent when virus administration generated immediate immune response to result in multi-organ failure and death [20].

## **1.2 Current scenario of gene therapy**

China was the first country to approve a gene therapy based product for clinical use named Gendicine™ in 2003 [21, 22]. Two years later, China's State Food and Drug Administration (SFDA) granted permission for clinical use of another product, Oncorine™ [23]. In 2004, Cerepro® , developed by Ark Therapeutics Group plc, received permission for its commercial supplies for the first time in the EU as gene-based medicines and by 2008 it became the first adenoviral vector to complete phase III clinical trial [24]. In addition, promising results have been observed in recent gene therapy clinical trials for Leber's

congenital amaurosis [25],  $\beta$ -thalassemia [26, 27], X-linked severe combined immunodeficiency (SCID-X1) [28] and ADA-SCID [29], haemophilia B [27], Wiskott-Aldrich syndrome [30], metachromatic leukodystrophy [31], choroideremia [32], and HIV [33]. Finally, the EMA recommended for the first time a gene therapy product Glybera, originally developed by Amsterdam Molecular Therapeutics and now marketed by UniQure, for clinical approval in the EU on July 19th 2012 [34]. Figure 1.2 shows the number of gene therapy clinical trials approved worldwide from 1989 to 2014 [17]. Since 1999 the number of clinical trials has increased worldwide to make gene therapy as the future treatment procedure and sooner or later be part of the standard care for a variety of genetically linked diseases. However, the majority of gene therapy clinical trials are in phase I, phase II or phase I/II trials [17, 35] to determine the maximum tolerable doses of gene delivery vectors and to identify the transgene products and the activity of the new agents in patients. Phase III, phase IV and single subject gene therapy clinical trials are limited but work is in progress to develop and translate this technique into a clinical reality (Figure 1.3).



Figure 1.3. Current scenario of the phases of gene therapy clinical trials.

Adopted from Ref [17].

### **1.3 Cancer gene therapy**

Contrary to the belief that only inherited single-gene disorders could be possibly treated with gene therapy [36], it was later realized in 1980s that cancer is also a disease of complex gene disorders where the technology could find its widespread application. After the first clinical trial for cancer gene therapy by Steven A. Rosenberg and R. Michael Blaese's groups [12] in 1991 a remarkable progress have been made in the past two decades in an attempt to meet the specific therapeutic needs and replace the conventional treatments with far reaching negative side effects. To date, 2076 gene therapy clinical trials have been approved for treating various diseases (Figure 1.4) [17], out of which cancer diseases outscores with 64.1% of maximum number of clinical trials.

The field of cancer gene therapy treatments can be broadly categorized into immunotherapy, oncolytic virotherapy and gene transfer.

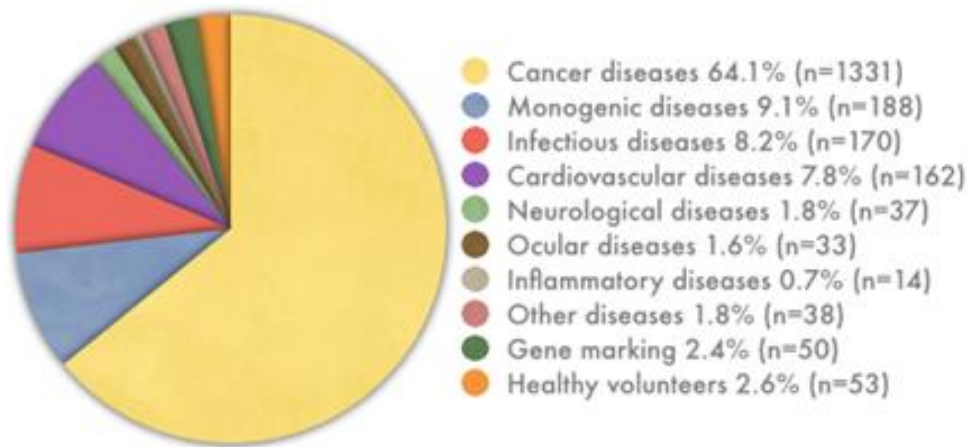


Figure 1.4. Graphical representation of the various diseases addressed by gene therapy in clinical trials, most of which were performed to treat cancer and soon became the major interest [17].

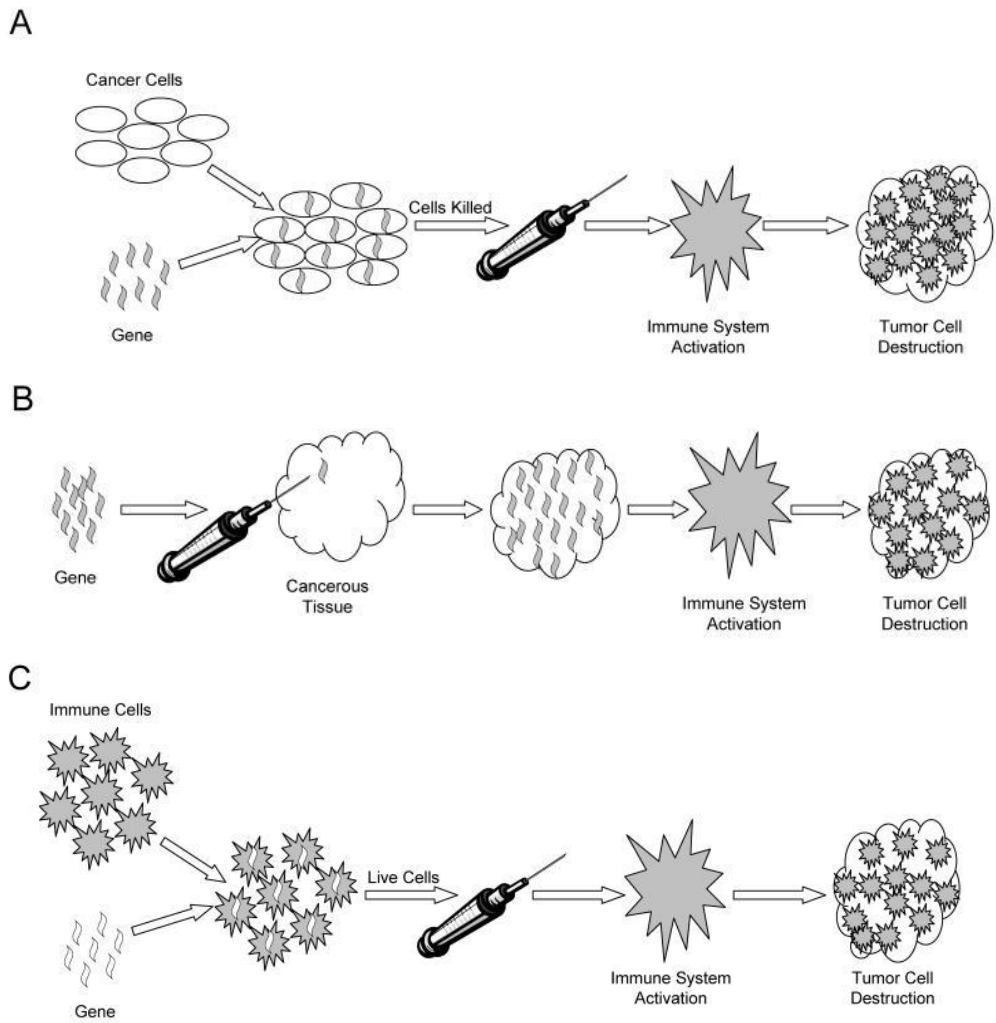


Figure 1.5. Schematic representation of immunotherapy. (A) Immunotherapy with altered cancer cells. (B) Immunotherapy with genes delivered in vivo. (C) Immunotherapy using patient's altered immune cells. Adopted from Ref [37].

**1.3.1. Immunotherapy:** Immunotherapy means to boost one's immune system to target and destroy cancer cells, but limited success has been achieved with traditional immunotherapy, as cancer cells tend to evolve mechanisms that evade immune detection [37]. Currently recombinant cancer vaccines are created to make the cancer cells more recognizable to patient's immune system by the addition of one or more genes (cytokine genes) that produce highly antigenic and immunostimulatory cellular debris. These cellular contents are incorporated into a vaccine (Figure 1.5 A) [38]. Alternatively, immunostimulatory genes (cytokines) can be delivered to the tumor in vivo which upon expression will unmask the cells from immune evasion (Figure 1.5 B) [39]. Another immunotherapy strategy is to directly alter the patient's immune system by adding a tumor antigen or other stimulatory gene into mononuclear circulating blood cells or bone marrow gathered from the patient in order to sensitize it to the cancer cells (Figure 1.5 C) [40].

**1.3.2. Oncolytic virotherapy:** In this strategy genetically engineered viruses are used to target and destroy cancer cells through the propagation of the virus, expression of cytotoxic proteins and cell lysis while remaining innocuous to the rest of the body cells (Figure 1.6)

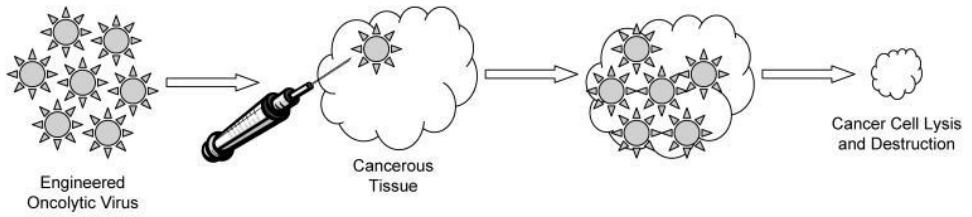


Figure 1.6. Schematic representation of oncolytic virotherapy. Adopted from Ref [37].

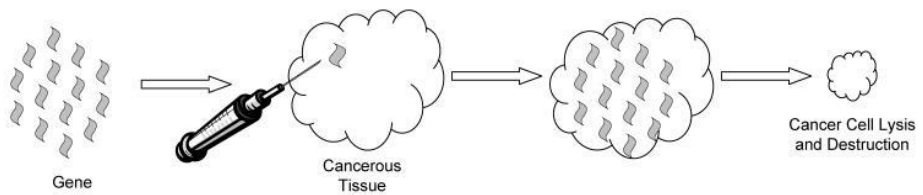


Figure 1.7. Schematic representation of gene transfer therapy. Adopted from Ref [37].

[41]. However, several stumbling blocks for oncolytic virotherapy in humans includes the clearance of viral particles before its infection in cancer cells by patient's immune system and the use of replication competent viral particles often calls for increased safety precautions, making clinical trials more expensive and cumbersome. **1.3.3. Gene transfer:** This is a radically new treatment paradigm which involves introduction of a foreign gene into the cancer cell or surrounding tissue. Genes including suicide genes, antiangiogenesis genes and cellular stasis genes are inserted into the cancer cell chromosome using either viral or non-viral gene delivery vectors, depending upon the desired specificity and length of time required for gene expression (Figure 1.7) [42]. However, this technique requires efficient delivery of therapeutic gene to the target cells without getting integrated into unwanted cell types, such as reproductive tissues.

In a summary, the strategies that have been designed and tested for cancer gene therapy are listed below [17, 35]:

1. The tumor suppressor genes such as p53 hold a check on the controlled division of cells by inducing apoptosis [43]. When

its function becomes awry, cancer establishment and progression could be controlled by replacing the defective tumor suppressor genes with wild type;

2. oncogenes e.g. ras transformed from its proto-oncogenic forms can be inactivated to block its expression;
3. drug sensitivity genes could be delivered that can convert a pro-drug to a cytotoxic drug upon their expression in cancer cells;
4. stimulation of immune responses against cancer cells; or
5. multi-drug resistance genes could be delivered to normal cells so that high chemotherapeutic doses could be given to cancer cells.

Specifically introducing these genetic materials at the target site could become a promising technology for the treatment of cancer, but targeting tumor cells and an appropriate gene transport vector are pre-requisites, the lack of which has rendered this approach clinically less effective.

### Vectors Used in Gene Therapy Clinical Trials

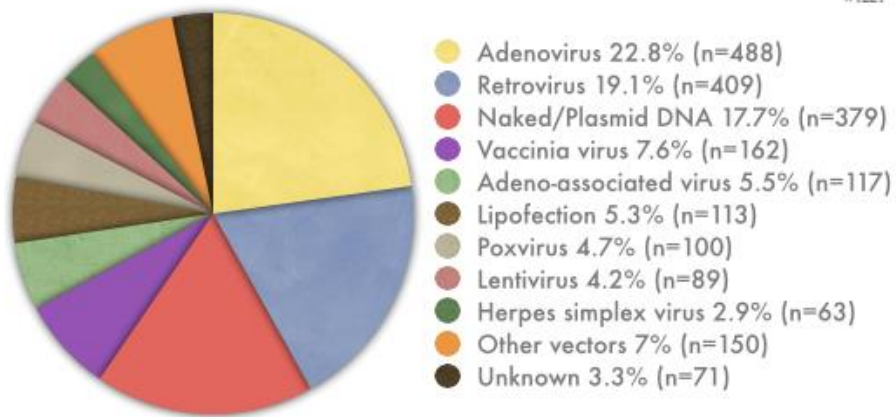


Figure 1.8. Various gene transporting vectors used in clinical trials. Adenovirus and retrovirus are most commonly used viral vectors in clinical trials. Non-viral mediated gene transfer, including naked DNA and liposomes has occupied 24% of all the clinical trials so far. Adopted from Ref [17].

## **1.4 Gene delivery vectors**

The various strategies to deliver exogenous, functional genes to cells could promise for the future treatment of a variety of human diseases, provided that these delivery methods are safe, efficient, and selective. To ensure efficient delivery of genes various vectors are being used in clinical trials including both viral and non-viral vectors, each with its own characteristic advantages and disadvantages. 42% of the clinical trials used adenovirus and retrovirus due to their high gene transfer efficiency and 24% of them used non-viral vectors chiefly considering the safety concerns in therapy (Figure 1.8). Viral vector mediated gene delivery is referred to as transduction while that mediated with non-viral vector is known as transfection.

## **1.5 Need for the non-viral vector mediated gene delivery**

Replication-defective recombinant viruses have considerable appeal in clinical use due to their natural ability to infect cells and delivering genes efficiently. However, these vectors do have significant practical

limitations. For instance, recombinant retroviruses do not transfer genes into non-replicating cells, though do so in culture cells and thus are generally inefficient *in vivo*. Due to the limited packaging capacity of many of these viruses large gene inserts cannot be delivered. In addition, the tropism of specific recombinant viruses can restrict their use. Some viral vectors can be cytotoxic by stimulating severe immune responses which was highlighted during the gene therapy treatment of an 18-year old young patient, Jesse Gelsinger, who died (1999) due to multiple organ failure as a result of the immune response against the infusion of genetically altered adenoviral vectors [20]. Moreover, non-pathogenic viral vectors might become activated following infection with wild-type or helper viruses and produce replication-competent recombinant virus [44], as evidenced in children with X-linked SCID who developed leukemia after receiving a retroviral gene therapy [45]. Because of primarily the safety concerns, the development of non-viral gene delivery vectors has received considerable attention. Moreover, non-viral vectors can be easily constructed and modified, scaled up for large production and show high gene carrying capacity.

## 1.6 Non-viral gene delivery systems

Non-viral systems include a variety of physical, non-infectious methods like calcium phosphate co-precipitation [46], liposomes [47], DEAE-dextran [48], microinjection [49], gene-particle bombardment [50], electroporation [51], ultrasound [52] and cationic polymers [53].

**1.6.1. Electroporation:** In this method electric pulses are applied across the cell membrane which creates transient membrane permeation due to trans-membrane potential difference. This destabilized membrane allows DNA insertion.

**1.6.2. Ultrasound:** This can be used to deliver ultrasound energy directly to an object and genes transport into cells can be achieved by the alteration of vascular permeability in a method called sonoporation.

**1.6.3. Gene-particle bombardment:** This method uses a gene gun for the direct injection of genes into the cell nucleus or other organelles. The payload used is a heavy metal particle coated with DNA.

**1.6.4. Cationic liposomes:** Cationic liposomes are synthetic vectors composed of lipid molecules with a positively charged head group. Liposomes do not encapsulate DNA, but instead the DNA becomes heavily condensed by cationic lipids that completely or partially cover the plasmid. Although it was initially believed that the lipid-DNA complexes fuse with the cell membrane and deliver DNA into the cytoplasm, it is now suggested that the DNA uptake requires endocytosis.

**1.6.5. Cationic polymers:** Cationic polymers are synthetic vectors which form condensed complexes (polyplexes) with nucleic acid due to electrostatic interactions between positive charge of polymers and negative charge on nucleic acid. This condensation results in nanosized particles which facilitate the delivery of genes into the cell. It is shown that the degree of condensation of the complexes is correlated with the level of transgene expression. Complexes measuring 80–100 nm in diameter are most effective for gene transfer [54]. Moreover, the use of polymeric vectors provides flexibility in their design, modification and synthesis for large scale production. Cationic molecules, such as

polymethacrylates [55], polypeptides [56, 57], celluloses [58], chitosan [59, 60], dendrimers including polyamidoamine or PAMAM dendrimers [61, 62], poly(vinyl pyrrolidone) [63], and polyamine polymers [64] are the most widely researched polymeric agents for their use in delivering genes. The excess positive charge present on their nanosized complexes in aqueous solutions lead to the interaction with anionic cell membranes and subsequent uptake into target cells. An effective gene delivery vector then disassembles to release the nucleic acid near nucleus to which it protected against the intracellular degradation [65]. Cyclodextrin based polymer has been used by Davis et al in phase I clinical trials in 2009 for delivering siRNA in patients with solid tumor [66].

## **1.7 Biological barriers for cellular uptake**

Non-viral gene therapy vectors which include naked DNA, cationic lipid/DNA complexes (lipoplex), polymer/DNA complexes (polyplex) or combinations of lipids and polymers are highly desirable tools for delivering genes into cells. However, they need to cross the various cellular barriers for trafficking of payload up till the nucleus (Figure

1.9). (i) The vector must traverse the plasma membrane, (ii) then escape the endosome and pass through the dense cytoskeletal network, (iii) and finally enter the nucleus for the desired transgene expression. Since the non-viral vectors lack the innate mechanisms to deliver and express the genetic material they carry, much work needs to be done at characterizing them to overcome these barriers.

**1.7.1. Plasma membrane:** Plasma membrane represents the first barrier for cellular uptake. Naked DNA is not able to associate efficiently with the cell membrane and get internalized due to the negative charge density present on both the DNA and the membrane [67]. Cationic polymers circumvent this problem by neutralizing the negative charge of DNA and forming nanosized polyplexes, thereby associating with the plasma membrane due to electrostatic interactions which is mediated by heparin sulfate proteoglycans on the cell surface. This trigger endocytosis of the polyplexes and nucleic acid gains entry inside the cell. Endocytosis leads to invagination of the plasma membrane at specific domains characterized by lipid raft/protein depending on the chosen endocytic pathways to form endocytic

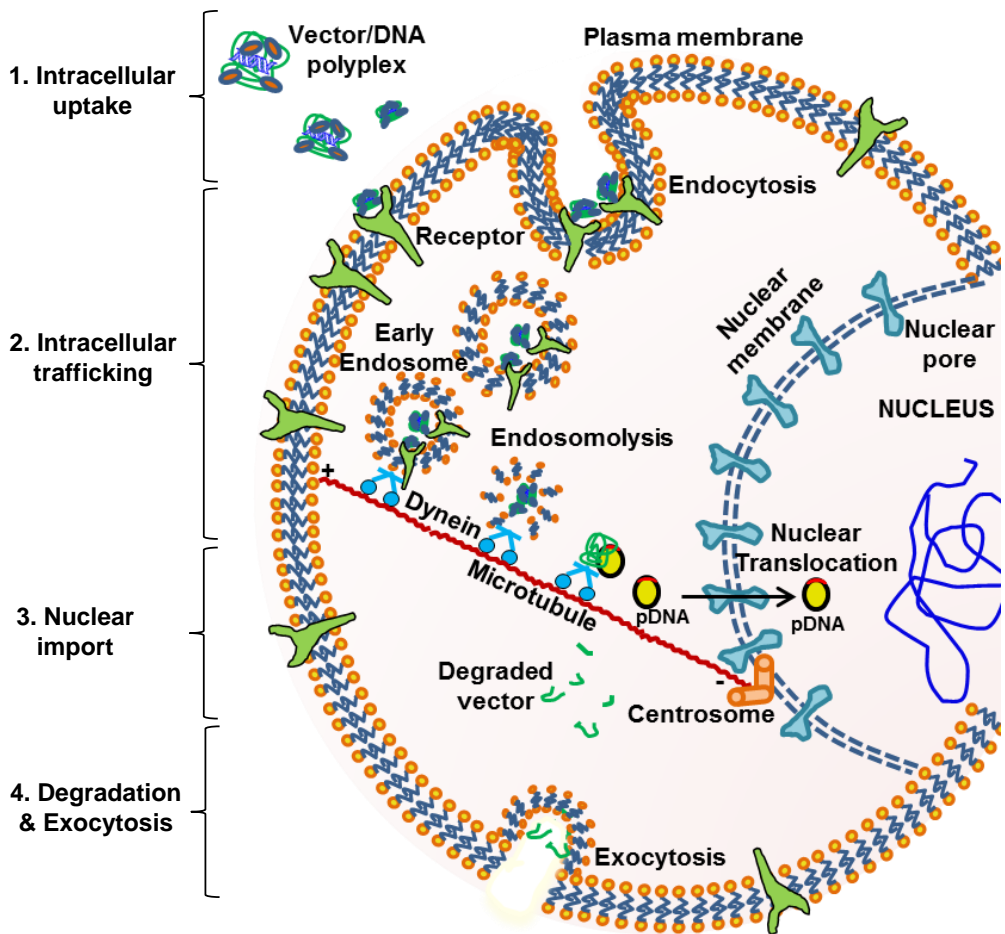


Figure 1.9. Intracellular barriers for non-viral gene transfer. Depiction of the journey of polyplexes after crossing the cellular uptake barriers, unloading the nucleic acid in cytoplasm, nuclear translocation, and transgene expression in the cell nucleus.

vesicles containing the polyplexes. The choice of endocytic pathways such as clathrin-mediated endocytosis, clathrin-independent endocytosis, caveolae-mediated endocytosis, macropinocytosis and phagocytosis [68-70] largely depends on the size of particle and the cell type [71, 72]. It was shown by Rejman et al. that the particles < 200 nm were taken up by the clathrin-dependent pathway, whereas larger particles (200-500nm) entered through another caveolae-mediated endocytosis [71]. Particles > 500 nm undergo micropinocytosis [73]. Alternatively, cell-penetrating peptides (CPPs) can be used to facilitate cell entry in an endocytosis-independent manner [74].

**1.7.2. Endosomal release and cytoplasmic trafficking:** The early endosomes carrying the polyplexes mature to late endosomes in ~ 5 min and is accompanied by a decrease in pH from 7.0 to 5.9. After about 30 min there is an additional pH drop from 6.0 to 5.0 when the late endosomes convert into lysosomes with aim to degrade the vesicular material [69]. Thus, escaping the endosomal trapping before its maturation into lysosomes becomes necessary for the polyplexes and becomes a rate-limiting step in the transgene expression.

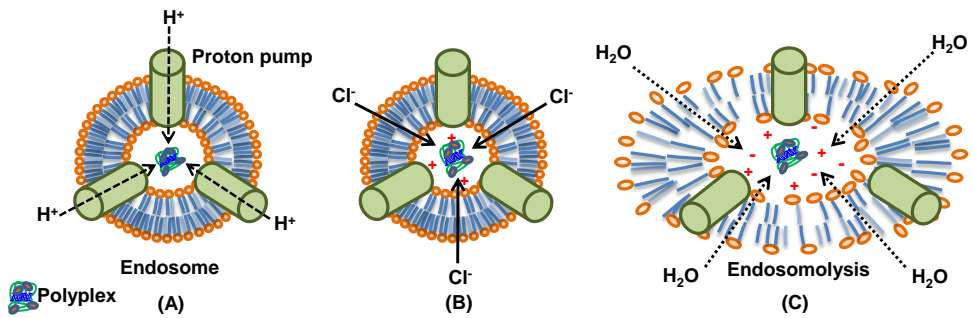


Figure 1.10. An artistic representation depicting the proton sponge hypothesis. (A) Accumulation of proton into endosomes by proton pumps; (B) the protons are accompanied with influx of chloride ions; and (C) builds up an osmotic pressure of water that eventually ruptures the endosomal membrane.

Degradation in the lysosomal acidic environment of the polyplexes can be avoided by employing the proton-sponge effect [75] or by incorporation of fusogenic and pore-forming peptides to the polymers [76]. The polyplexes of polyamidoamine (PAMAM) and pEI [77] can disrupt the endosomes by proton sponge mechanism (Figure 1.10) due to the presence of protonable amines in the polymer branches. PEI has amino nitrogen at every third atom which can be protonated within the acidifying endosomes to impart it a very high buffering capacity. Proton accumulation consequently leads to influx of chloride ions thereby resulting in osmotic swelling and subsequent lysis of endosome to release the entrapped components [75].

The released polyplex with bound nucleic acid is now exposed to cytoplasmic nucleases that can degrade the free nucleic acid. Although the condensed nucleic acids are protected against the nuclease degradation by the polymeric shield, it remains unprotected when once freed by the polymer [78]. Hence, it is of very importance that the polymer also dissociates the nucleic acid in the vicinity of nucleus so that the nucleic acid enters the nucleus before nuclease degradation.

Also the viscosity of cytoplasm poses another diffusional barrier for the mobility of macromolecules [79, 80]. It has been shown that the macromolecules utilize the microtubule network including the motor protein, dynein for its trafficking to the nucleus [81, 82]. A multiprotein complex mainly composed of transcription factors, is involved that bridges the interaction between the macromolecule and dynein and facilitates the movement of macromolecule along microtubules [83].

**1.7.3. Nuclear import:** The final physical barrier to transgene expression is the import of DNA into the nucleus. Nuclear trafficking of DNA from the perinuclear region into the interior of the nucleus largely depends on its size [84]. DNA fragments of size < 250 bp can enter the nucleus by passive diffusion through nuclear pore complexes (NPC), while larger fragments of DNA up to 1 kb need active transport which is a slow and highly inefficient process [82]. Several studies have shown that transfected DNA enters the nucleus during mitosis phase of cell division due to the breakdown of nuclear envelope [85], which could be the case for untroubled DNA entry in the nucleus of fast dividing cancer cells. In case of non-dividing cells the DNA can be

attached with single or multiple nuclear localization sequences (NLS) to stimulate its nuclear entry and augment transgene expression [86].

## **1.8 Criteria for successful cancer gene therapy**

Successful cancer gene therapy depends upon the ability of the vector to specifically target cancer cells, enter the cell and obtain sufficient levels of gene expression.

The following requirements should be fulfilled by an ideal delivering vector for efficient cancer gene therapy.

1. Safe to administer without generating immunogenicity,
2. should be inert to avoid causing any associated diseases,
3. large therapeutic gene carrying capacity,
4. protecting the therapeutic molecule against degradation during its voyage to the nucleus,
5. specifically target the cancer cells without harming the normal body tissues,
6. increase the cellular uptake for transgene expression, and
7. Its self-degradation after delivering the therapeutic molecule to

avoid cytotoxicity and detection by immune system.

Non-viral vectors fulfill most of the above mentioned criteria but usually at the expense of lower gene transfer efficiency than viral vectors. In addition, they result in short-lived expression and generally lack specificity making them difficult for delivering genes in vivo. However, if they can be perfected to a dependable and efficient vehicle for targeted gene delivery in vivo, will lead to further improvements in the overall technology and emerge as the future treatment procedure.

## **1.9 Strategies to use nanotechnology in cancer gene therapy**

The unique challenges for cancer treatment include their small size, high multiplicity and metastasis to diverse organs during advanced stages of cancer. Nanoparticles have many potential benefits for diagnosing and treating cancer, including the ability to transport therapeutic molecules to cancer sites, as well as targeting specific cell populations with erroneous cellular functions. Thus, integrating engineering sciences with cancer biology may expand the capabilities

of nanotechnology-based tools in targeting, detection and particle trafficking for treating cancer. Although nanotherapeutics have reached the clinic, for example, liposome-encapsulated doxorubicin (doxil) [88], protein nanoparticles containing paclitaxel (abraxane) [89], iron oxide nanoparticles (ferumoxytol) [90], we expect that future generation nanotherapeutics will ensure new capabilities in targeting and early detection of diseased cancer sites.

Nanomaterial-based therapeutic approaches are currently under huge development for the strategies to diagnose, treat and target cancer (Figure 1.11).

**1.9.1. Diagnosis:** Stimulus, such as molecular binding event or change in ionic concentration can be detected by the nanomaterial and may respond to the stimulus by releasing therapeutic molecule, or degrading, or chemically modifying drugs in vivo.

**1.9.1. Therapeutic mechanisms:** Nanotherapeutics can be used to carry small molecule drugs or biomacromolecules (proteins or siRNA), or act

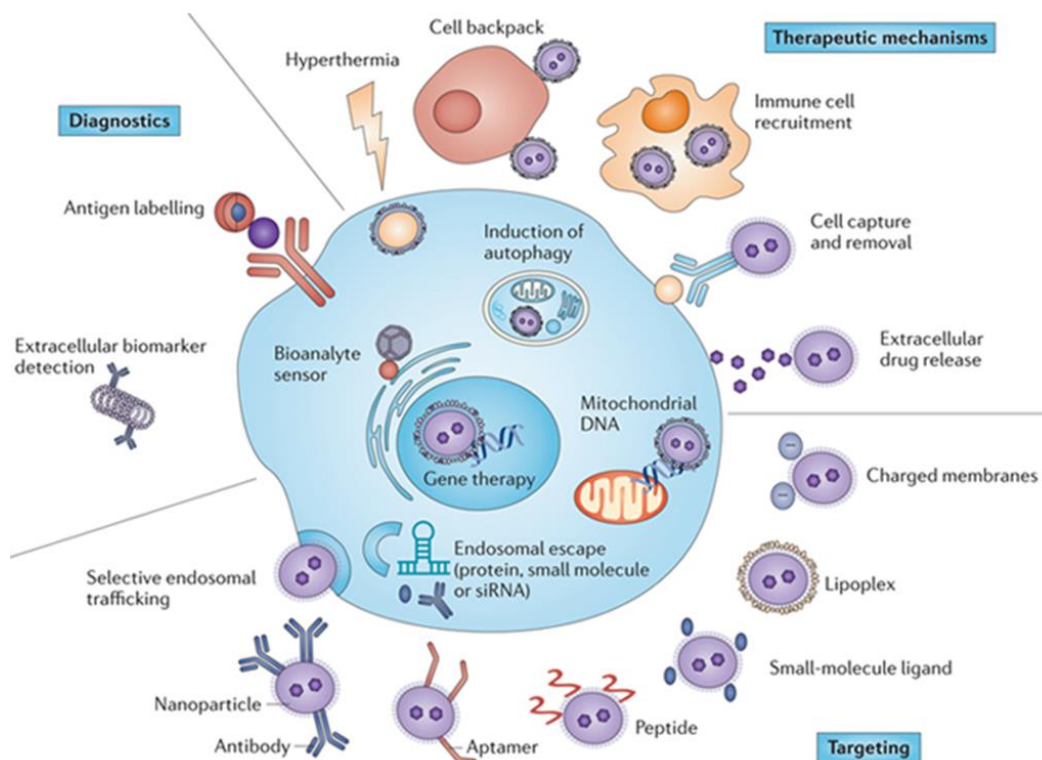


Figure 1.11. The figure summarizes nanotechnological strategies for diagnosis, treatment and specific targeting of cancer cells. Adopted from Ref [87].

as vehicles for immunotherapy and thermal absorption including targeting the diseased site, eliciting drug release, and increasing half-life of drug by changing its pharmacokinetics [91]. This ensures to reduce off-target effects on non-diseased cells and also lower the drug amount needed to be administered [88, 92]. Moreover, thermo-ablative therapy, that is, killing tumor cells by heat energy, can be augmented by activating nanomaterials localized in diseased tissue using magnetic fields, infrared light or radio-frequency[93-96]. Removal of nanomaterials from the in vivo system after its job is done is equally important as the therapeutic process. Hence, the nanomaterials are constructed with linkages to ensure its degradation or removal after a certain time.

**1.9.1. Targeting cancer:** Antibody-based targeting ligands, conjugated with drug or polymer are being used clinically as nanodelivery systems to target cancer cells [97, 98]. Similarly, linking short peptides [99, 100], such as RGD, or aptamers (nucleic acid ligands) [101, 102] to nanoparticles can increase their binding specificity. Peptide nucleic acids (PNAs) are also used in which they bind with high affinity to

complimentary DNA strand and the peptide backbone covalently modifies targeting ligand [103]. Small-molecule-binding domains, such as the folate receptor [104], vitamin B12 receptors [105] which are overexpressed in certain cancer cell types, demonstrate high affinity to the nanotherapeutics coated with their respective ligand molecules. The cellular uptake of such nanotherapeutics is enhanced by the receptor-mediated endocytosis in the specific cells with the receptors on their cell surface. This way indiscriminant transgene expression can be avoided. The ligand is covalently linked to a cationic polymer. The polymer electrostatically interacts with the negatively-charged phosphates of the DNA backbone and forms a stable polymer/DNA complex of nanoscale size suitable for cellular uptake. The polymer must also contain an endosomolytic agent to avoid degradation in the endosomal compartment [106].

Multiple therapeutic functions can be combined into a single platform and such nanoparticles can be used to target specific cells/tissues and reach particular subcellular compartments by carefully considering the biology of cancer process and engineer nanomaterials accordingly.

## **1.10 Objective of the study**

The research study focuses on enhancing the transfection efficiency of transgene transported by cationic polymer specifically to the cancer cells. For this a cationic polymer was constructed such that it is itself innocuous to the cells simultaneously contains a ligand to enhance its cellular uptake in cancer cells. Degradable linkages were incorporated to ensure its degradation after delivering the cargo in the vicinity of cell nucleus. The ligand vitamin B6 was inserted in the polymer branches via covalent bonding to incorporate targeting property in the polymer specifically for cancer. The next chapter 2 deals with this idea and demonstrates the synthesis and mechanistic investigations of the vitamin B6 coupled polymer, VBPEA, for the enhanced cellular uptake of cationic polyplexes by cancer cells.

## **1.11 Conclusion**

An ideal gene delivery system for cancer gene therapy should effectively condense and protect therapeutic nucleic acid, increase its cellular uptake specifically in cancer cells, and release the nucleic acid

at the site of action. Nanomaterial tools can address to the needs of cancer therapy that are only now starting to be realized in the clinic. Many of the past impediments to treatment, like safety, targeting, endosomal escape, polymer toxicity and non-degradability, lower transfection efficiency, etc. are being actively researched and overcome. In the present research study, the solution to the above mentioned problems in cancer gene therapy are tried to address and applied in vivo to discern its therapeutic potential.

# CHAPTER 2

## *Synthesis & Transfection Efficiency of Vitamin B6-Coupled Poly(ester amine) Gene Transporter*

---

### **2.1 Introduction**

Non-viral gene delivery systems are superior to highly-efficient viral methods in a way being safer as they do not induce unwanted immune responses or aberrant gene expressions [107, 108]. However, the low transfection efficiency of non-viral vectors remains a major drawback to their widespread clinical application. Therefore, method optimization for the development of non-viral vector is essential to improve host cell internalization and thus transfection activity so that

the efficacy equivalent to viral vector-mediated gene delivery can be achieved [109]. Recent research focused on these challenges is dedicated to make non-viral method a future treatment for a myriad of genetic disorders. Poly (L-lysine), polyethylenimine (PEI), chitosan, PAMAM dendrimer, and cationic liposomes are a few of the commonly studied non-viral agents that can self-assemble with and condense DNA into nanoplexes suitable for endocytosis [110, 111]. The PEI-based gene delivery system is an excellent candidate as a non-viral vector due to its unique endosome escape capability; however, its high molecular weight (HMW) increases cytotoxicity due to non-discharged aggregate accumulation on the cell surface, which impairs important membrane functions [64]. One approach to reduce cytotoxicity is to cross-link low molecular weight (LMW)-PEI with degradable linkages to make HMW polymer that can condense and protect nucleic acid for efficient transfection and can be discharged into small fragments upon degradation [112]. In addition, incorporation of ligands such as folic acid, mannose, galactose and synthetic peptides into vectors can enhance transfection by encouraging specific pathways of cellular internalization [113, 114]. Active targeting can be beneficial in two

ways: first, coupling a targeting moiety to the vector can facilitate its exclusive uptake into specific cell types, and second, non-specific interactions can be reduced by shielding the positive surface charges of the vector [115]. Hence, the target site, the targeting ligand, and the physicochemical properties of the polyplexes should be carefully considered in the development of gene delivery vectors [116] .

In general, vitamins achieve facilitated entry into most cells with relative specificity. The specific receptors/carriers involved in the uptake of vitamin B<sub>6</sub> (pyridoxine), B<sub>7</sub> (biotin), B<sub>9</sub> (folic acid), B<sub>12</sub> (cobalamin), and other vitamins have been previously studied [117-119]. Therefore, their specific receptor/carrier-mediated entry can be utilized as a biological mechanism for the delivery of pharmacological compounds into cells. Vitamin B<sub>6</sub> (VB<sub>6</sub>) is an essential micronutrient required for the normal growth and function of nearly all cell types. VB<sub>6</sub> plays a vital role as a cofactor for a large number of essential apoenzymes that carry out various metabolic functions [120]. Since tumor cells, owing to high metabolic activity, have high demand for VB<sub>6</sub>, the VB<sub>6</sub>-coupled molecules can also achieve entry into the tumor

cells through the specific VB<sub>6</sub> transporting membrane carriers (VTCs). In a previous work, VB<sub>6</sub> was found to facilitate the cellular uptake of small peptides and peptide-oligonucleotide conjugates through VTCs [121, 122]. Although VB<sub>6</sub> has been modified to transport small molecules, its ability to increase the cellular uptake of gene transporters with a higher affinity in cancer cells has never been documented.

Previously, poly(ester amine) (PEA) synthesized by a Michael addition reaction between LMW-PEI and glycerol dimethacrylate (GDM) as a cross linker was reported to show high transfection efficiency due to the glycerol backbone which facilitates cellular entry by exerting hyperosmotic effects along with PEI amine groups that help in fast endosomal release. Moreover, the polyester backbone ensures the degradability of the polymer into smaller fragments by its biphasic degradation pattern, making it easier to be exocytosed [123]. Based on these aforementioned characteristics, we synthesized a vitamin B<sub>6</sub>-coupled poly(ester amine) (VBPEA) gene transporter in which VB<sub>6</sub> was covalently coupled with a degradable PEA backbone synthesized from 1.2k branched PEI (bPEI) cross linked with GDM. The VBPEA

was expected to show enhanced transfection efficiency due to the specific uptake process of VB<sub>6</sub> combined with the degradable property of PEA. Hence, it was anticipated that VB<sub>6</sub> coupled to a polycationic gene delivery vehicle could encourage specific and enhanced cellular uptake via endocytosis and achieve a pharmacological response by binding to its specific membrane carrier.

## **2.2 Materials and Methods**

### **2.2.1. Materials**

bPEI (Mn: 1.2k and 25k), dimethyl sulfoxide (DMSO), pyridoxal 5'phosphate (PLP), sodium cyanoborohydride (NaCNBH<sub>4</sub>), and 3-(4, 5-dimethyl thiazol-2-yl)-2, 5-diphenyl tetrazolium bromide (MTT) reagent were purchased from Sigma (St. Louis, MO, USA). Luciferase reporter, pGL3- vector with SV-40 promoter and enhancer encoding firefly (*Photinus pyralis*) luciferase was obtained from Promega (Madison, WI, USA). The green fluorescent protein (GFP) gene was obtained from Clontech (Palo Alto, CA, USA). All other chemicals used in this study were of analytical reagent grade.

### **2.2.2. Synthesis of vitamin B<sub>6</sub>-coupled poly(ester amine) (VBPEA)**

VBPEA was synthesized in a two-step reaction in which LMW bPEI was cross linked with GDM to form PEA, which was then coupled with the active form of VB<sub>6</sub> (pyridoxal 5'phosphate, PLP) to produce the VBPEA gene transporter.

#### ***2.2.2.1. Synthesis of PEA***

PEA was synthesized by a Michael addition reaction between LMW-bPEI (1.2k) and GDM [124]. Briefly, GDM and LMW-PEI were separately dissolved in anhydrous methanol. The GDM solution was added slowly to the LMW-PEI solution at a stoichiometric ratio of 1:2 at 60°C with constant stirring for 24 h. The reaction mixture was subsequently dialyzed at 4°C for 24 h using a Spectra/Por membrane (MW cut-off 3.5k; Spectrum Medical Industries, Inc., Los Angeles, CA, USA) against distilled water. Finally, the copolymer was lyophilized and stored at 0°C.

#### ***2.2.2.2. Synthesis of VBPEA***

10 mol% of the total primary amines present in PEA were reacted with pyridoxal 5'phosphate (PLP) to form a transient Schiff base, which was subsequently reduced with NaCNBH<sub>4</sub> to obtain VBPEA [121] . Briefly, a 10 mL aqueous solution of PLP (1 mg/mL) was added dropwise to a 50 mL aqueous solution of PEA (1 g) and NaHCO<sub>3</sub> (100 mg) at RT and stirred vigorously for 24 h. Subsequently, NaCNBH<sub>4</sub> (50 mg) was added to reduce the Schiff base to a secondary amine. The reaction mixture was dialyzed with a Spectra/Por membrane (MW cut-off 3.5 k) against distilled water at 4°C for 24 h. The solution was finally lyophilized and stored at 0°C until use.

### **2.2.3. Characterization of VBPEA**

<sup>1</sup>H NMR spectra of VBPEA and PEA in D<sub>2</sub>O were recorded using an Advanced 600 spectrometer (Bruker, Germany). The absolute molecular weight of the VBPEA polymer was measured by gel permeation chromatography coupled with multiangle laser light scattering (GPC-MALLS) using a Sodex OHpack SB-803 HQ (Phenomenex, Torrells, CA, USA) column (column temperature 25°C; flow rate 0.5 mL/min).

#### **2.2.4. Gel retardation assay**

VBPEA was complexed with DNA (0.3 µg, pGL3 control) at various N/P ratios (0.5, 1, 3, 5 and 10) for 30 min at RT in autoclaved water with the total volume adjusted to 20 µL. 1X loading dye (Biosesang, Korea) was added, and the samples were resolved on a 0.8% agarose gel in 1X TAE buffer containing ethidium bromide (EtBr, 0.1 µg/mL). Gel electrophoresis was conducted at 100 V for 40 min in 1X TAE running buffer, and images were captured under ultraviolet illumination.

#### **2.2.5. DNA protection and release assay**

The ability of VBPEA to protect DNA was assessed by treating VBPEA/DNA (N/P 10) with DNase I. The prepared VBPEA/DNA complexes and free DNA were incubated separately with DNase I (1 µL, 50 units) in DNase/Mg<sup>2+</sup> digestion buffer containing Tris-Cl (50 mM, pH 7.6) and MgCl<sub>2</sub> (10 mM) at 37°C for 30 min. The DNase was inactivated by adding 4 µL EDTA (250 mM in 1 N NaOH) and incubated for another 30 min at RT. Finally, protected DNA was released from the complexes with the addition of 5 µL 1% sodium

dodecyl sulfate (SDS) in distilled water for 2 h. Released DNA was detected by resolving on a 0.8% agarose gel (with 0.1  $\mu\text{g}/\text{mL}$  EtBr) in 1X TAE running buffer at 100 V for 40 min.

#### **2.2.6. Measurement of particle size and zeta potential**

A dynamic light scattering spectrophotometer (DLS 8000, Otsuka Electronics, Osaka, Japan) was used to measure the size and zeta potential of the VBPEA/DNA complexes in comparison to the PEA/DNA and PEI25k/DNA complexes with 90 and 20 scattering angles at 25°C, respectively. The samples were incubated for 30 min in distilled water at N/P ratios of 5, 10, 20 and 30 with a 40  $\mu\text{g}/\text{mL}$  final DNA concentration in a total volume of 1 mL. In order to investigate the effects of serum proteins on the stability of VBPEA/DNA complexes (N/P 20) compared to PEA/DNA (N/P 20) and PEI25k/DNA complexes (N/P 10), serum concentrations of 0%, 10%, 20%, and 30% were added to the prepared complexes and their sizes were then measured.

#### **2.2.7. Observation of VBPEA/DNA complexes**

The morphology and size of the VBPEA/DNA complexes (at N/P 20) and the PEI25k/DNA complexes (at N/P 10) were confirmed by EF-TEM (LIBRA 120, Carl Zeiss, Germany). Prepared VBPEA/DNA and PEI25k/DNA complexes were loaded on a carbon grid, stained with 1% uranyl acetate for 10 s, washed with distilled water, and dried for an additional 10 min. Samples were then analyzed under an electron microscope.

#### **2.2.8. Cell culture and animals**

Adenocarcinoma human alveolar basal epithelial cells (A549) were maintained in Roswell Park Memorial Institute (RPMI)-1640 culture medium. Human cervix carcinoma cells (HeLa) and human liver hepatocellular carcinoma cells (HepG2) were cultured in Dulbecco's modified Eagle's medium (DMEM, low glucose) containing 10% heat-inactivated fetal bovine serum (FBS, HyClone, Logan, UT, USA) with 1% penicillin/streptomycin. All cells were maintained under standard culture conditions of 37°C and 5% CO<sub>2</sub>.

Animals were obtained from Orient Bio Inc. (Republic of Korea) and

kept in a laboratory animal facility maintained at  $23 \pm 2^{\circ}\text{C}$  and  $50 \pm 20\%$  relative humidity and under a 12 h light/dark cycle. All experimental protocols were reviewed and approved by the Animal Care and Use Committee at Seoul National University (SNU-120409-3).

### **2.2.9. Cytotoxicity assay**

VBPEA *in vitro* cytotoxicity was evaluated by MTT assay in three cell lines (A549, HeLa, and HepG2) and compared with that of PEA and PEI25k. At monolayer confluency, cells were trypsinized and seeded in a 24-well plate at  $10 \times 10^4$  initial cell density in 1 mL growth media and allowed to grow to 80% confluency prior to polyplex treatment. Cells were treated at various N/P ratios (5, 10, 20, 30, 40, and 50) in serum-free medium that was changed with serum-containing medium after 3 h. Thirty-six hours later, 500  $\mu\text{L}$  of MTT solution in 1X PBS (0.5 mg/mL) was added to each well and incubated for an additional 3 h. The medium was carefully aspirated, leaving purple formazan crystals, which were dissolved in DMSO (500  $\mu\text{L}$ ). Dissolved formazan (100  $\mu\text{L}$ ) from each well were transferred to 96-well plate and absorbance was

measured at 540 nm using a VERSAmax tunable microplate reader (Sunnyvale, CA, USA). All experiments were conducted in triplicate.

#### **2.2.10. In vitro transfection in the absence and presence of serum**

Transfection studies were performed in A549, HeLa and HepG2 cells at an initial cell density of  $10 \times 10^4$  in 24-well plate. At 80% cell confluency, VBPEA/pGL3 (1  $\mu$ g), PEA/pGL3, and PEI25k/pGL3 polyplexes were treated at various N/P ratios (5, 10, 20, 30 and 40) in serum-free medium, which was exchanged with fresh media containing serum (10% FBS) after 3 h. After the cells were kept under standard incubation conditions for 24 h, luciferase assay was performed according to the manufacturer's protocol. A chemiluminometer (Autolumat, LB953; EG&G Berthold, Germany) was used to measure relative light units (RLUs) normalized with protein concentration in cell extract estimated using a BCA protein assay kit (Pierce Biotechnology, Rockford, IL, USA). The effect of serum on polyplex stability for its possible use in biological systems was investigated in the A549 cell line. At N/P 20, cells were transfected with 0%, 10%, 20%, and 30% serum concentrations in 24-well plate, and luciferase

assay was performed as described above. Transfection activity was measured in triplicate as RLU/mg protein.

#### **2.2.11. Flow cytometry measurement**

Flow cytometry was performed to estimate the percent transfection efficiency of VBPEA/tGFP (1  $\mu$ g) polyplexes in A549 cells in comparison with PEA/tGFP and PEI25k/tGFP polyplexes. Transfected cells were harvested with 0.25% trypsin/EDTA and washed twice with 1X PBS. Cells expressing GFP acquired from a total of 10,000 cells were scored through a FACS calibrator system (Becton-Dickinson, San Jose, CA, USA) to determine the percent transfection.

#### **2.2.12. In vivo biodistribution**

Intravenous injection of VBPEA/pGL3 complexes was performed in Balb/c mice (4 mice/group) to analyze *in vivo* biodistribution. For these experiments, VBPEA and PEA (at N/P 20) were complexed with pGL3 (30  $\mu$ g) in normal saline (final volume 100  $\mu$ L). Similarly, naked DNA in normal saline was used as a control. Complexes were delivered to 6-week old Balb/c mice intravenously (i.v.) through the tail vein using a

40 U insulin syringe (1 mL with a needle size 0.30 x 8 mm). After four days of gene delivery, animals were sacrificed by cervical dislocation and all vital organs were dissected. Organs were washed with chilled normal saline, weighed, chopped, and suspended to 25% w/v homogenate in 2.5X cell lysis buffer (Promega, USA) and centrifuged (10,000 rpm, 10 min, 4°C). Cell lysate (100 µL) from each sample was assayed for luciferase activity using a chemiluminometer.

## **2.3 Results**

### **2.3.1. Synthesis and physicochemical characterization of VBPEA**

The terminal amines of PEA were reacted with the aldehyde group of VB<sub>6</sub> (pyridoxal 5'phosphate) at the 4' position to form an unstable transient Schiff base, which was reduced with NaCNBH<sub>4</sub> (Figure 2.1).

The synthesized VBPEA was characterized for its composition, DNA condensation and protection ability, size, zeta potential and morphology of its complexes with DNA. The composition of VBPEA as analyzed through <sup>1</sup>H NMR spectroscopy shows intense peaks at around 8.0 ppm, representing protons in the pyridoxal ring of VB<sub>6</sub>.

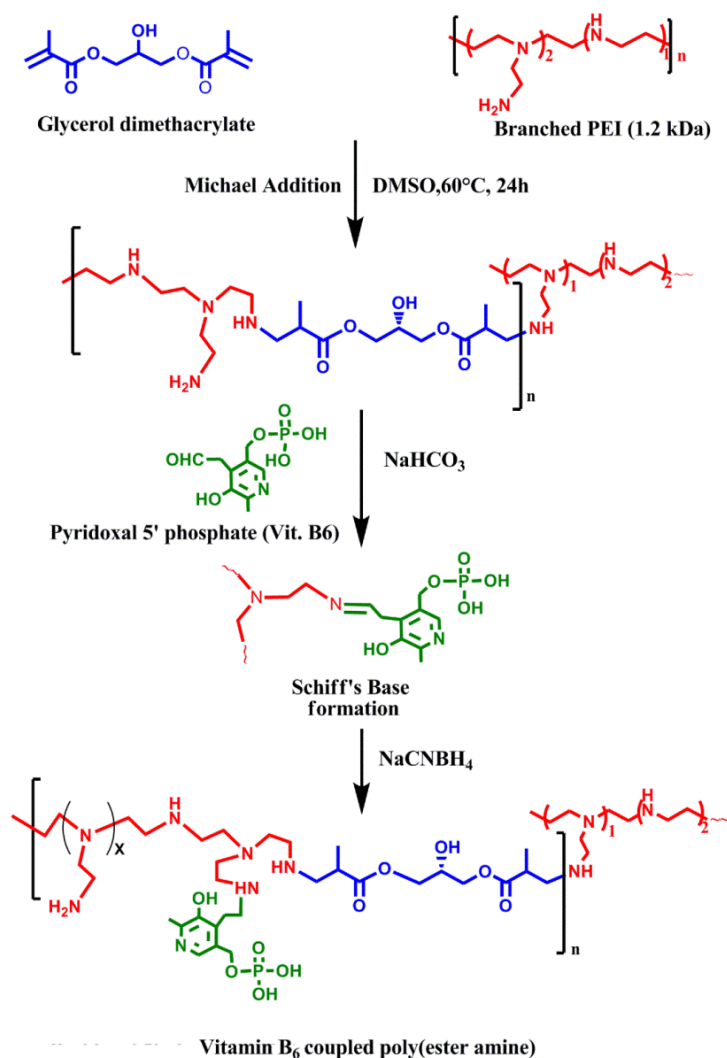


Figure 2.1. Synthesis scheme of vitamin B6-coupled poly(ester amine) (VBPEA). The terminal amines of poly(ester amine) (PEA) were reacted with the aldehyde group of VB6 to form an unstable Schiff base, which was reduced with  $\text{NaCNBH}_4$  to form VBPEA.

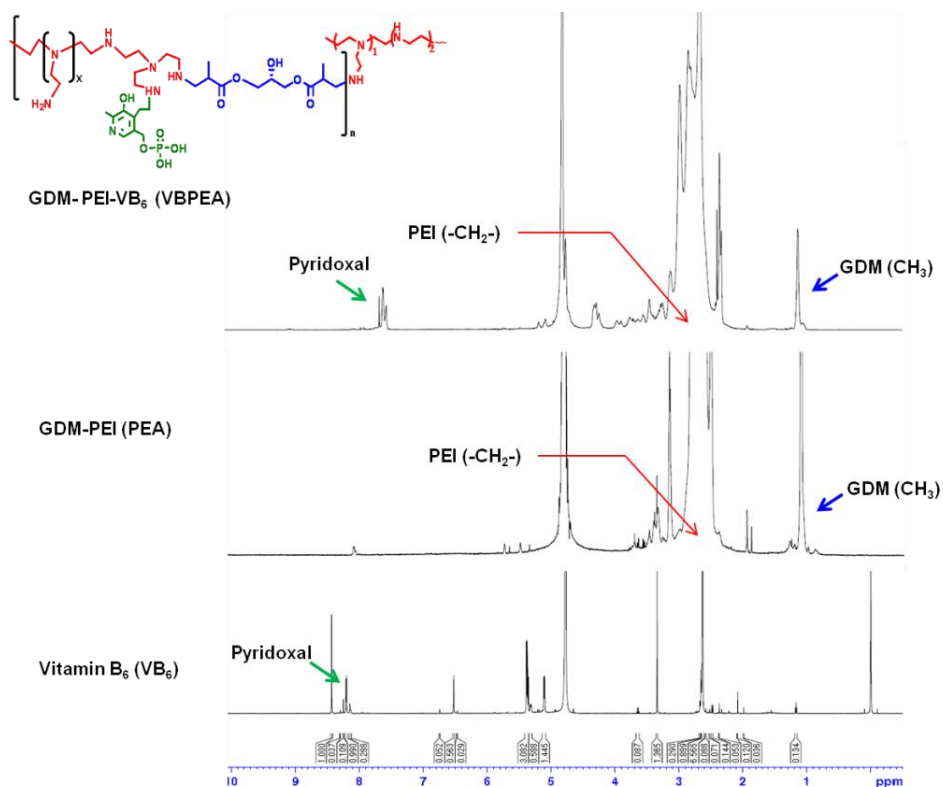


Figure 2.2. <sup>1</sup>H-NMR spectra of VBPEA, PEA, and VB6 in D<sub>2</sub>O.

Table 2.1. Characterization of VBPEA

MW of reactants (Da)		Composition of PEA (mol-%) *	Composition of VB <sub>6</sub> (mol-%) *	M.W. (Da) †	Polydispersity index (PDI)
PEA	VB <sub>6</sub>				
5,000	247	90.23	9.77	5,000-	1.12
-				6,150	
5,200					

\* Determined by <sup>1</sup>H NMR

† Determined by GPC

Presence of PEA backbone in VBPEA was confirmed by methyl peaks visible at 1.1 ppm and 2.4 ppm. A comparative NMR of VB<sub>6</sub> (pyridoxal), PEA, and VBPEA is shown in figure 2.2. The composition of VB<sub>6</sub> in VBPEA as estimated by NMR was about 9.77 mol-% and the MW of VBPEA measured by GPC was 5000-6000 Da (Table 2.1), which indicated appropriate size of polymer to link with DNA and form stable polyplexes.

Gel retardation assay further demonstrated the ability of VBPEA to condense DNA by completely retarding DNA migration in the agarose gel at an N/P ratio of 5 (Figure 2.3A), suggesting a high VBPEA complexation capacity. Further, through DNA protection and release assay VBPEA showed to protect the complexed DNA as visible in lane 4 of Figure 2.3B to suggest its protection against intracellular DNase degradation.

The condensation of DNA with VBPEA resulted in nanoscale particle sizes appropriate for cellular uptake, confirmed by dynamic light scattering spectrophotometer (DLS) and EF-TEM. DLS revealed a decreasing trend in VBPEA/DNA nanoplex sizes with increasing N/P

ratio (Figure 2.4A), which is in accordance with the increasing zeta potential from +35 to +41 mV (Figure 2.4B). The increase in zeta potential from lower to higher N/P ratio provides increased DNA condensation, leading to a decrease in nanoplex sizes. After a certain limit of compactness of ~ 110 nm (at N/P 20), nanoplex sizes began to increase, probably due to subtle play of electrostatic and repulsive forces of interaction. It is noteworthy that VBPEA showed a reduction in its zeta potential as compared to PEA, most likely due to VB<sub>6</sub> coupling.

The polyplex sizes estimated with increasing serum concentrations showed a continuous increase in the hydrodynamic diameter of PEI25k/DNA due to aggregation with serum proteins, which generates polyplex sizes unsuitable for cellular uptake. In contrast, VBPEA/DNA showed no significant change in polyplex sizes, suggesting minimal interaction with serum proteins and favorable transfection (Figure 2.5). This can be attributed to the coupled VB<sub>6</sub> and hydroxyl groups of PEA backbone, which obstructed interactions between serum proteins and

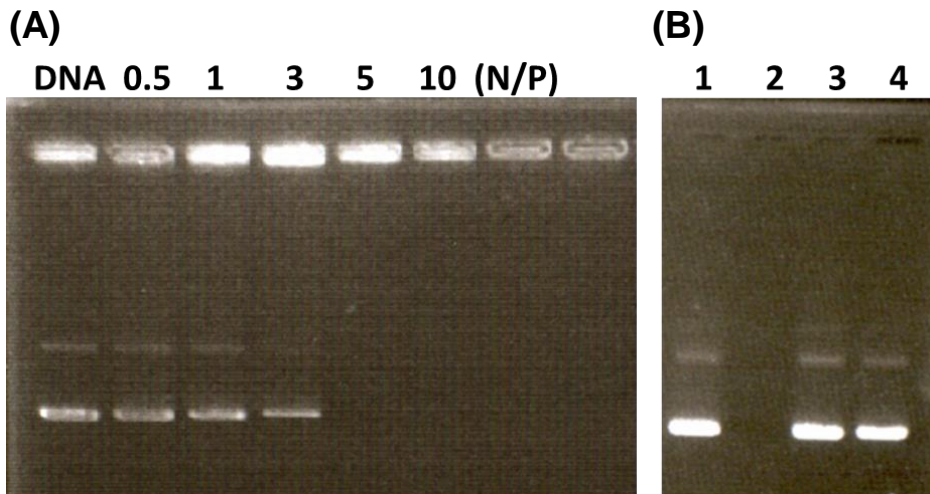


Figure 2.3. Electrophoretic mobility shift assay. (A) Gel electrophoresis of VBPEA/pGL3 (0.1  $\mu\text{g}$ ) complexes at various N/P ratios (0.5 to 10). (B) DNA protection and release assay. DNA was released by adding 1% SDS to VBPEA/pGL3 complexes at an N/P ratio of 10: (Lane 1) pGL3 without DNase I, (Lane 2) pGL3 with DNase I, (Lane 3) VBPEA/pGL3 complexes without DNase I, and (Lane 4) VBPEA/pGL3 complexes with DNase I.

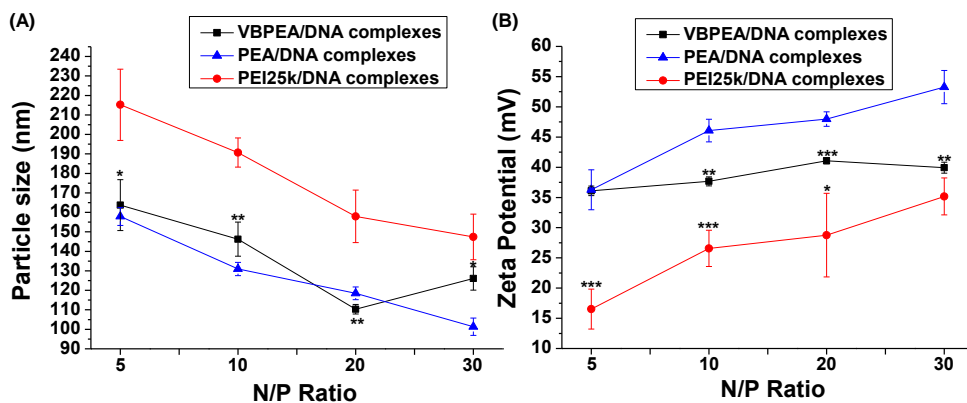


Figure 2.4. Dynamic light scattering microscopic measurements of VBPEA/DNA polyplexes at various N/P ratios. (A) VBPEA/pGL3 particle size without serum. (B) VBPEA/pGL3 zeta potential (n = 3, error bar represents SD) (\*p < 0.05; \*\*p < 0.01; \*\*\*p < 0.001, one-way ANOVA).

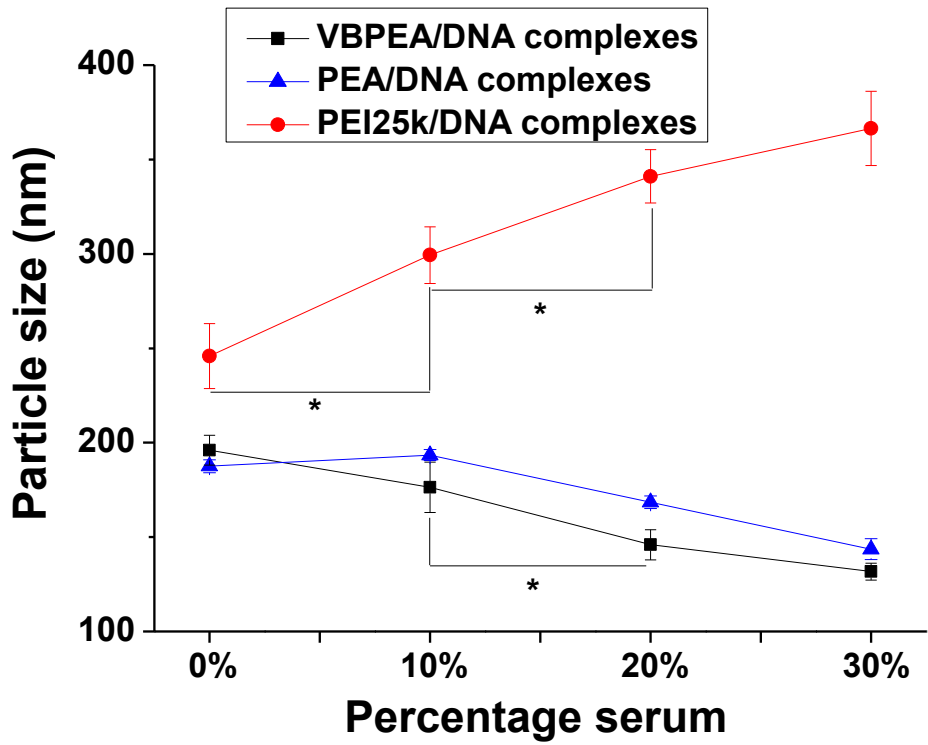


Figure 2.5. VBPEA/pGL3 particle size in various percent serum concentrations (n = 3, error bar represents SD) (\*p < 0.05; \*\*p < 0.01; \*\*\*p < 0.001, one-way ANOVA).

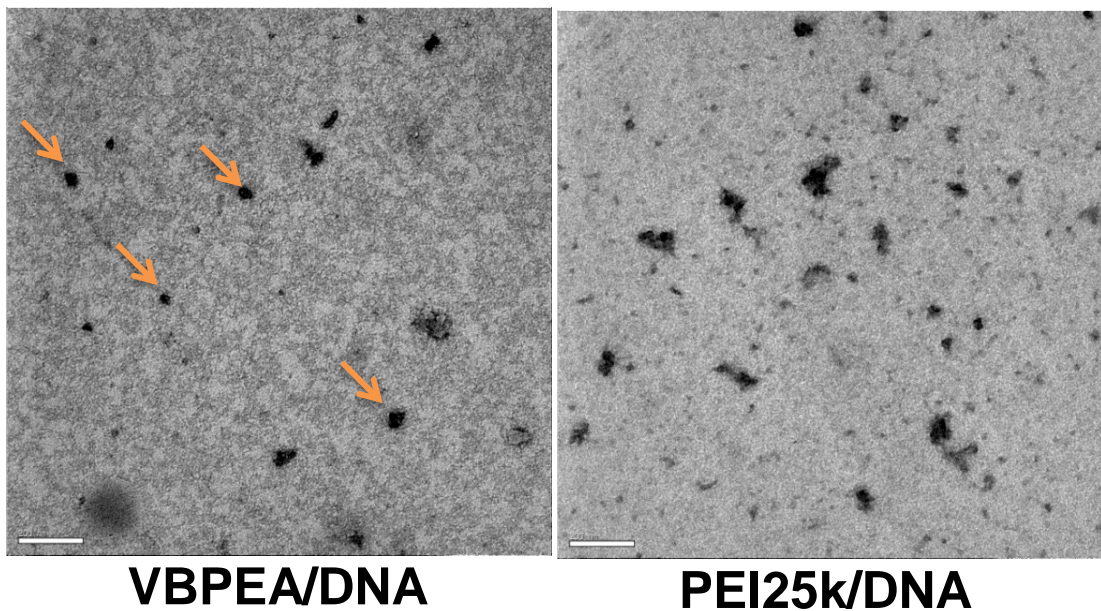


Figure 2.6. EF-TEM images of VBPEA/pGL3 and PEI25k/pGL3 complexes at an N/P ratio of 20.

the positive charges of the PEA backbone, ensuring its stability in an anionic environment. EF-TEM images also showed the VBPEA/DNA complexes to have a uniform size distribution (<120 nm) with well-defined spherical morphologies and no aggregation allowing their easy uptake, in comparison to PEI25k/DNA (Figure 2.6).

### **2.3.2. Enhanced in vitro cell viability and transfection efficiency of VBPEA/DNA complexes**

Enhancement in cell viability by VBPEA due to VB<sub>6</sub> coupling was demonstrated by MTT assay that shows >98% cell viability in A549, HeLa, and HepG2 mammalian carcinoma cell lines in comparison to PEA/DNA (~85-90%) and PEI25k/DNA (~70%) complexes (Figure 2.7).

*In vitro* VBPEA/pGL3 transfection in A549, HeLa, and HepG2 cell lines showed increase in transfection efficiency from N/P 5 to 40 due to the increasing positive charge density, leading to more efficient DNA complexation. However, the level of luciferase gene expression with PEA was comparatively lower than VBPEA. VBPEA (N/P 20)

resulted in a 5-20 fold increase in luciferase expression over PEA (N/P 20) and a 12-30 fold increase over PEI 25k (N/P 10) (Figure 2.8). VBPEA showed 40-45 % transfection efficiency compared to 30-35% efficiency of PEA and 10-13% efficiency of PEI 25k (Figure 2.9) as measured by flow cytometry (Figure 2.10). The crucial result is the increased transfection of VBPEA over PEA, which indicated the probable involvement of a VB<sub>6</sub>-mediated internalization.

Furthermore, VBPEA transfection in presence of serum (Figure 2.11) initially showed stable expression of transgenic product until 20% serum concentration, after which only a slight decrease in transfection was observed due to aggregated serum proteins on VBPEA. The results are in accordance with the aforementioned particle size measurements at various percent serum concentrations.

### **2.3.3. In vivo biodistribution of VBPEA/DNA complexes**

The biodistribution of VBPEA/pGL3 complexes in a Balb/c mouse model showed a moderate level of luciferase gene expression in most of the vital organs, with the highest expression in the spleen, followed

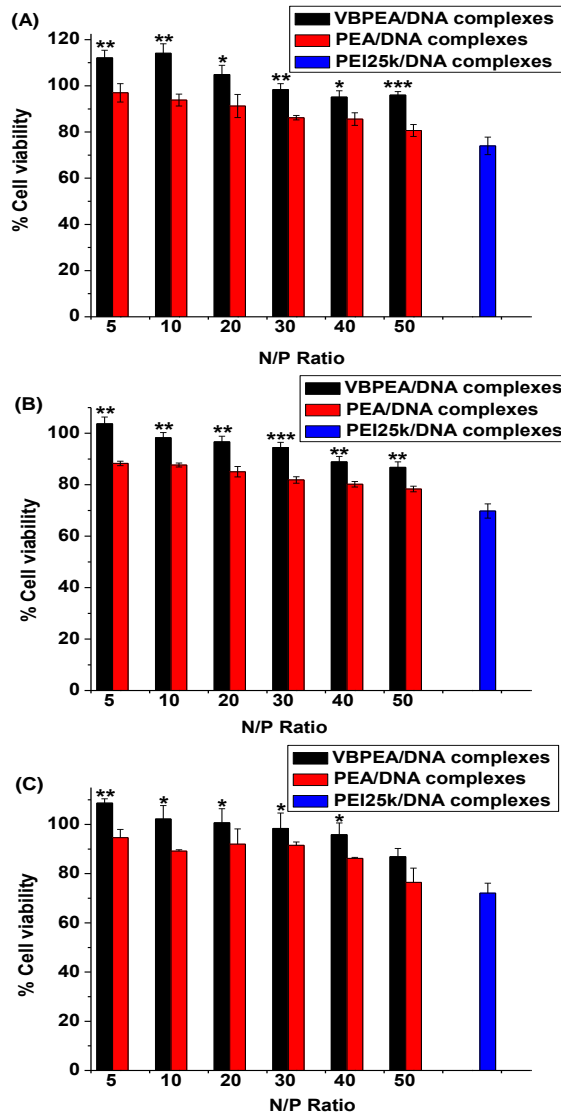


Figure 2.7. Cytotoxicity of VBPEA/DNA (pGL3) complexes at various N/P ratios in different cell lines. (A) A549, (B) HeLa, and (C) HepG2 (n= 3, error bar represents SD) (\*p < 0.05; \*\*p < 0.01; \*\*\*p < 0.001, one-way ANOVA).

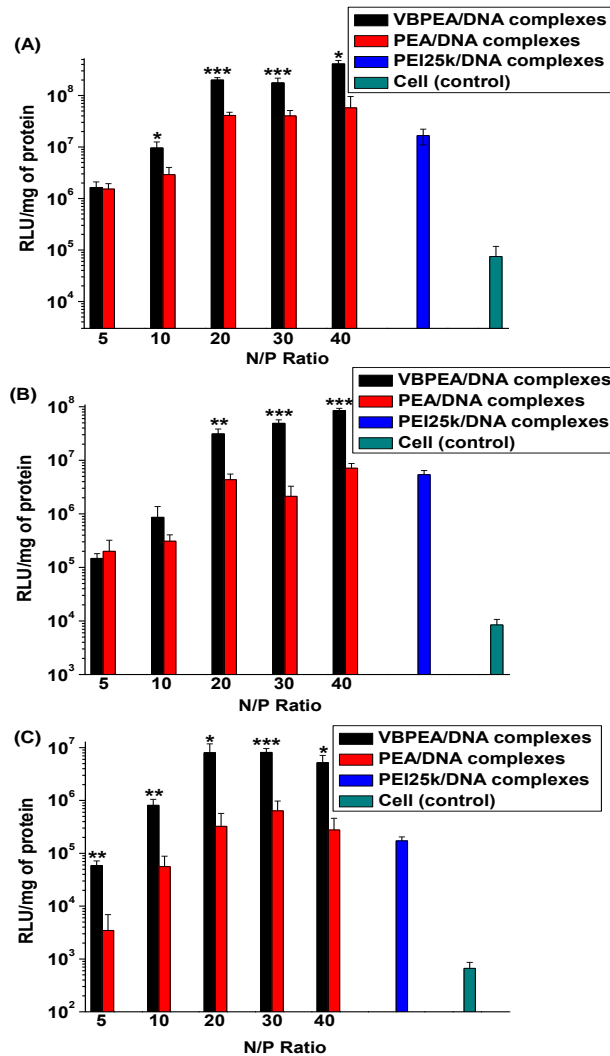


Figure 2.8. In vitro transfection studies of VBPEA/DNA complexes. In vitro transfection in serum free medium at various N/P ratios in different cell lines: (A) A549, (B) HeLa, and (C) HepG2 (n = 3, error bar represents SD) (\*p < 0.05; \*\*p < 0.01, \*\*\*p < 0.001, one-way ANOVA).

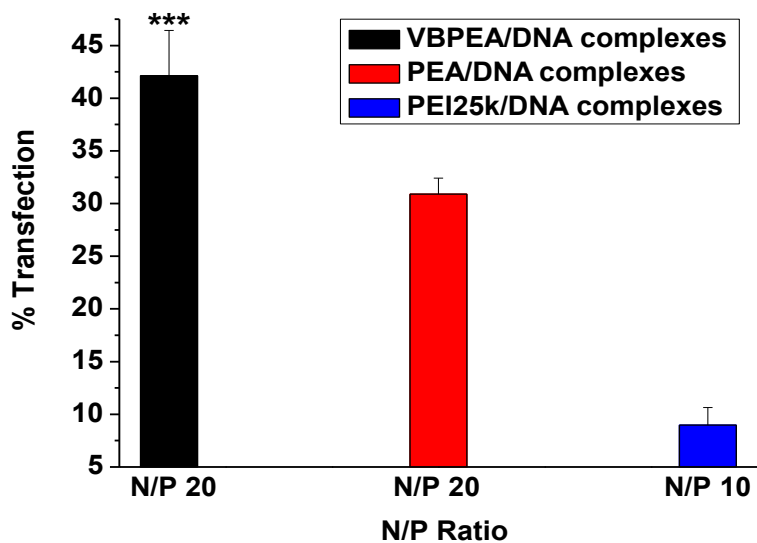


Figure 2.9. Percent transfection efficiency as measured by flow cytometry (n= 3, error bar represents SD) (\*p < 0.05; \*\*p < 0.01, \*\*\*p < 0.001, one-way ANOVA).

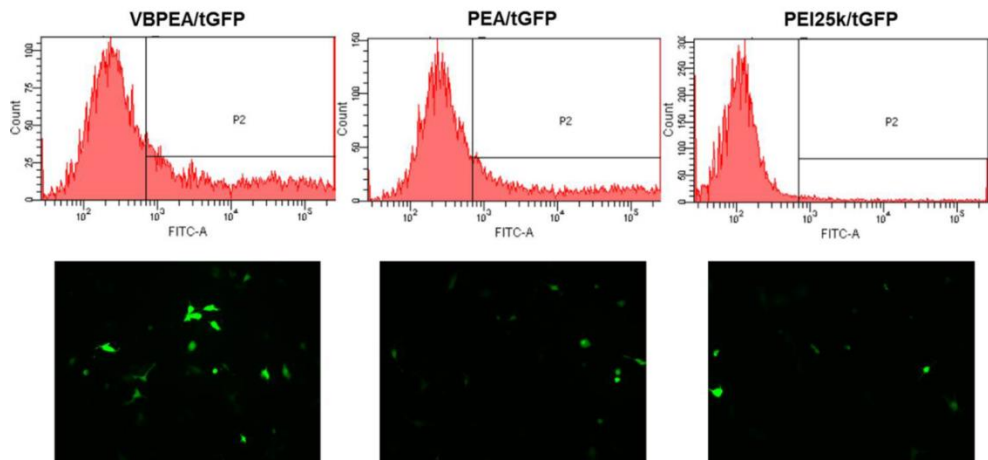


Figure 2.10. FACS studies showing transfection efficiency of VBPEA/tGFP, PEA/tGFP and PEI25k/tGFP complexes in A549 cells with corresponding transfection images.

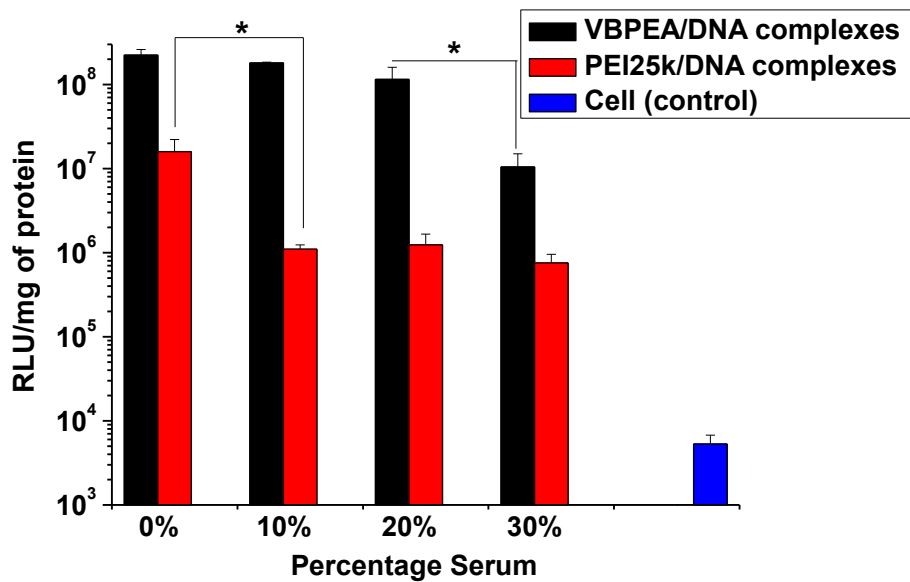


Figure 2.11. Transfection of VBPEA/DNA complexes in various percent serum concentrations in A549 cells (n= 3, error bar represents SD) (\*p < 0.05; \*\*p < 0.01, \*\*\*p < 0.001, one-way ANOVA).

by the lung, brain, liver, and kidney, with minimum expression in the heart (Figure 2.12). VB<sub>6</sub> enhanced the cellular uptake, especially in the liver, lung, and brain, which typically shows lower levels of transgene expression due to restricted entry of therapeutics [124, 125]. Immediately after i.v. injection, polyplexes tend to aggregate with blood cells and plasma components, resulting in a large accumulation of polyplexes in the fine capillaries of the lung, where they extravasate into lung tissues due to vascular leakage of ~60 nm polyplexes. Larger polyplexes are released into circulation, with high concentrations found in liver cells [115]. VB<sub>6</sub> is metabolized by the liver resulting in high accumulation in the liver [126]. Therefore, luciferase delivered by VBPEA, but not by PEA, was expressed in mouse liver.

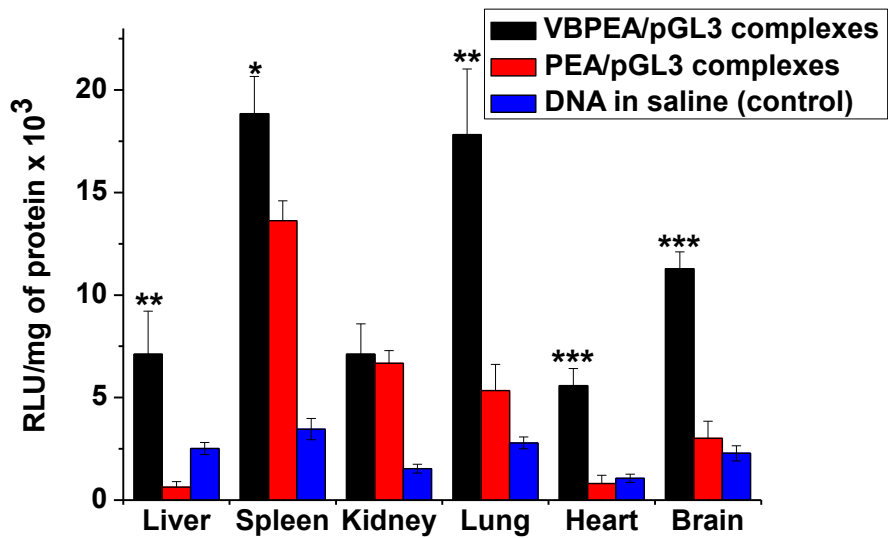


Figure 2.12. In vivo luciferase protein expression after i.v. injection in Balb/c mice showing biodistribution of VBPEA/pGL3 complexes in comparison to PEA/pGL3 complexes and naked pGL3 (n = 4, error bar represents SD) (\*p < 0.05; \*\*p < 0.01, \*\*\*p < 0.001, one-way ANOVA).

## 2.4 Discussion

Our findings show that, with the modification of internalization pathway and mode of cellular uptake, a gene transporter can enhance transfection efficiency in cancer cells. Using VB<sub>6</sub>, coupled to poly(ester amine) backbone, we sought that VB<sub>6</sub> could trail the gene transporter to its specific intracellular route. Interest aroused towards VB<sub>6</sub> due to its unequalled catalytic versatility as a cofactor and widespread involvement in various cellular processes [110, 127]. VB<sub>6</sub> utilizes the common reaction feature of forming a Schiff base (aldimine) between its electrophilic carbonyl group and nucleophilic amines on enzymes [128]. The amino groups of PEA play a similar elegant role in forming the VB<sub>6</sub>-coupled gene transporter via Schiff base formation. The robustness of VBPEA was demonstrated by its ability to protect nucleic acids against DNase degradation and its biocompatibility was verified by over 98% cell viability. The nanosized structure (<170 nm) with optimum surface charge of VBPEA/DNA polyplexes makes it suitable for cellular uptake. In addition, 20-30 folds higher transfection efficiency of VBPEA relative to PEA and PEI25k nanoplexes

demonstrated the involvement of VB<sub>6</sub> specific membrane carriers in uptake process, owing to which the VBPEA gene transporter showed potential for use in gene therapy.

The molecular weight and surface charge of polyplexes plays a crucial role in determining their cytotoxicity. High surface charge of PEI25k tends it to aggregate on the membrane surface and impairs important membrane functions, thereby reducing cell viability [123]. Therefore, LMW PEI was used in VBPEA. VB<sub>6</sub> coupled to the PEA backbone further reduced the surface charge and converted cytotoxic primary amines [129] to less toxic secondary amines, and resulted in the polyplexes no longer being deleterious to cells. In addition, formation of LMW degradation products after polyester backbone hydrolysis into respective acid and alcohol reduces the detrimental cytological effects [123]. The hydroxyl groups in PEA that offer greater cell viability by reducing the surface charge through the formation of hydrogen bonds with DNA gives further biocompatibility to VBPEA in addition to that conferred by the degradable ester linkages. These characteristics function together to give VBPEA an innocuous profile. Polyplex sizes

less than 200 nm helps in an easy cellular internalization, and a positive zeta potential enables it to condense DNA into nanoplexes that brings it in close proximity with the anionic cell membrane [130]. Despite the reduced zeta potential of VBPEA compared to PEA due to VB<sub>6</sub> coupling, the enhancement in the transfection efficiency of VBPEA both *in vitro* and *in vivo* is its most striking feature (Figure 2.8, 2.12), that suggests for the presence of a specialized cellular uptake mechanism due to incorporation of VB<sub>6</sub>.

## **2.5 Conclusion**

This study provides a proof-of-principle strategy for using vitamin B<sub>6</sub>-coupled poly(ester amine) (VBPEA) as a gene transporter for gene delivery to cancer cells with reduced cytotoxicity and increased transfection efficiency. The current research suggests VBPEA is a promising anticancer therapeutic entity that modulates vector delivery and will be able to perform myriad of productive gene modulations by the expression of transgenic products.

# CHAPTER 3

## *Membrane Transport Mechanism of Vitamin B<sub>6</sub>-Coupled Poly(ester amine)*

---

### **3.1 Introduction**

Vitamin B<sub>6</sub> (VB<sub>6</sub>) is an essential micronutrient required for the normal cellular growth and function. It is taken up by the body from exogenous food sources and absorbed by the intestine. Most of the absorbed VB<sub>6</sub> is transported to the liver and taken up by facilitated diffusion through specific VB<sub>6</sub> transporting membrane carriers (VTCs) into the cells [119]. VB<sub>6</sub> plays a vital role as a cofactor for a large number of essential apoenzymes that carry out various metabolic functions [120]. Serine hydroxymethyltransferase (SHMT) is one of the VB<sub>6</sub>-dependent enzymes involved in DNA biosynthesis. This enzyme activity is

enhanced for DNA duplication in the proliferating tumor cells that results in increased consumption of VB<sub>6</sub> [131]. Consequently, to meet the VB<sub>6</sub> needs of tumor cells, VB<sub>6</sub> uptake from neighboring tissues is increased [132, 133]. Since tumor cells have high demand for VB<sub>6</sub>, it was anticipated that the VB<sub>6</sub>-coupled molecules can also achieve VTC-mediated entry into the tumor cells with higher affinity than the normal cells.

## **3.2 Materials and Methods**

### **3.2.1. Materials**

bPEI 25kDa, pyridoxal 5'phosphate (PLP), genistein, chlorpromazine, methyl-β-cyclodextrin, bafilomycin A1 and 4'-deoxypyridoxine hydrochloride were purchased from Sigma (St. Louis, MO, USA). Luciferase reporter, pGL3- vector with SV-40 promoter and enhancer encoding firefly (*Photinus pyralis*) luciferase was obtained from Promega (Madison, WI, USA). Tetramethylrhodamine isothiocyanate (TRITC) and YOYO-1 iodide (Molecular Probes, Invitrogen, Oregon,

USA) fluorescent dyes were used for confocal microscopy. All other chemicals used in this study were of analytical reagent grade.

### **3.2.2. Cell culture and isolation of mouse primary lung cells**

Adenocarcinoma human alveolar basal epithelial cells (A549) and mouse lung adenoma cells (LA-4) were maintained in Roswell Park Memorial Institute (RPMI)-1640 culture medium. Human bronchial epithelial cells (16-HBE) were cultured in DMEM/Ham's F-12 medium containing 10% heat-inactivated fetal bovine serum (FBS, HyClone, Logan, UT, USA) with 1% penicillin/streptomycin. All cells were maintained under standard culture conditions of 37°C and 5% CO<sub>2</sub>.

To obtain lung single cell suspensions, lungs were removed from mice (6 weeks old) and kept separately in DMEM/F-12 medium containing 0.5 mg/mL collagenase D (Roche Applied Science, Indianapolis, IN, USA) and 100 µg/mL DNase I (Sigma-Aldrich). Tissues were minced with scissors, incubated for 1 h at 37°C and then passed through a 70 µm Falcon cell strainer (BD Labware). RBC lysis was performed using ACK lysis buffer (Gibco) followed by centrifugation (800 rpm, 10 min).

The cell pellet was resuspended in DMEM/Ham's F-12 medium (10% FBS and 1% antibiotic). Cells were counted and seeded in a 24-well plate.

### **3.2.3. In vitro transfection**

Transfection studies were performed in A549, LA-4 and 16-HBE cells at an initial cell density of  $10 \times 10^4$  in 24-well plate. At 80% cell confluency, VBPEA/pGL3 (1  $\mu$ g), PEA/pGL3, and PEI25k/pGL3 polyplexes were treated at various 20 N/P ratio in serum-free medium, which was exchanged with fresh media containing serum (10% FBS) after 3 h. After the cells were kept under standard incubation conditions for 24 h, luciferase assay was performed according to the manufacturer's protocol. A chemiluminometer (Autolumat, LB953; EG&G Berthold, Germany) was used to measure relative light units (RLUs) normalized with protein concentration in cell extract estimated using a BCA protein assay kit (Pierce Biotechnology, Rockford, IL, USA). Transfection activity was measured in triplicate as RLUs/mg protein.

### **3.2.4. Mechanistic studies for VBPEA high transfection efficiency:**

#### ***3.2.4.1. 4'-Deoxypyridoxine competition assay***

To investigate the role of VB<sub>6</sub> in enhancing cellular internalization, a competitive inhibition study was performed using 4'-deoxypyridoxine, a structural analogue of VB<sub>6</sub>. 4'-Deoxypyridoxine was added to 80% confluent A549 cells at concentrations of 0, 1, 2, 5, 10, and 20 mM, and the cells were incubated for 10 min before the addition of VBPEA/DNA and PEA/DNA polyplexes. *In vitro* luciferase assay was performed 24 h later.

#### ***3.2.4.2. VBPEA inhibition study by confocal microscopy***

A Carl Zeiss LSM 710 inverted laser scanning confocal microscope was used to monitor intracellular trafficking of TRITC-labeled VBPEA and YOYO-1-labeled pDNA in A549 cells in the presence and absence of 4'-deoxypyridoxine. TRITC (25 μL, 1 mg/100 μL in DMF) was added to VBPEA (1 mL, 10 mg/mL in H<sub>2</sub>O) to block ~1% of its total amines and stirred overnight. Unreacted TRITC was removed by washing with ethyl acetate (3 × 2 mL), which was then lyophilized and

resuspended in water. pDNA (1  $\mu$ g) was labeled with YOYO-1 iodide (2  $\mu$ L, 1 mM solution in DMSO) by stirring for 2 h at  $25 \pm 1^\circ\text{C}$  in the dark and then stored at  $-20^\circ\text{C}$ . A549 cells seeded in 6-well plate at  $20 \times 10^4$  cells/well were transfected with dual-labeled VBPEA/DNA complexes with and without 4'-deoxypyridoxine. After 120 min of incubation, cells were washed with  $1\times$  PBS 3 times with 500  $\mu$ L and fixed with 4% paraformaldehyde for 10 min at  $4^\circ\text{C}$ . DAPI was used to counter-stain the nuclear DNA of fixed cells, and images were procured from confocal microscopy.

#### ***3.2.4.3. Effect of free and coupled VB<sub>6</sub> on gene transfection***

The effect of VBPEA in comparison to VB<sub>6</sub> alone in enhancing transfection was demonstrated by transfecting A549 cells with PEA/pGL3 complexes (N/P 20) with 0, 5, 20, 50, and 100  $\mu$ M VB<sub>6</sub>. These transfection results were compared with VBPEA/pGL3 (N/P 20)-mediated transfection.

#### ***3.2.4.4. Comparison of VBPEA affinity towards cancer cells and normal cells***

Mouse primary lung cells seeded in 24-well plate at a density of  $10 \times 10^4$  cells/well were washed with PBS and transfected with VBPEA/DNA complexes (N/P 20) in serum-free medium. After 3 h, the medium was replaced with fresh DMEM/F-12 complete medium. Similarly, mouse lung adenoma LA4 cells, human adenocarcinoma A549, and human bronchial epithelial 16HBE cells were also transfected. After 24 h, luciferase expression was analyzed and compared between normal and cancer cells.

#### ***3.2.4.5. Comparison of PEA and VBPEA endocytosis pathways***

The route of VBPEA uptake was analyzed by inhibiting various endocytosis pathways and their subsequent effect on transfection was observed. For the investigation of clathrin-mediated endocytosis, A549 cells were treated with chlorpromazine at concentrations of 1, 2 and 3  $\mu\text{g/mL}$  and incubated for 1 h before adding VBPEA/DNA complexes. Similarly, caveolae-mediated uptake was examined using the inhibitors  $\beta$ -methyl cyclodextrin (2.5, 6.5 and 10  $\text{mg/mL}$ ) and genistein (100, 200, and 300  $\mu\text{M}$ ). After 1 h of incubation with inhibitors, A549 cells were transfected and luciferase expression was measured 24 h later.

#### ***3.2.4.6. Proton sponge effect by PEI in VBPEA***

To ensure the endosomal escape of VBPEA, the vacuolar-type H<sup>+</sup>-ATPase endosome proton pump was inhibited by bafilomycin A1 and the effect on transfection was observed. For this, A549 cells were seeded in 24-well plate at an initial cell density of  $10 \times 10^4$ . Confluent cells (80%) were pretreated with bafilomycin A1 (200 nM in DMSO) for 10 min, after which the inhibitor was aspirated and VBPEA/DNA and PEI25k/DNA polyplexes were added. Luciferase expression was measured after 24 h as described above.

### **3.3 Results**

#### **3.3.1. Competitive inhibition of VBPEA/DNA complexes by 4'-deoxyribose reveals VTC mediated uptake**

A549 cells transfected with VBPEA/DNA and PEA/DNA complexes in the presence of 4'-deoxyribose (structural analogue of VB<sub>6</sub>) showed a sudden decrease in VBPEA transfection to the level of PEA-mediated transfection efficiency at an inhibitor concentration of 1 mM (Figure 3.1). On the other hand, no significant inhibitor effect in

PEA/DNA transfection activity was observed, suggesting that 4'-deoxypyridoxine competitively inhibits the binding of VB<sub>6</sub> present in VBPEA/DNA polyplexes to VTC and decelerates polyplex uptake. Owing to the PEA backbone, VBPEA still retains transfection potential and does not completely lose transfection efficacy; instead, only VB<sub>6</sub>-specific uptake is hindered by 4'-deoxypyridoxine. This suggests the active participation of a VB<sub>6</sub>-specific uptake mechanism via a membrane carrier favoring accelerated internalization of VBPEA. Moreover, confocal images showed that VBPEA/DNA polyplexes internalization was decreased in the presence of 4'-deoxypyridoxine due to the decreased accessibility of VTC to VBPEA (Figure 3.2).

### **3.3.2. VB<sub>6</sub> coupling enhances cellular uptake of PEA polyplexes in cancer cells**

In order to prove the role of coupled VB<sub>6</sub>, we analyzed the transfection activity of PEA/DNA in the presence of free VB<sub>6</sub> compared to the amount of coupled VB<sub>6</sub> in VBPEA. VB<sub>6</sub> in a non-coupled state had no contribution in increasing the transfection activity of PEA even at 100  $\mu$ M concentration of VB<sub>6</sub> (Figure 3.3). In contrast, the VB<sub>6</sub> coupled to

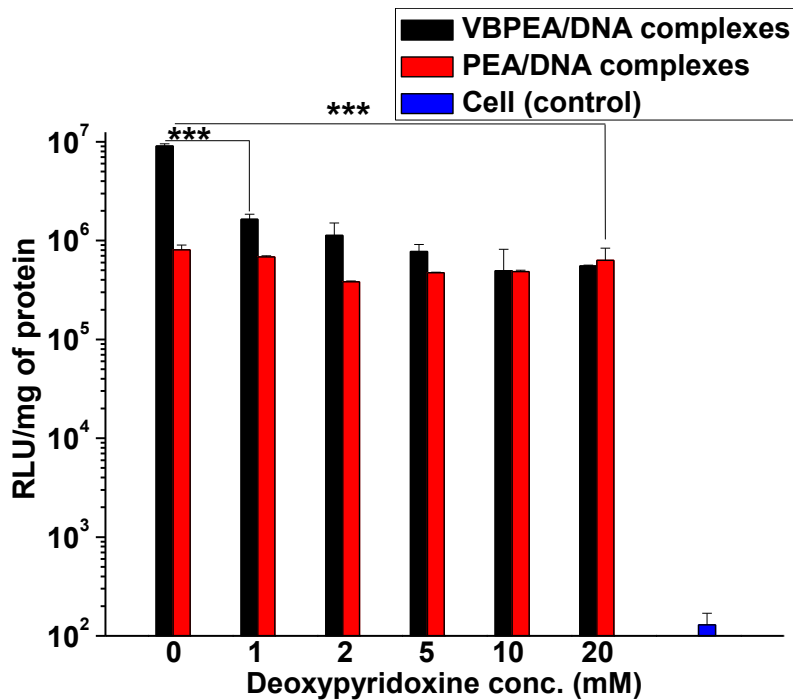


Figure 3.1. Carrier-mediated uptake of VBPEA evidenced by 4'-deoxyripyridoxine (a structural analog of VB6) competitive inhibition (n = 3, error bar represents SD) (\*\*\*)  $p < 0.001$ , one-way ANOVA).

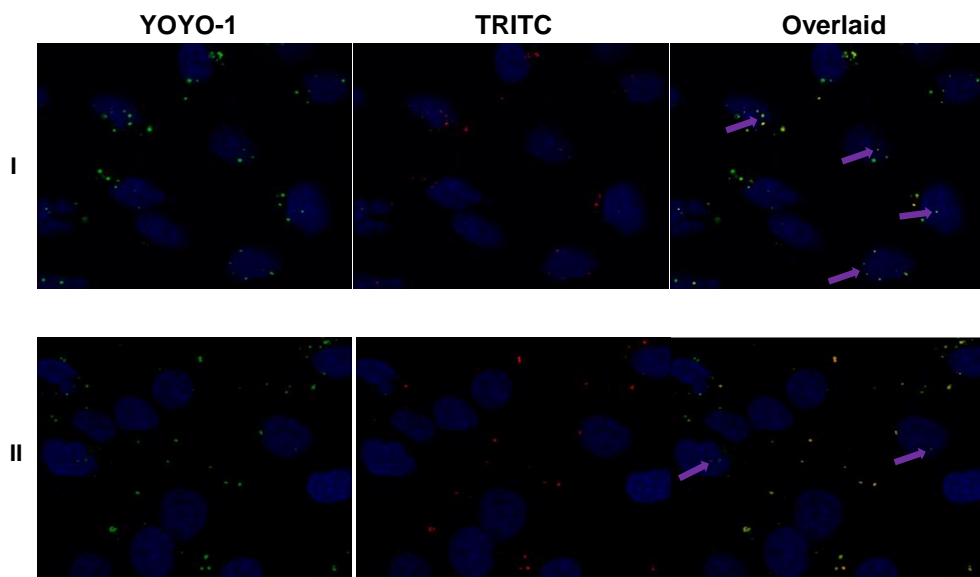


Figure 3.2. Confocal microscopic images of A549 cells taken after VBPEA/DNA polyplex treatment for 120 min (I) in the absence of 4'-deoxypyridoxine and (II) in the presence of 4'-deoxypyridoxine. VBPEA labeled with TRITC (red), pDNA labeled with YOYO-1 (green) and nuclear DNA labeled with DAPI (blue).

PEA drastically elevated the gene delivering capacity. Based on these results, it can be concluded that free VB<sub>6</sub> is easily transported across the cell membrane through VTC without affecting the transfection efficiency of PEA, whereas VB<sub>6</sub> coupled to PEA is unable to pass through the VTC owing to its large polyplex sizes, which may result in endocytosis of the inactivated VTC along with the VBPEA polyplex.

To investigate the increased affinity of cancer cells for VBPEA relative to normal cells, a comparative transfection study using human and mouse primary lung and cancer cells with VBPEA/DNA complexes was conducted. Primary cells showed lower transfection relative to their respective cancer cells (Figure 3.4), illustrating that VBPEA/DNA polyplex uptake is favored in tumors, most likely due to their need for excess VB<sub>6</sub> to support their uncontrolled growth and proliferation. However, normal cells, the growth and proliferation of which is under strong control, have a comparatively lower affinity for VB<sub>6</sub>, and thus showed lower transfection activity. To verify that normal cells were not affected by cellular cytotoxicity, a cell viability assay was performed to show no toxic effects of VBPEA/DNA complexes (Figure 3.5).

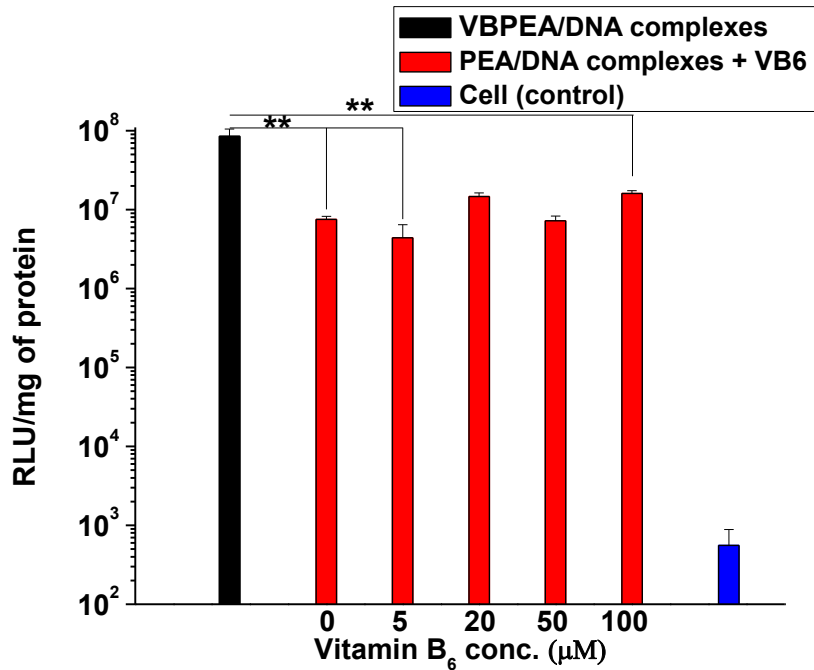


Figure 3.3. VB6 coupling enhances cellular uptake of PEA polyplexes in cancer cells. Effect of coupled VB6 in VBPEA compared to free VB6 in gene delivery (n = 3, error bar represents SD), (\*p < 0.05; \*\*p < 0.01, \*\*\*p < 0.001, one-way ANOVA).

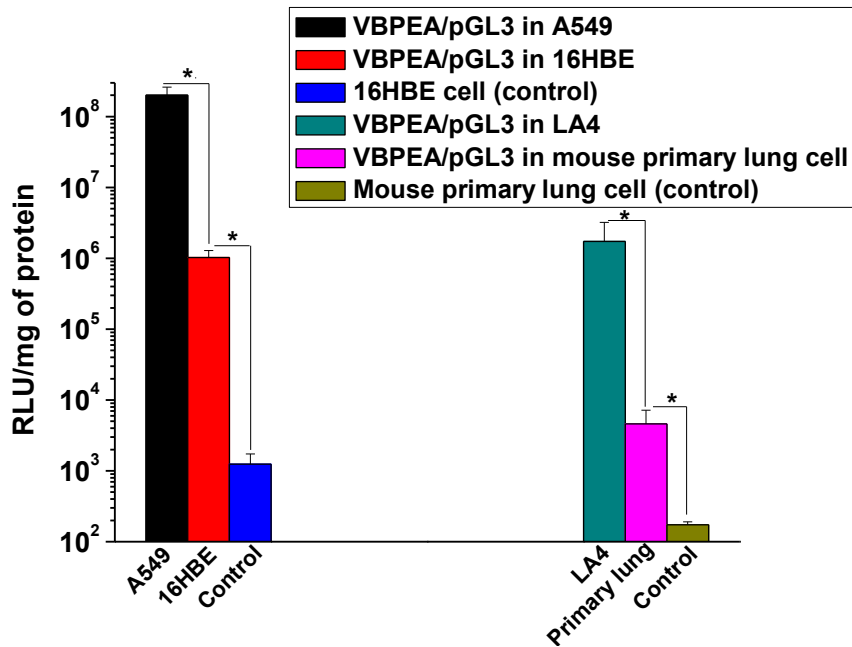


Figure 3.4. Uptake study of VBPEA/pGL3 by primary cells vs. cancer cells in human and mouse lung cell lines showing enhanced uptake by cancer cells (n = 3, error bar represents SD), (\*p < 0.05; \*\*p < 0.01, \*\*\*p < 0.001, one-way ANOVA).

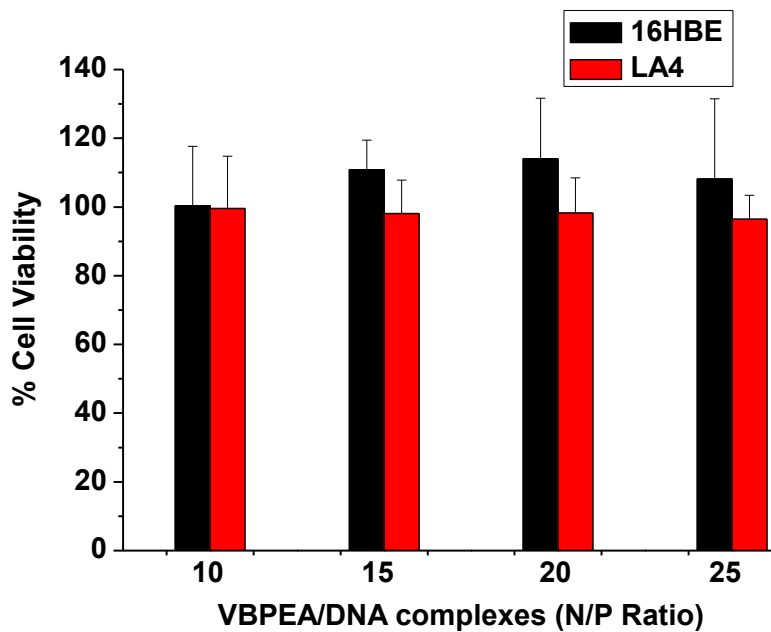


Figure 3.5. Cytotoxicity of VBPEA/DNA complexes in 16HBE (human) and LA4 (mouse) normal lung cell lines at various N/P ratios. (n = 3, error bar represents SD).

### **3.3.3. VBPEA elicit clathrin- and caveolae-mediated endocytosis and endosomal escape**

Caveolae endocytic inhibitors  $\beta$ -methyl cyclodextrin and genistein, which deplete the cholesterol rafts of caveolae, result in a gradual decrease in VBPEA and PEA-mediated transfection, suggesting a caveolae route of internalization utilized by both transporters. In contrast, clathrin-mediated endocytosis studied using chlorpromazine inhibitor showed decreased transfection of VBPEA/DNA complexes, whereas PEA/DNA complexes showed no loss in transfection (Figure 3.6). The clathrin pathway is likely to be initiated by VBPEA because of the involvement of VTCs in its uptake process, whereas PEA does not follow clathrin-mediated endocytosis due to the lack of carrier participation. Furthermore, inhibition of vacuolar type  $H^+$ -ATPases by bafilomycin A1 showed a 1000-fold decrease in the transfection of VBPEA, suggesting the ability of VBPEA to induce endosome acidification (Figure 3.7). The inhibitor prevented endosomal acidification and hence ceased its bursting to release the transporter.

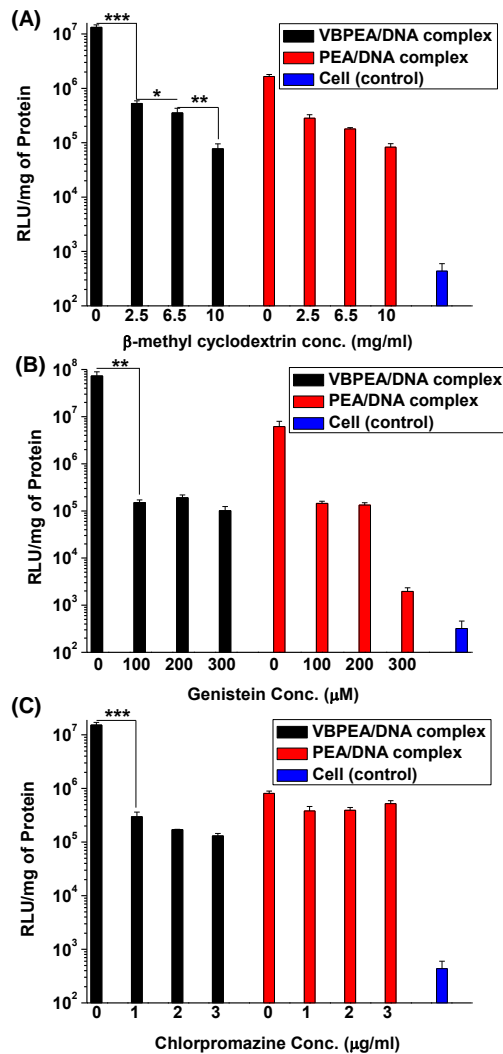


Figure 3.6. Effect of caveolae- and clathrin- endocytic inhibitors on transfection. Caveolae-endocytic inhibitors (A)  $\beta$ -methyl cyclodextrin, (B) genistein and clathrin-endocytic inhibitor (C) chlorpromazine. (n = 3, error bar represents SD), (\*p < 0.05; \*\*p < 0.01, \*\*\*p < 0.001, one-way ANOVA).

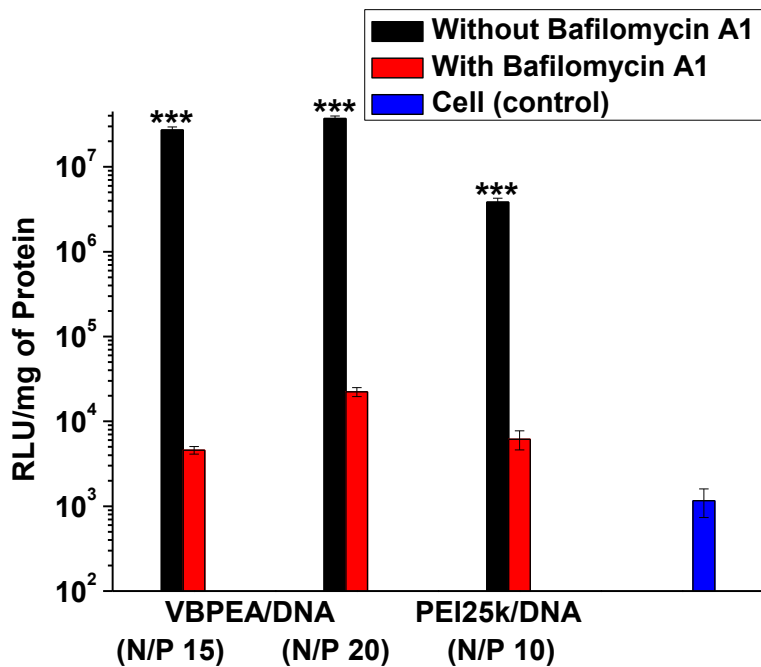


Figure 3.7. Bafilomycin A1 studies to show endosomal escape ability of VBPEA. (n = 3, error bar represents SD), (\*\*\*)p < 0.001, one-way ANOVA).

### 3.4 Discussion

The enhancement in transfection efficiency of VBPEA both *in vitro* and *in vivo* relative to PEA (Figure 2.8, 2.12), suggests the involvement of VB<sub>6</sub> specific membrane carriers in its uptake process due to incorporated VB<sub>6</sub>. The coupled VB<sub>6</sub>-mediated uptake of polyplexes was investigated by the effect of 4'-deoxyripyridoxine, which is a structural analog of VB<sub>6</sub>, on the transfection efficiency of VBPEA and PEA. It was observed that 4'-deoxyripyridoxine reduced the transfection activity of VBPEA but had no effect on PEA transfection, suggesting that 4'-deoxyripyridoxine competitively inhibited VBPEA cellular uptake by obstructing VB<sub>6</sub>-mediated cellular entry. This indicated the involvement of VTCs in polyplex transport into cells. When VTCs on the cell membrane were competitively inhibited, the VB<sub>6</sub> in VBPEA is unable to enhance transfection. Confocal studies in the presence of inhibitor also showed a reduction in the internalization of polyplexes compared to that in the absence of inhibitor. This hypothesis was further supported when PEA along with unbound VB<sub>6</sub> experienced no enhancement in expression of transgenic product. We concluded that

the addition of free VB<sub>6</sub> to PEA/DNA complexes exerted no effect on complex internalization; instead, VB<sub>6</sub> itself easily passed through the membrane carrier. This clearly demonstrated the role of VB<sub>6</sub>-coupled to PEA in enhancing polyplex uptake by co-transporting the vector with VB<sub>6</sub> attached to the VTC. A speculative representation of the involvement of VTC in VBPEA/DNA transport into cell is shown in Figure 3.8A. VBPEA-mediated transfection was found to be sensitive to bafilomycin A1, a specific inhibitor of vacuolar-type H<sup>+</sup>-ATPases [134], suggesting that PEI has a role in the endosomal release of VBPEA/DNA complexes via a ‘proton sponge’ effect, helping it to escape the aggressive endosomal nucleases in the cytoplasm. However, it is noteworthy that, even in the presence of bafilomycin A1, VBPEA showed an approximately 10-fold higher level of transfection than PEI25k (Figure 3.7), suggesting that increased cellular uptake is more important than endosomal escape in order to achieve high transfection.

In general, VB<sub>6</sub> is absorbed into the bloodstream from the intestine via simple diffusion, where it travels in its activated form (PLP). Before cellular uptake, it is dephosphorylated by a membrane-bound alkaline

phosphatase and enters the cell via a VTC through facilitated diffusion. Pyridoxal kinase rephosphorylates it to PLP so that it can participate in various cellular catalytic reactions [119, 126]. A schematic representation of a hypothetical mechanism of enhanced transfection of VBPEA based on available mechanistic studies is shown in figure 3.8B. Cells displaying VTC on their membrane specifically transport VB<sub>6</sub> inside cells; however, these membrane carriers are not able to transport the VB<sub>6</sub> in VBPEA/DNA polyplexes due to their large sizes. Consequently, polyplexes bound to the inactivated VTC are endocytosed as a cellular clearing mechanism. Its sojourn towards lysosomal fusion is halted due to the proton sponge effect, which leads to endosomal escape and subsequent gene delivery into the nucleus. In addition endocytosis inhibition studies of VBPEA showed both clathrin- and caveolae-mediated endocytosis, indicating the involvement of VTC in the VBPEA internalization process.

Since VB<sub>6</sub> is essential for the growth and proliferation of cells, it becomes an important requisite for cancerous tissues. In addition, there is evidence that serine hydroxymethyltransferase (SHMT), a VB<sub>6</sub>-

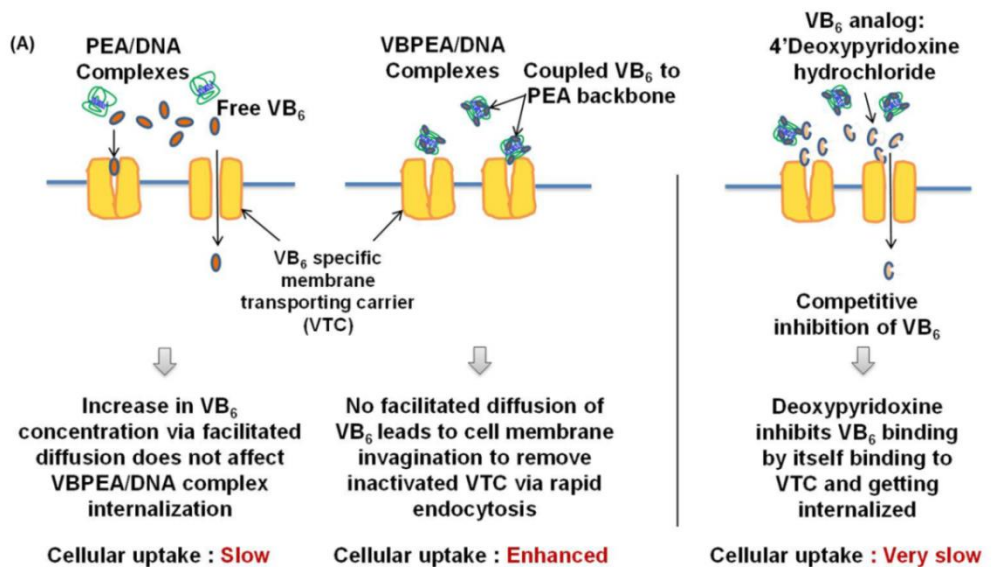


Figure 3.8. (A) A speculative representation of the involvement of a VTC in VBPEA/DNA transport. Figures do not represent the scale of the molecule.

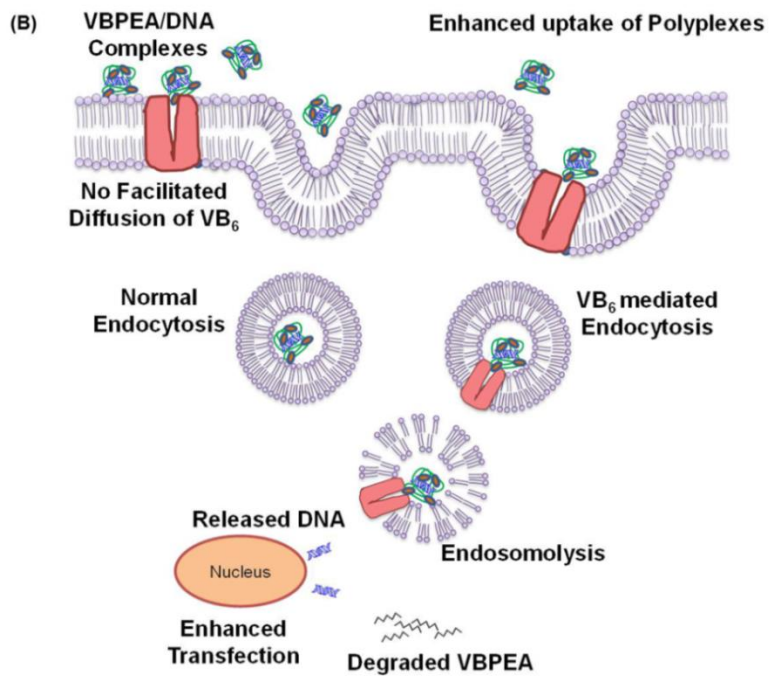


Figure 3.8. (B) A schematic representation of a hypothetical mechanism of cellular internalization of VBPEA/DNA complexes. Figures do not represent the scale of the molecule.

dependent enzyme, is associated with the increased demand for DNA biosynthesis during tumor proliferation. In order to support their uncontrolled proliferation, tumors have a constant need for this vitamin to synthesize DNA [133]. Due to this cancer cells show higher affinity towards VBPEA coupled with VB<sub>6</sub> and hence elevated transfection level was observed in comparison to normal cells. Therefore, we anticipate that our newly synthesized gene transporter can be used in cancer gene therapy with specificity and efficiency to deliver therapeutic siRNA targeting VB<sub>6</sub>-dependent enzymes. The attributes of VB<sub>6</sub> demonstrated in the present study show its potential applications in developing more profound gene and drug delivery systems.

### **3.5 Conclusion**

Competitive inhibition studies with 4'-deoxypyridoxine indicated that VTCs play a crucial role in enhancing the cellular uptake of VBPEA, which was inactivated by the attachment of large polyplexes and resulted in endosome formation. Although the exact mechanism of the enhanced affinity of VBPEA towards cancer cells is not clear at this point, we speculate that, in order to support their uncontrolled growth

and proliferation, cancer cells constantly require VB<sub>6</sub> for various metabolic reactions, resulting in increased VBPEA uptake. Ongoing studies are focusing on the cellular signaling mechanism involved in increasing the affinity of VBPEA in cancer cells and exploring its therapeutic applications using siRNA.

# CHAPTER 4

## *Gene Silencing Efficiency of Vitamin B6-Coupled Poly(ester amine)*

---

### 4.1 Introduction

The phenomena RNA interference (RNAi) first discovered in the nematode worm *Caenorhabditis elegans*, is a conserved biological response of double-stranded RNA (~ 21 nucleotides long) which impose resistance to both endogenous parasitic and exogenous pathogenic nucleic acids and regulates the expression of genes post transcriptionally [135]. Fire, Mello and colleagues discovered that dsRNA mixture was at least tenfold more potent in triggering silencing effect than the sense or antisense RNAs alone [136]. Since then RNAi has become a valuable research tool, both *in vitro* and *in vivo*, because

synthetic dsRNA can selectively and robustly suppress the products of specific genes of interest when introduced into cells.

RNAi can be induced either by miRNA or siRNA. Both function via the same mechanism and using the similar silencing machinery, the difference lies in their origin. miRNA originates from a single strand RNA looped on itself which on cutting by Dicer appears double stranded. On the other hand, siRNA is actually formed from a double stranded RNA. Moreover, miRNA is synthesized endogenously in the cell to regulate the expression of genes whereas siRNA has exogenous origin which is foreign to cell.

RNAi technology is welcomed as one of the greatest medical advancements since antibiotics, with the potential to knockdown the genes that are responsible for cancer advancement, yet most laboratories are working dedicatedly to translate this RNAi technology from just a research tool into a usable therapeutic strategy. A major obstacle for RNAi remains the efficient delivery of these small molecules to the targeted cell type in vivo. Hence, the development of a suitable vector candidate with a conjugated targeting ligand becomes

the major area of research. Therefore, owing to higher affinity towards cancer cells, VBPEA gene transporter portrays an appropriate vector for delivering siRNA into the cancer cells.

## **4.2 Literature Review**

### **4.2.1. Components of RNAi machinery**

**Dicer** is an endoribonuclease that cleaves dsRNA and generates short dsRNA fragments called small interfering RNA (siRNA ~ 20-23 nucleotides long) with two base long 3' overhang and 5' phosphorylated terminus, both required for activity [137].

**RISC** is RNA-induced silencing complex. This multiprotein complex has helicase, exonuclease, endonuclease and homology searching proteins. Initially RISC is inactive until it is transformed into active form by unwinding of the siRNA duplex; loss of sense strand called as passenger strand and remains attached with the another antisense strand of siRNA called as the guide strand.

**Antisense** (guide) strand of siRNA defines specificity of RNAi by

guiding the RISC complex to its complementary mRNA. This strand serves as a template for recognizing the specific mRNA after which RISC activates the RNase activity and cleaves the mRNA, resulting in decreased level of protein translation and efficiently turning off the gene [138].

**Argonaute** protein acts as a slicer which functions as the catalytic component of the RISC complex. These proteins are key players in RNA silencing which can bind small non-coding RNAs and control protein synthesis, affect mRNA stability and even participate in the production of a different class of RNAs called Piwi interacting RNAs. These proteins are also responsible to some extent for the selection of guide strand and destruction of passage strand [139].

#### **4.2.2. Mechanism of RNAi**

A sequential RNAi pathway is illustrated in figure 4.1.

**A.** Introduction of dsRNA precursor triggers the RNAi pathway in cell's cytoplasm which accounts for the initiation of gene silencing.

**B.** Dicer which is a large multidomain cytoplasmic RNase III endonuclease enzyme cleaves the dsRNA precursor to produce double stranded fragments of small interfering RNA (siRNA) of approximately 21-23bp length with two base long 3'overhangs. Dicer producing siRNA is ATP dependent process with substrate specificity to dsRNA. It also need a dsRNA binding protein called R2D2 which has two dsRNA binding domains and function in association with RNase enzyme of dicer forming a heterodimeric complex [141]. It is unclear which of these domains physically bind to siRNA but is believed that siRNA binds at the interface between dicer and R2D2. This induces a conformational change in either or both the proteins allowing them to bind to siRNA simultaneously [142].

**C.** The next step is characterized by the formation of silencing complex called RISC (RNA Induced Silencing Complex). The double stranded siRNA unwinds and one out of the two single strands referred to as guide strand assembles into RISC. The other strand called passenger strand is degraded. The core of the RISC complex was found to be composed of highly conserved Argonaute (Ago) protein which has

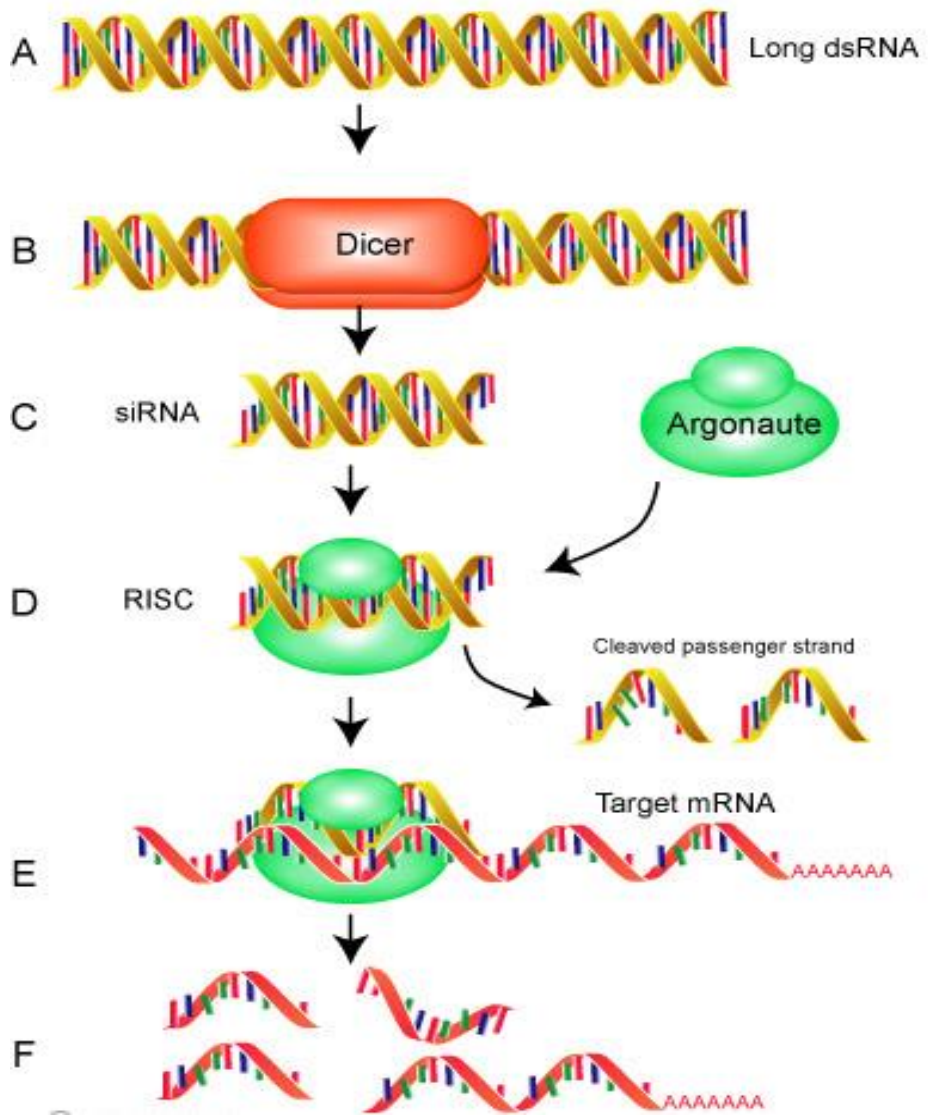


Figure 4.1. Mechanism of RNA interference. Adopted from Ref [140].

structural similarity with RNase H ribonuclease [143]. The Ago proteins serve to be the catalytic subunit of RISC. The orientation of the RISC with siRNA creates a thermodynamic asymmetry that helps in the separation of guide strand from the passenger strand [144].

This Ago protein dependent complex converts the pre-RISC containing the duplex siRNA into holo-RISC containing the guide strand of siRNA, by removing the passenger strand [144].

**D.** Antisense siRNA guide strand then guides the RISC to complementary mRNA molecules. The 5' end of siRNA acts as a target recognition site.

**E.** RISC cleaves the mRNA. The Ago subunit of holo-RISC acts as RNase H and cleaves the target mRNA backbone.

**F.** This leads to specific post transcriptional gene silencing.

## **4.3 Materials and Methods**

### **4.3.1. Materials**

bPEI 25kDa, and 3-(4, 5-dimethyl thiazol-2-yl)-2, 5-diphenyl tetrazolium bromide (MTT) reagent were purchased from Sigma (St. Louis, MO, USA). Luciferase reporter, pGL3- vector with SV-40 promoter and enhancer encoding firefly (*Photinus pyralis*) luciferase was obtained from Promega (Madison, WI, USA). The green fluorescent protein (GFP) gene was obtained from Clontech (Palo Alto, CA, USA). Nonspecific scrambled siRNA (siScr), luciferase siRNA and GFP siRNA (siGFP) (Table 4.1) were purchased from Genolution Pharmaceuticals, Inc. (Seoul, South Korea). All other chemicals used in this study were of analytical reagent grade.

#### **4.3.2. Synthesis and characterization of VBPEA/siRNA polyplexes**

The cationic VBPEA polymer at N/P 20 was electrostatically bound with siGFP (100 pM) in ultra-pure molecular grade water (WelGENE, S. Korea) (30 min incubation at RT) to form VBPEA/siGFP polyplexes. VBPEA/siRNA polyplexes were characterized using a transmission electron microscope (EF-TEM) (LIBRA 120, Carl Zeiss, Germany) and a dynamic light scattering spectrophotometer (DLS 8000, Otsuka Electronics, Osaka, Japan). The specimens for TEM were prepared by

Table 4.1. siRNA sequences

<b>siRNA</b>	<b>Sense (5'→3')</b>	<b>Anti-sense (5'→3')</b>
siRNA scrambled	CGUACGCGGAAUACUUCGAUU	UCGAAGUAUUCCGCGUACGUU
siRNA GFP	GUUCAGCGUGUCCGGCGAGUU	CUCGCCGGACACGCUGAACUU
siRNA Luciferase	CUUACGCUGAGUACUUCGAUU	UCGAAGUACUCAGCGUAAGUU

drop-coating the VBPEA/siRNA (N/P 20) polyplex dispersion onto a carbon grid and then dried for 2 h, after which it was stained with 1% uranyl acetate (10 s) and observed for its morphology. DLS samples were prepared at various N/P ratios (5, 10, 20, and 30) of VBPEA/siGFP polyplexes with 40  $\mu\text{g}/\text{mL}$  siGFP and then measured for their hydrodynamic size and zeta potential with  $90^\circ$  and  $20^\circ$  scattering angles at  $25^\circ\text{C}$ .

#### **4.3.3. Electrophoretic mobility shift assay (EMSA)**

VBPEA/siRNA polyplexes were characterized for siRNA retardation and protection assay. For siRNA retardation assay, VBPEA was complexed with siRNA (1  $\mu\text{g}$ ) for 30 min at RT at various N/P ratios (0.5, 1, 2, 3, and 5). The complexed samples and equivalent amounts of free siRNA with 1X loading dye (Biosesang, Korea) were added in individual wells in a 2% agarose gel (with 0.1  $\mu\text{g}/\text{mL}$  EtBr) casted in 1X TAE buffer. The samples were resolved for 40 min in 0.5X TAE running buffer at 100 V, and images were captured under ultraviolet illumination. For RNase protection assay, VBPEA/siRNA (N/P 20) polyplexes and free siRNA were incubated with RNase (1  $\mu\text{g}/\mu\text{L}$ ) at

37°C. After 30 min, RNase was inactivated by adding 5  $\mu$ L EDTA (100 mM) at 70°C for 10 min and incubated for another 30 min at RT. Finally, the protected siRNA was released from the complexes with the addition of 5  $\mu$ L 1% sodium dodecyl sulfate (SDS) for 2 h and resolved on a 2% agarose gel (with 0.1  $\mu$ g/mL EtBr) in 0.5X TAE running buffer at 100 V for 40 min.

#### **4.3.4. Cell culture**

Low passage adenocarcinoma human alveolar basal epithelial (A549) cells were cultured in T-75 culture flasks (Nunc, Thermo Scientific) in 15 mL complete medium containing Roswell Park Memorial Institute (RPMI)-1640 (HyClone Laboratories, USA) supplemented with 10% heat-inactivated fetal bovine serum (FBS, HyClone Laboratories, USA) and 1% antibiotic cocktail of streptomycin and penicillin. Cells were maintained under standard culture conditions of 37°C and 5% CO<sub>2</sub> for 4 or 5 days, with the culture duration selected to maintain cells under exponential growth and reach ~80% confluency. Cells were then trypsinized, centrifuged at 1200 RPM for 5 min to pellet cells and counted using hemocytometer to seed the cells for experimental assays.

#### **4.3.5. Confocal microscopy**

TRITC (Molecular Probes, Invitrogen, Oregon, USA) (25  $\mu$ L, 1 mg/100  $\mu$ L in DMF) was added to VBPEA (1 mL, 10 mg/mL in H<sub>2</sub>O) to block ~1% of its total amines, and the mixture was then stirred overnight (VBPEA<sup>T</sup>). Unreacted TRITC was removed by washing with ethyl acetate (3 x 2 mL), which was then lyophilized and resuspended in water. A549 cells were seeded at a density of 3 x 10<sup>5</sup> cells/well in a cover glass bottom dish (SPL Lifesciences, Korea) and incubated for 24 h in humidified chamber. Cells were transfected with VBPEA<sup>T</sup>/siRNA complexes and further incubated for 3 h, 2 d, 3 d, 5 d, 6 d, and 7 d to study the degradation profile of VBPEA polyplexes. The transfected A549 cells with fluorescently labeled complexes were washed 3 times with 1X PBS and then fixed with 4% paraformaldehyde for 10 min at 4°C. DAPI was used to counter-stain the nuclear DNA of fixed cells, and images were procured using a Leica SP8 X STED super-resolution laser scanning confocal microscope to monitor fluorescently labeled VBPEA<sup>T</sup>/siRNA complexes inside the treated A549 cells.

#### **4.3.6. Cell viability assay**

Cytotoxicity of VBPEA/siRNA (N/P 20), PEA/siRNA (N/P 20) and PEI25k/siRNA (N/P 10) polyplexes at various siRNA concentrations (0, 50, 100, 150 pM) and after different incubation times (3 h, 2 d, 5 d, 7d) were measured by the reduction of a tetrazolium component (3-(4,5-dimethylthiazol-2-yl)-2,5-diphenyltetrazolium bromide, or MTT) (Sigma, St. Louis, Mo, USA) into insoluble purple colored formazan crystals by the mitochondria of the viable cells. Polyplex transfected A549 cells that had been incubated in a 24-well plate ( $10 \times 10^4$  initial cell density/well) for 48 h were then incubated with MTT reagent (0.5 mg/mL in 1X PBS) for 3 h, followed by the addition of DMSO (500  $\mu$ L) to solubilize the colored crystals, and absorbance was measured at 540 nm using a Sunrise<sup>TM</sup> TECAN ELISA reader (Grödig, Austria).

#### **4.3.7. Silencing of luciferase activity**

A549 cell were transfected with Lipofectamine<sup>TM</sup>/pGL3 complexes in serum-free medium. After 3 h, the medium was aspirated and VBPEA/siLuc or siScr and PEA/siLuc or siScr complexes (N/P 20) were added containing 50, 75, 100 and 150 pM siRNA concentrations. Cells were incubated for additional 3 h, after which medium was

replaced with complete medium containing 10% serum. Finally, 24 h later luciferase expression was measured by luciferase assay and normalized with the protein concentration in the cell extract. The luciferase silencing efficiency was calculated as the relative percentage of luciferase activity to the control cells without siRNA treatment.

#### **4.3.8. GFP silencing efficiency by VBPEA**

A549 cells at 70% confluency ( $3 \times 10^5$  initial cell density/well) in a 6-well plate were transfected with Lipofectamine/tGFP (1  $\mu$ g) complex in serum-free medium according to the manufacturer's protocol (Invitrogen, Oregon, USA). After 3 hours, the medium was replaced with fresh serum-free RPMI-1640 medium with the VBPEA/siGFP complex (N/P 20) containing 100 pM of siRNA. The silencing efficiency was then compared with that of PEA/siGFP (N/P 20) and PEI25k/siGFP (N/P 10) mediated silencing. After 3 hours of incubation, the medium was again replaced with 10% serum-containing medium. After an additional 48 h, the silencing efficiency was measured using flow cytometry (BD Biosciences, San Jose, CA, USA). The percentage of GFP silencing in the cells treated with VBPEA/siGFP complexes

was calculated after normalizing the results with respective mock-treated cells and then compared to the silencing of the VBPEA/siScr-treated group. Nonspecific scrambled siRNA (siScr) and GFP siRNA (siGFP) (Table 4.1) were purchased from Genolution Pharmaceuticals, Inc. (Seoul, South Korea).

## **4.4 Results**

### **4.4.1. VBPEA represents an efficient siRNA transporter**

Electrophoretic mobility shift assay demonstrated VBPEA's high complexation ability with siRNA and its ability to protect siRNA against intracellular RNase degradation (Figure 4.2a, b). Dynamic light scattering spectrophotometry (DLS) and EF-TEM images showed nanosized VBPEA/siRNA polyplexes suitable for cellular uptake. A decreasing trend in VBPEA/siRNA polyplex size (from 180 to 110 nm) and zeta potential (from +44 to +38 mV) suggest stronger condensation of VBPEA with siRNA with increasing N/P ratios (Figure 4.2c). EF-TEM images showed a uniform particle size distribution (< 100 nm)

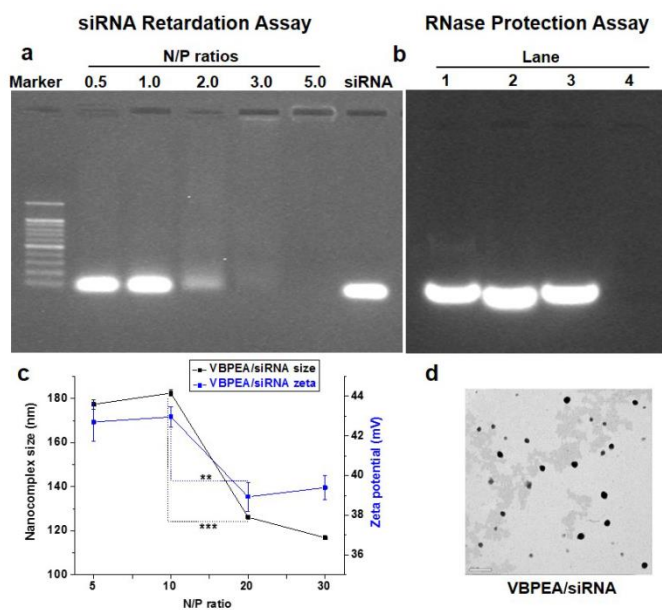


Figure 4.2. Physicochemical characterization of VBPEA/siRNA complexes. (a) Gel electrophoresis of VBPEA/siRNA (0.1  $\mu\text{g}$ ) complexes at various N/P ratios (0.5, 1, 2, 3, and 5) shows complete siRNA retardation at an N/P ratio of 3. (b) RNase protection and release assay. Complexed siRNA with VBPEA (N/P 20) was released using 1% SDS: (Lane 1) VBPEA/siRNA complexes without RNase; (Lane 2) VBPEA/siRNA complexes with RNase (1  $\mu\text{g}/\mu\text{L}$ ) demonstrates the protection of the siRNA; (Lane 3) free siRNA without RNase; (Lane 4) free siRNA with RNase (1  $\mu\text{g}/\mu\text{L}$ ) shows its complete degradation. (c) Particle size and zeta potential of VBPEA/siRNA complexes at various N/P ratios (5, 10, 20, and 30) shows its size  $\sim 110$  nm and zeta potential +38 mV ( $n = 3$ , error bar represents SD) (\*\* $P < 0.01$ ; \*\*\* $P < 0.001$ , one-way ANOVA). (d) EF-TEM image of VBPEA/siRNA (N/P 20) complexes shows its size  $\sim 100$  nm (scale bar: 200 nm).

without aggregation (Figure 4.2d), suggesting their efficient cellular uptake.

#### **4.4.2. Enhanced in vitro cell viability and degradation profile of VBPEA/siRNA complexes**

The lower surface charge and non-aggregation of the VBPEA polyplexes (Figure 4.2c, d) does not disrupt the integrity of the cell membrane surface [123, 145] which results in higher cell viability of VBPEA/siRNA complexes (> 98%) in comparison to PEA/siRNA (~85-95%) and PEI25k/siRNA (~60%) complexes (Figure 4.3) in A549 cells. In addition, the presence of degradable ester linkages in VBPEA backbone (Figure 2.1) ensured a gradual disappearance of VBPEA after 3 h, 2, 3, 5, 6, and 7 days of transfection (Figure 4.4) by hydrolyzing into smaller degradation products that can be exocytosed [146]. Therefore, the occurrence of vesicles was observed to increase with time (maximum on day 5). This further increases the cell viability of VBPEA complexes (Figure 4.5) and makes VBPEA innocuous for cellular uptake.

#### **4.4.3. GFP silencing efficiency of VBPEA/siGFP complexes**

The gene silencing efficiency of vectors was analyzed by suppressing transgenic GFP expression in A549 cells. VBPEA/siGFP exhibited 67% GFP silencing in comparison to 41% by PEA/siGFP, 32% by PEI25k/siGFP and negligible by naked siGFP and complexes with non-specific scrambled siRNA (siScr) (Figure 4.6).

#### **4.4.4. Luciferase silencing efficiency of VBPEA/siLuc complexes**

Luciferase expression was silenced with luciferase siRNA (siLuc). VBPEA/siLuc showed an increased silencing efficiency reaching upto 94% in comparison to PEA/siLuc. The silencing activity becomes stable after 100 pM of siRNA concentration. As expected, nonspecific scrambled siRNA (siScr) and naked siLuc exhibited negligible silencing (Figure 4.7). Cell viability assay verifies that the improved VBPEA-mediated gene silencing was not affected by cellular cytotoxicity (Figure 4.3). The results reflect the potential of VBPEA to silence VB<sub>6</sub> dependent enzymes which are involved in cancer cell proliferation as an anticancer therapeutic strategy.

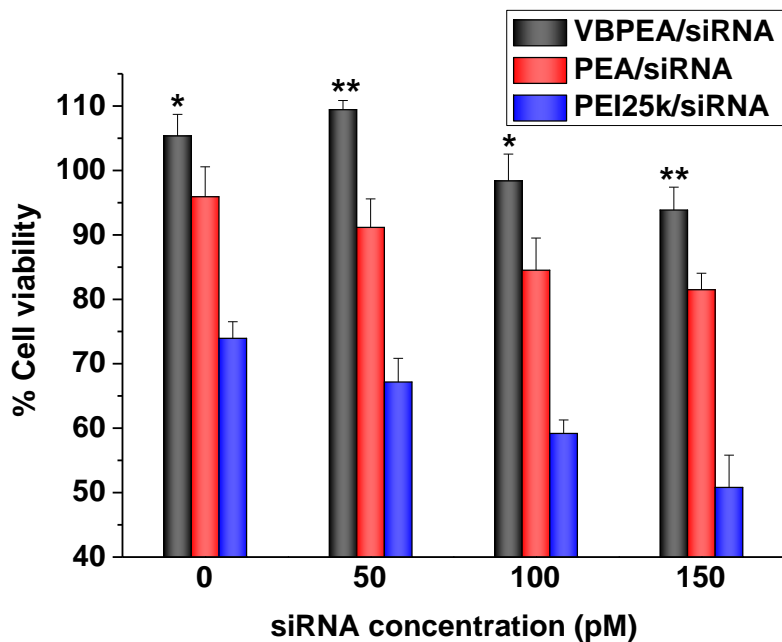


Figure 4.3. Cytotoxicity of VBPEA/siRNA complexes at various siRNA concentrations (0, 50, 100, 150 pM) show no cytotoxicity. (n = 3, error bar represents SD) (\*P < 0.05; \*\*P < 0.01, one-way ANOVA).

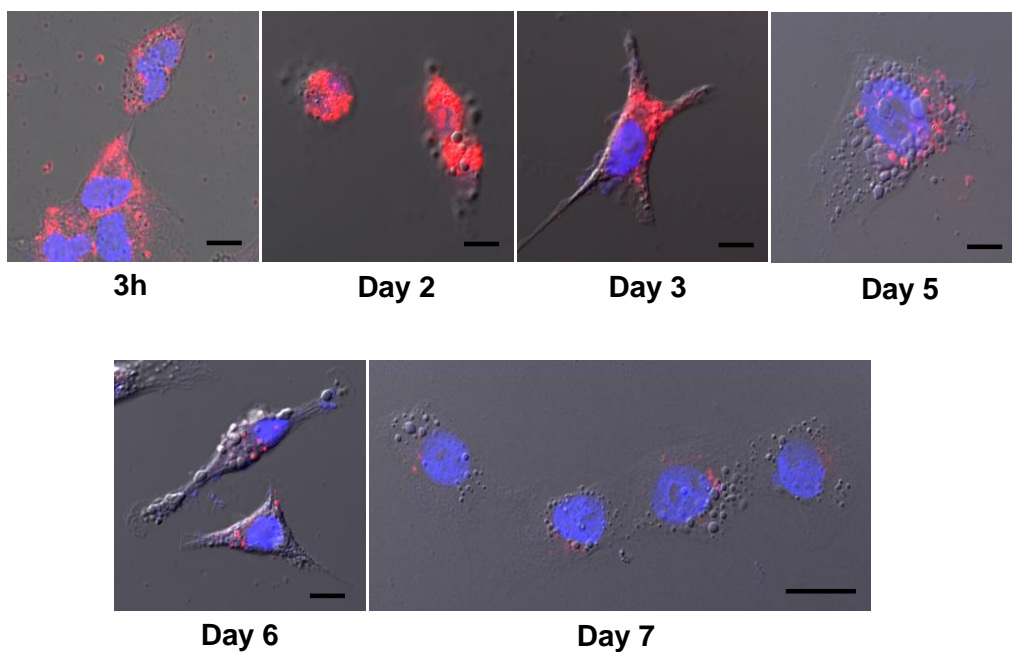


Figure 4.4. Study of VBPEA<sup>T</sup>/siRNA nanoplex uptake and degradation in A549 cells. Confocal microscopic images of A549 cells with DAPI nuclear staining (blue), observed up to 7 days following transfection with TRITC-labeled VBPEA<sup>T</sup> (red). VBPEA<sup>T</sup> after cellular uptake (3 h) (scale bar: 10  $\mu\text{m}$ ) is gradually degraded up to day 7 (scale bar: 20  $\mu\text{m}$ ), and the occurrence of vesicular structures represents the increased exocytosis of fragmented VBPEA<sup>T</sup>.

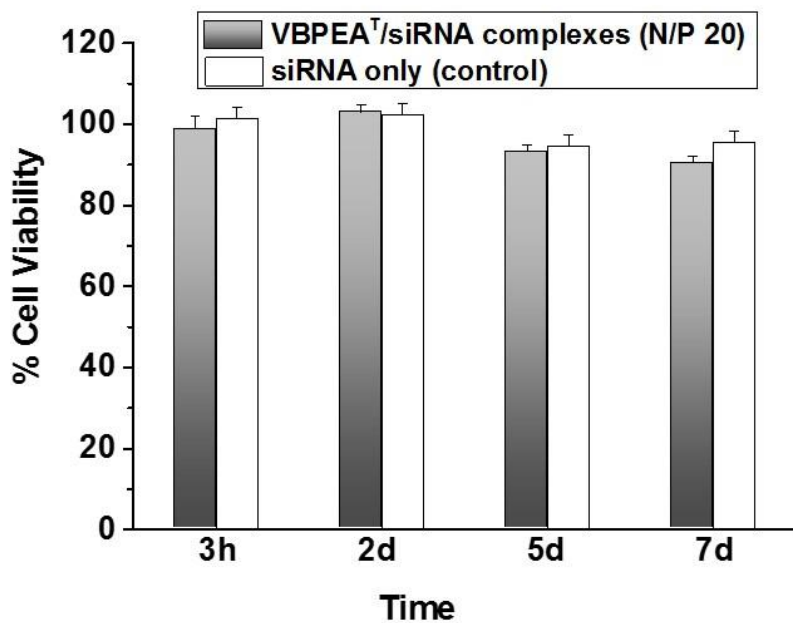


Figure 4.5. Cytotoxicity measurements of VBPEAT/siRNA (N/P 20) complexes by MTT assay after 3 h, 2d, 5d, and 7d of transfection in A549 cells show no cytotoxic effects. Statistical significance was determined using one-way ANOVA (n = 3, error bar represents SD).

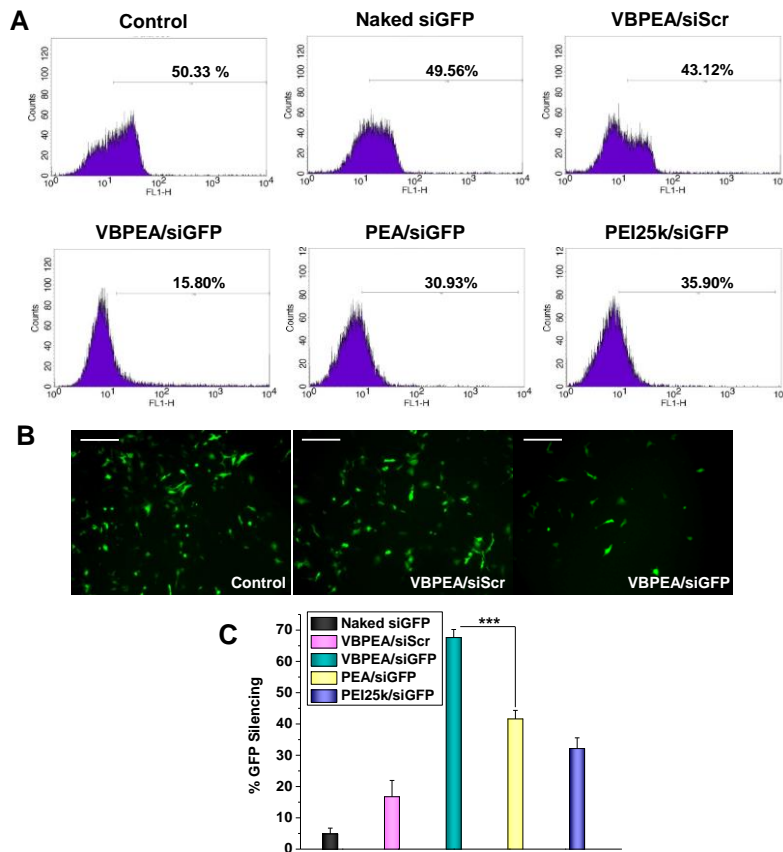


Figure 4.6. GFP silencing efficiency of VBPEA/siRNA complexes in A549 cells. (A) Pre-transfected GFP gene was silenced using siGFP (100 pM) complexed with VBPEA (N/P 20), and transgene expression was measured using FACS. (B) Corresponding transfection images were taken with a Nikon fluorescence microscope (scale bar: 500  $\mu$ m) to show maximum GFP suppression by VBPEA mediated siGFP delivery. (C) %GFP silencing was calculated in reference to the control cells without siGFP treatment, and maximum silencing was found to be mediated by VBPEA (67%) (n = 3, error bar represents SD) (\*P < 0.05; \*\*P < 0.01, one-way ANOVA).

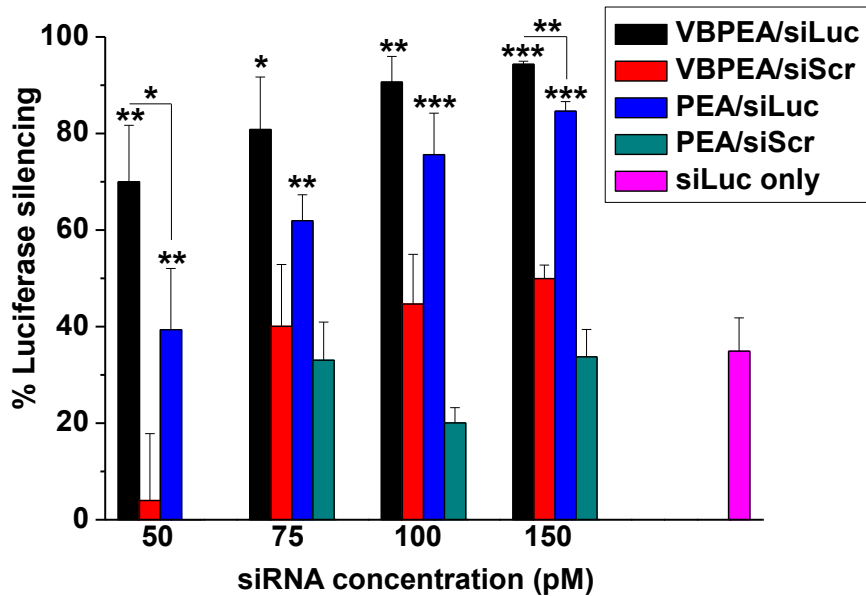


Figure 4.7. Silencing efficacy of VBPEA/siLuc and PEA/siLuc complexes in A549 cells compared to the respective scrambled siRNA (siScr) group (n = 3, error bar represents SD), (\*p < 0.05; \*\*p < 0.01, \*\*\*p < 0.001, one-way ANOVA).

## **4.5 Discussion**

VBPEA resulted not only in ~100 nm size of compact nanoplexes after complexation with siRNA, but also demonstrated to protect the complexed siRNA against nuclease degradation in the biological milieu. VBPEA/siRNA complexes showed high cell viability due to the presence of ester linkages in the polymer backbone. This was responsible for its gradual degradation and subsequent exocytosis by hydrolyzing into respective acid and alcohol degradation products of smaller molecular weights. Therefore, a higher silencing efficiency of VBPEA over PEA and PEI25k nanoplexes was achieved in cancer cells that showed the potential of VBPEA gene transporter for its use in cancer gene therapy.

## **4.6 Conclusion**

RNA interference through siRNA, shRNA, miRNA has contributed to the better understanding of neoplasia and proposes a great promise for anti-cancer therapeutics. A long term accumulation of genetic and epigenetic aberrations take the form of cancer. There is not one reason

for the cause of cancer and creates heterogeneity among patients. Therefore, there are different responses to the standard therapeutic approaches. It necessitates for analyzing molecular profiles of individual cancer patients and to develop a personalized therapy programs. This therapeutic approach requires specificity and adaptability to the particular patient which could be rendered by the RNAi technique. To imply the RNAi technology against cancer, the limitations of target selection, delivery agent, and off-target effects need to be considered. However, novel RNAi and delivery vectors with the conjugated vitamin B6 as a targeting ligand may solve the problem and hopefully help in the development of effective anti-cancer therapy.

# CHAPTER 5

## *Nucleotide Biosynthesis Arrest by Silencing SHMT1 Function*

---

### 5.1 Introduction

Serine hydroxymethyltransferase (SHMT) is one of the components of a multi-enzyme complex involved in the *de novo* thymidylate biosynthesis pathway that catalyzes a reaction to generate one-carbon supply for the downstream synthesis of thymidylate, purine and methionine [147]. During cell proliferation, SHMT isoforms cytoplasmic SHMT1 & mitochondrial SHMT2 $\alpha$  are found in high concentrations due to their active participation in DNA biosynthesis [148] performing two major functions. First, it catalyzes the reversible conversion of serine to glycine by transferring serine-carbon to tetrahydrofolate (THF) yielding methylene-THF, the one-carbon donor

which methylates dUMP to dTMP for the synthesis of thymine nucleotides [147, 149]. Second, it serves as a scaffold protein essential for multi-enzyme complex formation [148]. This metabolic complex associates with the nuclear lamina and is enriched at sites of DNA replication initiation during the S and G2/M phases of cell cycle [148] (Figure 5.1A, B). Due to its pivotal role in the *de novo* thymidylate biosynthesis, the only cellular pathway for thymine synthesis [149], SHMT expression becomes a rate limiting factor [148]. Therefore, SHMT activity is correlated with an increased demand for DNA biosynthesis and is evidenced in fast proliferating tumor cells to preferentially channel serine for rapid DNA duplication [133, 150, 151]. Alternatively, the abnormal SHMT overexpression may influence the process of carcinogenesis in terms of both the development and genesis of tumor. Consequently, the central role of SHMT in nucleotide biosynthesis makes SHMT an attractive target [151], whereby reducing its activity could cease the DNA synthesis machinery of cancer cells. Moreover, cancer cells have greater requirements for nucleotides and, therefore, are more sensitive than normal cells towards the inhibition of nucleotide biosynthesis [149]. Although SHMT2 found to be

overexpressed in certain cancer cell lines and silencing of this isoform slows down proliferation to some extent [152], the effect of SHMT1 silencing on cancer progression has yet not been sufficiently explored.

Among the three enzymes of the thymidylate synthase cycle, SHMT1 is the only enzyme that remains uninvestigated as a target for chemotherapy [153]. The other two enzymes, thymidylate synthase (TYMS) and dihydrofolate reductase (DHFR) are targeted by clinically practiced chemotherapeutic drugs [149, 154-156]. However, the emergence of drug resistance is a major problem for the prolonged use of these drugs [157, 158], making it necessary for an alternative approach to target SHMT1. In this study, we propose a siRNA technology based SHMT1 silencing-mediated cancer therapy with presumably no chance for the development of drug resistance. However, in spite of specificity, potency and versatility to silence the expression of a desired gene [159], the high therapeutic potential of siRNA approach to the treatment of severe and chronic diseases has not yet been successfully translated clinically, owing to major limitations such as difficult cellular uptake, low transfection capability, short half-life

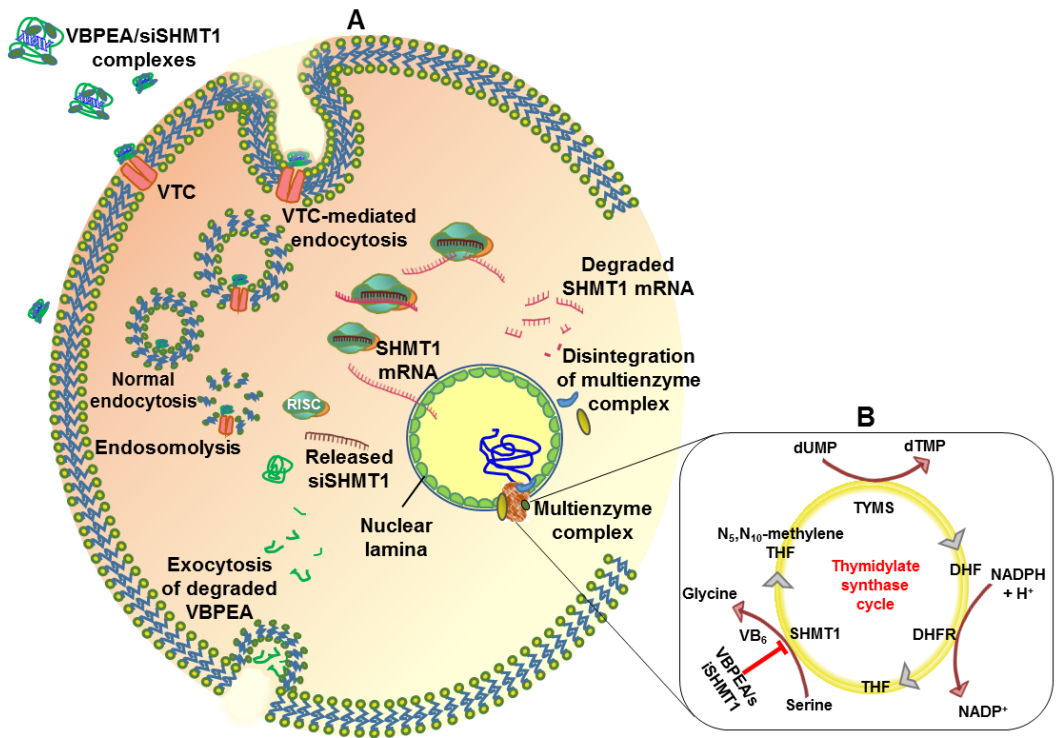


Figure 5.1. Schematic illustration of silencing events after the delivery of VBPEA-mediated siSHMT1 (A) VBPEA-mediated SHMT1 silencing, (B) interruption of thymidylate synthase cycle. Figures do not represent the scale of the molecules.

and insufficient bioavailability [160]. Thus, an efficient transporter for SHMT1 siRNA (siSHMT1) delivery is a vital requisite between siRNA technology and its therapeutic applications.

Vitamin B<sub>6</sub>-coupled poly(ester amine) (VBPEA) recently synthesized in our laboratory (Figure 2.1) shows high transfection activity in cancer cells, due to VB<sub>6</sub> coupling that utilizes the VB<sub>6</sub> transporting membrane carrier (VTC)-mediated uptake mechanism, leading to enhanced vector transport [146, 161, 162].

Interestingly, SHMT1 is one of the VB<sub>6</sub>-dependent enzymes that become functional when the VB<sub>6</sub> cofactor is bound to its active site [151, 163]. Due to its involvement in various cellular metabolic processes, VB<sub>6</sub> availability is expected to augment the process of carcinogenesis by keeping the DNA synthesis machinery functional through SHMT1 catalyzed reactions [164]. Consequently, VB<sub>6</sub> uptake from the neighboring tissues increases to support tumor growth [132, 133]. In short, the increased DNA requirement enhances SHMT1 activity [151, 165] which enforces increased VB<sub>6</sub> uptake in cancer cells than normal cells [146, 151, 164] and therefore a vector coupled to VB<sub>6</sub>

may experience enhanced cellular uptake [146, 166, 167]. Hence, we hypothesize that due to the increased membrane transport efficiency of VBPEA [146], the complexed siSHMT1 could be trailed along with the vector inside the cell. Accordingly, we investigated the efficacy of VBPEA/siSHMT1 system to down regulate the overexpressed SHMT1 gene responsible for rapid DNA synthesis in cancer cells both *in vitro* and in xenograft mice. Because SHMT1 controls a fundamental rate limiting step in DNA synthesis, silencing its activity is anticipated to result in decreased cell proliferation and tumor growth inhibition. Therefore, the impact of SHMT1 knockdown on the integrity of multi-enzyme complex, cell cycle and DNA synthesis of cancer cells was assessed.

## **5.2 Literature Review**

Cancer being one of the most prevalent diseases of the world reflects disturbances of the basic rules of cell behavior in a multicellular organism. The body of an animal represents a society or ecosystem composed of individual cells which are reproducing by programmed cell division and well organized into collaborative tissues. The only

difference from ecological system is the lack of natural selection and competition where the basic rule is self-sacrifice as all the somatic cells are destined to die after propagating their clonal progeny. But in cancer selfish behavior of individual mutant cells within the population of somatic cells prosper at the expense of their neighbors leading to the destruction of the whole cellular society [168].

Cancer cells are neoplastic (uncontrolled proliferation) and malignant (invade and colonize surrounding tissues). A general concept is that a single cell mutation causes additional mutations on proliferation of the cell to result in a full blown tumor. The tumor cells may further metastasize giving rise to secondary tumors, difficult to eradicate surgically. Therefore, in order to devise rational ways to cure it, the understanding of the cancer cell's inner malfunctioning and intercommunication with other cells is necessary [169]. Neoplastic cell proliferation is often associated with a block in differentiation whereby the stem cells continue to divide which can be curbed by promoting cell differentiation. The tumor cells must cross the basal lamina to become malignant which can be obstructed by designing specific antibodies to

interfere its invasion. The characteristic of the cancer cells to easily mutate helps them to develop resistance to anticancer drugs. However, the DNA metabolism underlying such mutations can be selected for therapeutic attack which is the focus of discussion in this chapter.

The prevailing anticancer therapy includes surgical removal of the benign tumor if detected at an early stage, or destruction with toxic chemicals or radiation which are toxic to the normal cells as well. Moreover, eradication of every single cancer cell is very difficult. Hence, an alternative approach is in demand for cancer therapy. Fire and Mello who received Noble Prize for discovering RNA interference (RNAi) in 1998, have opened an era for increased understanding of the molecular mechanisms involved in the development of cancer and devising probable therapeutics against cancer by performing targeted gene silencing [136]. RNAi is a post-transcriptional process whereby the transcribed mRNA is degraded by a double stranded RNA molecule to regulate the gene expression [170]. Since the remarkable breakthrough, RNAi therapeutics has gained considerable advancements against various diseases including viral infections and

cancer [171].

## **5.2.1. Cancer cell growth and proliferation**

### ***5.2.1.1. Key behavior of cancer cells in general***

1. Self-sufficient – the cancer cells reproduce in defiance to normal restraints because they become self-supportive for the supply of nutrients and oxygen.
2. Insensitive to anti-proliferative extracellular signals –The normal cells that stop dividing due to contact inhibition, the abnormal cells continue dividing to give rise to neoplasm – a relentlessly growing mass of abnormal cells, which become impervious to anti-proliferative signals.
3. Less prone to apoptosis – Due to development of certain mutations cancer cells escape the programmed cell death mechanism and keep dividing to form a tumor.
4. Defective in intracellular control mechanisms (abnormal proliferation) - The cancer cells in contrast to normal cells

which are under strong vigilance of cell cycle check points, defy and surpass the cell cycle control system.

5. Induce help from normal stromal cells – To compensate the increased demand of nutrition, cancer cells drive it from their neighboring stromal cells.
6. Induce angiogenesis – Angiogenesis is a key feature of tumor growth and proliferation to support their need for blood supply and exchange of gases in deep seated compact cell mass.
7. Escape from their home tissue – Tumor becomes seriously dangerous when it becomes malignant, that is, capable of invading the surrounding tissues usually far away from the original tissue. Tumor cells break loose, enter the blood stream and form secondary tumors at other sites in the body (Figure 5.2).
8. Genetically unstable – Cancer is caused by mutations that cause cells not only to grow indefinitely but also uncontrollably and invasively. They are genetically unstable due to establishment



Figure 5.2. Metastasis shown in the bone marrow from carcinoma of prostate gland. Adopted from Ref [140].

of multiple mutations which may be developed as an effect of mutagens.

9. Produce telomerase - Telomeres are specialized sequence of hundreds to thousands of tandem repeats at the ends of eukaryotic chromosomes which in normal somatic cells are lost (50-200 nucleotides) per cell division. DNA polymerase is unable to replicate these lost nucleotides. This loss of genetic material is what leads to aging and apoptosis (programed cell death). Telomerase is a ribonucleoprotein (enzyme) that synthesizes telomeric DNA which prevents the loss in telomere length. Although telomerase is suppressed in normal somatic cells, it is activated in cancer cells allowing the cells to replicate indefinitely as an immortal cell line [172].

#### ***5.2.1.2. Normal cell division with various check points***

The cell cycle control system is a set of coordinating proteins functioning cyclically which regulates the cell division at specific check points (Figure 5.3). These proteins have been conserved over a billion years through evolution. The two basic components of this system are: activating proteins called cyclins and cyclin dependent

kinases (Cdk), the complexes of which together regulate the normal cell cycle [173].

#### ***5.2.1.3. Tumor proliferation and uncontrolled division***

When the cell crosses all the cell cycle barriers it leads to duplication of cell. Cancer cells due to mutation keeps the cell cycle proteins in their active state to continuously replicate the DNA and divide the cell in uncontrolled fashion. The localized tumor mass is called benign which can be surgically removed but when it takes the form of metastases it migrates and invades other tissues to colonize in various body parts impossible to surgical removal and usually fatal (Figure 5.4 & 5.5).

#### ***5.2.1.4. Most cancers derive from a single abnormal cell***

A single cell that has undergone some heritable changes enables it to outgrow its neighbors. A single mutation is not sufficient to convert a healthy cell into a cancer cell. The genesis of a cancer is evidenced by the fact that it requires several independent mutational accidents to occur together in one cell. These events may then cause the establishment of cancer which further proliferate and invade the neighboring tissues (Figure 5.6).

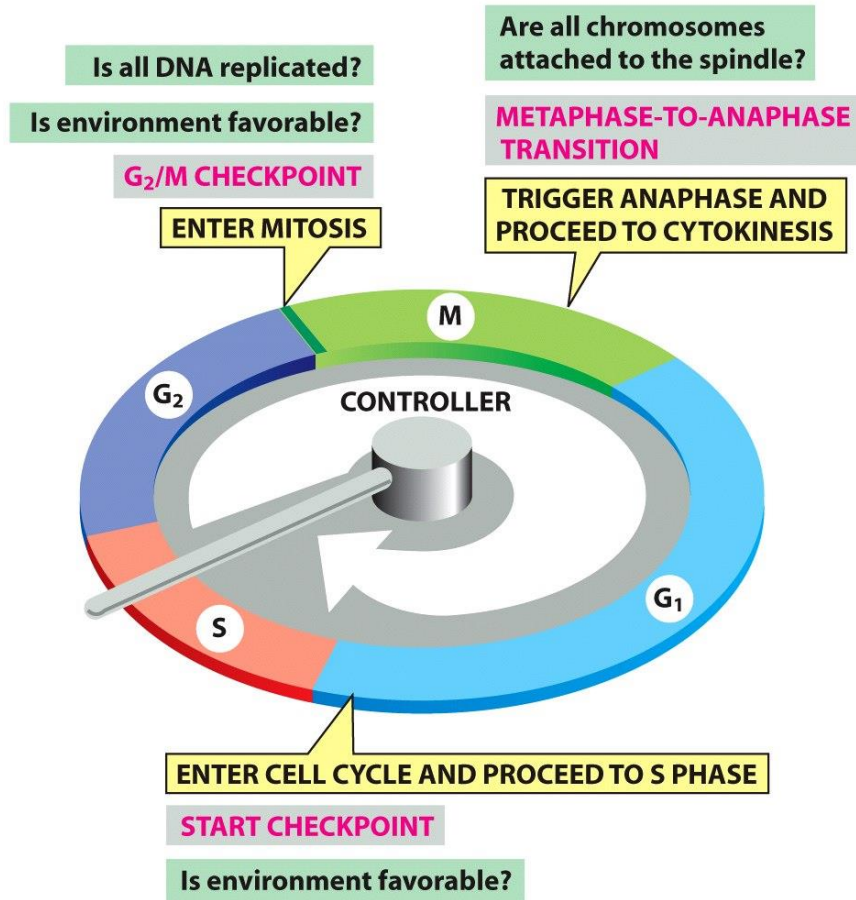


Figure 5.3. Checkpoints and inputs of regulatory information to the cell cycle control system. Adopted from Ref [140].

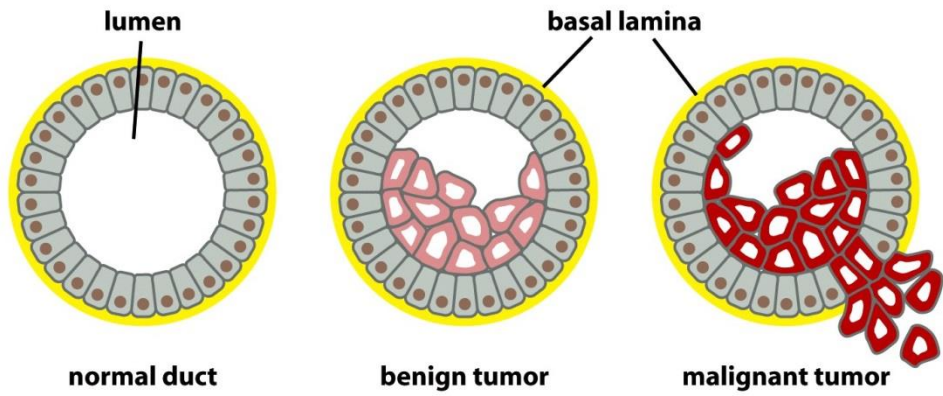


Figure 5.4. Progression of benign tumor (adenoma) to malignant tumor (adenocarcinoma). Adopted from Ref [140].

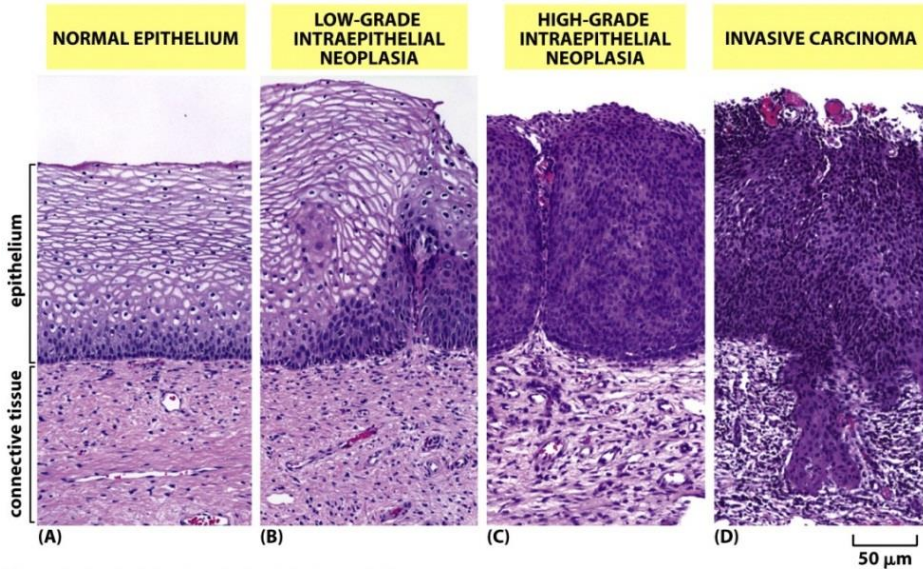


Figure 5.5. The stages of progression in cancer development of epithelium of uterine cervix. Adopted from Ref [140].

#### ***5.2.1.5. Cancer develop in slow stages from mildly aberrant***

Cancer begins as a disorder characterized by nonlethal overproduction of cells which continues for several years before changing into a much more rapid cell proliferation and illness progression that usually leads to death of the patient in few months. The descendants of a single mutant ancestor evolve through successive cycles of mutation and natural selection. The later rapidly dividing cells are characterized with the presence of large nucleus and comparatively less cytoplasm due to the rapid division of cells without paying attention to cell growth as visible in figure 5.7c.

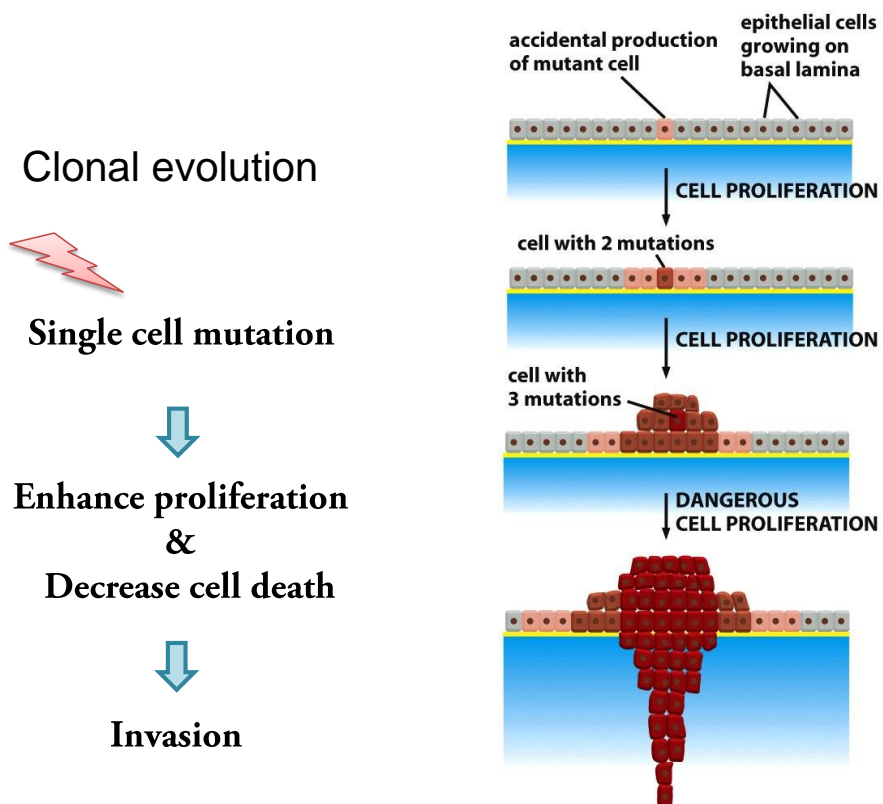


Figure 5.6. A single mutation is not enough to cause cancer. Adopted from Ref [140].

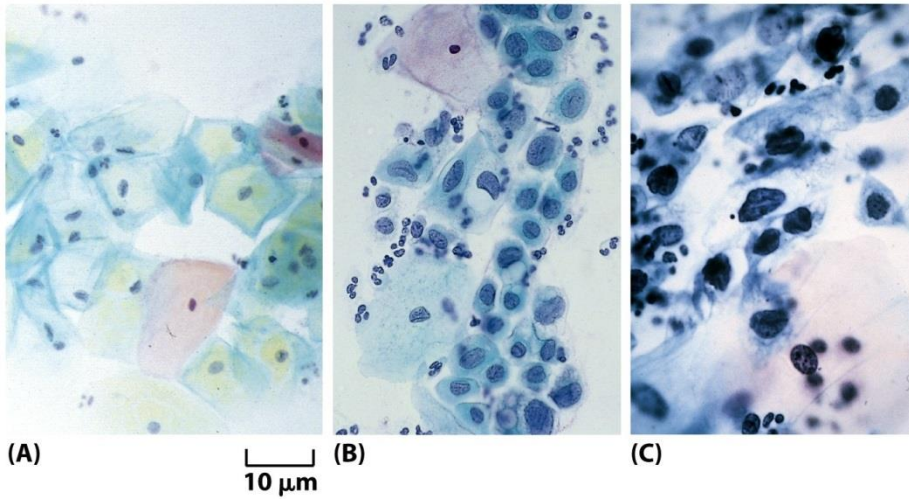


Figure 5.7. Photograph of cells collected from the surface of uterine cervix. Adopted from Ref [140].

## **5.2.2. DNA synthesis**

### ***5.2.2.1. DNA synthesis activity increases during cancer development***

DNA replication, together with repair mechanisms and cell cycle control, are the most important cellular processes necessary to maintain correct transfer of genetic information to the progeny [174]. The cell divides when DNA is completely replicated. Any error during DNA synthesis is proofread by DNA polymerase to replace with the correct nucleotide otherwise in the next cell division it may become a permanent mutation which is read as a normal nucleotide by cellular machinery. These mutated cells lead to aberrant cell proliferation with increased DNA synthesis activity during the cancer advancement [175, 176].

DNA replication means polymerization of pre-synthesized nucleotides which is composed of purines and pyrimidines. Both the purines and pyrimidines have some common points in their biosynthetic pathways. The basic difference is in their size due to ring system and therefore their N and C donors differ slightly. The smaller pyrimidine ring has

two fewer nitrogens, and one less carbon than purine ring. A purine is synthesized from 3 amino acids, two formyl-THFs, and one CO<sub>2</sub> whereas a pyrimidine requires two amino acids and CO<sub>2</sub>. For these extra N's and C's the purine ring needs twice as many glutamines and depends on 2 formyl-THFs. Thus, purine assembly relies on multiple amino acids (Figure 5.8).

#### ***5.2.2.2. Regeneration of N<sup>5</sup>,N<sup>10</sup> Methylene tetrahydrofolate - key to DNA synthesis***

The thymidylate synthase cycle shown in figure 5.9 is central to DNA replication as it recycles the folate involved in DNA synthesis. Thymidylate is a key precursor of DNA which is synthesized by the tetrahydrofolate-dependent methylation of deoxyuridylate catalyzed by thymidylate synthase (TYMS) [177]. The methyl group (recall that thymine is 5-methyl uracil) is donated to dUMP by N<sup>5</sup>,N<sup>10</sup>-methylene THF. The produced dTMP is quickly consumed by cancer cells for direct incorporation during DNA replication. Thymidylate synthase shows its unique property by converting THF to dihydrofolate (DHF), the only reaction that yields DHF from THF. In order to continue the

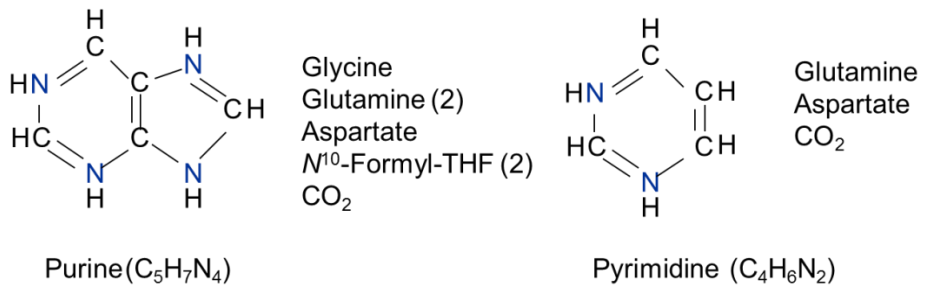


Figure 5.8. The basic structure of nitrogenous bases: purines and pyrimidines and their synthetic requirements.

thymidylate synthase reaction, THF must be regenerated from DHF which is accomplished through dihydrofolate reductase (DHFR). THF is then converted to  $N^5,N^{10}$ -THF via serine hydroxymethyl transferase (SHMT) enzyme by methyl transfer from serine. Serine is reduced to glycine which a precursor for purine synthesis as mentioned in previous section. All the three enzymes TYMS, DHFR and SHMT function in cyclic coordination to generate the precursors of nucleotides displaying the central hub for DNA synthesis.

#### ***5.2.2.3. Role of Serine hydroxymethyltransferase (SHMT)***

Folate dependent one carbon metabolism is essential for the biosynthesis of numerous cellular constituents required for cell growth, and serine hydroxymethyltransferase (SHMT) is central to this process. Folate coenzymes function as donor and acceptor of one carbon unit and the  $\beta$ -carbon of serine is its major source. SHMT is a highly conserved enzyme that catalyzes the reversible conversion of serine and THF into glycine and 5,10-methylene THF, respectively (Figure 5.10). During the S-phase of cell cycle when the cells prepare to proliferate, incorporation of  $\beta$ -carbon of serine into DNA and SHMT activity are

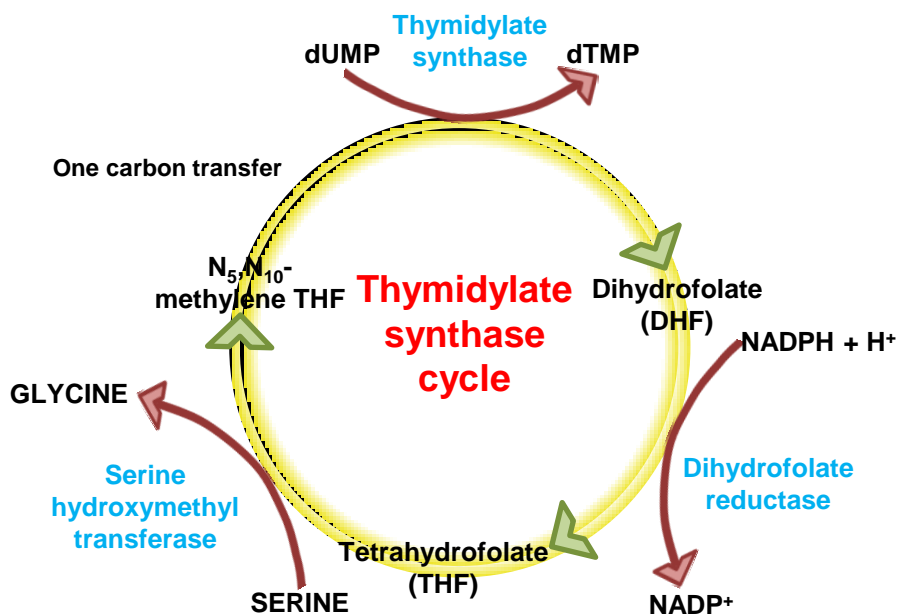


Figure 5.9. Thymidylate synthase cycle displaying the central hub for DNA synthesis by the action of three enzymes TYMS, DHFR and SHMT.

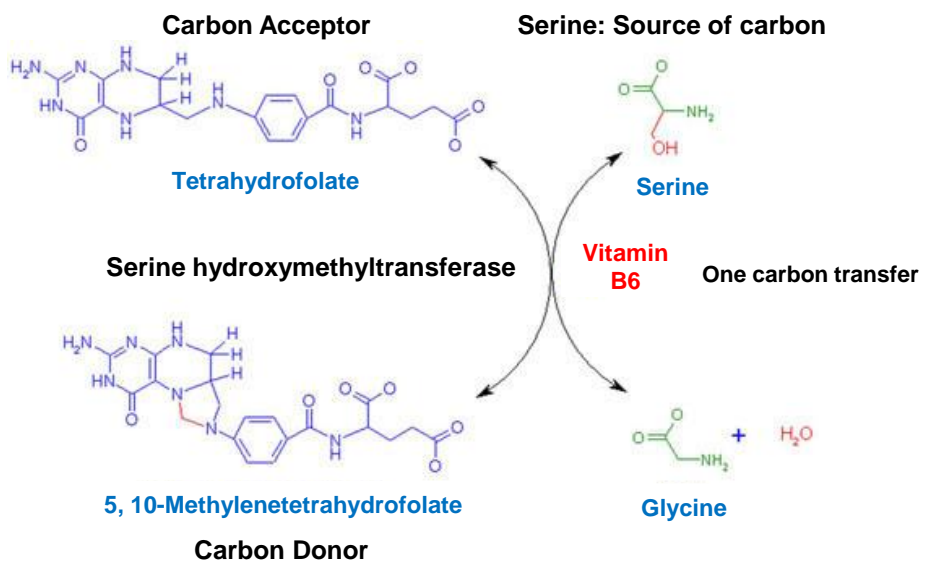


Figure 5.10. The transfer of hydroxyl methyl group of serine to THF to form glycine and 5,10-THF catalyzed by SHMT.

both increased [178].

### **5.2.3. Target proteins for retarding DNA biosynthesis**

DNA is replicated during S-phase of the cell cycle one for each daughter cell. If the DNA replication machinery which involves DNA polymerase and four deoxynucleotides faces incapability in duplicating the DNA, the cell does not divide. Since SHMT, a component enzyme of thymidylate synthase cycle, along with the TYMS and DHFR are involved in DNA synthesis, they may function as the potential anticancer targets.

There could be various technologies and strategies applied to cease the growth and proliferation of cancer cells by interfering their DNA synthesis mechanism. Chemotherapy drugs are used to interfere with thymidylate synthase reaction to decrease dTMP production or dihydrofolate reductase step can be stopped competitively by DHF analogs. Fluorodeoxyuridylate an irreversible inhibitor of TYMS also affects rapidly growing normal cells (hair follicles, bone marrow, immune system, intestinal mucosa). Anti-folates such as aminopterin,

methotrexate, trimethoprim are clinically used as inhibitors for DNA synthesis. But a common problem encountered by using these inhibitors is the emergence of drug resistance because the enhanced mutability of cancer cells help them evade destruction by anticancer drugs [179]. Several researches have been conducted to inhibit TYMS and DHFR but little has been focused on SHMT. Elevated SHMT activity has been shown to be coupled with the increased demand for DNA synthesis in rapidly proliferating cells. It is also found that complete knockout of SHMT leads to glycine auxotrophy. Therefore the central role of SHMT in nucleotide biosynthesis makes it a suitable anticancer target [179, 180].

Another strategy to control the proliferation of cancer cells is the use of RNAi technology (discussed in later section) which will selectively silence the SHMT to shut down the whole DNA synthesis machinery in cancer cells. However, the immense potential of RNAi in anti-cancer therapy is impeded by the non-availability of a suitable delivery agent, off-target effects and induction of innate immune response. These obstacles can be overcome by using nanoparticles of the size below 100

nm which can effectively deliver the siRNA via endosome mediated cellular uptake. The RNAi specificity not only depends upon the sequence homology between siRNA and target mRNA, but also on the homology of 5' end of guide strand which is the major determinant of off-target silencing. Hence, to avoid cross homology of 5' end, siRNA design should be thoroughly considered.

### **5.3 Materials and Methods**

#### **5.3.1. Cell culture and animals**

Low passage adenocarcinoma human alveolar basal epithelial (A549) cells were cultured in T-75 culture flasks (Nunc, Thermo Scientific) in 15 mL complete medium containing Roswell Park Memorial Institute (RPMI)-1640 (HyClone Laboratories, USA) supplemented with 10% heat-inactivated fetal bovine serum (FBS, HyClone Laboratories, USA) and 1% antibiotic cocktail of streptomycin and penicillin. Cells were maintained under standard culture conditions of 37°C and 5% CO<sub>2</sub> for 4 or 5 days, with the culture duration selected to maintain cells under exponential growth and reach ~80% confluency. Cells were then

trypsinized, centrifuged at 1200 RPM for 5 min to pellet cells and counted using hemocytometer to seed the cells for experimental assays.

For animal study four weeks old nude Balb/c mice were obtained from Orient Bio Inc. (Republic of Korea) and kept in a laboratory animal facility maintained at  $23 \pm 2^\circ\text{C}$  and  $50 \pm 20\%$  relative humidity under a 12 h light/dark cycle. All experimental protocols were reviewed and approved by the Animal Care and Use Committee at Seoul National University (SNU-120409-3).

### **5.3.2. Transfection for RNAi silencing of SHMT1**

A549 cells were cultured according to standard techniques as described above. Cells were seeded at a density of  $3 \times 10^5$  cells/well in a 6-well plate; and after 24 h (70% confluent) were transfected with VBPEA/siSHMT1 complexes. The SHMT1 siRNA (siSHMT1) (Sigma, St. Louis, MO, USA) was reconstituted in ultra-pure water (DNase/RNase free) and mixed with VBPEA at an N/P ratio of 20 to a final concentration of 100 pM of SHMT1 siRNA. After 30 min of incubation, A549 cells at ~70% confluency were transfected for 3 h in

serum-free medium. PEA (N/P 20) and PEI25k (N/P 10) were used as positive controls, whereas naked siSHMT1 and scrambled sequence (siScr) negative controls were used in all experiments. For assessment of SHMT1 knockdown, 24 h, 48 h, and 72 h post-transfection total RNA was isolated from cells using QuickGene RNA kit (Fujifilm, Tokyo, Japan), and real-time quantitative PCR (Q-PCR) was performed for SHMT1. Extracted RNA was reverse transcribed to cDNA using the Finnzymes cDNA synthesis kit with MMLV reverse transcriptase (Thermo Fisher Scientific Inc., Vantaa, Finland) and a random primer. The relative abundance of each mRNA species was quantified by qPCR using the hSHMT1 5'-GCTGGGCTACAAAATAGTCA-3' (forward) and 5'-AGGCAATAGAACAGGCTTC-3' (reverse) and hGAPDH 5'-GCCCAATACGACCAAATCC-3' (forward) and 5'-AGTCAGCCGCATCTTCTT-3' (reverse) specific primers from Cosmogenetech, Seoul, Korea. PCR mixtures were prepared with 2X Prime Q-Mastermix containing 2X SYBR<sup>®</sup> Green I (Genet Bio, Nonsan, Korea) according to the manufacturer's protocol. Q-PCR was performed in quadruplicate for each group, with GAPDH as reference gene, using a C1000 Thermal Cycler (BioRad, CA, USA) starting with

10 min of pre-incubation at 95°C followed by 50 amplification cycles with an annealing temperature at 61.3°C. The fluorescent signal intensities were measured and analyzed using C1000Manager Software (BioRad, Hercules, CA, USA).

### **5.3.3. Western blot analysis**

At 48 h post-transfection, cells were harvested and lysed with 1X RIPA lysis buffer (Millipore, MA, USA). A BCA protein assay kit (Thermo scientific, MA, USA) was used to measure the protein concentrations. Equal amounts of the protein (25 µg) from each sample were separated by a Novex NuPAGE 4-12% SDS-PAGE gel (Life technologies, CA, USA), transferred to nitrocellulose membrane using iBlot (Invitrogen, USA) and then non-specific binding sites were pre-blocked with 5% skim milk for 1 h at RT. The membrane was washed and probed with anti-SHMT1 (Santa Cruz Biotechnology Inc., CA, USA) and anti-β-actin (Abfrontier, Seoul, Korea) antibodies (1:500 dilution) overnight at 4°C. Then, the membrane was incubated with secondary antibody (1:1000 dilution) conjugated with HRP (Invitrogen, Carlsbad, CA, USA). Bands were captured using a ChemiDoc<sup>TM</sup> XRS<sup>+</sup> (Biorad, CA,

USA) imaging system. The band intensities were analyzed quantitatively using ImageJ software (NIH, USA) and plotted as the mean pixel value.

#### **5.3.4. Confocal microscopy**

TRITC (Molecular Probes, Invitrogen, Oregon, USA) (25  $\mu$ L, 1 mg/100  $\mu$ L in DMF) was added to VBPEA (1 mL, 10 mg/mL in H<sub>2</sub>O) to block ~1% of its total amines, and the mixture was then stirred overnight (VBPEA<sup>T</sup>). Unreacted TRITC was removed by washing with ethyl acetate (3 x 2 mL), which was then lyophilized and resuspended in water. A549 cells were seeded at a density of 3 x 10<sup>5</sup> cells/well in a cover glass bottom dish (SPL Lifesciences, Korea) and incubated for 24 h in humidified chamber. Cells were transfected with VBPEA<sup>T</sup>/siRNA complexes and further incubated for 120 min. The transfected A549 cells with fluorescently labeled complexes were washed 3 times with 1X PBS and then fixed with 4% paraformaldehyde for 10 min at 4°C. DAPI was used to counter-stain the nuclear DNA of fixed cells, and images were procured using a Carl Zeiss LSM 710 inverted laser scanning confocal microscope with ZEN software to monitor

fluorescently labeled VBPEA<sup>T</sup>/siRNA complexes inside the treated A549 cells.

### **5.3.5. Immunocytochemistry (ICC)**

A549 cells were seeded in an 8-well chamber slide (Lab Tek, Sigma, USA) at  $5 \times 10^4$  initial cell density/well and transfected with the VBPEA/siSHMT1 complexes together with the positive controls. After 48 h, cells were rinsed in 1X PBS and fixed with 4% paraformaldehyde at 37°C for 10 min and then with 1:1 (v/v) methanol:acetone solution at -20°C for an additional 10 min. After fixation, cells were washed twice with ice cold PBS and then permeabilized with ice-cold 0.2% Tween 20 in PBS for 10 min. Non-specific binding was blocked using 10% BSA in 1X PBS for 5 min at RT and then at 4°C for 1 h because cooling prevents endocytosis of antibodies. Cells were incubated with SHMT1 (100 µg/mL) (Santa Cruz Biotechnology Inc., CA, USA) and nuclear lamina specific LAP2 (20 µg/mL) (Millipore, CA, USA) antibodies diluted in 3% BSA at 4°C overnight. After washing several times with PBS, cells were incubated with fluorophore-conjugated secondary antibodies diluted in 3% BSA for 2 h at RT away from light.

Nuclei were stained with DAPI (0.1  $\mu\text{g}/\text{mL}$ ) for 10 min and mounted with Aqua poly/mount (Polysciences, PA, USA). The images were procured from confocal microscopy and the percentage of colocalization was evaluated using a custom designed MATLAB program.

### **5.3.6. EdU and WST proliferation assay**

A549 cells in an 8-well chamber slide were transfected and further grown in complete media containing EdU (5-ethynyl-2'-deoxyuridine, 10 $\mu\text{M}$ ) for 48 h. EdU is a nucleoside analog of thymidine that is incorporated into DNA during active DNA synthesis. The cells were then fixed in 4% paraformaldehyde and permeabilized with 0.5% Triton X-100. EdU detection is based on a copper catalyzed click reaction between an alkyne in EdU and an azide in the Alexa Fluor dye, and was conducted according to the manufacturer's protocol (Click-iT EdU imaging kit, Invitrogen). This is a direct qualitative method for the detection of cell's proliferative ability to evaluate anti-cancer activity. The images were captured using image restoration microscopy (DeltaVision RT, USA). WST colorimetric assay (EZ-Cytox Cell

Viability Assay Kit; Daeillab, Korea) quantified the proliferation ability of the transfected A549 cells in a 96-well plate (10000 initial cell density/well), which was proportional to the intensity of the water soluble formazan formed by the cleavage of tetrazolium salt by the mitochondria of the viable cells. After 0, 1, 2, 3, 4 days of treatment, WST assay was performed according to manufacturer's protocol, and the absorbance was measured at 450 nm using a Sunrise™ TECAN ELISA reader (Grödig, Austria).

#### **5.3.7. In vitro and in vivo TUNEL assay**

The transfected A549 cells in the 8-well chamber slide and the *in vivo* treated tumor sections were analyzed for apoptotic death using a DeadEnd colorimetric TUNEL (TdT mediated dUTP nick end labeling) system from Promega, USA, which end-labels the fragmented DNA of apoptotic cells. The paraffin embedded tissue sections were deparaffinized using xylene and rehydrated by sequentially immersing the slides into 100%, 95%, 85%, 70%, and 50% ethanol. The tissue sections and the cultured cells were fixed with 4% paraformaldehyde for 25 min at RT and washed twice with PBS. The tissue cells and

cultured cells were then permeabilized using proteinase K (20  $\mu\text{g}/\text{mL}$ ) and 0.2% Triton X-100 respectively, for 10 min at RT and rinsed twice with PBS. Biotinylated nucleotides were incorporated at the 3'-OH DNA ends using a recombinant terminal deoxynucleotidyl transferase, (rTdT) enzyme. Horseradish peroxidase-conjugated streptavidin was then bound to biotinylated nucleotides, which were detected with hydrogen peroxide and diaminobenzimide (DAB). The images were captured using a light microscope. Cells treated with DNase I to induce DNA strand breaks were used as a positive control.

#### **5.3.8. Annexin V-FITC Apoptosis Detection Assay**

The supernatant medium from the transfected cells and trypsinized adherent cells were collected and washed twice with cold 1X PBS at 2000 rpm for 5 min at RT. Cells were then washed with cold 1X binding buffer diluted in 1X PBS, and 1.8  $\mu\text{L}$  of FITC-conjugated Annexin V (200  $\mu\text{g}/\text{mL}$ ) (Komabiotech, Korea) which has high affinity for translocated membrane phospholipid phosphatidylserine (PS), was added and incubated for 15 min at RT in dark. The supernatant was removed by centrifugation and the cells were washed with cold 1X

binding buffer (0.5 mL). 10  $\mu$ L of propidium iodide (PI) (30  $\mu$ g/mL) which can bind with nucleic acids, was added and the cells were then analyzed using a BD FACSCalibur I equipped with dual laser (488 nm argon ion laser and 635 nm red diode laser) for the detection of multicolored fluorescent particles in the single sample. As the fluorescent particles intercept the laser light, the scattering of the fluorescent light is detected and the particle's fluorescent intensity is acquired by using BD FACStation software version 6.0.

#### **5.3.9. 4'-Deoxyripyridoxine inhibition study**

A549 cells were transfected with VBPEA/siSHMT1 and PEA/siSHMT1 complexes in the presence and absence of 4'-deoxyripyridoxine hydrochloride (structural analog of VB<sub>6</sub>) (10 mM) (Sigma, MO, USA) and were harvested 48 h later for western blot analysis as described above to evaluate their effect on the silencing efficiency of SHMT1. Confocal microscopy was also used to visualize the intracellular trafficking of the TRITC-labeled VBPEA<sup>T</sup>/siRNA complexes with and without 4'-deoxyripyridoxine. After 120 min of

transfection, the cells were processed for confocal microscopy as previously explained.

#### **5.3.10. Cell synchronization**

After 48 h of treatment, A549 cells in an 8-well chamber slide were provided with Ham's F-12 medium supplemented with 10% FBS, 1% antibiotics, and 2 mM thymidine and incubated for 8 h at 37°C in a CO<sub>2</sub> incubation chamber. The cells were washed twice with 1XPBS and Ham's F-12 medium supplemented with 10% FBS and 1% antibiotics was then added. Cells were incubated for an additional 12 h to progress through S phase.

#### **5.3.11. Cell cycle analysis**

Transfected A549 cells were harvested after 12 h, 24 h, and 72 h, and then washed, pelleted and resuspended in 0.5 mL PBS into a monodisperse cell suspension before fixing it with ice-cold 70% ethanol for 2 h at -20°C. Before the cell cycle analysis, cells were hydrolyzed and stained with PI (50 µg/mL) and RNase (1 µg/mL) in 1X PBS. Analysis was performed using single-color flow cytometry with a

BD FACSCanto II at an excitation wavelength of 488 nm (blue laser) and an emission wavelength range of 564 to 606 nm. Cell fluorescence was measured using a pulse-width area signal which discriminated G2/M cell singlets from G0/G1 cell doublets and gated out the latter. The data was analyzed using BD FACSDiva 5.0 software and the ModFit (Verity software) deconvolution algorithm was used to deconvolute the histograms.

#### **5.3.12. Fluorescence studies for genomic DNA quantification**

At 72 h post-transfection, A549 cells were harvested and genomic DNA was extracted using a PureLink genomic DNA kit (Invitrogen, CA, USA). The purity of the extracted DNA was analyzed by using NanoVue (GE Healthcare Life Sciences, USA) (Table 5.1). The total DNA contents of the samples were measured using a fluorescence based DNA quantitation kit from Sigma. Fluorescence based DNA measurement is highly sensitive and accurate method. The fluorescent dye, Hoechst 33258, bound primarily to AT sequences in the minor groove of double-stranded DNA excites at 360 nm and gives emission spectra at 460 nm. The emission spectra of samples with unknown

Table 5.1. Purity of genomic DNA from the transfected A549 cells after 72 h.

<b>Sample</b>	<b>Control</b>	<b>Naked siSHMT1</b>	<b>VBPEA/ siScr</b>	<b>VBPEA/ siSHMT1</b>	<b>PEA/siSHMT1</b>
<b>Purity</b>	1.948 ± 0.02	1.774± 0.11	1.918± 0.03	1.810± 0.31	1.911± 0.02

DNA concentrations and standard DNA solutions were obtained using a FluoroMate FS-2 fluorescence spectrophotometer (Scinco, WI, USA). A standard DNA curve was calibrated by plotting the known DNA concentrations versus relative fluorescence units. The DNA concentrations of samples were calculated from the standard DNA curve.

### **5.3.13. Tumor implantation, treatment and in vivo bioimaging**

Five weeks old nude Balb/c mice (male, 4 mice/group) were subcutaneously injected with 100  $\mu$ L of a single cell suspension containing  $3 \times 10^6$  luciferase expressing A549 cells (PerkinElmer, MA, USA). The treatment of tumors with siSHMT1 was started after 1 month when the tumor size reached 800-1000  $\text{mm}^3$ . 100  $\mu$ L of VBPEA/siSHMT1 (30  $\mu$ g) complexes (N/P 20) in normal saline was injected directly into the tumor at an interval of 48 h, which continued for one month. PEA/siSHMT1 (N/P 20) and PEI25k/siSHMT1 (N/P 10) complexes prepared under identical conditions were used as vector controls, and normal saline was used as a negative control. The IVIS Imaging system 100 (Xenogen) with Living Image software was used

for tumor bioimaging to analyze the effect of treatment on tumor size. The mice were anaesthetized by intraperitoneal (IP) injection of a Zoletil (40 mg/kg): Rompun (10 mg/kg) (4:1) mixture diluted 8 times in sterile 1X PBS. 200  $\mu$ L of D-luciferin (15 mg/mL stock solution in DPBS) for a 20 g mouse (3 mg/mouse) was injected intraperitoneally and was quickly distributed throughout the body. Tumor-expressed luciferase reacts with luciferin to emit luminescence, which was captured by the IVIS system to show images with intensity proportional to tumor size. Images were captured in the plateau phase which usually occurs after 15 min and lasts for 15-20 min. Tumor volume was also measured using Vernier caliper every week during the treatment. Tumor volume was calculated by using its mean diameter and applying the formula  $m = 0.5 \times a \times b^2$ , where  $a$  and  $b$  are the smallest and largest diameters, respectively. After treatment over one month, the tumors were dissected, chopped, and homogenized, and the protein concentrations of the lysates were measured. Equal amounts of protein (25  $\mu$ g) were separated by SDS-PAGE and transferred onto a nitrocellulose membrane for immunoblot analysis.

#### **5.3.14. Immunohistochemistry (IHC)**

The dissected tumors were fixed in 10% neutral buffered formalin and embedded in paraffin wax. Tissue sections (4-12  $\mu\text{m}$  thick) were prepared using a microtome and placed on positively charged slides and dried in an oven at 60°C. The slides were then deparaffinized, rehydrated and processed for antigen retrieval using 10 mM sodium citrate buffer, pH 6.0 at 95-100°C. Immunostaining with SHMT1 antibody (1:50 dilution) was performed using a mouse specific HRP/DAB detection IHC kit (Abcam, Cambridge, UK). Harris hematoxylin solution (Sigma) was used to stain the nuclei, and images were taken using a light microscope.

#### **5.3.15. Statistical analysis**

Statistical analysis was carried out by one-way ANOVA in conjunction with Bonferroni's test for the comparison of means. A value of  $P < 0.05$  was taken as statistically significant.

### **5.4 Results**

#### **5.4.1. VBPEA efficiently delivers siSHMT1 to silence SHMT1**

SHMT1 suppression by VBPEA/siSHMT1 was observed in A549 cells up to 72 h post-transfection using quantitative real time (Q)-PCR. A remarkable suppression of SHMT1 (~90%) was observed after 48 h of VBPEA/siSHMT1 treatment in comparison to PEA/siSHMT1 (42%) (Figure 5.11A), indicating an enhanced gene silencing efficiency. Further, western blot showed that VBPEA mediated delivery of siSHMT1 resulted in ~60% knockdown of SHMT1 protein expression, which was higher than that obtained by PEA/siSHMT1 (33%) or PEI25k/siSHMT1 (~32%) polyplexes in reference to the control after 48 h (Figure 5.12). Immunocytochemical analysis also showed the suppressed gene expression of SHMT1 by VBPEA/siSHMT1 treatment (Figure 5.11B). The crucial result is the increased gene silencing efficiency of VBPEA over PEA, which is indicative of the involvement of VB<sub>6</sub> in internalization of the polyplex.

#### **5.4.2. Competitive inhibition by 4'-deoxypyridoxine suggests VTC-mediated uptake of VBPEA polyplexes**

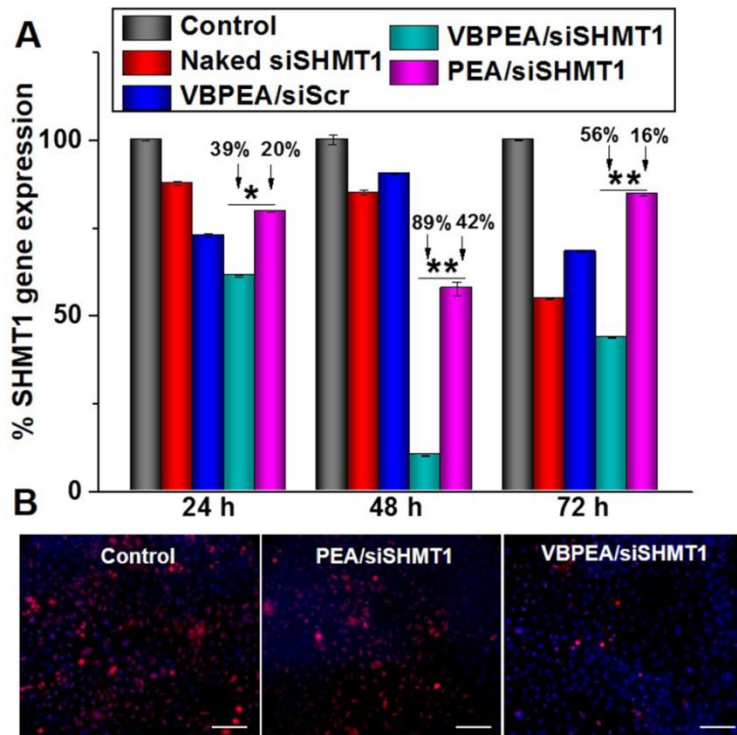


Figure 5.11. SHMT1 gene silencing efficiency of VBPEA/siSHMT1 complexes. (A) SHMT1 gene expression monitored at 24, 48, and 72 h post-transfection in A549 cells using quantitative real-time PCR (Q-PCR). Maximum SHMT1 suppression (~90%) was observed after 48 h by VBPEA/siSHMT1 complexes. Data are expressed as the mean  $\pm$  SEM of 3 experiments. Statistical significance was determined using one-way ANOVA (\* $P < 0.05$ ; \*\* $P < 0.01$ ). (B) Immunocytochemical analysis shows least SHMT1 expression (red) in VBPEA-treated A549 cells in comparison to PEA-treated and control cells after 48 h of transfection (scale bar: 200  $\mu$ m).

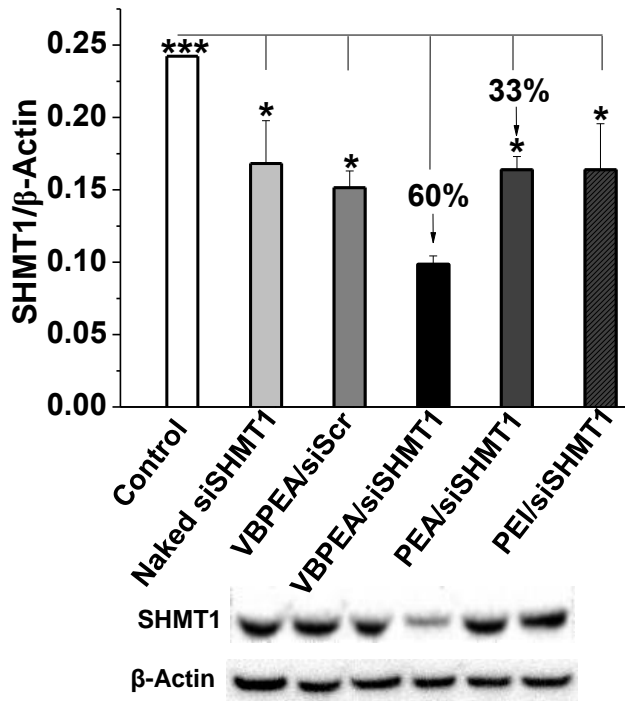


Figure 5.12. Western blot analysis of SHMT1 protein from the lysate of transfected A549 cells after 48 h showing no change in  $\beta$ -actin (42-kDa band) protein expression and a significant decrease in SHMT1 (50-kDa band) protein expression in cells treated with VBPEA/siSHMT1 complexes in contrast to other treated controls. Densitometric analysis of the SHMT1 protein band in reference to the untreated control cells (100% SHMT1 expression) shows a 60% decrease in SHMT1 expression in VBPEA/siSHMT1 treated cells. Data are shown as the mean  $\pm$  SD of 3 independent experiments (\* $P < 0.05$ ; \*\*\* $P < 0.001$ , one-way ANOVA).

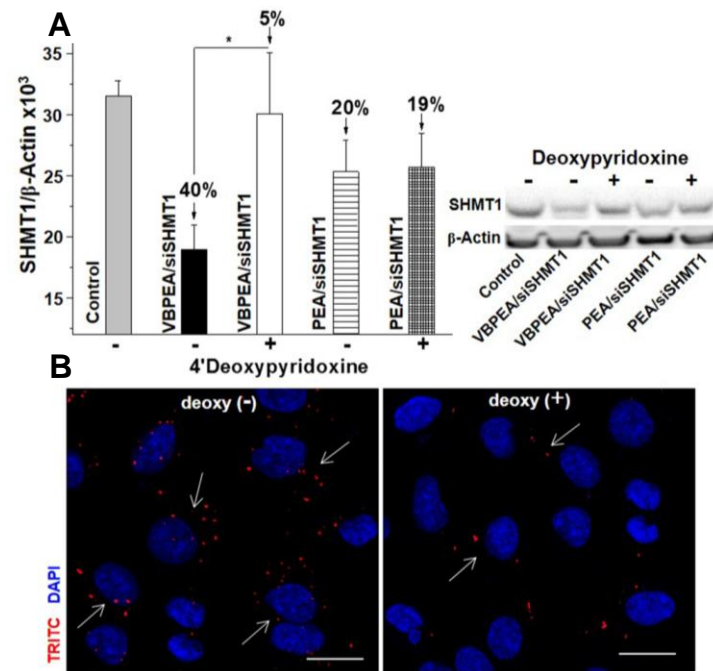


Figure 5.13. SHMT1 gene silencing efficiency of VBPEA/siSHMT1 complexes is enhanced by VTC-mediated endocytosis. (A) Western blot analysis of the A549 cells treated with VBPEA/siSHMT1 and PEA/siSHMT1 complexes (N/P 20) in the absence and presence of 4'-deoxyypyridoxine shows the effect of inhibition only on VBPEA-mediated delivery, whereas the PEA-mediated delivery remained unaffected by the inhibitor. Data are shown as the mean  $\pm$  SD of 3 independent experiments (\* $P < 0.05$ , one-way ANOVA). (B) Confocal microscopic images of A549 cells (scale bar: 20  $\mu$ m) after transfection with the VBPEAT/siRNA polyplex after 120 min show reduced polyplex internalization in the presence of 4'-deoxyypyridoxine (deoxy) competitive inhibitor than in its absence. VBPEA was labeled with TRITC (red) and nuclear DNA was counter-stained with DAPI (blue).

The western blot analysis of A549 cell lysates from VBPEA/siSHMT1 transfected cells showed no suppression of the SHMT1 gene in the presence of 4'-deoxypyridoxine (structural analog of VB<sub>6</sub>) (~5%) than the otherwise silenced SHMT1 in absence of the inhibitor (~40%) (Figure 5.13A). Contrary to this, no significant inhibitory effect was observed in PEA/siSHMT1 transfected cells in the presence (~19%) or absence (~20%) of 4'-deoxypyridoxine, suggesting that 4'-deoxypyridoxine competitively inhibits the binding of VB<sub>6</sub> present in VBPEA/siSHMT1 polyplexes to VTC [146] and decelerates polyplex uptake. Confocal studies in the presence of inhibitor also resulted in reduced polyplex internalization compared to that in the absence of inhibitor due to the decreased accessibility of VTC to VBPEA (Figure 5.13B). This suggests the active participation of a VB<sub>6</sub>-specific uptake mechanism via a membrane carrier (VTC) favoring the accelerated internalization of VBPEA.

#### **5.4.3. SHMT1 knockdown resulted in reduced cell proliferation and increased apoptotic events**

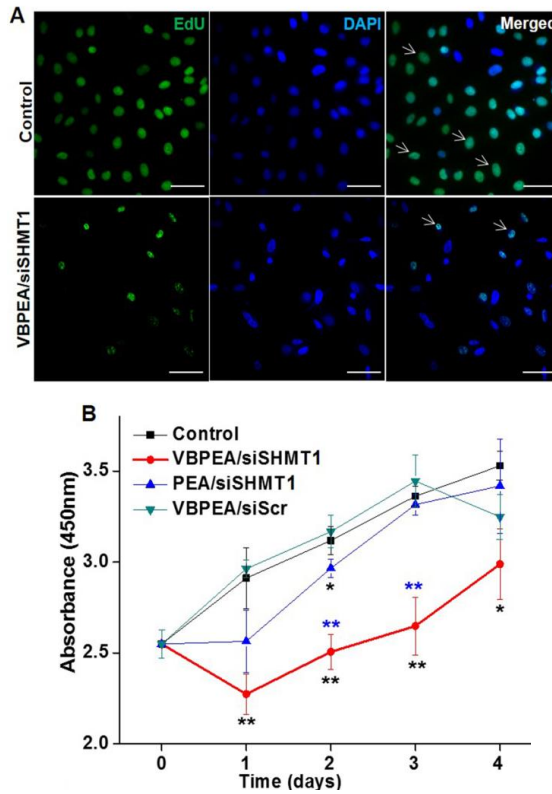


Figure 5.14. Effect of SHMT1 knockdown on the proliferative behavior of A549 cells. (A) EdU proliferation assay showing diminished cell proliferation in the VBPEA/siSHMT1 treated group compared to the untreated control group due to lower EdU nucleotide incorporation in fewer dividing A549 cells (scale bar: 50  $\mu$ m). The arrows indicate the proliferated nuclei (green). (B) WST proliferation assay at day 0, 1, 2, 3, 4 after treatment with polyplexes shows the lowest metabolic activity in VBPEA/siSHMT1 treated A549 cells up to day 3, indicating less cell proliferation. Statistical significance was determined using one-way ANOVA (\* $P < 0.05$ ; \*\* $P < 0.01$ ,  $n = 3$ , error bar represents SD).

VBPEA/siSHMT1 transfected A549 cells exhibited comparatively lesser proliferative behavior than the untreated control cells. EdU incorporation in proliferating cells (green fluorescence) can be assessed for the direct analysis of DNA synthesis and cell proliferation. The results showed hampered cell proliferation (lower number of green nuclei) due to the knockdown of SHMT1 protein expression, in comparison to the untreated control (Figure 5.14A). In addition, WST assay also showed a reduced proliferation of VBPEA/siSHMT1 treated cells until day 3, after which proliferative behavior was restored, due to consumption of the single dose of siSHMT1 (Figure 5.14B). The proliferation was also halted to some extent, but less efficiently by PEA/siSHMT1. PEI25k was excluded due to its high cytotoxicity, which may produce false results.

The non-proliferative cancer cells with silenced SHMT1 are supposed to gradually proceed towards apoptosis, which was evident from features such as cell rounding, membrane blebbing, and detachment from the tissue culture dish. Loss of membrane asymmetry and nuclear disintegration are the characteristic features of apoptotic cells

distinguishable from the necrotic cells [181, 182]. Therefore, enumeration of apoptosis in the treated cancer cells was done for assuring the induction of apoptosis, which serves as a prognostic marker for cancer treatment [183, 184]. The results of colorimetric TUNEL assay, where ends of the apoptosis-induced DNA strand breaks were labeled and detected as dark brown stained nuclei, showed higher DNA fragmentation (dark brown) in VBPEA/siSHMT1 treated cells than the cells treated with PEA and the controls (Figure 5.15A). AnnexinV-PI staining also detects apoptosis, based on the binding of Annexin V with the exposed phospholipid phosphatidylserine and propidium iodide (PI) with DNA on loss of plasma membrane integrity of apoptotic cells [185]. From the FACS results of VBPEA/siSHMT1 treated group, cells that are negative for both Annexin V and PI are considered viable (~35%), whereas cells in early apoptosis are Annexin V positive and PI negative (~3%), and late apoptotic or dead cells are positive for both Annexin V and PI (~62%) (Figure 5.15B). The presence of these three phenotypes within a mixed cell population suggests apoptosis. The proliferation and apoptosis assays suggest that

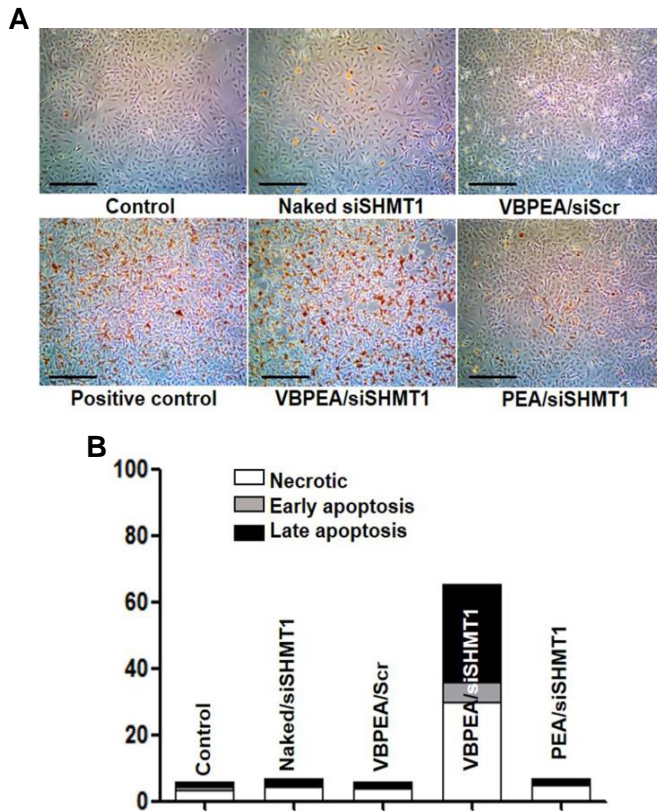


Figure 5.15. SHMT1 knockdown onsets the apoptotic events in A549 cells. (A) TUNEL assay in A549 cells for the comparison of apoptotic events in the various treatment groups shows the maximum apoptosis induction in the VBPEA-mediated siSHMT1 delivery; apoptosis is represented by brown stained nuclei (scale bar: 500  $\mu$ m). (B) AnnexinV-PI staining of transfected A549 cells show >50% apoptotic cell death in VBPEA/siSHMT1 treated cells after 48 h.

antagonizing SHMT1 expression resulted in reduced cell division and apoptotic death of cancer cells.

#### **5.4.4. Knockdown of SHMT1 drastically affects cellular DNA synthesis and arrests cell cycle at sub-G<sub>1</sub> phase**

The three constituent enzymes of the thymidylate biosynthetic pathway, which translocate to the nucleus for DNA replication, form a multienzyme complex where SHMT isoforms (SHMT1 & SHMT2 $\alpha$ ) anchor this metabolic complex at the nuclear lamina [148]. Therefore, the co-localization of SHMT1 with nuclear lamins was investigated during DNA replication at the S phase (cells synchronized at S phase) of the cell cycle. We demonstrated that VBPEA-mediated delivery of siSHMT1 resulted in the decreased incidence of SHMT1 co-localization with the nuclear lamina (Figure 5.16). The results showed approximately 91% co-localization of SHMT1 (red) with the nuclear lamina (green) in the control group, with no significant difference in the siScr treated group (89%), suggesting continued DNA synthesis and cell division (indicated by an arrow in Figure 5.16). In contrast, VBPEA/siSHMT1 treated cells displayed reduced amount of SHMT1

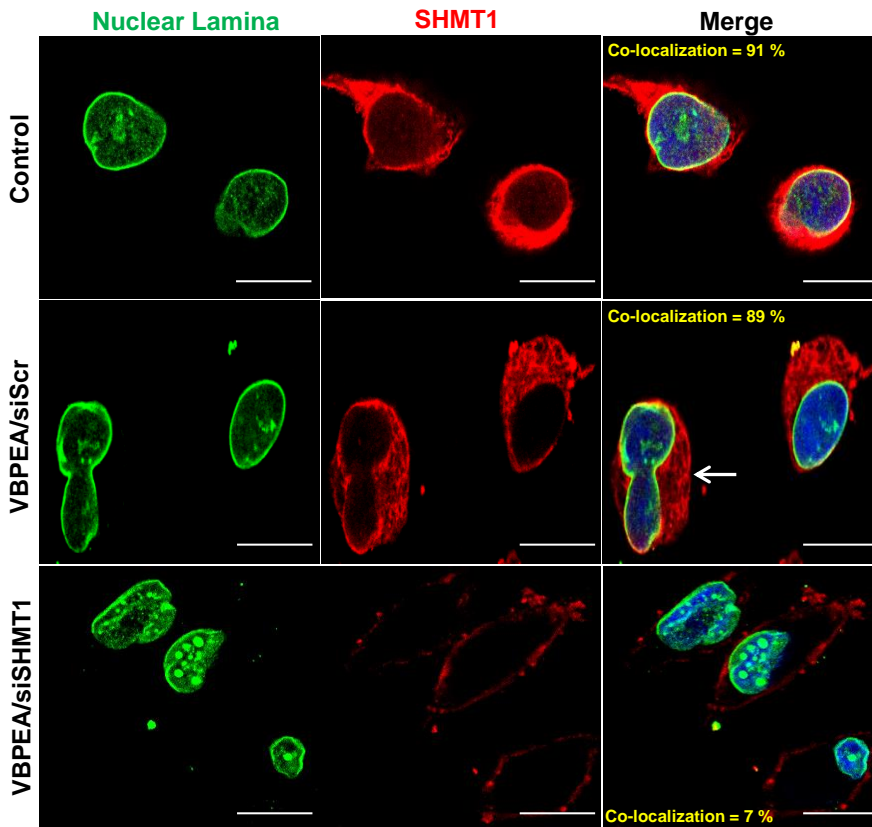


Figure 5.16. SHMT1 knockdown affected DNA synthesis. Co-localization study of SHMT1 (red) with the nuclear lamina (green) of post-transfected A549 cells, synchronized at S phase, showed the least co-localization (7%) with VBPEA/siSHMT1 treated cells in contrast to the control in which ~90% co-localization suggests active DNA synthesis and cell division. The dividing cell in the negative control (VBPEA/siScr treated cells) is indicated by an arrow (scale bar: 20  $\mu$ m).

(less intense red fluorescence), showing only 7% co-localization with the nuclear lamina. These SHMT1 silencing results indicate the disintegration of the *de novo* thymidylate biosynthetic multienzyme complex, which leads to the cessation of DNA synthesis and cell cycle arrest in adenocarcinoma cells.

The cell growth arrest after the delivery of siSHMT1 using VBPEA was confirmed by cell cycle analysis. Since the incidence of DNA replication is much higher in cancer cells than in normal cells, their growth pattern is different where most cells skip cell cycle check points and remain in the G1 phase without exiting the cell cycle [186]. VBPEA-mediated delivery of siSHMT1 is demonstrated to arrest cell cycle progression (Figure 5.17B) that occurred due to the deprivation of nucleotides. A549 cells treated with VBPEA/siSHMT1 together with positive and negative controls were monitored for their growth pattern after 12 h, 24 h, and 72 h of transfection using FACS. On the basis of differences in intensity of PI fluorescence (proportional to DNA content), the population of cells in G0/G1, S, and G2/M phases were identified. A population of cells in G0/G1 phase had uniform, low

DNA content values compared to G2/M cells with twice the DNA content, and S cells with intermediate DNA content. 12 h post-transfection, not much differences were observed in all of the treated and control groups, with most cancer cells (~70%) being present in G1 phase, indicating their re-entry into the cell cycle. 24 h later, while the control cells again entered G1 phase in preparation for the next division cycle, the VBPEA/siSHMT1 treated cells were not observed in G1 phase (2%), suggesting initiation for their retreat from cell division. The crucial results after 72 h showed that the VBPEA/siSHMT1 treated cells exhibited cell cycle arrest in the sub-G1 phase (38%) and were prevented from entering the G1 phase of cell division (Figure 5.17A & 5.18). It is noteworthy that the decrease in the number of S phase cells (after 24 h) has appeared at the sub-G1 phase, where they can be induced for apoptosis. The results are in accordance with the WST proliferation assay where the cell proliferation is seen reduced until day 3 (72 h) (Figure 5.14B).

Because cells were found in the sub-G1 phase after 72 h, the total genomic DNA from all of the treated and control groups were

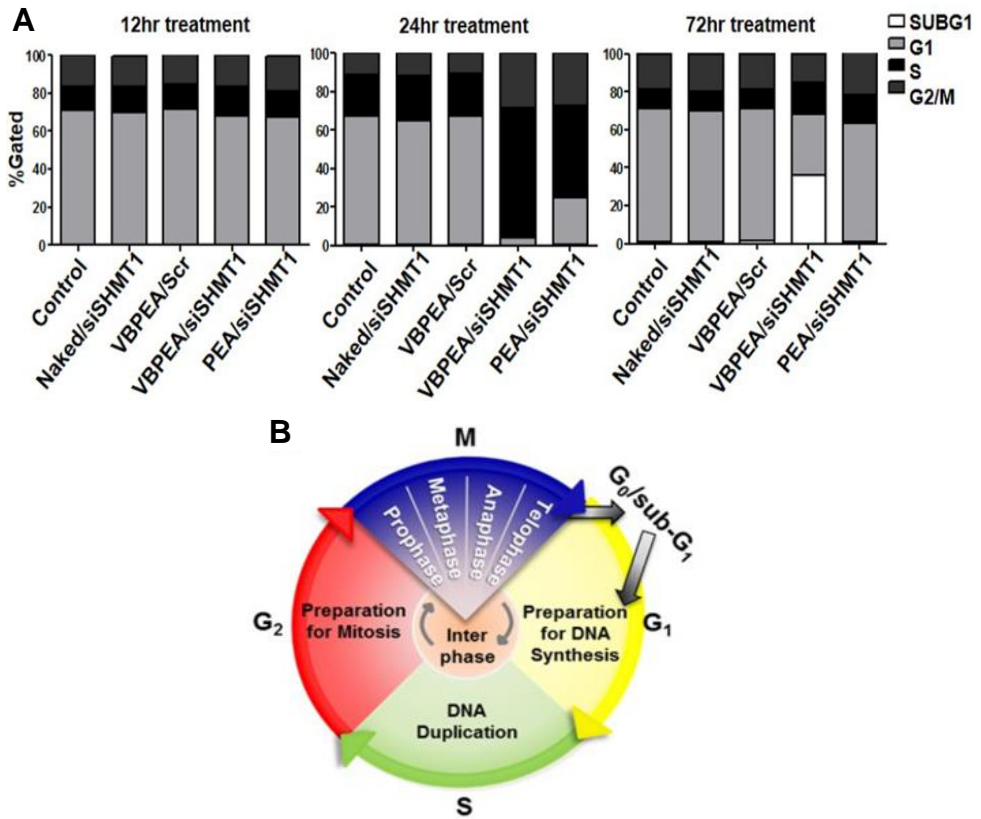


Figure 5.17. SHMT1 knockdown resulted in cell cycle arrest. (A) FACS analysis of the population of A549 cells in different cell growth phases after 12 h, 24 h, and 72 h of treatment with VBPEA/siSHMT1 and PEA/siSHMT1 complexes (N/P 20), showing cell growth arrest due to suppression of SHMT1 gene expression after 72 h. (B) Pictorial presentation of cell cycle progression.

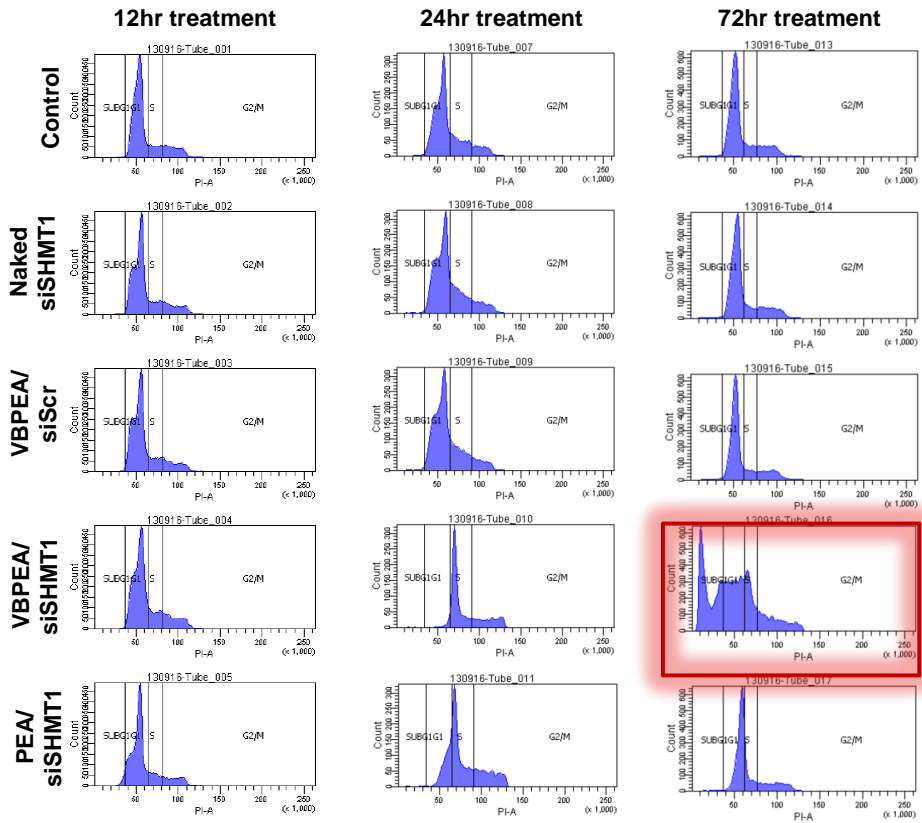


Figure 5.18. FACS analysis of the population of A549 cells present in different cell growth phases after 12 h, 24 h, and 72 h of treatment with VBPEA/siSHMT1 and PEA/siSHMT1 complexes.

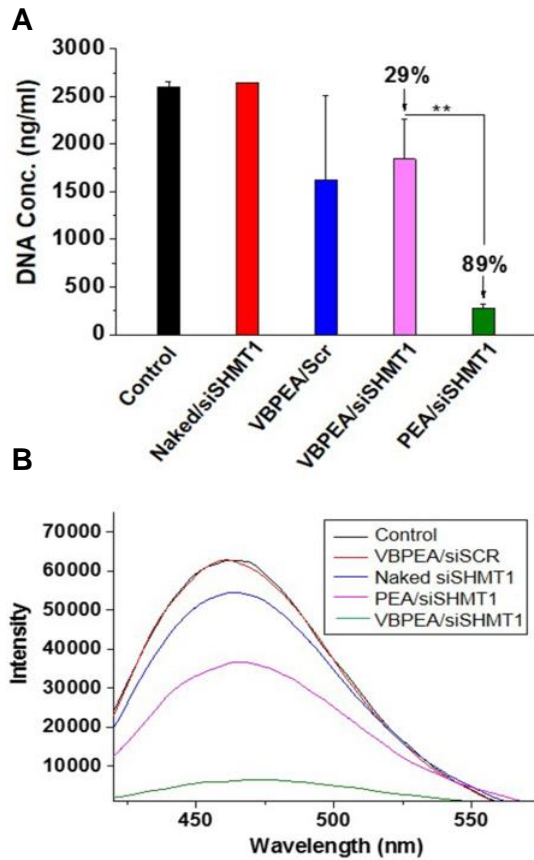


Figure 5.19. SHMT1 knockdown decreased the total genomic DNA content of the cells. (A) The total genomic DNA content and (B) fluorescence intensity of treated A549 cells shows a drastic decrease in genomic DNA content of VBPEA treated cells after 72 h. The fluorescent dye, Hoechst 33258, bound to DNA excites at 360 nm and gives emission spectra at 460 nm. Statistical significance was determined using one-way ANOVA (\*\*P < 0.01, n = 3, error bar represents SD).

quantified after 72 h. The VBPEA group showed an 89% decrease in the genomic DNA concentration, whereas the PEA group showed a 29% decrease in reference to control (Figure 5.19A, B). The results suggest that VBPEA-mediated silencing of SHMT1 arrested the thymidylate synthase cycle and consequently stopped nucleotide biosynthesis. As a result, cell proliferation was also inhibited, leading to apoptotic cell death and lower genomic DNA concentration.

#### **5.4.5. VBPEA-mediated knockdown of SHMT1 retarded tumor growth in xenograft mice**

Instead of systemic, local administration of siRNA avoids the obstacles of low bioavailability, systemic toxicity, rapid excretion and inefficient targeting [187]. Therefore, the luciferase-expressing subcutaneous tumor ( $\sim 1000 \text{ mm}^3$ ) bearing xenograft mice were treated with the local administration of VBPEA/siSHMT1. Bioluminescence images were captured every two weeks during polyplex injection. A gradual decrease in bioluminescence intensity (Figure 5.20) and tumor volume (56%)(Table 5.2) of the VBPEA/siSHMT1 treated group demonstrated

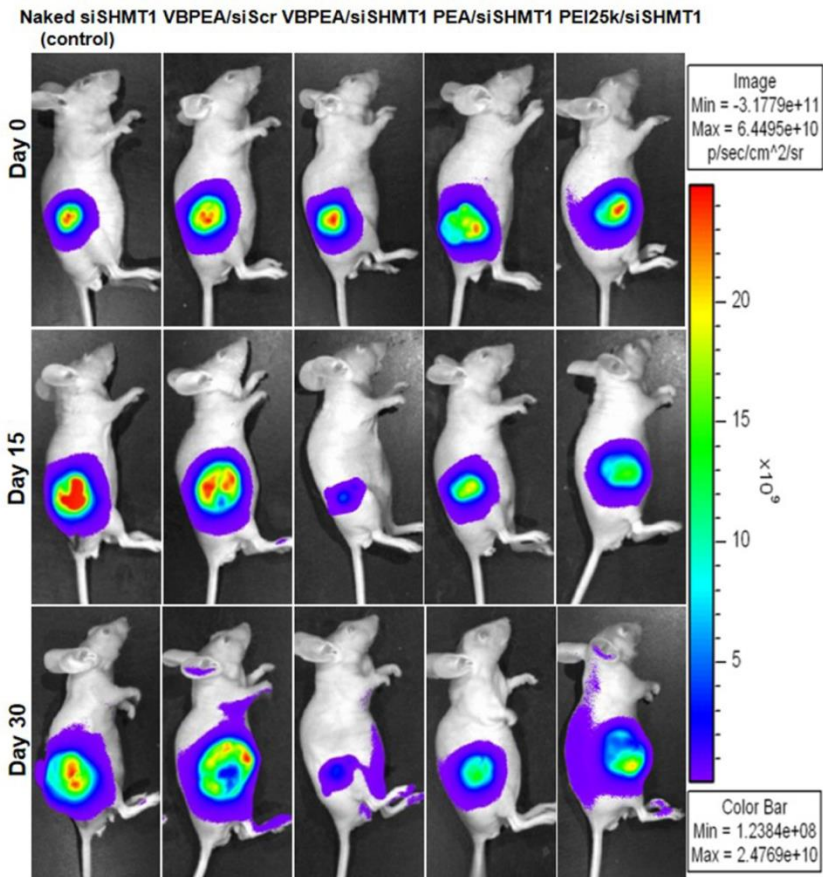


Figure 5.20. The subcutaneous injection of luciferase expressing A549 cells in 5 weeks old nude Balb/c mice ( $n = 4$ ) resulted in tumors  $\sim 1000$  mm<sup>3</sup> in size after a month. VBPEA/siSHMT1 (N/P 20), PEA/siSHMT1 (N/P 20) and PEI25k/siSHMT1 (N/P 10) complexes (with 30  $\mu$ g siSHMT1) were directly administered in the tumor with alternate doses after every 48 h for 4 weeks. Bioluminescence images taken every 15 days show a maximum in vivo tumor retardation resulting from VBPEA-mediated delivery of siSHMT1.

tumor growth inhibition, in contrast to the control groups where tumor has grown several folds than the initial volume (Figure 5.21A). Although the PEA/siSHMT1 and PEI/siSHMT1 treated mice did not show a multifold increase in tumor size, they failed to retard the tumor growth comparative to VBPEA, certainly due to their lower gene transport efficiency. In the subsequent experiments, VBPEA treated group showed a 59% decrease in SHMT1 expression in reference to the control (similar to *in vitro* SHMT1 suppression of 60%), which was higher than that of the PEA (26% decrease) or PEI (19% decrease) treated groups (Figure 5.21B). Immunohistochemical analysis also showed decreased brown staining of the SHMT1 protein throughout the tumor section of VBPEA/siSHMT1-treated group (Figure 5.22). The effect of SHMT1 suppression in VBPEA/siSHMT1-treated tumor is not only seen as diminution in tumor volume but also by the presence of apoptotic cells in tumor section (Figure 5.23) which suggests the significance of SHMT1 inactivation in treating cancer and applicability of VB<sub>6</sub>-coupled vector in enhancing siSHMT1 delivery.

Table 5.2. Tumor volume measurements using Vernier caliper every week during the one month treatment in xenograft mice (n = 4).

<b>Sample</b>	<b>Untreated (mm<sup>3</sup>)</b>	<b>Naked siSHMT1 (mm<sup>3</sup>)</b>	<b>VBPEA/ siScr (mm<sup>3</sup>)</b>	<b>VBPEA/ siSHMT1 (mm<sup>3</sup>)</b>	<b>PEA/ siSHMT1 (mm<sup>3</sup>)</b>	<b>PEI/ siSHMT1 (mm<sup>3</sup>)</b>
<b>Initial</b>	961.4 ± 24.7	889.4± 38.4	1000.5± 31.8	1066.6± 31.1	1138.4± 40.5	1166.4± 40.5
<b>Week 1</b>	2016.5 ± 66.4	1608.2± 69.5	1846.0± 85.6	956.3 ± 52.9	1241.9 ± 93.9	1203.6 ± 76.9
<b>Week 2</b>	2740.8 ± 49.2	2282.8± 68.6	2794.8± 20.7	802.1 ± 79.0	1283.5 ± 56.5	1405.9 ± 56.1
<b>Week 3</b>	3662.0 ± 49.2	3187.1± 60.9	3593.7± 51.6	590.5± 45.6	1488.4± 64.9	1583.5± 45.0
<b>Week 4</b>	4428.9 ± 66.6	4397.7± 53.2	4763.0± 173.2	471.5± 25.0	1504.6± 14.1	1884.9± 77.1

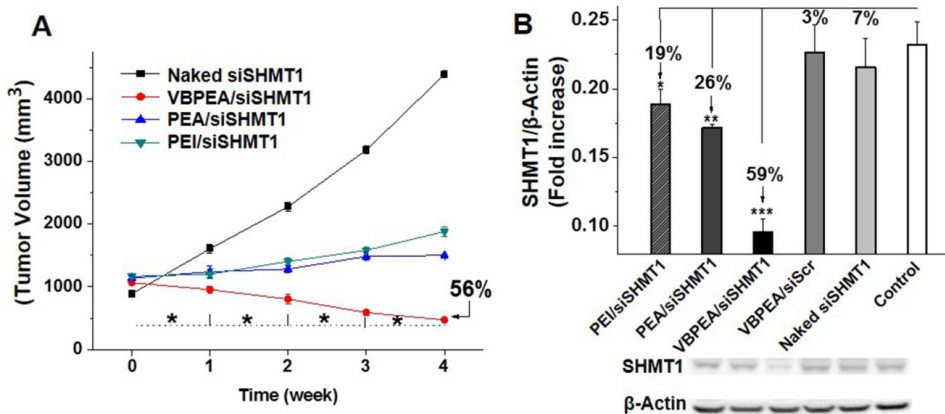


Figure 5.21. Reduction of tumor size in xenograft mice (n = 4). (A) Tumor volumes were measured using Vernier caliper every week during the treatment and ultimately resulted in ~56% reduction in tumor size. Statistical significance was determined using one-way ANOVA (\*P < 0.05, error bar represents SD). (B) Western blot analysis of the tumor mass after 1 month of treatment shows suppressed SHMT1 expression in VBPEA-mediated treated tumor. Data are shown as the mean ± SD of 3 independent experiments (\*P < 0.05; \*\*P < 0.01; \*\*\*P < 0.001, one-way ANOVA).

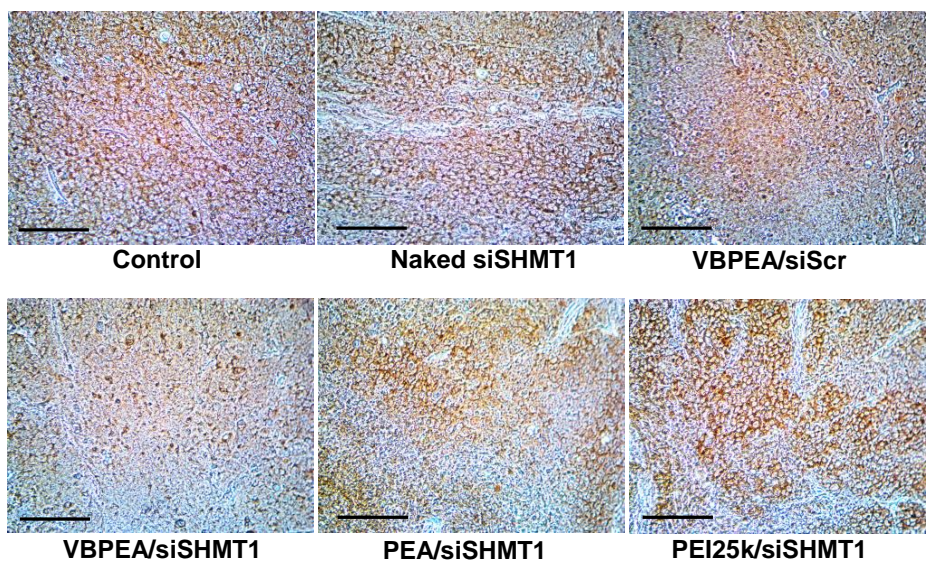


Figure 5.22. Immunohistochemistry of the formalin fixed tumor sections show decreased staining in VBPEA treated tumor section of xenograft mice (n = 4) (scale bar: 500  $\mu$ m), suggesting suppression of SHMT1 gene expression.

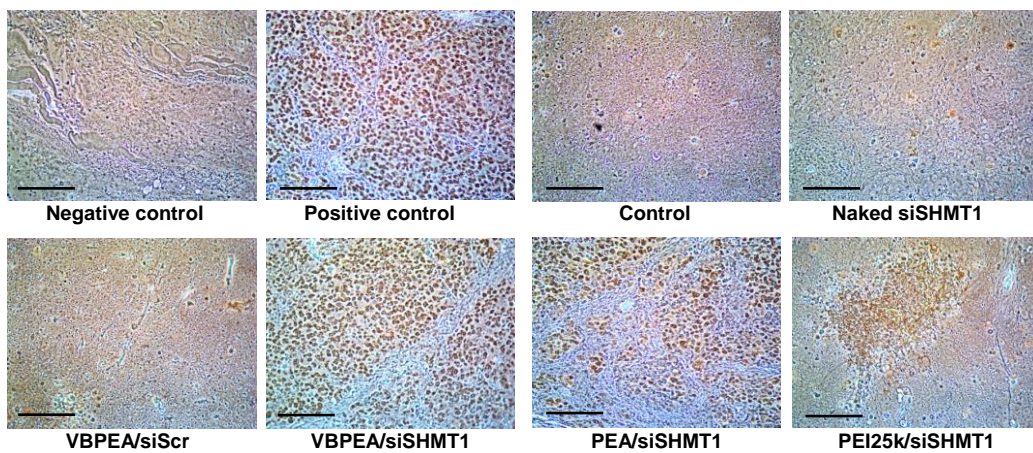


Figure 5.23. In vivo TUNEL assay of formalin fixed tumor sections show a high level of apoptotic events occurring in VBPEA/siSHMT1 treated tumors in xenograft mice (n = 4) (scale bar: 500  $\mu$ m).

## 5.5 Discussion

Our findings show that, by combining the gene silencing technology with the modification of the mode of cellular uptake of polyplex, a control on the growth of the tumor cells could be achieved. Using VB<sub>6</sub>, coupled to poly(ester amine), we sought that VB<sub>6</sub> could trail the vector along with the complexed therapeutic siRNA through its specific VTC-mediated endocytosis [146]. VB<sub>6</sub> has gained attention due to its unequalled catalytic versatility as a cofactor where VB<sub>6</sub> forms a Schiff base (aldimine) between its electrophilic carbonyl group and nucleophilic amines of an enzyme [110, 127, 128]. Similarly, the amines of PEA form a Schiff base with VB<sub>6</sub> and get reduced during the formation of VBPEA. Despite the reduction in the total number of primary amines of the backbone polymer, the enhancement in the transfection capability of VBPEA is its most striking feature [146], which underscores its potential as an efficient carrier of siRNA molecules.

SHMT catalyzed reaction in the thymidylate synthase cycle in addition to dTMP synthesis also produces glycine and methylene-THF, both of

which are the precursors for nucleotide biosynthesis [151]. During cancer progression, the SHMT enzyme is extremely required for continuous synthesis of DNA [151] and therefore, is in constant need for its cofactor, VB<sub>6</sub>. For unobstructed DNA synthesis the cellular uptake of VB<sub>6</sub> is increased in tumor cells [132, 164], due to which VB<sub>6</sub>-coupled VBPEA gains quick entry into the tumor cells in comparison to non-coupled vectors (Figure 5.13A). SHMT plays a central role in carcinogenesis and therefore its therapeutic manipulation raises exciting opportunities as well as challenges in the path towards clinical development. Inhibition of the thymidylate biosynthesis pathway due to SHMT1 knockdown by enhanced delivery of SHMT1 siRNA is expected to introduce a nanotechnology-based approach for the treatment of cancer. The mechanism of VBPEA-mediated SHMT1 silencing was demonstrated to occur via VTC-mediated endocytosis (Figure 5.13A, B). Antagonizing SHMT1 expression severely hampers the DNA synthesis mechanism by disrupting the multienzyme complex, shown by only 7% co-localization (Figure 5.16), which impairs the thymidylate synthase cycle components to assemble at nuclear lamina. The growth pattern of VBPEA/siSHMT1-treated cancer cells showed

~40% of the cell fraction in the sub-G1 phase which secondarily underwent apoptosis. Suppressed SHMT1 could not anchor the multienzyme complex to the nuclear lamina for DNA synthesis that preferentially impaired rapidly proliferating cancer cells and slowed down the tumor growth. That is why, VBPEA/siSHMT1 treated cells displayed inhibition of cell proliferation as well as induction of apoptosis. So, it can be deduced that the loss of SHMT1 function results in the cessation of thymidylate nucleotide (dTMP) synthesis from the thymidylate biosynthesis pathway. Subsequently, dUMP (deoxyuracil monophosphate) instead of dTMP is incorporated into DNA strand during DNA synthesis which leads to high genomic instability and DNA strand breaks in cancer cells [188]. Consequently, this results in apoptotic cell death and a reduction in the genomic DNA content. A speculative representation of the silencing events has been documented in Figure 5.1A.

The obtained *in vivo* results further illustrate that even at an advanced tumor state; the inactivation of SHMT1 *in situ* can bring about substantial decrease in tumor volume. We may conclude that silencing

the SHMT1 expression radically inhibits cancer growth and that this effect is enhanced by delivery via VB<sub>6</sub>-coupled vector comparable to non-coupled vector. Therefore, it is strongly recommended to study and use VB<sub>6</sub>-coupled vectors for carrying the cargo in cancer cells, which has also been suggested by Zhang et al. [122]. The attributes of VBPEA-mediated siSHMT1 delivery demonstrated in the present study suggest its potential applications in developing more profound therapeutic molecules against the uninvestigated therapeutic target SHMT1 and other VB<sub>6</sub>-dependent enzymes involved in cancer sustenance.

## **5.6 Conclusion**

Antagonizing SHMT1 expression in cancer cells using siRNA whose enhanced delivery was ensured by the VB<sub>6</sub>-coupled vector, VBPEA, showed its detrimental effect on the cell cycle and proliferation of cancer cells with subsequent onset of apoptosis. 4'-Deoxypyridoxine inhibition studies indicated the crucial involvement of VTCs in enhancing the cellular uptake of VBPEA complexes by resulting in endosome formation on the attachment of large polyplexes. Based on

the silencing results we infer that in order to support their uncontrolled growth and proliferation, cancer cells constantly need VB<sub>6</sub> for continuous functioning of thymidylate synthase cycle, resulting in enhanced VBPEA uptake. With further success in the xenograft mice model, we offer an efficient alternative to inhibit cancer growth by using VBPEA to curb SHMT1 activation that will envision a new target for cancer treatment.

# CHAPTER 6

## *SUMMARY*

---

To address the safety and specific delivery of the therapeutics to the cancer cells, vitamin B6 coupled cationic polymer was developed as a non-viral vector. PEI 1.2 kDa was used to ensure negligible polymer cytotoxicity and was linked with GDM to make poly(ester amine) (PEA) as the backbone polymer. To ~10% of the nucleophilic amines present throughout the branches of the PEA backbone, VB6 was attached via a Schiff base formation due to its electrophilic carbonyl groups. The vector, vitamin B6 coupled poly(ester amine) (VBPEA), was constructed such that (i) the VB6 provides specificity to the polymer for cancer cells, (ii) the PEI component incorporates endosomal escape property into the vector, and (iii) the PEA backbone contains degradable ester linkages which facilitate the polymer removal from the system after delivering the payload. VB6 serves as a cofactor

to various apoenzymes for cell growth and proliferation. A specific VB6 transporting carrier (VTC) facilitates the entry of VB6 in cells. VB6 present in VBPEA also utilizes this pathway for its cellular uptake. VBPEA due to its size limitation cannot pass through the VTC and consequently end up in VTC-mediated endocytosis of the polyplex. VBPEA owing to endosomal osmolysis property ruptures the endosome and enters the cell cytoplasm to deliver the therapeutic gene in the vicinity of cell nucleus. The cancer cells need VB6 more frequently and in larger amounts to support its rapid proliferation. And, subsequently it takes up the VB6 from the neighboring normal cells. Therefore, cancer cells have higher affinity for VBPEA than the normal cells and VBPEA is spontaneously channeled towards the diseased cancer tissue. Further, therapeutic study using VBPEA was done in vitro and in vivo.

Serine hydroxymethyltransferase (SHMT), a vitaminB6 (VB6)-dependent enzyme, plays a key role during DNA synthesis by generating precursors for nucleotide biosynthesis. Therefore, SHMT expression is drastically increased during cancer proliferation, making it an attractive target for cancer therapy; however, the impact of

SHMT1 knockdown on DNA synthesis machinery of cancer cells was entirely uninvestigated. To address this, SHMT1 siRNA was used and its efficient delivery was ensured by a VB6 coupled vector. The mechanism and detrimental effect of SHMT1 silencing on the cell cycle and proliferation of cancer cells with subsequent onset of apoptosis was demonstrated. SHMT1 silencing resulted in disintegration of the multienzyme complex and thus prevented the functioning of thymidylate synthase cycle in cancer cells. Xenograft tumor mice models were used to show the inhibition of tumor growth by silencing SHMT using VBPEA vector. With the success in xenograft mice model, an efficient alternative to inhibit cancer growth by curbing SHMT1 activation is offered that will envision a new target for cancer treatment.

## *REFERENCES*

---

- [1] Culver K. Gene Therapy—A Handbook for Physician. Mary Ann Liebert, Inc, New York. 1994.
- [2] Griffith F. The Significance of Pneumococcal Types. *Epidemiology & Infection*. 1928;27:113-59.
- [3] Avery OT, MacLeod CM, McCarty M. Studies on the chemical nature of the substance inducing transformation of pneumococcal types: induction of transformation by a desoxyribonucleic acid fraction isolated from pneumococcus type III. *The Journal of Experimental Medicine*. 1944;79:137-58.
- [4] Zinder ND, Lederberg J. Genetic exchange in Salmonella. *Journal of Bacteriology*. 1952;64:679-99.
- [5] Szybalska EH, Szybalski W. Genetics of human cell lines, IV. DNA-mediated heritable transformation of a biochemical trait. *Proceedings of the National Academy of Sciences*. 1962;48:2026-34.

- [6] Wirth T, Parker N, Ylä-Herttuala S. History of gene therapy. *Gene*. 2013;525:162-9.
- [7] Temin HM. Mixed infection with two types of Rous sarcoma virus. *Virology*. 1961;13:158-63.
- [8] Rogers S, Pfuderer P. Use of viruses as carriers of added genetic information. *Nature*. 1968;219:749-51.
- [9] Rogers S, Lowenthal A, Terheggen HG, Columbo JP. Induction of arginase activity with the Shope papilloma virus in tissue culture cells from an argininemic patient. *The Journal of Experimental Medicine*. 1973;137:1091-6.
- [10] Terheggen HG, Lowenthal A, Lavinha F, Colombo JP, Rogers S. Unsuccessful trial of gene replacement in arginase deficiency. *Z Kinder-Heilk*. 1975;119:1-3.
- [11] Mercola KE, Bar-Eli M, Stang HD, Slamon DJ, Cline MJ. Insertion of new genetic information into bone marrow cells of mice:

comparison of two selectable genes. *Annals of the New York Academy of Sciences*. 1982;397:272-80.

[12] Rosenberg SA, Aebersold P, Cornetta K, Kasid A, Morgan RA, Moen R, et al. Gene transfer into humans — Immunotherapy of patients with advanced melanoma, using tumor-infiltrating lymphocytes modified by retroviral gene transduction. *New England Journal of Medicine*. 1990;323:570-8.

[13] Rosenberg SA, Packard BS, Aebersold PM, Solomon D, Topalian SL, Toy ST, et al. Use of tumor-infiltrating lymphocytes and interleukin-2 in the immunotherapy of patients with metastatic melanoma. *New England Journal of Medicine*. 1988;319:1676-80.

[14] Rosenberg SA. Gene therapy for cancer. *JAMA*. 1992;268:2416-9.

[15] Rosenberg SA, Anderson WF, Blaese M, Hwu P, Yannelli JR, Yang JC, et al. The development of gene therapy for the treatment of cancer. *Annals of Surgery*. 1993;218:455-63.

[16] Blaese RM, Culver KW, Miller AD, Carter CS, Fleisher T, Clerici M, et al. T lymphocyte-directed gene therapy for ADA- SCID: Initial trial results after 4 years. *Science*. 1995;270:475-80.

[17] Edelstein ML. Gene therapy clinical trials worldwide. website at: <http://www.wiley.co.uk/genmed/clinical>. *The Journal of Gene Medicine* 2014.

[18] Bordignon C, Notarangelo LD, Nobili N, Ferrari G, Casorati G, Panina P, et al. Gene therapy in peripheral blood lymphocytes and bone marrow for ADA- immunodeficient patients. *Science*. 1995;270:470-5.

[19] Puumalainen AM, Vapalahti M, Agrawal RS, Kossila M, Laukkanen J, Lehtolainen P, et al.  $\beta$ -galactosidase gene transfer to human malignant glioma in vivo using replication-deficient retroviruses and adenoviruses. *Human Gene Therapy*. 1998;9:1769-74.

[20] Stolberg SG. The biotech death of Jesse Gelsinger. *NYTimes Mag*. 1999:136-40, 49-50.

[21] Peng Z. Current status of gendicine in China: Recombinant human Ad-p53 agent for treatment of cancers. *Human Gene Therapy*. 2005;16:1016-27.

[22] Wilson JM. Gendicine: The first commercial gene therapy product. *Human Gene Therapy*. 2005;16:1014-5.

[23] Bischoff JR, Kirn DH, Williams A, Heise C, Horn S, Muna M, et al. An adenovirus mutant that replicates selectively in p53-deficient human tumor cells. *Science*. 1996;274:373-6.

[24] Wirth T, Samaranayake H, Pikkarainen J, Määttä AM, Ylä-Herttuala S. Clinical trials for glioblastoma multiforme using adenoviral vectors. *Current Opinion in Molecular Therapeutics*. 2009;11:485-92.

[25] Maguire AM, High KA, Auricchio A, Wright JF, Pierce EA, Testa F, et al. Age-dependent effects of RPE65 gene therapy for Leber's congenital amaurosis: a phase 1 dose-escalation trial. *The Lancet*. 2009;374:1597-605.

[26] Cavazzana-Calvo M, Payen E, Negre O, Wang G, Hehir K, Fusil F, et al. Transfusion independence and HMGA2 activation after gene therapy of human  $\beta$ -thalassaemia. *Nature*. 2010;467:318-22.

[27] Jessup M, Greenberg B, Mancini D, Cappola T, Pauly DF, Jaski B, et al. Calcium upregulation by percutaneous administration of gene therapy in cardiac disease (CUPID): A phase 2 trial of intracoronary gene therapy of sarcoplasmic reticulum  $\text{Ca}^{2+}$ -ATPase in patients with advanced heart failure. *Circulation*. 2011;124:304-13.

[28] Hacein-Bey-Abina S, Hauer J, Lim A, Picard C, Wang GP, Berry CC, et al. Efficacy of gene therapy for X-linked severe combined immunodeficiency. *New England Journal of Medicine*. 2010;363:355-64.

[29] Aiuti A, Cattaneo F, Galimberti S, Benninghoff U, Cassani B, Callegaro L, et al. Gene therapy for immunodeficiency due to adenosine deaminase deficiency. *New England Journal of Medicine*. 2009;360:447-58.

[30] Boztug K, Schmidt M, Schwarzer A, Banerjee PP, Díez IA, Dewey RA, et al. Stem-cell gene therapy for the Wiskott-Aldrich syndrome. *New England Journal of Medicine*. 2010;363:1918-27.

[31] Biffi A, Montini E, Lorioli L, Cesani M, Fumagalli F, Plati T, et al. Lentiviral hematopoietic stem cell gene therapy benefits metachromatic leukodystrophy. *Science*. 2013;341.

[32] MacLaren RE, Groppe M, Barnard AR, Cottrill CL, Tolmachova T, Seymour L, et al. Retinal gene therapy in patients with choroideremia: initial findings from a phase 1/2 clinical trial. *The Lancet*. 2014;383:1129-37.

[33] Tebas P, Stein D, Tang WW, Frank I, Wang SQ, Lee G, et al. Gene editing of CCR5 in autologous CD4 T cells of persons infected with HIV. *New England Journal of Medicine*. 2014;370:901-10.

[34] Ylä-Herttuala S. Endgame: Glybera finally recommended for approval as the first gene therapy drug in the European union. *Molecular Therapy*. 2012;20:1831-2.

- [35] Edelstein ML, Abedi MR, Wixon J. Gene therapy clinical trials worldwide to 2007—an update. *The Journal of Gene Medicine*. 2007;9:833-42.
- [36] Friedmann T, Roblin R. Gene therapy for human genetic disease? *Science*. 1972;175:949-55.
- [37] Cross D, Burmester JK. Gene Therapy for cancer treatment: past, present and future. *Clinical Medicine & Research*. 2006;4:218-27.
- [38] Kowalczyk DW, Wysocki PJ, A M. Cancer immunotherapy using cells modified with cytokine genes. *Acta Biochimica Polonica*. 2003;50:613-24.
- [39] Nawrocki S, Wysocki PJ, Mackiewicz A. Genetically modified tumour vaccines: an obstacle race to break host tolerance to cancer. *Expert Opinion on Biological Therapy*. 2001;1:193-204.
- [40] Kikuchi T. Genetically modified dendritic cells for therapeutic immunity. *The Tohoku Journal of Experimental Medicine*. 2006;208:1-8.

[41] Mullen J, Tanabe K. Viral oncolysis for malignant liver tumors. *Ann Surg Oncol.* 2003;10:596-605.

[42] Patil S, Rhodes D, Burgess D. DNA-based therapeutics and DNA delivery systems: A comprehensive review. *AAPS J.* 2005;7:E61-E77.

[43] Fridman JS, Lowe SW. Control of apoptosis by p53. *Oncogene.* 2003;22:9030-40.

[44] Ziady A, Ferkol T. DNA condensation and receptor-mediated gene transfer. *Gene therapy technologies, applications and regulations: from laboratory to clinic* editor: Anthony Meager 2001:13-34.

[45] Kohn DB, Sadelain M, Glorioso JC. Occurrence of leukaemia following gene therapy of X-linked SCID. *Nat Rev Cancer.* 2003;3:477-88.

[46] Graham FL, van der Eb AJ. A new technique for the assay of infectivity of human adenovirus 5 DNA. *Virology.* 1973;52:456-67.

- [47] Fraley R, Subramani S, Berg P, Papahadjopoulos D. Introduction of liposome-encapsulated SV40 DNA into cells. *Journal of Biological Chemistry*. 1980;255:10431-5.
- [48] Pagano JS, McCutchan JH, Vaheiri A. Factors influencing the enhancement of the infectivity of poliovirus ribonucleic acid by diethylaminoethyl-dextran. *Journal of Virology*. 1967;1:891-7.
- [49] Gordon JW, Scangos GA, Plotkin DJ, Barbosa JA, Ruddle FH. Genetic transformation of mouse embryos by microinjection of purified DNA. *Proceedings of the National Academy of Sciences*. 1980;77:7380-4.
- [50] Klein TM, Wolf ED, Wu R, Sanford JC. High-velocity microprojectiles for delivering nucleic acids into living cells. *Nature*. 1987;327:70-3.
- [51] Andreason G. Electroporation as a technique for the transfer of macromolecules into mammalian cell lines. *Journal of Tissue Culture Methods*. 1993;15:56-62.

[52] Noble ML, Kuhr CS, Graves SS, Loeb KR, Sun SS, Keilman GW, et al. Ultrasound-targeted microbubble destruction-mediated gene delivery Into canine livers. *Mol Ther.* 2013;21:1687-94.

[53] Samal SK, Dash M, Van Vlierberghe S, Kaplan DL, Chiellini E, van Blitterswijk C, et al. Cationic polymers and their therapeutic potential. *Chemical Society Reviews.* 2012;41:7147-94.

[54] Wagner E, Cotten M, Foisner R, Birnstiel ML. Transferrin-polycation-DNA complexes: the effect of polycations on the structure of the complex and DNA delivery to cells. *Proceedings of the National Academy of Sciences.* 1991;88:4255-9.

[55] Funhoff AM, van Nostrum CF, Lok MC, Kruijtz JAW, Crommelin DJA, Hennink WE. Cationic polymethacrylates with covalently linked membrane destabilizing peptides as gene delivery vectors. *Journal of Controlled Release.* 2005;101:233-46.

[56] Pouton CW, Lucas P, Thomas BJ, Uduehi AN, Milroy DA, Moss SH. Polycation-DNA complexes for gene delivery: a comparison of the

biopharmaceutical properties of cationic polypeptides and cationic lipids. *Journal of Controlled Release*. 1998;53:289-99.

[57] Zeng J, Wang S. Enhanced gene delivery to PC12 cells by a cationic polypeptide. *Biomaterials*. 2005;26:679-86.

[58] Fayazpour F, Lucas B, Alvarez-Lorenzo C, Sanders NN, Demeester J, De Smedt SC. Physicochemical and transfection properties of cationic hydroxyethylcellulose/DNA nanoparticles. *Biomacromolecules*. 2006;7:2856-62.

[59] Borchard G. Chitosans for gene delivery. *Advanced Drug Delivery Reviews*. 2001;52:145-50.

[60] Huang M, Fong C-W, Khor E, Lim L-Y. Transfection efficiency of chitosan vectors: Effect of polymer molecular weight and degree of deacetylation. *Journal of Controlled Release*. 2005;106:391-406.

[61] Lee CC, MacKay JA, Frechet JMJ, Szoka FC. Designing dendrimers for biological applications. *Nat Biotech*. 2005;23:1517-26.

[62] Bielinska A, Kukowska-Latallo JF, Johnson J, Tomalia DA, Baker JR. Regulation of in vitro gene expression using antisense oligonucleotides or antisense expression plasmids transfected using starburst PAMAM dendrimers. *Nucleic Acids Research*. 1996;24:2176-82.

[63] Mendiratta SK, Quezada A, Matar M, Wang J, Hebel HL, Long S, et al. Intratumoral delivery of IL-12 gene by polyvinyl polymeric vector system to murine renal and colon carcinoma results in potent antitumor immunity. *Gene Therapy*. 1999;6:833-9.

[64] Lungwitz U, Breunig M, Blunk T, Göpferich A. Polyethylenimine-based non-viral gene delivery systems. *European Journal of Pharmaceutics and Biopharmaceutics*. 2005;60:247-66.

[65] Heidel JD, Yu Z, Liu JY-C, Rele SM, Liang Y, Zeidan RK, et al. Administration in non-human primates of escalating intravenous doses of targeted nanoparticles containing ribonucleotide reductase subunit M2 siRNA. *Proceedings of the National Academy of Sciences*. 2007;104:5715-21.

[66] Davis ME. The first targeted delivery of siRNA in humans via a self-assembling, cyclodextrin polymer-based nanoparticle: from concept to clinic. *Molecular Pharmaceutics*. 2009;6:659-68.

[67] Gottfried LF, Dean DA. Extracellular and intracellular barriers to non-viral gene transfer. *Novel Gene Therapy Approaches*. 2013.

[68] Mellman I. Endocytosis and mmolecular sorting. *Annual Review of Cell and Developmental Biology*. 1996;12:575-625.

[69] Mukherjee S, Ghosh RN, Maxfield FR. Endocytosis. *Physiological Reviews*. 1997.

[70] Goldstein JL, Anderson RGW, Brown MS. Coated pits, coated vesicles, and receptor-mediated endocytosis. *Nature*. 1979;279:679-85.

[71] Rejman J, Oberle V, Zuhorn IS, Hoekstra D. Size-dependent internalization of particles via the pathways of clathrin- and caveolae-mediated endocytosis. *Biochem J* 2004;377:159-69.

[72] Douglas KL, Piccirillo CA, Tabrizian M. Cell line-dependent internalization pathways and intracellular trafficking determine

transfection efficiency of nanoparticle vectors. *European Journal of Pharmaceutics and Biopharmaceutics*. 2008;68:676-87.

[73] Nakase I, Tadokoro A, Kawabata N, Takeuchi T, Katoh H, Hiramoto K, et al. Interaction of arginine-rich peptides with membrane-associated proteoglycans is crucial for induction of actin organization and macropinocytosis. *Biochemistry*. 2006;46:492-501.

[74] Luedtke NW, Carmichael P, Tor Y. Cellular Uptake of aminoglycosides, guanidinoglycosides, and poly-arginine. *Journal of the American Chemical Society*. 2003;125:12374-5.

[75] Varkouhi AK, Scholte M, Storm G, Haisma HJ. Endosomal escape pathways for delivery of biologicals. *Journal of Controlled Release*. 2011;151:220-8.

[76] Lee H, Jeong JH, Park TG. A new gene delivery formulation of polyethylenimine/DNA complexes coated with PEG conjugated fusogenic peptide. *Journal of Controlled Release*. 2001;76:183-92.

[77] Sonawane ND, Szoka FC, Verkman AS. Chloride accumulation and swelling in endosomes enhances DNA transfer by polyamine-DNA polyplexes. *Journal of Biological Chemistry*. 2003;278:44826-31.

[78] Lechardeur D, Sohn KJ, Haardt M, Joshi PB, Monck M, Graham RW, et al. Metabolic instability of plasmid DNA in the cytosol: a potential barrier to gene transfer. *Gene Therapy*. 1999;6:482-97.

[79] Kao HP, Abney JR, Verkman AS. Determinants of the translational mobility of a small solute in cell cytoplasm. *The Journal of Cell Biology*. 1993;120:175-84.

[80] Dauty E, Verkman AS. Actin cytoskeleton as the principal determinant of size-dependent DNA mobility in cytoplasm: A new barrier for non-viral gene delivery. *Journal of Biological Chemistry*. 2005;280:7823-8.

[81] Vaughan EE, Dean DA. Intracellular trafficking of plasmids during transfection is mediated by microtubules. *Mol Ther*. 2006;13:422-8.

[82] Mesika A, Kiss V, Brumfeld V, Ghosh G, Reich Z. Enhanced intracellular mobility and nuclear accumulation of DNA plasmids associated with a karyophilic protein. *Human Gene Therapy*. 2005;16:200-8.

[83] Badding MA, Vaughan EE, Dean DA. Transcription factor plasmid binding modulates microtubule interactions and intracellular trafficking during gene transfer. *Gene Ther*. 2012;19:338-46.

[84] Lukacs GL, Haggie P, Seksek O, Lechardeur D, Freedman N, Verkman AS. Size-dependent DNA mobility in cytoplasm and nucleus. *Journal of Biological Chemistry*. 2000;275:1625-9.

[85] Brunner S, Sauer T, Carotta S, Cotten M, Saltik M, Wagner E. Cell cycle dependence of gene transfer by lipoplex, polyplex and recombinant adenovirus. *Gene Therapy*. 2000;7:401-7.

[86] Young JL, Benoit JN, Dean DA. Effect of a DNA nuclear targeting sequence on gene transfer and expression of plasmids in the intact vasculature. *Gene Ther*. 0000;10:1465-70.

[87] Schroeder A, Heller DA, Winslow MM, Dahlman JE, Pratt GW, Langer R, et al. Treating metastatic cancer with nanotechnology. *Nat Rev Cancer*. 2012;12:39-50.

[88] Safra T, Muggia F, Jeffers S, Tsao-Wei DD, Groshen S, Lyass O, et al. Pegylated liposomal doxorubicin (doxil): Reduced clinical cardiotoxicity in patients reaching or exceeding cumulative doses of 500 mg/m<sup>2</sup>. *Annals of Oncology*. 2000;11:1029-33.

[89] Tomao S, Miele E, Spinelli GP, Miele E, Tomao F. Albumin-bound formulation of paclitaxel (Abraxane<sup>®</sup> ABI-007) in the treatment of breast cancer. *Int J Nanomedicine*. 2009;4:99-105.

[90] Harisinghani MG, Saksena M, RW R. A pilot study of lymphotropic nanoparticle-enhanced magnetic resonance imaging technique in early stage testicular cancer: a new method for noninvasive lymph node evaluation. *Urology*. 2005;66:1066-71.

[91] Gabizon A, Shmeeda H, Barenholz Y. Pharmacokinetics of pegylated liposomal doxorubicin. *Clin Pharmacokinet*. 2003;42:419-36.

- [92] Lee J, Sohn JW, Zhang Y, Leong KW, Pisetsky D, Sullenger BA. Nucleic acid-binding polymers as anti-inflammatory agents. *Proceedings of the National Academy of Sciences*. 2011;108:14055-60.
- [93] Lal S, Clare SE, Halas NJ. Nanoshell-enabled photothermal cancer therapy: Impending clinical impact. *Accounts of Chemical Research*. 2008;41:1842-51.
- [94] W. Y, M. A, M. E, A. HES, S. LT, R. SR, et al. Do liposomal apoptotic enhancers increase tumor coagulation and end-point survival in percutaneous radiofrequency ablation of tumors in a rat tumor model? *Radiology*. 2010;257:685-96.
- [95] Baker I, Zeng Q, Li W, Sullivan CR. Heat deposition in iron oxide and iron nanoparticles for localized hyperthermia. *Journal of Applied Physics*. 2006;99:08H106-08H-3.
- [96] Ivkov R, DeNardo SJ, Daum W, Foreman AR, Goldstein RC, Nemkov VS, et al. Application of high amplitude alternating magnetic fields for heat induction of nanoparticles localized in cancer. *Clinical Cancer Research*. 2005;11:7093s-103s.

[97] Jain RK, Lee JJ, Hong D, Markman M, Gong J, Naing A, et al. Phase I oncology studies: Evidence that in the era of targeted therapies patients on lower doses do not fare worse. *Clinical Cancer Research*. 2010;16:1289-97.

[98] Brannon-Peppas L, Blanchette JO. Nanoparticle and targeted systems for cancer therapy. *Advanced Drug Delivery Reviews*. 2004;56:1649-59.

[99] Sarfati G, Dvir T, Elkabets M, Apte RN, Cohen S. Targeting of polymeric nanoparticles to lung metastases by surface-attachment of YIGSR peptide from laminin. *Biomaterials*. 2011;32:152-61.

[100] Yang W, Luo D, Wang S, Wang R, Chen R, Liu Y, et al. TMTP1, a novel tumor-homing peptide specifically targeting metastasis. *Clinical Cancer Research*. 2008;14:5494-502.

[101] Farokhzad OC, Jon S, Khademhosseini A, Tran T-NT, LaVan DA, Langer R. Nanoparticle-aptamer bioconjugates: A new approach for targeting prostate cancer cells. *Cancer Research*. 2004;64:7668-72.

- [102] Shigdar S, Lin J, Yu Y, Pastuovic M, Wei M, Duan W. RNA aptamer against a cancer stem cell marker epithelial cell adhesion molecule. *Cancer Science*. 2011;102:991-8.
- [103] Hanvey J, Peffer N, Bisi J, Thomson S, Cadilla R, Josey J, et al. Antisense and antigene properties of peptide nucleic acids. *Science*. 1992;258:1481-5.
- [104] Wang X, Li J, Wang Y, Koenig L, Gjyzezi A, Giannakakou P, et al. A folate receptor-targeting nanoparticle minimizes drug resistance in a human cancer model. *ACS Nano*. 2011;5:6184-94.
- [105] Arendt JFB, Pedersen L, Nexø E, Sørensen HT. Elevated plasma vitamin B12 levels as a marker for cancer: A population-based cohort study. *Journal of the National Cancer Institute*. 2013.
- [106] Michael SI, Curiel DT. Strategies to achieve targeted gene delivery via the receptor-mediated endocytosis pathway. *Gene Therapy*. 1994;1:223-32.

- [107] Lehrman S. Virus treatment questioned after gene therapy death. *Nature*. 1999;401:517-8.
- [108] Marshall E. Gene therapy a suspect in leukemia-like disease. *Science*. 2002;298:34-5.
- [109] Zhu K, Guo C, Lai H, Yang W, Wang C. Novel hyperbranched polyamidoamine nanoparticle based gene delivery: Transfection, cytotoxicity and in vitro evaluation. *International Journal of Pharmaceutics*. 2012;423:378-83.
- [110] Luo D, Saltzman, W. Mark. Synthetic DNA delivery systems. *Nat Biotech*. 2000;18:33-7.
- [111] Morille M, Passirani C, Vonarbourg A, Clavreul A, Benoit J-P. Progress in developing cationic vectors for non-viral systemic gene therapy against cancer. *Biomaterials*. 2008;29:3477-96.
- [112] Arote RB, Hwang S-K, Lim H-T, Kim T-H, Jere D, Jiang H-L, et al. The therapeutic efficiency of FP-PEA/TAM67 gene complexes via

folate receptor-mediated endocytosis in a xenograft mice model. *Biomaterials*. 2010;31:2435-45.

[113] Delgado D, Gascón AR, del Pozo-Rodríguez A, Echevarría E, Ruiz de Garibay AP, Rodríguez JM, et al. Dextran–protamine–solid lipid nanoparticles as a non-viral vector for gene therapy: In vitro characterization and in vivo transfection after intravenous administration to mice. *International Journal of Pharmaceutics*. 2012;425:35-43.

[114] Liang B, He M-L, Chan C-y, Chen Y-c, Li X-P, Li Y, et al. The use of folate-PEG-grafted-hybranched-PEI nonviral vector for the inhibition of glioma growth in the rat. *Biomaterials*. 2009;30:4014-20.

[115] Merdan T, Kopeček J, Kissel T. Prospects for cationic polymers in gene and oligonucleotide therapy against cancer. *Advanced Drug Delivery Reviews*. 2002;54:715-58.

[116] Hughes JA, Rao GA. Targeted polymers for gene delivery. *Expert Opinion on Drug Delivery*. 2005;2:145-57.

[117] Said HM, Kumar C. Intestinal absorption of vitamins. *Current Opinion in Gastroenterology*. 1999;15:172.

[118] Carver LA, Schnitzer JE. Caveolae: mining little caves for new cancer targets. *Nat Rev Cancer*. 2003;3:571-81.

[119] Said HM, Ortiz A, Ma TY. A carrier-mediated mechanism for pyridoxine uptake by human intestinal epithelial Caco-2 cells: regulation by a PKA-mediated pathway. *American Journal of Physiology - Cell Physiology*. 2003;285:C1219-C25.

[120] Merrill AH, Henderson JM. Diseases associated with defects in vitamin B6 metabolism or utilization. *Annual Review of Nutrition*. 1987;7:137-56.

[121] Zhu T, Stein S. Preparation of vitamin B6-conjugated peptides at the amino terminus and of vitamin B6-peptide-oligonucleotide conjugates. *Bioconjugate Chemistry*. 1994;5:312-5.

[122] Zhang ZM, McCormick DB. Uptake of N-(4'-pyridoxyl)amines and release of amines by renal cells: a model for transporter-enhanced

delivery of bioactive compounds. Proceedings of the National Academy of Sciences. 1991;88:10407-10.

[123] Arote RB, Hwang S-K, Yoo M-K, Jere D, Jiang H-L, Kim Y-K, et al. Biodegradable poly(ester amine) based on glycerol dimethacrylate and polyethylenimine as a gene carrier. The Journal of Gene Medicine. 2008;10:1223-35.

[124] L. B. Thomsen ABL, J. Lichota, T. Moos. Nanoparticle-derived non-viral genetic transfection at the blood-brain barrier to enable neuronal growth factor delivery by secretion from brain endothelium. Current Medicinal Chemistry. 2011;18:3330-4.

[125] Begley DJ. Delivery of therapeutic agents to the central nervous system: the problems and the possibilities. Pharmacology & Therapeutics. 2004;104:29-45.

[126] Merrill AH, Henderson JM. Vitamin B6 metabolism by human liver. Annals of the New York Academy of Sciences. 1990;585:110-7.

[127] Mooney S, Leuendorf J-E, Hendrickson C, Hellmann H. Vitamin B6: A long known compound of surprising complexity. *Molecules*. 2009;14:329-51.

[128] Ortega-Castro J, Adrover M, Frau J, Salvà A, Donoso J, Muñoz F. DFT studies on schiff base formation of vitamin B6 analogues. Reaction between a pyridoxamine-analogue and carbonyl compounds. *The Journal of Physical Chemistry A*. 2010;114:4634-40.

[129] Breunig M, Lungwitz U, Liebl R, Goepferich A. Breaking up the correlation between efficacy and toxicity for nonviral gene delivery. *Proceedings of the National Academy of Sciences*. 2007;104:14454-9.

[130] Merkel OM, Mintzer MA, Sitterberg J, Bakowsky U, Simanek EE, Kissel T. Triazine dendrimers as nonviral gene delivery systems: Effects of molecular structure on biological activity. *Bioconjugate Chemistry*. 2009;20:1799-806.

[131] Skelly JV, Renwick SB, Chave KJ, Sanders PG, Snell K, Baumann U. Purification, crystallization and preliminary X-ray analysis of human recombinant cytosolic serine

hydroxymethyltransferase. *Acta Crystallographica Section D*. 1998;54:1030-1.

[132] Gregory JF. A novel vitamin B6 metabolite may be a circulating marker of cancer. *Nutrition Reviews*. 1992;50:295-7.

[133] Hellmann H, Mooney S. Vitamin B6: A molecule for human health? *Molecules*. 2010;15:442-59.

[134] Yoshimori T, Yamamoto A, Moriyama Y, Futai M, Tashiro Y. Bafilomycin A1, a specific inhibitor of vacuolar-type H(+)-ATPase, inhibits acidification and protein degradation in lysosomes of cultured cells. *Journal of Biological Chemistry*. 1991;266:17707-12.

[135] Hannon GJ. RNA interference. *Nature*. 2002;418:244-51.

[136] Fire A, Xu S, Montgomery MK, Kostas SA, Driver SE, Mello CC. Potent and specific genetic interference by double-stranded RNA in *Caenorhabditis elegans*. *Nature*. 1998;391:806-11.

- [137] Zamore PD, Tuschl T, Sharp PA, Bartel DP. RNAi: Double-stranded RNA directs the ATP-dependent cleavage of mRNA at 21 to 23 nucleotide intervals. *Cell*. 2000;101:25-33.
- [138] Gregory RI, Chendrimada TP, Cooch N, Shiekhattar R. Human RISC couples microRNA biogenesis and posttranscriptional gene silencing. *Cell*. 2005;123:631-40.
- [139] Hutvagner G, Simard MJ. Argonaute proteins: key players in RNA silencing. *Nat Rev Mol Cell Biol*. 2008;9:22-32.
- [140] Bruce Alberts, Alexander Johnson, Julian Lewis, Martin Raff, Keith Roberts, Walter P. Cancer, *Molecular biology of the cell* 5th Edition: Garland Science; 2007.
- [141] Jiang F, Ye X, Liu X, Fincher L, McKearin D, Liu Q. Dicer-1 and R3D1-L catalyze microRNA maturation in *Drosophila*. *Genes & development*. 2005;19:1674-9.

- [142] Liu X JF, Kalidas S, Smith D, Liu Q. Dicer-2 and R2D2 coordinately bind siRNA to promote assembly of the siRISC complexes. *RNA*. 2006;12:1514-20.
- [143] Song J-J, Smith SK, Hannon GJ, Joshua-Tor L. Crystal structure of argonaute and its implications for RISC slicer activity. *Science*. 2004;305:1434-7.
- [144] Schwarz DS, Hutvágner G, Du T, Xu Z, Aronin N, Zamore PD. Asymmetry in the assembly of the RNAi enzyme complex. *Cell*. 2003;115:199-208.
- [145] Lim Y-b, Kim S-m, Suh H, Park J-s. Biodegradable, endosome disruptive, and cationic network-type polymer as a highly efficient and nontoxic gene delivery carrier. *Bioconjugate Chemistry*. 2002;13:952-7.
- [146] Pandey S, Garg P, Lim KT, Kim J, Choung Y-H, Choi Y-J, et al. The efficiency of membrane transport of vitamin B6 coupled to poly(ester amine) gene transporter and transfection in cancer cells. *Biomaterials*. 2013;34:3716-28.

[147] Anderson DD, Stover PJ. SHMT1 and SHMT2 are functionally redundant in nuclear *de novo* thymidylate biosynthesis. PLoS ONE. 2009;4:e5839.

[148] Anderson DD, Woeller CF, Chiang E-P, Shane B, Stover PJ. Serine hydroxymethyltransferase anchors *de novo* thymidylate synthesis pathway to nuclear lamina for DNA synthesis. Journal of Biological Chemistry. 2012;287:7051-62.

[149] Nelson DL, Cox MM. Biosynthesis of amino acids, nucleotides, and related molecules. Lehninger Principles of Biochemistry: W. H. Freeman Publishers; 2013. p. 833-80.

[150] Thorndike J, Pelliniemi T-T, Beck WS. Serine hydroxymethyltransferase activity and serine incorporation in leukocytes. Cancer Research. 1979;39:3435-40.

[151] Renwick SBS, Skelly JVJ, Chave KJK, Sanders PGP, Snell KK, Baumann UU. Purification, crystallization and preliminary X-ray analysis of human recombinant cytosolic serine

hydroxymethyltransferase. *Acta Crystallogr D Biol Crystallogr*. 1998;54:1030-1.

[152] Jain M, Nilsson R, Sharma S, Madhusudhan N, Kitami T, Souza AL, et al. Metabolite profiling identifies a key role for glycine in rapid cancer cell proliferation. *Science*. 2012;336:1040-4.

[153] Amadasi A. Pyridoxal 5'-phosphate enzymes as targets for therapeutic agents. *Current medicinal chemistry*. 2007;14:1291.

[154] Papamichael D. The use of thymidylate synthase inhibitors in the treatment of advanced colorectal cancer: Current status. *The Oncologist*. 1999;4:478-87.

[155] Marsh S. Thymidylate synthase pharmacogenetics. *Invest New Drugs*. 2005;23:533-7.

[156] Schweitzer BI, Dicker AP, Bertino JR. Dihydrofolate reductase as a therapeutic target. *The FASEB Journal*. 1990;4:2441-52.

[157] Wang T-L, Diaz LA, Romans K, Bardelli A, Saha S, Galizia G, et al. Digital karyotyping identifies thymidylate synthase amplification as

a mechanism of resistance to 5-fluorouracil in metastatic colorectal cancer patients. *Proceedings of the National Academy of Sciences of the United States of America*. 2004;101:3089-94.

[158] Banerjee D, Mayer-Kuckuk P, Capioux G, Budak-Alpdogan T, Gorlick R, Bertino JR. Novel aspects of resistance to drugs targeted to dihydrofolate reductase and thymidylate synthase. *Biochimica et Biophysica Acta (BBA) - Molecular Basis of Disease*. 2002;1587:164-73.

[159] Vicentini F, Borgheti-Cardoso L, Depieri L, Macedo Mano D, Abelha T, Petrilli R, et al. Delivery systems and local administration routes for therapeutic siRNA. *Pharm Res*. 2013;30:915-31.

[160] Ozpolat B, Sood AK, Lopez-Berestein G. Nanomedicine based approaches for the delivery of siRNA in cancer. *Journal of Internal Medicine*. 2010;267:44-53.

[161] Grant BD, Donaldson JG. Pathways and mechanisms of endocytic recycling. *Nat Rev Mol Cell Biol*. 2009;10:597-608.

[162] Wu F, Christen P, Gehring H. A novel approach to inhibit intracellular vitamin B6-dependent enzymes: proof of principle with human and plasmodium ornithine decarboxylase and human histidine decarboxylase. *The FASEB Journal*. 2011;25:2109-22.

[163] Schirch V, Szebenyi DME. Serine hydroxymethyltransferase revisited. *Current Opinion in Chemical Biology*. 2005;9:482-7.

[164] GP T, HP M, GP S. Vitamin B6 and cancer (review). *Anticancer Research*. 1981;1:263-7.

[165] Hans-Georg Eichler RH, Keith Snell. The role of serine hydroxymethyltransferase in cell proliferation: DNA synthesis from serine following mitogenic stimulation of lymphocytes. *Bioscience Reports*. 1981;1:101-6.

[166] Tripathi SK, Gupta N, Mahato M, Gupta KC, Kumar P. Selective blocking of primary amines in branched polyethylenimine with biocompatible ligand alleviates cytotoxicity and augments gene delivery efficacy in mammalian cells. *Colloids and Surfaces B: Biointerfaces*. 2014;115:79-85.

- [167] Arif M, Tripathi SK, Gupta KC, Kumar P. Self-assembled amphiphilic phosphopyridoxyl-polyethylenimine polymers exhibit high cell viability and gene transfection efficiency in vitro and in vivo. *Journal of Materials Chemistry B*. 2013;1:4020-31.
- [168] Cairns J. Mutation selection and the natural history of cancer. *Nature*. 1975;255:197-200.
- [169] Nowell P. The clonal evolution of tumor cell populations. *Science*. 1976;194:23-8.
- [170] Elbashir SM, Harborth J, Lendeckel W, Yalcin A, Weber K, Tuschl T. Duplexes of 21-nucleotide RNAs mediate RNA interference in cultured mammalian cells. *Nature*. 2001;411:494-8.
- [171] Whitehead KA, Langer R, Anderson DG. Knocking down barriers: advances in siRNA delivery. *Nat Rev Drug Discov*. 2009;8:129-38.

[172] Kim NW, Piatyszek MA, Prowse KR, Harley CB, West MD, Ho PL, et al. Specific association of human telomerase activity with immortal cells and cancer. *Science (New York, NY)*. 1994;266:2011-5.

[173] Weinert LHaT. Checkpoints: controls that ensure the order of cell cycle events. *Science*. 1989;246:629-34.

[174] Viviane Castelo Branco Reis FAGT, Marcio José Poças-Fonseca, Marlene Teixeira De-Souza, Diorge Paulo de Souza, João Ricardo Moreira Almeida, Camila Marinho-Silva, Nádia Skorupa Parachin, Alessandra da Silva Dantas, Thiago Machado Mello-de-Sousa, Lídia Maria Pepe de Moraes. Cell cycle, DNA replication, repair, and recombination in the dimorphic human pathogenic fungus *Paracoccidioides brasiliensis*. *Genet Mol Res*. 2005;4:232-50.

[175] Nio Y, Tamura K, Kan N, Inamoto T, Ohgaki K, Kodama H. In vitro DNA synthesis in freshly separated human breast cancer cells assessed by tritiated thymidine incorporation assay: relationship to the long-term outcome of patients. *British Journal of Surgery*. 1999;86:1463-9.

[176] Shirasaka T, Fujii S. DNA synthesis in tumor-bearing rats. *Cancer Research*. 1975;35:517-20.

[177] Narasimha Rao K, Bhattacharya RK, Venkatachalam SR. Thymidylate synthase activity in leukocytes from patients with chronic myelocytic leukemia and acute lymphocytic leukemia and its inhibition by phenanthroindolizidine alkaloids pergularinine and tylophorinidine. *Cancer Letters*. 1998;128:183-8.

[178] Elsea SH, Juyal RC, Jiralerspong S, Finucane BM, Pandolfo M, Greenberg F, et al. Haploinsufficiency of cytosolic serine hydroxymethyltransferase in the Smith-Magenis syndrome, 1995.

[179] Appaji Rao N, Talwar R, Savithri HS. Molecular organization, catalytic mechanism and function of serine hydroxymethyltransferase — a potential target for cancer chemotherapy. *The International Journal of Biochemistry & Cell Biology*. 2000;32:405-16.

[180] Renwick SB, Snell K, Baumann U. The crystal structure of human cytosolic serine hydroxymethyltransferase: a target for cancer chemotherapy. *Structure*. 1998;6:1105-16.

[181] Duvall E, Wyllie AH. Death and the cell. *Immunology Today*. 1986;7:115-9.

[182] Wyllie AH, Kerr JFR, Currie AR. Cell Death: The significance of apoptosis. *International Review of Cytology*: Academic Press; 1980. p. 251-306.

[183] Carson DA, Ribeiro JM. Apoptosis and disease. *The Lancet*. 1993;341:1251-4.

[184] Hickman J. Apoptosis induced by anticancer drugs. *Cancer Metast Rev*. 1992;11:121-39.

[185] van Engeland M, Nieland LJW, Ramaekers FCS, Schutte B, Reutelingsperger CPM. Annexin V-affinity assay: A review on an apoptosis detection system based on phosphatidylserine exposure. *Cytometry*. 1998;31:1-9.

[186] Sherr CJ. Cancer cell cycles. *Science*. 1996;274:1672-7.

[187] Durcan N, Murphy C, Cryan S-A. Inhalable siRNA: Potential as a therapeutic agent in the lungs. *Molecular Pharmaceutics*. 2008;5:559-66.

[188] Herbig K, Chiang E-P, Lee L-R, Hills J, Shane B, Stover PJ. Cytoplasmic serine hydroxymethyltransferase mediates competition between folate-dependent deoxyribonucleotide and S-adenosylmethionine biosyntheses. *Journal of Biological Chemistry*. 2002;277:38381-9.

## *LIST OF PUBLICATIONS*

---

1. **S Pandey\***, P Garg\*, Somin Lee, Yun-Hoon Choung, Pill-Hoon Choung\*\*, and Jong Hoon Chung, Nucleotide biosynthesis arrest by silencing SHMT1 function via vitamin B6-coupled vector and effects on tumor growth inhibition, **Biomaterials**, 35 (2014), 9332-9342.
2. **S Pandey\***, P Garg\*, KT Lim, J Kim, YH Choung, YJ Choi, PH Choung, CS Cho and JH Chung, The efficiency of membrane transport of vitamin B6 coupled to Poly(ester amine) gene transporter and transfection in cancer cells, **Biomaterials**, 34 (2013), 3746-3728.
3. P Garg, **S Pandey**, B Kang, J Kim, K T Lim, M H Cho, T-E Park, Y J Choi, P H Choung, C S Cho and J H Chung, Highly efficient gene transfection by hyperosmotic polymannitol based gene

- transporter through regulation of caveolae and COX-2 induced endocytosis, **J. Mater. Chem. B**, 2 (2014), 2666-2679.
4. J Kim, HN Kim, KT Lim, Y Kim, **S Pandey**, P Garg, YH Choung, PH Choung, KY Suh and JH Chung, Synergistic Effects of Nanotopography and Co-Culture with Endothelial Cells on Osteogenesis of Mesenchymal Stem Cells, **Biomaterials**, 34 (2013), 7257-7268.
  5. P Garg\*, S Kumar\*, **S Pandey**, H Seonwoo, PH Choung, J Koh and JH Chung, Triphenylamine coupled chitosan with high buffering capacity and low viscosity for enhanced transfection in mammalian cells in vitro and in vivo, **J. Mater. Chem. B**, 1 (2013), 6053-6065.
  6. P. Garg\*, S. Pandey\*, Seonwoo Hoon, Seungmin Yeom, Choung Yun-Hoon, Cho Chong-Su, Choung Pill-Hoon and Chung Jong Hoon, Hyperosmotic polydixylitol for crossing blood brain barrier and efficient nucleic acid delivery, **ChemComm**.

NOTE: \*equal contributions